Parathyroid Glands in Marsupials and Monotremes

by
Julie Irene Haynes
B.Sc. University of Adelaide

A thesis submitted for the degree of Doctor of Philosophy,
Department of Anatomical Sciences,
University of Adelaide,
South Australia

List of Contents

List of Diagrams and Plates

Abstract

The gross anatomy and microscopic morphology of the parathyroid glands were studied in 140 animals from twelve species of marsupials and monotremes. In marsupials parathyroid III was found bilaterally in the vicinity of the carotid bifurcation dorsolateral to the larynx. Two parathyroids IV were present in the mediastinum of most species. Parathyroid glands were often associated with the thymus but never thyroid.

Monotremes had one pair of glands located adjacent to the origins of the carotid arteries in the mediastinum. Endocrine glands, found lateral to the origin of the trachea, were confirmed by immunostaining to be ultimobranchial bodies.

Parathyroid parenchymal cells were arranged in strands and clumps separated by capillaries and supported by minimal connective tissue, except in the kangaroo where principal cells were clustered into lobules separated by quite thick septa. Follicles and cysts were observed in parathyroids of dunnarts, bandicoots, wombats, koalas and possums. Light and dark principal cell variants that were either inherent structural features or artefacts of fixation were present in most, but not all species. 'Non-secretory' cells, present in the parathyroids of antechinus, wombat and echidna, were identified as leukocytes, macrophages, and epithelial reticular cells respectively. Immunostaining for PTH showed, at the light microscopic level, a diffuse distribution of the hormone in parathyroid cells of all species examined. At the electron microscopic level only weak labelling of PTH was obtained and labelling was restricted to sparse small granules. Oxyphil cells were identified only in the wombat, and water-clear cells were found in parathyroids of the possum and echidna. The water-clear cells in some possums were thought to be related to stress and prompted a study into the relationship between the ultrastructure of the parathyroids and chronic stress in antechinuses during the post-mating period.

The effect of age on parathyroid morphology was studied in the kangaroo. The number of mitochondria per $10\mu m^2$ of parenchymal cell cytoplasm was analysed for young adult and very old (more than ten years) male kangaroos. No increase in the number of mitochondria was detected in the old group.

Declaration

This thesis contains no material which has been accepted for the award of any other degree or diploma in any university or other institution and, to the best of my knowledge and belief, contains no material previously published or written by another person, except where due reference has been made in the text.

I give consent to this copy of my thesis, when deposited in the University Library, being available for loan and photocopying.

Julie Irene Haynes

December, 1997.

Publications

Haynes, J.I. (1991) Cervical lymph nodes and mast cells in the marsupial *Sminthopsis crassicaudata*. Anat Rec 231: 7 - 13.

Haynes, J.I. (1995) Parathyroid morphology of the brush-tail possum, *Trichosurus vulpecula*. Anat Rec 241: 401 - 410.

Future Publications

Haynes, J.I. Parathyroid glands in monotremes. (In preparation)

Haynes, J.I. The marsupial parathyroid gland. (In preparation)

Haynes, J.I. Thoracic and cervical thymuses in Australian marsupials and monotremes. (In preparation)

Acknowledgements

This study was conducted under the auspices of the Faculty of Medicine, University of Adelaide and I am very grateful to The University of Adelaide giving me the opportunity to complete this thesis during my study leave. I wish to thank my supervisors, Dr Robert Barbour and Dr Jeffrey Trahair, for their advice and help in the preparation of this manuscript, Dr Adam Locket for translating several German scientific articles, and Mrs Gini Gooden for her assistance with the graphics used on the first page of each chapter. My sincere thanks are extended to the staff members of the Department of Anatomical Sciences, particularly Mr Chris Leigh and Mrs Gail Hermanis for their expert technical advice and help as well as their continual encouragement and friendship. Finally the project would not have come to fruition if it had not been for the support and understanding of my husband, Peter and three daughters, Sally, Emily and Alice.

The Marsupial Parathyroid Gland

The marsupial parathyroid gland,
A topic on which I shall expand,
Is usually present in four parts:
Two in the neck; two near the heart.
The former are where the carotids branch,
The latter near the aortic arch.

From the third and fourth branchial pouches rise
Glands numbered the same, no surprise.
Parathyroid III may contain some thymus,
'IV' is near the thoracic thymus.
PIII's rostral in metatherians
But is caudal in most eutherians.

Diprotodonts, like possums have four
Which compared with dunnarts is one more.
Other animals that were looked at-
Bandicoot, koala, and wombat,
All showed several variations
In the parathyroid formations.

Often merging with the parathyroid
Was thymic tissue but not thyroid.
The mingling was seen sometimes complete
With basal laminae incomplete,
Leaving only thymic ER cells
Between thymocytes and the chief cells.

Most glands included some follicles
Where small clusters of cells formed circles.
Large cysts were also often present,
Sometimes rounded shapes but sometimes bent.
Different cells were on their edges
Enclosing colloid with macrophages.

Glands studied had only the chief cell
But wombats showed oxyphils as well,
Where the mitochondria packed tight
Were coloured by eosin, pink and bright.
Bizarre the mitochondria did look
But why, is not recorded in a book.

In possums some cells were water-clear,
Transformed by disease is one idea.
These strange cells in healthy glands are rare,
They look as though they are filled with air,
With lots of droplets large and small
The cytoplasm doesn't stain at all.

Chapter 1

Introduction, Aims and Objectives

1.1. Introduction

This study of the parathyroid glands in marsupials and monotremes has been done on 140 animals from six families of Australian marsupials and two families of Australian monotremes. The thesis is presented in eleven chapters. Chapter 1 includes the aims and objectives of the project. Literature review is covered in chapter 2; chapter 3, Materials and Methods, summarises the animals and numbers used and the general techniques employed in the study. Specific details of tissue processing and staining are given in the Appendices.

The investigations of the parathyroid glands in marsupials are described in chapters 4 to 8 with each chapter covering one or more species, representative of a marsupial family. The exception to this format is chapter 6 where the studies on the wombat, *Lasiorhinus latifrons*, and the koala, *Phascolarctos cinereus*, are presented under the heading of the superfamily Vombatoidea. Chapter 9 describes the parathyroid glands in two monotreme families. Chapters 4 to 9 have a similar format with three major sections - Introduction, Results and Discussion. The introduction includes details of the individual species studied and descriptions of materials and methods if they were not fully covered in chapter 3. The Results and Discussion have subsections of gross anatomy, light microscopy, and electron microscopy for each species. If similar results were found for several families then the findings are discussed in chapter 11, General Discussion, as well as in the individual chapters.

During the course of studies on the parathyroid glands in marsupials and monotreme species, tissue samples that were suitable for immunocytochemistry were collected. The immunocytochemical study is the topic for chapter 10.

(The sources of the figures in the graphics are given at the end of the bibliography, page 227.)

1.2. Aims and Objectives

For each marsupial and monotreme species examined the main aims of the study were:-

- To describe the gross anatomy, light microscopic structure, and ultrastructure of the parathyroid glands and to compare the morphology with that of other vertebrates, especially mammals.
- To identify parathyroid hormone in tissue sections of the glands at the light, and where possible, electron microscopic levels by employing immunocytochemistry.
- To determine the occurrence of oxyphil and water-clear cells, compare them with similar cells found in other mammalian species, and to speculate on the possible causes that influence the formation of oxyphil cells and water-clear cells.

Additional aims for the individual species or chapters were:-

Chapter 4 - Dasyurid Marsupials

- To investigate the influence of the mode of fixation (i.e. perfusion, immersion) on the microscopic morphology of the parathyroid glands*.
- To examine the effect of chronic stress in *Antechinus flavipes* and *Antechinus stuartii* on the microscopic morphology of the parathyroid glands.

Chapter 5 - Peramelid Marsupials

- To investigate the occurrence of thymic tissue in the neck in order to determine the absence or presence of the cervical thymus in *Isoodon* species.

Chapter 6 - Vombatoidae; Wombat and Koala

- To investigate the occurrence of thymic tissue in the neck and thorax of the wombat (*Lasiorhinus latifrons*) and the koala (*Phascolarctos cinereus*) in order to determine the status of cervical and / or thoracic thymuses in these two species.

Chapter 7 - Phalangerid Marsupial, *Trichosurus vulpecula*

- To investigate the influence of the mode of fixation (i.e. perfusion, immersion) on the microscopic morphology of the parathyroid glands*.

Chapter 8 - Macropod Marsupial, *Macropus fuliginosus*

• To investigate the influence of the mode of fixation (i.e. perfusion, immersion) on the microscopic morphology of the parathyroid glands*.

• To determine if there was a significant increase in the number of mitochondria per $10\mu m^2$ of cytoplasm in parenchymal cells of old kangaroos compared with young kangaroos.

• Associated with the above aim was: to determine the approximate age of kangaroos from which specimens were collected.

Chapter 9 - Monotremes

• To describe the gross anatomy, including the relationship to the parathyroid glands, and histology of thymus, thyroid, ultimobranchial bodies, and cervical and mediastinal lymph nodes in mature echidnas and platypuses.

Chapter 10 - Immunocytochemical Study

• To identify parathyroid hormone in tissue sections of the glands at the light, and where possible, electron microscopic levels by employing immunocytochemistry.

• To confirm by immunostaining the identification of glands as ultimobranchial bodies in the echidna.

* The influence of the mode of fixation (i.e. perfusion, immersion) on the microscopic morphology of the parathyroid glands was investigated in dunnarts, possums and kangaroos because for these animals two groups could be identified where environmental conditions at the time of death and the processing of specimens were similar for each group with the only known difference being the mode of fixation.

Chapter 2

Literature Review

2.1. Introduction

This literature review will focus on the mammalian parathyroid gland with minor references to parathyroids in birds, reptiles and amphibians. The parathyroid glands are endocrine glands located in the neck and sometimes thorax of all animals in the phyletic scale above and including air breathing amphibians (Roth and Schiller, 1976). Parathyroid glands develop from the endoderm of the third and fourth branchial pouches in the embryo. Most animals have two pairs of glands labelled PIII and PIV indicating their embryological origins. In some species, for example rat and mouse, one pair of glands either fails to develop or involutes early in development resulting in the final presence of only one pair of parathyroids (Roth and Schiller, 1976). The established function of the parathyroid glands is to secrete parathyroid hormone or parathormone (PTH) which increases the concentration of calcium in the blood as a result of a variety of different physiological actions.

In fish, PTH is replaced by stanniocalcin as the primary hormone for the homeostatic control of extracellular calcium (Wendelaar Bonga and Pang, 1991). Stanniocalcin is produced by the corpuscles of Stannius which are associated with the kidneys. Unlike PTH, stanniocalcin reduces extracellular calcium. The target organs are the gills and intestines where entry of calcium from the external environment is prevented (Perry et al. 1989). Hence while PTH and stanniocalcin are the primary hormones for controlling calcium levels in air-breathing vertebrates and fish respectively their modes of action are quite different.

2.2. History

Sandström is recognized as being the first to present a comprehensive description of the parathyroid glands in a scientific journal in 1880 (Seipel, 1938). Prior to this date several references had been made to these structures but no significance had been placed on the observations. Remak in 1855 (cited by Sandström, 1880) reported the presence of a gland-like structure located on the superior tip of the thymus in a new-born cat. Histologically, the gland was distinct from thyroid, lymphoid, or thymic

tissue. Virchow in 1863 (cited by Sandström, 1880) described the constant appearance of pea-shaped structures on the lateral masses of the human thyroid, and stated that the histology of these structures resembled lymphoid tissue rather than thyroid. Owen (1862) also mentioned the presence of glands, later interpreted as being parathyroids, in the rhinoceros.

In the paper published by Sandström in 1880, he described "hemp-seed like" structures attached to the thyroids of dogs. Microscopic examination revealed that they were unique glands which, from their position, were appropriately named parathyroid glands. Similar structures were identified in the cat, rabbit, ox, horse and human (Sandström, 1880). Detailed anatomical and histological aspects of the human parathyroid glands that were based upon studies of 50 individuals were included in the paper. No duct systems were observed and parenchymal cells were described as being arranged in clumps or irregular rows (Sandström, 1880). Baber (1881) without prior knowledge of Sandström's work, made an independent observation of parathyroids in dogs. Fortunately he did not complicate the issue by assigning a name to them. Since Sandström's paper was originally in Swedish, its impact would have been restricted to Sweden had it not been for the publication of an abstract, translated into German, by Retzius in 1880 (cited by Seipel, 1938) which enabled the wider scientific world to have access to the report.

By the turn of the century the existence of the parathyroid glands in a wide range of animals had been established. The literature was reviewed by Welsh (1898) and Hammer (1908). The anatomy and histology were accurately described but all these early anatomists believed that the parathyroid glands represented embryonic residues of the thyroids and that parathyroid cells were able to differentiate into thyroid cells. The occasional presence of parathyroid cells clustered into small follicles, imitating typical thyroid histological structure, probably added support to this hypothesis (Welsh, 1898; Hammer, 1908). Gley (1893, cited by Welsh, 1898) was one of the first researchers to reject this function of the parathyroid glands. Using rabbits, he removed the thyroid glands in which the internal parathyroids were present, and examined the external parathyroids at various intervals after thyroidectomy. Slight hypertrophy was initially noticed in the remaining glands but at no time was there any evidence of parathyroid tissue transforming into thyroid tissue.

In 1908, MacCallam and Voegtlin noticed increased neuromuscular excitability following parathyroidectomy and that hypocalcemia resulted in similar conditions. Consequently they postulated that the parathyroid glands controlled calcium metabolism (MacCallam and Voegtlin, 1908 & 1909). It was not until sixteen years later that the function of the parathyroid glands was determined more directly when Collip (1925) successfully extracted an active principle from bovine parathyroid glands which corrected hypocalcemia and tetany in parathyroidectomized dogs.

Since the establishment of the function of the parathyroid glands, an exponential growth in the knowledge of the parathyroids has occurred. The applications of new biochemical, histological, and immunological techniques that have been developed over the past 72 years have increased the understanding of the function and structure of the parathyroid glands (DeGroot, 1979; Potts et al., 1995).

2.3. Physiology and Biochemistry

The known, well documented function of the parathyroid glands is to secrete PTH (Potts et al., 1995). This hormone and calcitonin, which in most mammals, is secreted from parafollicular cells in the thyroid gland, are concerned with the maintenance of the serum calcium level within very narrow limits (DeGroot, 1979). Blood calcium concentrations are raised by PTH and decreased by calcitonin. The secretion of PTH raises the plasma calcium level in several ways. It liberates calcium from bone to blood by fast and slow mechanisms. Calcium is present in bone as a solid phase in the calcified matrix and as soluble calcium ions in bone fluid at the interface of the bone matrix with osteocytes and with osteoblasts on the surface of bone (Malluche and Faugere, 1986). Within minutes of being released from the parathyroid glands, PTH causes the rapid, active transfer of calcium ions from bone fluid to extracellular fluid (Parsons, 1979). This fast mechanism relies on PTH activating existing intracellular enzyme pathways in the osteoblasts. Short-term decreases in blood calcium levels are corrected in this manner (Talmage et al., 1978). The slower mechanism for the movement of calcium from bone to blood involves PTH activating catabolic enzymes in osteoclasts. This process takes several hours and results in the destruction of all the components of bone and the release of calcium ions from the matrix to blood (Parsons, 1979; Malluche and Faugere, 1986; Potts et al., 1995).

In addition to PTH having a catabolic effect on bone, the normal physiological levels of this hormone also have an anabolic effect resulting in an overall increase in bone mass. Initially PTH removes calcium from bone to blood but the action of PTH in increasing the absorption of calcium from the renal tubules and small intestine gives slight hypercalcemia ultimately leading to the deposition of calcium in bone by osteoblasts (Parsons, 1979; Malluche and Faugere, 1986).

Calcium absorption and phosphate secretion from the renal tubules are promoted by PTH (Potts et al., 1995). Also in the kidneys, PTH regulates the hydroxylation of 25-hydroxy-vitamin D to 1,25-dihydroxy-vitamin D. The latter compound is what enhances the absorption of calcium from the small intestine (Irving, 1973; Aurbach and Chase, 1976; Harper et al., 1979).

The secretion of PTH is controlled predominately by a simple feedback mechanism where decreasing blood calcium levels trigger the release of PTH from the parathyroid glands (Cohn and MacGregor, 1981). However this inverse relationship only occurs for plasma calcium concentrations between 7.5 and 10.5mg/100ml which are in the normal to slightly hypocalcemic range. In severe hypocalcemia and hypercalcemia the rate of secretion of PTH is independent of plasma calcium concentrations (Blum et al., 1974).

Parathyroid cells have surface receptors for calcium that induce transient increased intracellular calcium levels which, in turn, lead to PTH release (Potts et al., 1995). The surface receptor has been identified as a 500-kDa protein and its role in PTH secretion has been shown in a study where the presence of a monoclonal antibody to the receptor blocked the release of PTH in response to hypocalcemia (Juhlin et al., 1989).

Other ions and compounds have been shown to affect the secretion of PTH. Very high levels of magnesium inhibit the release of PTH but physiological concentrations of the cation have negligible influence (Kemper, 1984). Adrenalin and other beta-adrenergic agents increase PTH secretion. Dopamine D1 and histamine H2 receptors have been identified on parathyroid cells, and both biogenic amines raise plasma levels of PTH (Fairney, 1983; Kemper, 1984). A metabolite of vitamin D, 24,25-dihydroxy-vitamin D has an inhibitory effect (Mayer, 1979). Calcitonin and other hormones have been reported to affect PTH secretion by affecting the intracellular levels of cyclic AMP in the parathyroid cells. The physiological significance of these additional controlling agents is unclear (Kemper, 1984).

Parathyroid hormone is a linear basic polypeptide containing 84 amino acids residues (Potts et al., 1995). Close homology has been found among samples of PTH from different species. Analyses of the hormone from humans, cows, pigs, dogs, rats and chickens all show strong similarities (Kemper, 1984). Within the cells of the parathyroid glands PTH is initially synthesized in rough endoplasmic reticulum as preProPTH which consists of 115 amino acids. A cleavage of this polypeptide as it enters the cisternae of the rough endoplasmic reticulum, results in ProPTH which contains 90 amino acids and is conveyed to the Golgi region where it is converted to PTH (Cohn and Elting, 1983).

From the Golgi region PTH is packaged into secretory vesicles and appears to follow one of two routes prior to its release from the cell by exocytosis (Habener, 1979). Either PTH is stored in secretory granules that form an intracellular storage pool from which the hormone is secreted when required (Habener, 1979), or PTH is directly released from the cell after its formation in the Golgi region and it does not form part of the storage pool (MacGregor et al., 1975; Kemper,1984). The majority of PTH released from parathyroid cells appears to follow the latter course. Evidence is gained from the poor correlation between secretory activity and secretory granule numbers (Roth and Raisz, 1966; MacGregor et al., 1975) and

from studies using radioactive labelled leucine, where the major amount of secreted PTH was newly synthesized, and released directly from the Golgi body rather than the storage pool (MacGregor et al., 1975). Hence secretory activity is better indicated by the size of the Golgi complex (MacGregor et al., 1975). Studies using *in situ* hybridization techniques for PTH mRNA coupled with immunostaining of PTH showed similar results where in physiological conditions, an inverse relationship was shown to exist between the synthesis and storage of PTH (Kendall et al., 1993).

The parathyroid gland is unlike any other endocrine gland in that excess production of hormone occurs constantly and the main controlling mechanism of hormone secretion acts by varying the proportion of release or degradation of the hormone from the cytoplasm (Wendelaar Bonga and Pang, 1991). Many stored PTH secretory granules are degraded by lysosomal enzymes within the parathyroid cells with hypocalcemia decreasing degradation and increasing secretion of the stored PTH vesicles (Habener, 1979). Conversely, when PTH release is suppressed the number of lysosomes increases. In a mechanism apparently unique to the parathyroid gland, some of the products of the degradation of storage granules are secreted, thus contributing to the heterogeneity of circulating PTH derived products (Wendelaar Bonga and Pang, 1991). The synthesis of PTH is less affected by acute hypocalcemia than is the release of PTH from the parathyroid cells. The long delay between the onset of hypocalcemia and increased production of PTH suggests a controlling influence at the level of transcription rather than translation (Kemper, 1984).

In addition to PTH, parathyroid cells produce an accessory secretory protein. The identification of this protein was made simultaneously by two groups of investigators working independently (Morrissey and Cohn, 1978; Ravazzola et al., 1978), resulting in the same protein being named secretory protein-I by the former group and parathyroid secretory protein by the latter. Currently, both names are still used in journals and books (Oka et al., 1988; DeLellis, 1993). The pattern of secretion of this acidic protein is similar to that of PTH. Secretory protein-I contains 3 to 18% carbohydrate. In solution the protein consists of two to four subunits each of which has a molecular weight of approximately 70,000 daltons (Kemper, 1984). Immunofluorescence studies (Ravazzola et al., 1978) have shown identical intracellular locations for SP-I and PTH. This suggests that SP-I may be involved in the storage and secretion of PTH. No biological function has yet been associated with secreted SP-I (Kemper, 1984).

Secretory Protein-I is chemically and physically very similar to chromogranin A which is the major soluble protein associated with adrenalin and noradrenalin secretory granules in adrenal medullary cells and polypeptide hormone secretory cells (Cohn et al, 1982). Antibodies to SP-1 and chromogranin A cross-react with both proteins (O'Connor et al., 1983) and indeed antibodies to chromogranin A have been used in studies of SP-I in parathyroid glands (Oka et al., 1988). Chromogranin A, like SP-I, is assumed to play a

role in the storage and secretion of polypeptides and amines from endocrine cells and sympathetic nerves (O'Connor et al, 1983). Indeed, chromogranin A has been found to have an autocrine regulatory effect on the secretion of PTH (Fasciotto et al., 1990).

Several forms of PTH are present in the blood. Hormone proteolysis which probably occurs in the kidneys and other tissues, results in several fragments with differing potency and half lives (Potts et al., 1995). Cleavage at residue 34 from the amino terminal of the polypeptide results in biologically active and inactive fragments with the first 25 amino acids at the amino terminal responsible for the hormonal activity (Segre, 1979). The biologically inactive part of PTH (i.e. amino acid residues 35 to 84, including the carboxy terminal) is the main form of the immunoreactive part of PTH and has a longer half life than the biologically active amino terminal (i.e. amino acid residues 1 to 34). Hence immunoassays and immunocytochemical techniques for PTH may not always give direct indications of the amount of biologically active PTH present (Segre, 1979). Carboxyl-terminal specific antisera detect 90% of the total immunoreactive PTH in serum whereas amino-terminal specific antisera detect between 10-20% (Segre et al., 1972). Parathyroid hormone levels in serum are most accurately estimated using noncompetitive, two-site immunoassays where two antibodies are used to bind simultaneously to different regions (1 - 34; 39 - 84) of the hormone (Blind et al., 1988).

In the last decade another protein that is similar to PTH and causes hypercalcemia has been identified; it has been named parathyroid hormone related protein (PRP) (Broadus et al., 1988). The major sources of PRP are malignant tumour cells and PRP is responsible for the hypercalcemia observed late in malignancies. However, PRP is also found in very low concentrations in normal tissues where it is thought to have a paracrine action of regulating calcium transport. Negligible amounts of PRP enter the circulatory system in normal conditions (Martin and Moseley, 1995). Locations include smooth muscle, kidney tubules, keratinocytes, bronchioles, and male and female reproductive tracts (Kramer et al., 1991).Parathyroid hormone related protein relaxes smooth muscle of the vascular system, stomach and oviducts and in epithelia its role has been proposed as influencing cellular turnover and differentiation of epithelial cells (Martin and Moseley, 1995). In the placenta, PRP has a role in foetal calcium homeostasis (Emly et al., 1994). Parathyroid hormone related protein and PTH share homologies at their N-terminal portions allowing PRP to bind to PTH receptors in bone and kidney and cause hypercalcemia (Broadus et al., 1988). Additional receptors, unique to PRP are thought to be present in a wide range of tissues whereby PRP expresses its paracrine function (Orloff et al., 1989).

2.4.1. Anatomy and Embryology

The parathyroid glands develop in bilaterally symmetrical fashion from the endoderm of the third and fourth pharyngeal pouches (Fig. 2.1). Roman numerals are used to designate the origin of the two pairs of glands. In eutherians, the endoderm of the ventral extremity of the third pharyngeal pouch gives rise to the thymus, while the endoderm of the dorsal angle gives rise to parathyroid III (Gilmour, 1937; Norris, 1937; Roth and Schiller, 1976; Larsen, 1997). The growth of these two endodermal structures fills the third pouch and then, influenced by the descent of the heart into the thorax, they migrate caudally (Fig. 2.1). Parathyroid III splits from the larger cellular mass, the thymus, and two distinct organs are formed. The thymus, located in the thorax is displaced further from its origin compared with parathyroid III which usually stays near the caudal tip of the thyroid (Fig. 2.1). However, sometimes incorrect cleavage leads to accessory thymic or parathyroid tissue. The location of parathyroid III can also be variable. It can migrate with the descending thymus and reside in the mediastinum associated with the thymus (Roth and Schiller, 1976). In humans the position of parathyroid III is on or near the surface of the inferior tip of the thyroid (57%), within the superior regions of the thymus (39%), or rarely, deep in the mediastinum (2%). The remaining 2% develop abnormally and are found high in the neck, sometimes associated with the carotid sheath (Wang, 1976).

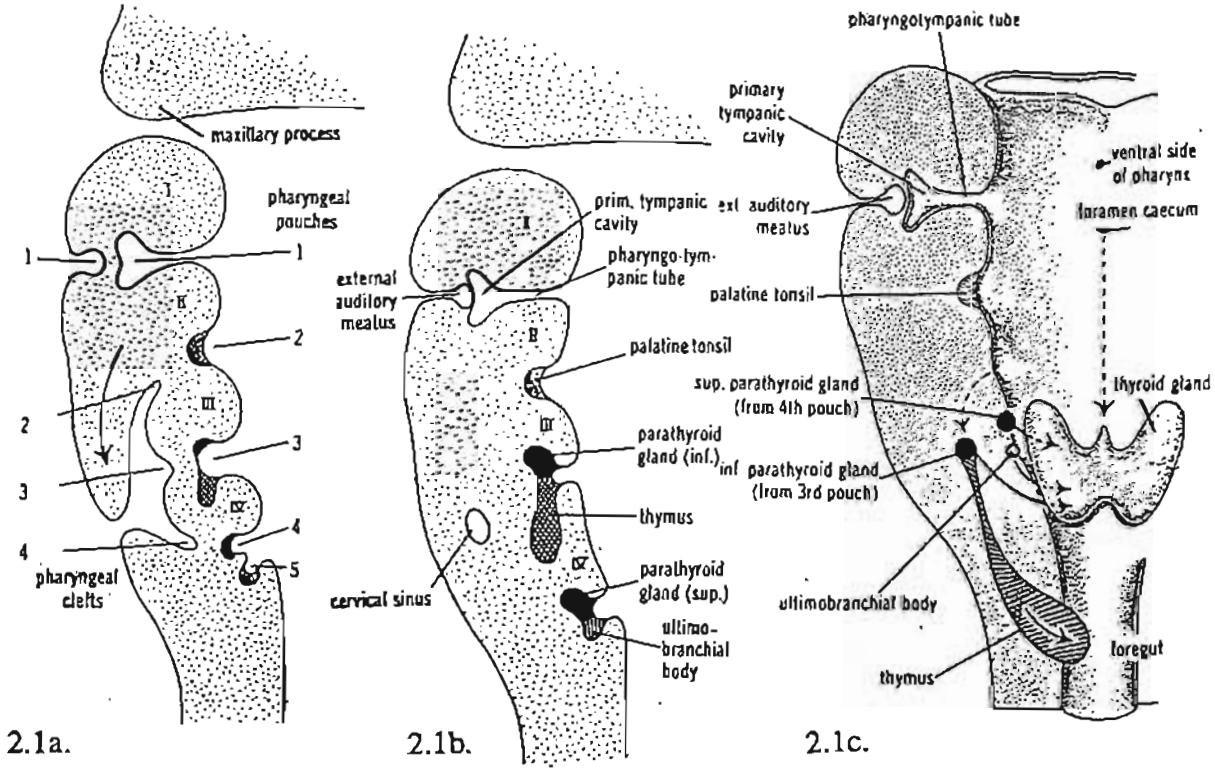

Fig. 2.1. A diagrammatic representation of the development of the pharyngeal pouches and clefts in humans to show the formation of the cervical sinus and the migration of the thyroid, thymus, parathyroid, and ultimobranchial anlagen. Early developmental stages are shown in Figs. 2.1a. & 2.1b. and a later stage in Fig 2.1c. (modified after Langman, 1969).

The dorsal wing of the fourth pharyngeal pouch forms the cephalic parathyroid gland (IV). The anlage of parathyroid IV attaches to the downwardly migrating thyroid gland that originates from the floor of the pharynx. The former gland is also connected by a thin stalk to the ultimobranchial body that arises from the poorly delineated fifth pouch (Fig. 2.1). This connection is lost as the cells of the ultimobranchial body in metatherians and eutherians penetrate the thyroid and give rise to parafollicular cells which secrete calcitonin (Larsen, 1997; Roth, 1979). In eutherians, parathyroid IV has a constant position on the dorsal surface of the thyroid gland (Roth and Schiller, 1976). In humans, parathyroid IV is found at the level of the cricothyroid junction, near where the middle thyroid artery crosses the recurrent laryngeal nerve (77%) , or on the dorsal aspect of the upper pole of the thyroid (22%). Parathyroid IV is rarely located in an ectopic position (1%) associated with the pharynx or oesophagus (Millzner, 1931; Wang, 1976). Accessory parathyroid glands are not uncommon in humans. Serial sections of 14 foetuses revealed three with more than four glands (Gilmour, 1937) and Millzner (1931) reported the presence of accessory parathyroids in 36 of 42 dissections on adults.

In eutherians some variations occur in the number and location of the parathyroid glands. Indeed, within a species, abnormal migration or cleavage of embryonic pharyngeal derivatives can result in additional glands in the neck or thorax. The importance of location and number of parathyroid glands in a species becomes apparent when experimental parathyroidectomy is performed because sometimes it can be doubtful that complete ablation of parathyroid tissue has occurred. The comparative anatomy of the parathyroid that is reviewed below represents the anatomy of parathyroid glands from those eutherian species on which most parathyroid research has been done.

In rats and mice, parathyroid IV never develops because the fourth pharyngeal pouch does not develop (Rogers, 1929; Roth and Schiller, 1976). During development, parathyroid III separates from the thymus in its caudal migration and comes into close contact with the lateral aspect of the thyroid. The rabbit has parathyroid III on or near the dorsocaudal surface of the thyroid, whereas parathyroid IV is found embedded in the thyroid. In very young rabbits parathyroid III occurs in a more cranial position than in mature animals (Kohn, 1896, cited by Welsh, 1898).

The cat normally has four parathyroid glands but accessory glands were noticed in 35% of 107 cats studied by Nicholas and Swingle (1925). Parathyroid IV is located at the cephalic pole of the thyroid on the ventral surface. Parathyroid III is more variable in number and location. It can occur anywhere on the tracheal surface of the thyroid gland or be embedded in it. The location of the parathyroid glands in the dog is similar to the general eutherian pattern (Godwin, 1937). However, every embryonic, foetal and post-natal specimen examined by Godwin contained accessory glands. In cows, sheep and goats, parathyroid IV is usually found a short distance from the thyroid near the common carotid artery or its

bifurcation. Parathyroid III is found on or just under the medial surface of the thyroid (Forsyth, 1908; Roth and Schiller, 1976).

2.4.2. Anatomy and Embryology of the Marsupial Parathyroid

There is a dearth of information on the marsupial and monotreme parathyroid glands and the majority of available references come from the first half of this century. In marsupials, the positions of the parathyroids and their associations with other organs can be influenced by the unusual development of the marsupial thymus (Fig. 2.2). All polyprotodont marsupials (e.g. Didelphidae, Dasyuridae, and Peramelidae) have a thoracic thymus derived from the third and fourth pharyngeal pouches. Diprotodonts (e.g. Phalangeridae and Macropodidae) have a cervical thymus as well as a thoracic thymus (Johnstone, 1898; Symington, 1898: Fraser, 1915; Fraser and Hill, 1915; Yadav, 1973). The cervical thymus arises mainly from the ectoderm of the cervical sinus (Fig. 2.2) with much smaller contributions from the second, third, and maybe fourth pharyngeal pouches (Fraser, 1915, Fraser and Hill, 1915). In the diprotodont phascolarid species of wombats and koalas, a cervical thymus is present whereas the thoracic thymus is usually absent. The absence of a thoracic thymus in the wombat has been indicated by all investigators but is disputed in the koala. This topic will be expanded later.

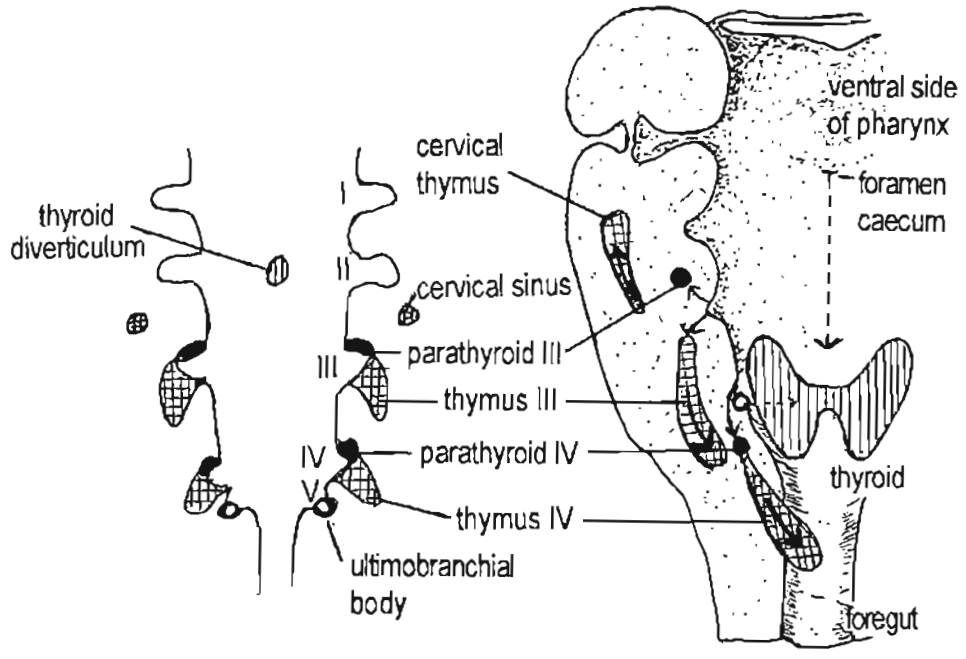

Fig. 2.2. A diagrammatic representation of the pharyngeal pouches to show the embryological derivation (Fig. 2.2a) and migration (Fig. 2.2b) of the parathyroid glands, thoracic and cervical thymuses, ultimobranchial body, and thyroid in *T. vulpecula*. The drawings summarise the descriptions and illustrations given by Fraser and Hill (1915).

The embryology and anatomy of the parathyroid glands has been described thoroughly for the brush-tailed possum, Trichosurus *vulpecula* (Fraser and Hill, 1915; Adams, 1955) and the opossum, *Didelphis virginiana*, (McCrady, 1938; Kingsbury, 1940; McCrady, 1941). From the examination of more than twenty uterine embryos and pouch young specimens of *T. vulpecula*, Fraser and Hill (1915) concluded that the cranial, dorsal wall of the third pouch and not the ventral extremity as in eutherians, gives rise to parathyroid III. Thymus III is derived from the entire ventral as well as the caudal, dorsal wall of the third pouch. The fourth pharyngeal pouch not only gives rise to parathyroid IV from its dorsal wall but also to thymus IV from its ventral wall. The participation of the fourth pharyngeal pouch in the formation of the thymus is also different from eutherians, in which the thymus is derived solely from the third pouch. The ultimobranchial body in *T. vulpecula*, arises from a vestigial fifth pouch and associates with the thyroid gland where it forms diffuse parafollicular cells. Parathyroid III migrates as a tubular, elongated structure to a position near the carotid bifurcation. In the adult it is usually present as a flattened, ovoid, encapsulated gland at the same location (Fraser and Hill, 1915; Adams, 1955). Isolation of groups of cells from the tubular elongated parathyroid III seen in developing possums, may produce aberrant or additional parathyroid glands in the adult. Thymus III and IV migrate to the thorax where they remain separate or join together. The position of parathyroid IV is much more variable than parathyroid III. It usually retains its proximity to thymus IV and hence is present in the thorax near or embedded in the thymus. Fraser and Hill (1915) noticed several "accessory epithelial bodies" and "accessory thymic bodies" in specimens of *T. vulpecula*. It was assumed that these structures were derived from cells interrupted in their migration by the intervention of other developing pharyngeal structures. The descriptions and illustrations given by Fraser and Hill (1915) for *T. vulpecula* are summarised in Figure 2.2.

Early in the differentiation of the pharyngeal pouches in *D. virginiana*, the anlage of parathyroid III moulds over the dorsal surface of the adjacent internal carotid artery. This association results in parathyroid III being an annular structure on the base of the internal carotid artery in the adult (McCrady, 1938: Kingsbury, 1940; McCrady, 1941). The dorsal wall of the fourth pouch gives rise to parathyroid IV which has been traced in embryos to migrate into the mediastinum with thymic tissue (McCrady, 1938). Evidence suggests that only limited development of parathyroid IV occurs. Although it could usually be detected as a small gland variable in position and often fragmented in embryos and pouch young (Kingsbury, 1940), no trace of parathyroid IV was found in the neck or mediastinum of adults (McCrady, 1941).

The other marsupials for which the anatomy and embryology of the parathyroid glands have been described are the koala, *Phascolarctos cinereus*, the common wombat, *Vombatus ursinus* (referred to as *Phascolomys mitchelli* in Fraser's paper, 1915) and two species of bandicoots, the long-nosed bandicoot, *Perameles nasuta*, and the southern brown

bandicoot, *Isoodon obesulus*. These descriptions have been based on examination of embryos and pouch young specimens. The only reference to parathyroids in an adult koala is by Sonntag (1921) who concluded that some of the many glands present at the root of the neck may have been parathyroids. In pouch young parathyroid III is in the vicinity of the carotid bifurcation. Parathyroid III arises from almost the entire third pharyngeal pouch with a very small part contributing to the cervical thymus and possibly the thoracic thymus (Fraser, 1915). As mentioned above, the presence of a thoracic thymus in the koala is disputed. There have been four reported investigations of the existence of the thoracic thymus in the koala (Johnstone, 1898; Symington, 1900; Fraser, 1915; Yadav, 1973). A thoracic thymus was identified in three of the total fifteen dissections described by the four authors. A thoracic thymus was not found in the koalas dissected by Symington (1900) (one specimen, 30cm in length) and Johnstone (1898) (two specimens, 20cm in length). Fraser (1915) found this structure in only one of ten uterine and pouch young specimens. However, Yadav (1973) identified this structure in two koalas (animals were either pouch young or juveniles). Even in the wombat, although researchers have indicated the thoracic thymus is usually absent, its presence has been recorded in three out of sixteen animals examined. Symington (1898) found a thoracic thymus in one of three adult wombats and Yadav (1973) found very small examples in two of eight pouch young or juvenile animals but only cervical thymuses were present in five embryos examined by Fraser (1915).

Parathyroid IV may or may not be present in the koala. It is derived from practically all the fourth pharyngeal pouch but its development may cease in the embryo. Its presence was verified on one or both sides in four out of nine embryonic and pouch young specimens (Fraser, 1915). The position of parathyroid IV was variable, from just caudal to parathyroid III to just cephalic of the pericardium near the origin of the left common carotid. Two specimens revealed parathyroid IV near the thyroid. This position was influenced by the retention of a connecting stalk between the developing parathyroid IV and the ultimobranchial body which in its migration to the thyroid dragged the parathyroid with it (Fraser, 1915). Thymus IV does not occur.

Information on the parathyroids in the wombat, *V. ursinus*, comes from only one study, also made by Fraser (1915). The derivation and location of parathyroid III were found to be similar to those in the koala. In two embryos the fourth pharyngeal pouch completely degenerated without giving rise to parathyroid IV or thymus IV. In the other three embryos, glands which were probably parathyroid IV were found in the lower neck caudal to the thyroids. There was no evidence of thymic tissue arising from the fourth pharyngeal pouch.

The embryological development of the third and fourth pouches in the bandicoot is similar to that in *T. vulpecula* (Fraser, 1915). Parathyroid III migrates to the carotid bifurcation, and a thoracic thymus results from thymus III and IV. The derivation and final position of

parathyroid IV are not always clear. Of the six specimens (three *P. nasuta* and three *I. obesulus*) examined, four had parathyroid IV on each side, one had a gland on one side only, and no parathyroid could be detected in the other animal. The position of parathyroid IV varied from near the origins of the common carotids to regions adjacent to the thymus (Fraser, 1915).

Other references to marsupial parathyroid glands are rather superficial and lack conviction in the true identification of the parathyroids. Zuckerkandl (1902) was the first to describe the parathyroids in marsupials. In *Didelphis azura* he described parathyroid III as a large lobulated structure, measuring 15.5 x 7 x 5 mm, pierced by the internal carotid artery. Parathyroid IV was found in the dorsal parts of the thyroid lobes (Zuckerkandl, 1902). These dimensions are the largest recorded for any mammal and perhaps should be viewed with suspicion. In the adult possum, *T. vulpecula*, the largest reported size of the parathyroid is 2.5 x1.5 mm (Fraser and Hill, 1915; Adams, 1955). From the size, locations and histological descriptions given for *D. azure*, later researchers (Fraser and Hill, 1915; Adams, 1955) have questioned the true identity of the "epithelial bodies" given by Zuckerkandl in 1902. Furthermore, in no other marsupial has the parathyroid been found associated with the thyroid (Roth and Schiller, 1976).

In a comparative study of the thyroid and parathyroids in 37 different species of mammals, Forsyth (1908) examined *Petaurus breviceps* and *T. vulpecula*.. His descriptions for both species were very inadequate. In the former species, a parathyroid was not found; in the latter species a structure located near an 'accessory thyroid gland' was identified as the parathyroid. A similar lack of accurate information is contained in the descriptions by MacKenzie and Owen (1919) on the Tasmanian devil, wombat, koala, kangaroo and possum.

2.4.3. Anatomy and Embryology of the Monotreme Parathyroid

The knowledge of the embryology and anatomy of the monotreme parathyroids comes from only two sources. Maurer (1899) thoroughly described the embryology of the parathyroid glands and other pharyngeal derivatives in the echidna, *Tachyglossus aculeatus*, (*Echidna hystrix*) and the location of many of these pharyngeal derivatives in the adult (Fig. 2.3). The third pharyngeal pouch gives rise to parathyroid III and thymus III, while the two recesses of the fourth pouch give rise to parathyroid IV and the ultimobranchial body. The fourth pouch does not contribute to the thymus. Both pairs of parathyroids and the thymus associate themselves with the caudally migrating thyroid to form a complex of organs in the thoracic cavity (Fig. 2.3). In the adult this fatty conglomerate of tissue spreads over a diffuse area which includes the trachea, the aortic arch and its branches. The parathyroids were not located in the mature animal (Maurer, 1899). In contrast to the situation in marsupials and eutherian mammals, the ultimobranchial body does not become integrated

into the thyroid. Instead, it remains as a discrete body lateral to the first or second cartilaginous ring of the trachea (Maurer, 1899).

Very little is known about the parathyroids in the platypus, *Ornithorhynchus anatinus*. MacKenzie and Owen (1919) identified a pair of endocrine glands near the commencement of the trachea as parathyroids. Histologically they showed "typical parathyroid gland structure". However, from the size, 3 x 2 mm, and location, these structures would better fit the description of ultimobranchial bodies given by Maurer (1899) in the echidna. Adjacent to each side of the thoracic thymus, MacKenzie and Owen (1919) identified a ductless gland, 10 x 7.5 x 0.25 mm with a tubular arrangement of cuboidal to columnar secretory cells. This structure was named "parathymus gland".

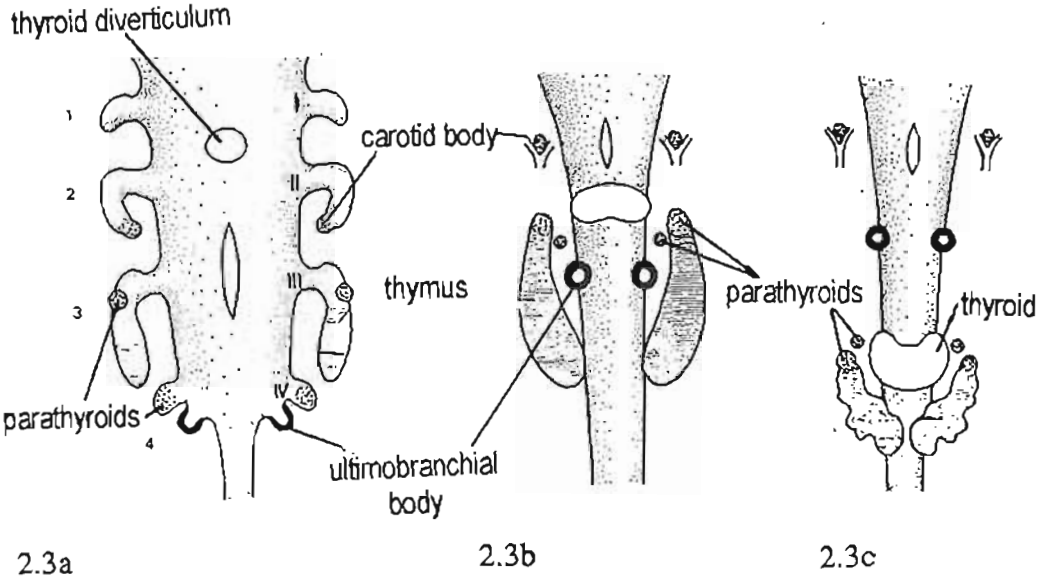

Fig. 2.3. A diagrammatic representation of the development of the derivatives of the pharyngeal pouches in *Tachyglossus*. (After Maurer, 1899). Figs. 2.3a & 2.3b show early stages in embryological development. Fig. 2.3c shows the pharyngeal derivatives in a 12cm pouch young.

2.5.1. Light Microscopy

Histological studies of the parathyroid glands from a wide variety of animals reveal similar morphology (Roth and Schiller, 1976). The histology of parathyroid III and parathyroid IV is identical. In humans, each gland in the young adult is surrounded by a thin capsule from which narrow irregular septa penetrate the underlying parenchymal cells. Reticular fibres, arising from the septa, support the clumps and strands of secretory cells and the rich capillary network. Varying numbers of fat cells also occur in the stroma (Roth, 1979). The most common parenchymal cell is the chief or principal cell. The diameter of this round to polygonal cell is 8 to 15 μm and there is a central moderately hyperchromatic nucleus. Principal cells are small compared with those of other endocrine glands, for example, those of the anterior pituitary and pancreas (Gilmour, 1939). In resin sections of well fixed tissue, principal cells can be divided into several categories which correlate with ultrastructural stages of the secretory cell cycle (DeLellis, 1993). The secretory cycle of each cell is independent of adjacent cells (Roth, 1979). In routine paraffin sections stained with haematoxylin and eosin the cytoplasm of the principal cells has an even, pale acidophilic appearance. The secretory granules in the principal cells have been demonstrated with chrome-alum haematoxylin, iron haematoxylin and argyrophilic techniques (Munger and Roth, 1963; Frigerio et al., 1982).

Before the advent of electron microscopy, several different classifications of parenchymal cells were made (Morgan, 1936; Gilmore, 1939). Several types of principal and oxyphil cells were described and classifications appear to have been influenced by the quality and type of fixation. Many criteria used to classify cells in these two detailed and thorough descriptions are now considered outmoded or unimportant.

In addition to principal cells another parenchymal cell type found in some parathyroid glands is the oxyphil or oncocytic cell. Although oxyphil cells were first noticed by Sandström (1880), they were described and named by Welsh (1898). Oxyphil cells occur usually in clumps in the parathyroid glands of older individuals in many species (Roth and Schiller, 1976). Fat cells are not present in these clumps (Christie, 1967). Compared with principal cells, oxyphil cells are slightly larger, have a smaller, more condensed nucleus and an intense acidophilic cytoplasm with a fine granular appearance. Histochemical studies have demonstrated high levels of activity for various enzymes associated with tricarboxylic acid cycle, fatty acid oxidation, glucose metabolism and electron transport system (i.e. mitochondrial enzymes) (Tremblay and Pearse, 1959; Tremblay and Cartier, 1961). Oxyphil cells are thought to be derived from principal cells and the presence of cells with a morphology intermediate between principal and oxyphil cells supports this hypothesis (Morgan, 1936; Roth and Schiller, 1976; Nilsson, 1977).

The third cell type, seldom encountered in normal parathyroid histology, is the water-clear or wasserhelle cell (Morgan, 1936; Gilmour, 1939). In routine sections the slightly enlarged cell is filled with vacuoles giving a clear appearance to the cytoplasm. Water-clear cells have been described in the hyperplastic parathyroid and curiously in normal golden hamsters (Emura et al., 1991). The light microscopic appearance of these cells is best shown in thin resin sections stained with toluidine blue (DeLellis, 1993). These sections reveal distinct outlines to the water-clear cells and often eccentric, hyperchromatic nuclei (DeLellis, 1993).

Although the parenchymal cells usually exhibit a typical endocrine arrangement, it is not uncommon for follicles and cysts to be present in the parathyroid glands (Gilmour, 1939; DeLellis, 1993). Appropriate definitions of these structures were given by Gilmour (1939). A follicle (actually referred to as an alveolus in Gilmore's paper) was defined as a spherical structure with a luminal diameter less than 40μm and consisting of a single layer of cells surrounding a structureless, weakly acidophilic substance. A substitution in terminology has been made because of the modern connotations of this histological term in reference to a spherical secretory unit in an exocrine gland (Cormack, 1987). Cysts were defined as large, often irregular structures occurring at the periphery of parathyroid glands; they were lined by heterogeneous cells and the cystic contents were variable in nature (Gilmour, 1939). Cysts formed from the persistence of small tubular diverticula that arose in the embryological formations of the parathyroid glands and thymus from the branchial pouches (Gilmour, 1937; 1939). Seven different types of cysts were described by Gilmour with the classifications dependent on embryological origins. The lining cells varied from squamous to ciliated columnar and mucous glands were observed opening into the cysts. Within the lumina, phagocytes, granulation tissue, giant cells, cholesterol crystals, and mucus have been identified in the acidophilic material (Morgan, 1936; Gilmour, 1939).

2.5.2. Light Microscopy of the Marsupial Parathyroid Glands

Although there are very few reports in the literature on the histology of the parathyroid glands in adult marsupials and monotremes, the limited information does indicate that the microscopic structure of these glands is similar to that found in eutherian species (Roth and Schiller, 1976). The only detailed descriptions have been given for the brushtail possum, *T. vulpecula* by Fraser and Hill (1915) and Adams (1955). In the former study, the parathyroid parenchymal cells were described as pale staining and closely packed into clumps or columns which were separated by sinusoids. Surrounding the gland was a thin connective tissue capsule from which extended a delicate reticular network that supported the glandular cells. A similar arrangement of cells was found by Adams (1955) except for the presence of a cyst or follicle in a gland taken from one of his nine animals. Aberrant thymic tissue was also observed embedded within a parathyroid gland without the apparent

intervention of a connective tissue septum. Oxyphil cells were not found in the parathyroids.

Only scant information is available on the histology of the parathyroid glands from other marsupials. Parathyroids from the opossum, *D. virginiana*, show typical endocrine morphology (Kingsbury, 1940). Other descriptions (Forsyth, 1908; Sonntag, 1921) are extremely brief, and indicate nothing peculiar about the marsupial parathyroid histology.

2.5.3. Light Microscopy of the Monotreme Parathyroid Glands

Almost no information is available on the histology of the monotreme parathyroid glands. Detailed histological descriptions were not included in the studies of the parathyroid glands that were made on the echidna by Maurer (1899) and the platypus by MacKenzie and Owen (1919). In the latter study, the parathyroids that were found at the commencement of the trachea showed typical parathyroid histology and the structure labelled 'parathymus gland' had a tubular glandular arrangement.

No reports of histological investigations of the marsupial or monotreme parathyroid have been found in the literature since 1955. Hence the results of applying ultrastructural, immunocytochemical, and *in situ* hybridization techniques to these two interesting groups of mammals are yet to be revealed.

2.6. Electron Microscopy

Electron microscopic studies of the parathyroid glands yield a similar uniformity in structural details as do light microscopic studies (Roth and Schiller, 1976). The ultrastructural appearance of the principal cell varies with its secretory cycle. Light cells are inactive principal cells and are characterized by abundant glycogen, lipid and lipofuscin granules with a small Golgi apparatus and few secretory granules. Synthesis of PTH precursors correlates with increasing amounts of RER and an enlarging Golgi complex with more and more associated vesicles and vacuoles. The presecretory stage corresponds to the dark principal cell. The cell is slightly smaller with short, irregular, cytoplasmic extensions. Glycogen and lipid inclusions have been replaced with numerous secretory vesicles at various stages of maturation and prominent polyribosomes. Since some dark principal cells contain fewer mature secretory granules than pancreatic islet cells and 'immature' granules from the Golgi apparatus are more abundant than mature granules at the periphery, it has been suggested that not all granules undergo maturation prior to secretion (MacGregor et al., 1975). Once the secretory granules have been released by exocytosis, the Golgi apparatus decreases in size, ribosomes disperse and the number of lysosomes increases together with glycogen and lipid inclusions, thus completing the secretory cycle of the cell (Munger and Roth, 1963; Roth and Raisz, 1966; Shannon and Roth, 1974). Within the parenchymal cells, degradation of some of the stored PTH is known to occur (Kemper,

1984) but the mechanisms involved are poorly understood. There appears to be a relationship between the degradation of PTH and the increased number of lysosomes and lipid inclusions that are seen when the cell converts from a secretory phase to a resting phase (Thiele, 1984). In the normal adult human parathyroid gland the ratio of resting (light) cells to active (dark) cells is 3 - 5: 1 (Roth and Munger, 1962).

Ultrastructural studies of the parathyroid glands include descriptions of a wide array of vesicles and granules (Roth and Schiller, 1976; Setoguti et al., 1995). In the rat a distinction has been made between 'immature', non-stored, secretory granules and mature, stored secretory granules and links established between extracellular calcium levels and granular types (Setoguti et al., 1995). Both types of vesicles ranged in sizes from 400 to 700nm. Type I granules, 'immature', secretory granules, are defined as vesicles with an electron dense core greater than two-thirds the diameter of the granule and type II, storage granules, have a more pronounced halo surrounding the core (core diameter is less than two-thirds the diameter of the granule). Type II granules usually have a more granular texture to the core. Type I granules emerge from the Golgi complex and release their contents by exocytosis in response to hypocalcemia. Type II storage granules remain longer in the cytoplasm and represent an emergency supply of PTH that can be released in response to extreme or rapid hypocalcemic stress. The contents of type II granules are more likely to be degraded than secreted. Degradation results in the formation of vacuolar bodies (Setoguti et al., 1995).

Contrary to ultrastructural interpretations, semi-quantitative studies of PTH mRNA in principal cells have shown that dark cells do not always represent active cells (Kendall et al., 1991). Instead, synthetically active cells with high levels of PTH mRNA are characterised by an euchromatic nucleus and abundant cytoplasm; cells with small dense nuclei and scant cytoplasm exhibit low levels of PTH mRNA (Kendall et al., 1991).

The division of parenchymal cells into light and dark cells may be partially artefactual (Setoguti, 1977) with the appearance of the cells influenced by swelling or shrinkage as a result of fixation. After fixation by perfusion with glutaraldehyde, Setoguti (1977) noticed that most principal cells had a uniform medium electron density whereas light and dark cells were more noticeable when excised tissue specimens had been immersed in fixatives.

The prominent ultrastructural feature of the oxyphil cell is the vast number of mitochondria that fill the cytoplasm almost to the exclusion of other cytoplasmic structures except glycogen (Trier, 1958). Oxyphil cells have the highest mitochondrial density of any animal cells (Christie, 1967). The large number of these organelles often results in changes to the shape of adjacent mitochondria. The mitochondrial cristae are closely packed which suggests that high oxidative phosphorylation occurs in the mitochondria (Munger and Roth, 1963; Hackenbrock, 1968). In normal physiological conditions, the synthesis and secretion

of PTH associated with oxyphil cells are negligible and PTH mRNA has been shown to be either absent or very low in these cells (Kendall et al., 1991). Apart from a very low rate of secretion of PTH, the only other function assigned to oxyphil cells in normal glands is the production of PRP (See Section 2.3, Physiology and Biochemistry, in this chapter) (Kitazawa et al., 1992). Immunocytological and *in situ* hybridization studies showed PRP and PRP mRNA were present in most oxyphil and transitional oxyphil cells whereas principal cells were only faintly positive. The production of this protein was also demonstrated to persist in oxyphil and transitional cells of parathyroid adenomas with principal cells secreting PTH and no or minimal amounts of PRP (Matsushita et al., 1992). The detection of PRP in oxyphil cells (Kitazawa et al., 1992) supports a hypothesis made nearly 30 years ago that oxyphil cells produce a hormone different from PTH (Christie, 1967). The postulation was made in an attempt to link the usual pronounced increase in oxyphil cell numbers associated with menopause and with chronic renal disease (Christie, 1967).

Water-clear cells generally have a central nucleus and the cytoplasm contains many membrane bound, electron lucent vacuoles which contain fine granular material (Sheldon, 1964). Sometimes the nucleus is located at the basal end of the cell and the vacuoles coalesce to form a single large vacuole (DeLellis, 1993). Most of the other organelles and inclusions are reduced in number and size and are located mainly at the periphery of the cell (Nilsson, 1977). The origin of the vacuoles and the nature of their contents is unknown, but the presence of ribosomes on the encasing membrane in some instances suggests that some vacuoles may arise from the accumulation of material within RER (Sheldon, 1964; Faccini, 1970; Emura et al., 1991).

2.7. Immunostaining and *In Situ* Hybridization Techniques

The location of PTH by immunostaining has been complicated by the low levels of stored PTH in the parenchymal cells and difficulties with the production of antibodies to PTH (See section 2.3 in this chapter) (DeLellis, 1993). The cellular distribution of PTH, PRP and parathyroid secretory protein-I in normal and pathological parathyroid glands has been illustrated by the use of immunostaining and *in situ* hybridization techniques. Since details of studies incorporating these techniques have been given previously in this chapter, sections 2.3 and 2.6, then only a brief summary of some applications will be included here.

Immunofluorescence staining of PTH (Hargis et al., 1964; Ali, 1980) and indirect peroxidase labelled antibody staining of PTH (Futrell et al., 1979; DeLellis, 1993; Kendall et al., 1993) have revealed an even distribution of PTH throughout the cytoplasm of the principal cells with no staining occurring in the nuclei. At the ultrastructural level, positive immunostaining for PTH has been observed in secretory granules of principal cells

(Ravazzola et al., 1978; Futrell et al., 1979; Kendall et al., 1993) with minimal activity also recorded in RER (Futrell et al., 1979; Kendall et al., 1993).

In situ hybridization techniques have demonstrated that correlations between cellular appearance and PTH synthesis are more accurate if the nuclear appearance, i.e. euchromatic or heterochromatic, rather than the appearance of the cytoplasm, i.e. dark or light, is evaluated (Kendall et al., 1991; Kendall et al., 1993). Synthesis of PTH is gauged more accurately by using *in situ* hybridisation techniques rather than by immunocytochemistry (DeLellis, 1993). The secretory products of oxyphil cells are usually produced in minute quantities and have been characterized by immunostaining and *in situ* hybridization techniques where PRP and PRP mRNA have been detected in these cells (Kendall et al., 1991; Kitazawa et al., 1992; Kendall et al., 1993).

In addition to the immunocytochemical studies of PTH, PRP, and parathyroid secretory protein-I, the profile of intermediate filaments for the parathyroid parenchymal cells has been described using immunocytochemistry (Miettinen et al., 1985). Principal, oxyphil, and water-clear cells all contained keratins 8, 18, and 19 that are characteristic of many types of epithelium except epidermis and some stratified epithelia (Cooper et al., 1985). Neurofilaments (200-K subunit protein) were detected in some keratin-containing parathyroid adenoma cells (Miettinen et al., 1985). This phenomenon has also been noticed in certain other adenomas and carcinomas, including pancreatic islet cell tumours and bronchial carcinoid tumours. The significance of the additional intermediate filaments in the tumour cells is unknown (Miettinen et al., 1985).

2.8. Effects of Certain Physiological Conditions and Age on Parathyroid Gland Morphology

In pathological conditions, including parathyroid tumours and hypo- and hyper-parathyroidism, the parathyroid shows many histological changes (Nilsson, 1977; DeLellis, 1993). The presence of oxyphil and water-clear cells in some of these pathological conditions has already been mentioned in section 2.5.1. Histological variations, usually subtle, have also been observed in the parathyroid glands associated with the changing demands for calcium in various physiological conditions such as growth, pregnancy, lactation and hibernation. However, the most noticeable normal changes that occur in the histology of the parathyroid glands are those related to age.

Correlative ultrastructural and histochemical studies have been made on the parathyroid glands of pregnant and lactating cows (Capen et al., 1965) and pregnant and puerperal mice (Yamahira et al., 1980). In the non-pregnant and non-lactating bovine parathyroid glands, light and intermediate principal cells are plentiful and their ultrastructure correlates with a quiescent state of protein production and secretion. This histology is in contrast to that of the parathyroid glands from cows just before and just after parturition where the glands are

dominated by dark principal cells with increased numbers of organelles and inclusions that are involved in PTH synthesis and secretion (Capen et al., 1965).

A morphometric study of the parathyroid glands from pregnant and puerperal mice (Yamahira et al., 1980) showed the volume of Golgi bodies increased and the number of storage granules decreased just prior to parturition. These ultrastructural changes were indicative of increased synthesis and secretion of PTH. However, during lactation when PTH secretion is also increased, equivocal results were obtained for the cytological profile of the principal cells, i.e. the volume of Golgi complexes and lipid droplets, and the number of storage granules fluctuated but remained higher than the control values.

Structural changes to endocrine glands including the parathyroids occur in relation to hibernation (Wang, 1982). Hypercalcemia and osteoporosis have been observed during hibernation of hamsters, squirrels and bats. The significance of the hypercalcemia is not fully understood but since dietary sources of calcium are non-existent then the calcium stores in the bones are targeted by PTH to provide the increased circulating levels of calcium. In a study of hibernating bats the histology of the parathyroids indicated increases in PTH synthesis and secretion during hibernation (Nunez et al., 1972).

The histology of the aging parathyroid gland has been most thoroughly recorded for humans where the number of stromal fat cells as well as oxyphil cells increases with advancing age. Up to adolescence few fat cells are present in the stroma of the parathyroid gland; fat content then increases until approximately 30 years where the volume of the stromal fat remains slightly less than 20% for the rest of adult life (Akerström et al., 1981; Dufour and Wilkerson, 1982). The amount of stromal fat is determined by the nutritional status and general body fat of the individual. Generally the increased stromal fat in adult parathyroid glands highlights the clustering of parenchymal cells into lobules whereas in children the glands are devoid of lobulation (Abu-Jawdeh and Roth, 1992). Earlier studies of the parathyroid that did not use morphometric techniques found that stromal fat in the older adult occupies approximately half the volume of the gland (Morgan, 1936; Gilmour, 1939). In the past emphasis has been placed on the stromal fat content in the diagnosis of parathyroid hyperplasia (DeLellis, 1993).

A widespread characteristic of the parathyroid glands from older individuals of many species of vertebrates is the large number of oxyphil cells (Roth and Schiller, 1976). Besides humans and other primates, oxyphil cells have been identified in cows, horses, dogs, bats and turtles (Roth and Schiller, 1976; Setoguti, 1977). In humans, single oxyphil cells first appear in early childhood and groups can be detected in young adults of 20 years. With advancing age, large masses become obvious (Morgan, 1936; Gilmour, 1939) with larger increases occurring in women over fifty than in men of the same age group (Christie, 1967).

Ultrastructural changes in the parathyroid gland associated with aging have been described for dogs (Setoguti, 1977). Syncytial cells between which adjacent membranes are absent, are a normal component of the parathyroid glands (Bergdahl and Boquist, 1973) and these cells become more numerous in senile dogs. Similarly follicles and oxyphil cells increase in number with age (Setoguti, 1977). Instead of colloid being present in the follicles, the lumina are filled with a heterogeneous substance which Setoguti believed is necrotic material produced by the surrounding, degenerating parenchymal cells (Setoguti, 1977). Often the mitochondria of oxyphil cells are enlarged and in the shapes of rings, bulbs, cups, or hooks with cristae running parallel to the long axis (Setoguti, 1977).

Several hypotheses have been presented in order to explain the increased numbers of oxyphil cells that occur in old age in many species. Oxyphil cells may represent a metaplastic change of principal cells where, for reasons unknown , mitochondria proliferate (Ordonez et al., 1982). However, the transformation from principal cell to oxyphil cell is apparently permanent and no reversals have been suggested in the literature. Boquist (1980) suggested that the mitochondrial proliferation which heralds the formation of oxyphil cells is triggered by annulate lamellae. Although the precise role of annulate lamellae is an enigma, many studies (Kessel, 1992) indicate this organelle has a function in regulation of gene expression where, by mechanisms unknown, the interval between transcription and translation is controlled. One of the many other postulated functions of this organelle includes the biogenesis of mitochondria (Kessel, 1992). Boquist (1980) speculated that annulate lamellae are not commonly seen in principal cells because they have a temporary existence, appearing just prior to the transition of a principal cell to an oxyphil cell when the production of mitochondria is initiated. Christie (1967) speculated that in view of oxyphil cell numbers increasing significantly in the fifth decade in humans or as a result of renal disease, then perhaps oxyphil cell hyperplasia is an attempt to readjust electrolyte equilibrium by mechanisms different from the normal production and physiological action of parathyroid hormone. The identification of PRP in oxyphil cells (Kitazawa et al., 1992) gives some credence to this suggestion. The different mechanisms may also be reflected by the unusual morphology of many mitochondria in many oxyphil cells (Setoguti, 1977). Alternatively, instead of different mechanisms being present, perhaps the mitochondria are defective and large numbers are needed to perform the same function as normal mitochondria (Tandler et al., 1970). Tremblay (1969) believed the mitochondria of aging cells retain all their enzymes (e.g. succinic dehydrogenase, ATP synthetase) but they become functionally inefficient. Although earlier studies also failed to detect a lack of any mitochondrial enzymes in oxyphil cells (Balogh and Cohen, 1961), Muller-Hocker (1992) linked functional impairment to enzyme deficiency. In histochemical studies on parathyroid glands Muller-Hocker (1992) showed a lack of cytochrome-c-oxidase in some but not all oxyphil cells. Hence it was proposed that oxyphil cells are a manifestation of cellular aging where first proliferation of mitochondria occurs, followed by the loss of cytochrome-c-

oxidase (Muller-Hocker, 1992). Another theory (Feldman et al., 1972) proposes that the increase in mitochondria is due to either an increased lifespan or decreased rate of elimination of these organelles.

Chapter 3

Materials and Methods

3.1. Animal Species and Numbers

In this study of the parathyroid glands, thirteen species were selected as representatives of eight families of Australian marsupials and monotremes. The details and number of each species used are given in Table 3.1.

Table 3.1 - List of Marsupial and Monotreme Species.

Order Marsupialia			
Common name	**Scientific name**	**Family**	**N**
fat-tailed dunnart	*Sminthopsis crassicaudata*	Dasyuridae	33
Tasmanian devil	*Sarcophilus harrisii*	Dasyuridae	1
yellow footed antechinus	*Antechinus flavipes*	Dasyuridae	2
brown antechinus	*Antechinus stuartii*	Dasyuridae	10
northern short-nosed bandicoot	*Isoodon macrourus*	Peramelidae	2
southern brown bandicoot	*Isoodon obesulus*	Peramelidae	1
brush-tail possum	*Trichosurus vulpecula*	Phalangeridae	23
western grey kangaroo (Kangaroo Island)	*Macropus fuliginosus fuliginosus*	Macropodidae	4
western grey kangaroo (Adelaide Hills)	*Macropus fuliginosus melanops*	Macropodidae	31
southern hairy-nosed wombat	*Lasiorhinus latifrons*	Vombatidae	13
koala	*Phascolarctos cinereus*	Phascolarctidae	6
Order Monotremata			
echidna	*Tachyglossus aculeatus*	Tachyglossidae	12
platypus	*Ornithorhynchus anatinus*	Ornithorhynchidae	2

3.2. Sources of Animals Used in the Study.

All animals that were used in this study were obtained with permission of the Animal Ethics Committee, University of Adelaide, and all experimental work was performed under the guidelines established by the same Committee. Most of the animals from which specimens were obtained formed part of other research projects.

The fat-tailed dunnarts came indirectly from the colony of *S. crassicaudata* maintained in the Genetics Department, University of Adelaide. These animals were used initially for studies involving sperm-egg interactions (Breed and Leigh, 1988) and immunocytochemical investigations of the pancreatic islets (Leigh and Edwin, 1991). Two yellow footed antechinuses were trapped at Inman Valley, 60Km south of Adelaide. *Antechinus stuartii* specimens came from ten fixed carcasses that were kindly supplied by Dr D.A. Taggart, Department of Anatomy, Monash University. The animals had been used previously in reproductive studies (Taggart and Temple-Smith, 1990a&b; Taggart and Temple-Smith, 1991a&b).

Specimens from the Tasmanian devil and five koalas came from autopsies performed on these animals by Dr Peter Phillips at the Institute of Medical and Veterinary Science, Adelaide. The Tasmanian devil came from the Adelaide Zoo and the koalas came from Cleland Wildlife Reserve in the Adelaide Hills.

Possums were from the Central Animal House, University of Adelaide and the bandicoots came from a colony at the Roseworthy Agricultural College, University of Adelaide. Prior to obtaining specimens from the bandicoots, they were used in reproductive research by Dr William Breed (Department of Anatomical Sciences, University of Adelaide) and Dr David Taggart (Taggart et al., 1994). Specimens from wombats were also from animals used in biological and reproductive studies (Taggart et al., 1994; 1996). Tissues from koalas came from post-mortems carried out by Dr Peter Phillips at the Institute of Medical and Veterinary Science, Adelaide. Four koalas were from the Adelaide Zoo and two were killed on the road.

Kangaroo specimens were a result of culling programs by National Parks and Wildlife Service at both Murray's Lagoon Conservation Park, Kangaroo Island and Para Wirra Recreation Park and Wildlife Reserve near Adelaide. These two locations are populated by two different subspecies of western grey kangaroos. *Macropus fuliginosus fuliginosus* is found in Kangaroo Island and *Macropus fuliginosus melanops* inhabits the Adelaide Plains and Hills.

Monotreme specimens came from animals which had been used in a variety of scientific studies. Specimens from two echidnas and the platypuses came from Dr U. Proske, Department of Physiology, Monash University, Victoria. The other echidnas were from the University of Adelaide, either from Dr N.A. Locket, Dr W.G. Breed, Department of Anatomy and Histology, or from Prof. B.P. Setchell, Department of Animal Science.

3.3. Anatomical Methods

The number of animals used in the various investigative techniques is indicated in the introduction of each appropriate chapter. Where possible, the weight and other relevant details of the animals at the time of death were recorded. The anatomical locations of the parathyroid glands in each species were determined in several ways. Either the whole dead animal was dissected or a large piece of tissue which included the ventral areas of the neck and upper thorax was removed from each animal and placed in 10% buffered formalin. Then, with the aid of a dissecting microscope, careful examination of the tissue was made and dissections were recorded either by photography or by drawings using a camera lucida attachment to the microscope. The positive identification of many structures encountered during dissection was possible only after viewing histological sections of paraffin processed blocks. Details of tissue processing and staining with haematoxylin and eosin are given in the Appendix, part A. Alternatively, the locations of the parathyroid glands were determined by examining serial sections of the reasonably intact, formalin-fixed specimens of ventral neck and thoracic tissue. The size and shape of the glands were determined either during dissection or during microscopic examination of serial sections.

3.4. Methods for Light Microscopy

Since serial sections revealed that the structure of parathyroid III and parathyroid IV was virtually identical and that a similar conclusion has been reached in previous investigations (Roth and Schiller, 1976), then parathyroid III was selected for the majority of the light and electron microscopic studies in the marsupials. In marsupials, parathyroid III appears to have a more constant location than parathyroid IV with the former gland occurring near the carotid bifurcation (Fraser and Hill, 1915; McCrady, 1941; Adams, 1955). Hence for histological studies, the carotid bifurcations and tissue within a radius of 7 to 15mm were removed from each animal and placed in 10% formalin, Bouins or electron microscopic fixative (see Appendix B). With the aid of a dissecting microscope, likely parathyroid structures were isolated and processed for paraffin (see Appendix A) or resin (see Appendix C) sections. Light microscopic studies were done on five micron paraffin sections and one micron resin sections. Resin sections were stained with toluidine blue (see Appendix E). Additional special staining techniques were used for some species. Details have been included in the appropriate chapters.

3.5. Methods for Electron Microscopy

Electron microscopic studies of the parathyroid glands were done on animals for which the period of time between death and immersion in an electron microscopic fixative was less than 20 minutes or on animals that were fixed by perfusion. In the latter situation, each animal (except kangaroos) was anaesthetised with Nembutal and the heart with its major blood vessels and lungs exposed. A small incision was made in the wall of the heart and a cannula inserted into the left ventricle, through the aortic valve and secured near the origin of the aorta. For five minutes rinse solution (Appendix, part B) was passed through the circulatory system and allowed to flow out from the severed right atrium. The fixative solution (Appendix, part B) was then perfused for the same time. Both perfusing solutions were located at a height above the animal to give approximately 140mm Hg pressure. The electron microscopic fixative contained 3% paraformaldehyde and 3% glutaraldehyde in a 0.1M phosphate buffered solution pH 7.4. Sometimes a fixative solution, containing a lower concentration (0.25%) of glutaraldehyde, was used in order to retain tissue antigenicity for immunocytochemical studies.

Structures resembling parathyroid glands were dissected out with the use of a dissecting microscope, diced if necessary into 1mm cubes and fixed for 2 - 12 hours in fresh electron microscopic fixative (see Appendix B). Specimens were washed three times for 15 minutes in each wash in 0.2M phosphate buffer pH 7.4, and post-fixed in 1% osmium tetroxide in 0.1 phosphate buffer pH 7.4 for one hour at room temperature. Specimens were again washed in phosphate buffer before being processed for electron microscopy (see Appendix C). Some samples were en bloc stained with uranyl acetate following post-fixation with osmium tetroxide. Details of en bloc staining are given in Appendix D.

Tissue was embedded in TAAB TK3 epoxy resin. Survey sections were cut on a Reichert - Jung ultramicrotome with glass knives, and stained with toluidine blue (see Appendix E). Silver-gold ultrathin sections for electron microscopy were cut with a diamond knife on the same ultramicrotome. Sections were mounted on 200 mesh copper nickel grids and stained with uranyl acetate and lead citrate (see Appendix F). Stained sections were examined at 60kV in a Jeol 100S transmission electron microscope or at 80kV in a Philips CM100.

3.6. Kangaroo Samples

3.6.1. Collection of Tissues.

Specimens from kangaroos were obtained under some difficulties in reserves at night-time. Kangaroos were shot in the head by park rangers as part of culling programs to control the number of animals within the reserves. As soon as each animal had been killed, the weight, sex and overall condition was recorded. Within minutes of death occurring, the carotid bifurcations and sometimes the thoracic thymus with adjoining

tissue were dissected out and placed in either 10% buffered formalin or electron microscopic fixative for approximately nine hours during which time the specimens were conveyed back to the laboratory. Samples were then treated by techniques described above. Three kangaroos were perfused with electron microscopic fixative in the field. Details of these procedures are given in chap., section 8.1.

3.6.2. Ageing Techniques

In addition to neck and thoracic tissue being taken from kangaroos, the mandible was removed from each animal and used for age estimations. The teeth present on the left and right sides were recorded and the jaw was lightly crushed to reveal the presence of unerupted teeth. Details are given in chap. 8, section 8.2.1.

3.7. Specimens for Immunocytochemistry

Coinciding with obtaining specimens for light and electron microscopy was the collection of suitable tissue for immunocytochemistry. Unstained paraffin sections of formalin fixed tissue were kept so that the immunostaining could be done collectively on all the different species. Specimens for electron microscopic immunostaining were fixed in an electron microscopic fixative with a low concentration of glutaraldehyde, not post-fixed with osmium tetroxide, and usually embedded in LR White resin. More detailed descriptions are given in chap. 10, Immunocytochemical Study of Marsupial and Monotreme Parathyroid Glands and the Ultimobranchial body in the Echidna.

Chapter 4.

Parathyroid Glands in Dasyurid Marsupials

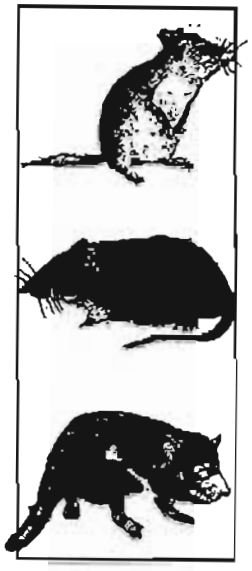

4.1. General Introduction

There are no known, previous scientific records of the parathyroid glands in dasyurid marsupials. Information on the anatomy, histology, and ultrastructure of the parathyroid glands was attained here using four dasyurid species, viz: the Tasmanian devil (*Sarcophilus harrisii*), the fat-tailed dunnart (*Sminthopsis crassicaudata*), the brown antechinus (*Antechinus stuartii*) and the yellow footed antechinus (*Antechinus flavipes*). Specimens from one Tasmanian devil, 33 dunnarts, two yellow footed and ten brown antechinuses were used in the study.

Sarcophilus harrisii is the largest of the surviving Australian carnivorous marsupials with an average adult body weight of 8kg for males and 6kg for females (Strahan, 1983), whereas *S. crassicaudata* represents one of the smallest marsupials with an average adult weight of 15g (Bennett et al., 1990). Both *Antechinus* species are also relatively small animals; average adult weights for *Antechinus stuartii* males and females are 35g and 20g respectively (Strahan, 1983). Similar data for *Antechinus flavipes* are 56g and 34g (Strahan, 1983). Both *Antechinus* species exhibit the unusual characteristic of post-mating male mortality where immediately following mating, death results from a state of chronic stress and associated impaired immunity (Barker et al., 1978).

4.1.1. Introduction - *S. crassicaudata*

For the 33 dunnarts a variety of techniques (See chap. 3, Materials and Methods) was employed to elucidate the anatomy, histology, and ultrastructure of the parathyroid glands. Serial sections of tissue from the ventral neck and upper thorax were prepared from four dunnarts; six dunnarts were dissected under a dissecting microscope and the dissections were recorded with either camera lucida drawings or photographs. The identification of structures observed during dissection was confirmed by the examination of histological sections. Samples for electron microscopy were taken from 23 dunnarts, but due to difficulties in locating and positively identifying the minute parathyroid glands with the dissecting microscope, only nine of 49 specimens processed were parathyroid glands. At least ten sections from each specimen were viewed with the electron microscope.

4.1.2. Introduction - *S. harrisii*

The female Tasmanian devil used in this study was at least nine years old and died of natural causes at the Adelaide Zoo. The previous maximum recorded age for Tasmanian devils was seven to eight years (Strahan, 1983). Since only one animal was available, investigations were limited to the anatomical and histological information derived from the examination of a superficial dissection of the excised tissue, consisting of the tongue, neck, mediastinum, heart and lungs and serial sections that were prepared from three lots of tissue. Two lots contained the carotid bifurcations and surrounding tissues and the other lot included tissue extending from the more caudal regions of the ventral neck to the base of the heart. Every tenth section was mounted, stained with haematoxylin and eosin (see Appendix A) and examined with the light microscope. If parathyroid tissue was present in consecutive sections then the other sequential paraffin sections were mounted and stained. Altmann's technique for mitochondria (see Appendix G) and staining with 0.15% toluidine blue formed part of the histological studies.

4.1.3. Introduction - *Antechinus* spp.

The two male yellow footed antechinuses were caught on August 9, 1993, at a period in the life cycle of *A. flavipes* when the males had mated, experiencing chronic stress and about to die. The imminent death of the males in the population was inferred by the fact that no animals were subsequently caught on August 20, and on September 2, 1993 only a female with pouch young was trapped; all males had vanished. The parathyroid glands in one animal were fixed by perfusion, in the other animal the glands were immersed in fixative. The perfusion, fixation and subsequent treatment of the specimens were the same as the electron microscopic techniques described for the dunnarts (See Materials and Methods, chap. 3).

The specimens from *A. stuartii* came from animals which were previously used for specific reproductive studies (Taggart and Temple-Smith, 1990a&b; Taggart and Temple-Smith, 1991a&b) before being stored for several years in 70% alcohol. Each animal had a median ventral incision extending from the sternum to the pelvis to allow fixation of the internal organs. The ten male *A. stuartii*, labelled As1 to As10, were collected at different times of the year:- As4 in late July, i.e. the mating season and a time of chronic stress; As2 and As3 in early July, just prior to the mating season; and the remaining animals were killed at various times of the year when presumably they were not stressed. Each *A. stuartii* was dissected with the aid of a dissecting microscope and structures likely to be parathyroid glands were processed for electron microscopy, not for the purpose of ultrastructural studies but because the dimensions of the specimens were too tiny for paraffin processing techniques. One dissection (As8) was photographed to illustrate the anatomy of the parathyroids.

4.2. Results

4.2.1.1. Anatomy - *S. crassicaudata*

In *S. crassicaudata* parathyroid III was located near the carotid bifurcation which is dorsolateral to the laryngopharynx (Figs. 4.1b & 4.2a). Overlying these complexes ventrally, on both sides, are the posterior belly of the digastric and the cephalic parts of the infrahyoid muscles (Fig. 4.1b) and more superficially , the sublingual and submandibular salivary glands (Figs. 4.1a & b). No cervical thymus is found in *S. crassicaudata*, but four large pigmented lymph nodes are consistently present near the salivary glands (Fig. 4.1a).

Macroscopically, the identification of the parathyroids was often hindered by the presence of small structures of similar dimensions in the vicinity of the carotid bifurcation. Hence histological examination was necessary in order to identify a structure as a parathyroid gland and not a lymph node, thymic tissue or ganglion (Figs. 4.2b, 4.2c, and 4.2d). The shape of parathyroid III was ovoid, often flattened with approximate dimensions of 1mm in length and 0.5mm in width. Parathyroid III was found either at the carotid bifurcation, often on the dorsal aspect (Fig. 4.2a) or a short distance from the bifurcation loosely associated with the common carotid artery or its two branches. The arteries that supplied blood to parathyroid III originated from either the common carotid or the external carotid near the bifurcation.

The location of parathyroid IV was sought in four animals, S5, S6, S8, and S9. It was only found by examining serial sections of the ventral neck region and mediastinum. Parathyroid IV was found in three of the four animals and in each only one parathyroid IV was identified near the midline. It was a minute structure being less than 0.5mm in diameter. In animal, S6, parathyroid IV was nestled between the aortic arch, the cephalic extent of atrial heart muscle and one of the two anterior venae cavae (Fig. 4.4b). (Two anterior venae cavae are a common feature of the marsupial cardiovascular system (Pearson, 1940). In animal S8, parathyroid IV was adjacent to thymic tissue, ventral and just cephalic to the aortic arch (Fig. 4.3) and in animal S9, parathyroid IV was ventral to the trachea, near the commencement of the brachiocephalic artery (Fig. 4.4a).

4.2.1.2. Anatomy - *S. harrisii*

In the Tasmanian devil, the locations of the two parathyroids III were determined by examining serial sections of the carotid bifurcations and the surrounding areas. The carotid arteries lay on the lateral aspects of the trachea and larynx with the bifurcations occurring at the level of the caudal end of the cornua of the thyroid cartilage.

On the left hand side, parathyroid III was located dorsomedial to the left common carotid, just caudal to the bifurcation. The size of the slightly ovoid gland was estimated to be 2 x 2.4 mm with the larger diameter parallel to the length of the carotid artery. On the right

hand side, parathyroid III was more cephalic in position, occurring just anteriorly to the bifurcation but caudal to the hypoglossal nerve. The ovoid gland measuring 3.6 x 1.5 mm was dorsomedial to the right internal carotid artery. No parathyroid IV was found in the serial sections that were cut from the tissue between the larynx, cephalically, and the atria of the heart, caudally.

4.2.1.3. Anatomy - *Antechinus* spp.

In both *Antechinus* species, the parathyroids were round to elongated ovoid structures; the longer axis was approximately 0.4mm. Antechinuses were similar to dunnarts in that the identity of the glands could be properly established only by examining resin sections stained with toluidine blue. Parathyroids were found in the vicinity of the carotid bifurcations. In *A. stuartii* the typical position of the parathyroid gland is illustrated in Figs. 4.5a and b. The parathyroid was on the dorsal side of a right-angled triangle, framed medially by the carotid artery. The glossopharyngeal nerve was the cephalic transverse boundary and the diagonally located sympathetic trunk formed the hypotenuse. The superior cervical ganglion and a small sensory ganglion relating to the vagus nerve were also associated with the nerves. The artery to the parathyroid branched from the common carotid just caudal to the bifurcation. The existence of the caudal pair of glands in *Antechinus* was not investigated because suitable specimens were unavailable.

4.2.2.1. Light microscopy - *S. crassicaudata*

In *S. crassicaudata* the histology of parathyroid III and IV was the same. The parathyroid glands were surrounded by a thin capsule with narrow connective tissue septa penetrating the mass of epithelial cells. Mast cells were quite numerous in the connective tissue (Fig. 4.6a). Parenchymal cells were compactly arranged into strands and clumps separated by capillaries (Fig 4.6a). Follicles were present in five of the twenty glands examined with the light microscope. Each follicle had a single layer of flattened cells which surrounded a homogeneous, acidophilic material (Fig. 4.6b) that was PAS positive. A patch of lymphocytes was seen in one parathyroid gland (Fig. 4.6c). It was concluded this lymphoid tissue was thymus (see section 4.3.2. Discussion).

The parathyroid parenchymal cells were all similar in appearance and could not be categorised as light or dark cells from light microscopic observation of resin sections stained with toluidine blue. Each cell had a central round nucleus with chromatin granules and a nucleolus. The cytoplasmic staining was moderately dense and occasional minute lipid inclusions or dark granules were present.

When parathyroid III was found at the carotid bifurcation between the internal and external carotid arteries, it was easily distinguished from the carotid body. The latter structure could not be identified as a separate entity with the dissecting microscope and was associated with

the outer layers of the internal and external carotid arteries at their origins from the common carotid artery. The carotid body did not have a distinct capsule like the parathyroid gland and lacked the compact arrangement of epithelial cells seen in the gland. Instead the chemoreceptor had numerous sinusoidal structures and dark staining epithelioid cells (Fig. 4.6d). Several small unmyelinated nerves were adjacent to the structure.

4.2.2.2. Light Microscopy - *S. harrisii*

The histological structure of the parathyroid gland from *S. harrisii* was also typical of a reticulate endocrine gland (Fig. 4.7). The cells were compactly arranged within the encapsulated gland and only one kind of principal cell could be identified. No follicular arrangement of cells was present. Altmann's technique applied to human and Tasmanian devil parathyroid glands showed mitochondrial rich cells were present only in the former species, sections from which were used as positive controls. Toluidine blue stain did not show mast cells in the Tasmanian devil, even though the same technique demonstrated these cells in *S. crassicaudata*.

4.2.2.3. Light Microscopy - *Antechinus* spp.

The parathyroid glands from *Antechinus* spp. showed a typical reticulate endocrine structure. In the parathyroid from *A. flavipes* fixed by perfusion, the capillaries were somewhat distended and the perivascular spaces enlarged. Connective tissue cells were sparse in the supporting mesenchymal framework of the gland; only one mast cell was identified. The parenchymal cells were generally clumped together with little or no intercellular space except for several patches where cells had a crenated outline (Fig. 4.8a). Only principal cells appeared to be present and light and dark variants could not be distinguished.

The parathyroid gland from *A. flavipes*, fixed by immersion, had a compressed arrangement of its parenchymal and mesenchymal components. Capillaries were accentuated by the dark staining of their red blood cells, no perivascular spaces were obvious, and minimal intercellular spaces were seen between parenchymal cells. Small dark staining cells, identified as lymphocytes, were abundant in the connective tissue (Fig. 4.8b). They appeared not to be forming a discrete nodular structure reminiscent of the thymic tissue observed in *S. crassicaudata* (Fig. 4.6c). The staining densities of the parenchymal cells varied slightly but it was difficult to categorise most principal cells as light or dark cells.

Inadequate fixation of the parathyroid glands from *A. stuartii* resulted in poor morphological detail. In resin sections parenchymal cells had numerous small granules stained with toluidine blue in mainly unstained cytoplasm. Connective tissue was minimal (Fig. 4.8c).

4.2.3.1. Electron Microscopy - *S. crassicaudata*

The study of the ultrastructure of the parathyroid glands in *S. crassicaudata* revealed a compact arrangement of parenchymal cells with little intercellular space. Cells were often slightly elongated and had irregular outlines and numerous short processes interdigitating with adjacent cells (Figs. 4.9a & b). Each cell had one nucleus with a typical appearance of a nucleolus and peripheral heterochromatin. Amounts of heterochromatin varied from cell to cell (Figs. 4.9b & 4.11b). Desmosomes were quite numerous (Fig. 4.10a) and along straight lengths of opposing cell membranes gap junctions were present. All parathyroid glands used in this study, regardless of fixation techniques, had light and dark cells as well as many cells of intermediate density (Figs. 4.9a & b). For example, the parathyroid featured in Figure 4.9a was fixed by perfusion whereas the parathyroid shown in Figure 4.9b was immersed in fixative. Compared with light cells, dark cells contained less glycogen, had a more compact arrangement of cytoplasmic contents and a more electron dense appearance to the fine granular texture of the cytoplasmic matrix. Ribosomes were more often free in light cells whereas RER was more obvious in dark cells. The lumina of the RER and the nuclear envelope in the latter cells were usually more dilated than in light cells (Fig. 4.9b).

Lipid inclusions were occasionally seen in the chief cells (Fig. 4.10b); lysosome-derived inclusions with heterogeneous contents were sparse. The Golgi complex was generally inconspicuous in all the subclasses of chief cells that were viewed in this study and its structure (Fig. 4.11a) was unremarkable. Mitochondria were quite sparse in light, dark, and intermediate cells. They were often elongated, sometimes U-shaped and had a matrix that was more electron dense than the cytoplasmic matrix (Fig. 4.11b). No oxyphil cell with the characteristic high density of mitochondria was observed.

There were two types of unit-membrane-bounded vesicles in the chief cells. One contained electron dense, homogeneous material; the other had a granular texture (Fig. 4.10b). The estimated diameter of the former was 280nm whereas that of the latter was 190nm. From this study it could not be established if the vesicles represented different stages in maturation of secretory vesicles, or if some were lysosomes. Similarly, no correlations could be made between cell type and vesicle numbers. In different specimens and in different areas of the same section, the number of vesicles in light, dark, and intermediate cells showed no definite trend. Many cells had a paucity of granules while others had many and showed a peripheral concentration of granules.

4.2.3.2. Electron Microscopy - *Antechinus* spp.

Ultrastructural studies were only possible on parathyroids from *A. flavipes*; specimens from *A. stuartii* had poorly preserved morphological details. The structure of the gland was generally similar to that in *S. crassicaudata*. Both the immersed and the perfused glands

showed cells with differing densities (Figs. 4.12a & b). Very pale cells had sparsely scattered organelles and inclusions set in an electron lucent matrix with finely dispersed granular and fibrillar material (Figs 4.12 &4.13). Cells with a denser matrix were similar to many principal cells described in *S. crassicaudata.*

In animal Af1, fixed by perfusion the perivascular space appeared to be artefactually enlarged (Fig. 4.12a). Apart from pericytes (Fig. 4.12a) few cells were present in tissue accompanying the capillaries but interspersed among the principal cells were dark staining cells that appeared to be leukocytes (Figs. 4.13a & b). Cells identified as lymphocytes had a single, reasonably electron-dense nucleus, abundant ribosomes and few or no granules (Figs 4.12b & 4.13a) whereas cells identified as neutrophils had very irregular outlines, nuclei that were often hyperchromatic and lobulated, and a variety of cytoplasmic granules (Fig. 4. 12b & 4.13b). In many leukocytes the perinuclear space was enlarged and many profiles of the endoplasmic reticulum appeared to be dilated. Mitochondria and secretory granules had normal appearances but the plasmalemma was very tortuous with short cytoplasmic processes covering the surface of the cell (Figs. 4.13a & b).

4.3 Discussion

4.3.1.1. Anatomy - *S. crassicaudata*

From the anatomical study, it appears that in *S. crassicaudata* there are usually three parathyroid glands. The location of parathyroid III is similar to the position previously described for this gland in other marsupials (Fraser, 1915; Fraser and Hill, 1915; McCrady, 1938; Kingsbury, 1940; Adams, 1955). Parathyroid IV is a minute structure and seems to be present in most specimens of *S. crassicaudata* as a single structure in the connective tissue of the mediastinum. The occurrence of parathyroid IV in other polyprotodont marsupials is unclear. It has been detected in immature opossums, *D. virginiana*, (Kingsbury, 1940) but McCrady (1941) found no trace of parathyroid IV in adults of the same species. The other polyprotodont marsupial for which relevant information is available is the bandicoot and parathyroid IV has only been described in embryos and pouch young (Fraser, 1915). The presence of a single parathyroid IV, near the midline, in *S. crassicaudata* is unusual. Perhaps during embryological development, the fate of the bilateral parathyroid IV anlage is similar to that of thymic tissue. In polyprotodonts thoracic thymic tissue is derived bilaterally from the third and fourth branchial pouches and migrates caudally with left and right derivatives often merging together to form a single thoracic thymus (Fraser, 1915).

4.3.1.2. Anatomy - *S. harrisii* and *Antechinus* spp.

Since only one specimen of *S. harrisii* was examined in the current study it is not possible to generalise that this anatomy is typical of the species. However the presence of only

bilaterally located parathyroid III and not parathyroid IV is similar to the location of parathyroid glands in other adult polyprotodonts (Fraser, 1915; McCrady, 1941).

The location of parathyroid glands in *Antechinus* spp. was also similar to parathyroid anatomy of other polyprotodonts.

4.3.2. Light Microscopy

Histological studies of the parathyroid glands of *S. crassicaudata*, *S. harrisii*, and *Antechinus* spp. demonstrated similarities to the microscopic structure of these glands in eutherians (Roth and Schiller, 1976) and other marsupials. The typical reticulate endocrine morphology described in this study has also been shown to exist in parathyroid glands from *D. virginiana* (Kingsbury, 1940) and from *T. vulpecula* (Fraser and Hill, 1915; Adams, 1955). Similarly, the lack of fat in the connective tissue septa corresponds to other descriptions of the marsupial parathyroid glands given by the above authors.

With the light microscope principal cells in both paraffin and resin sections generally could not be classified as light or dark variants and the mode of fixation by immersion or perfusion appeared not to influence the staining intensity of the principal cells. This issue is addressed more fully in the discussion of ultrastructure, section 4.3.3.

4.3.2.1. Light Microscopy - *S. crassicaudata*

The occurrence of follicles and cyst-like structures seems to be quite common in *S. crassicaudata*. Small cysts or follicles were found in 20% of the glands examined with the light microscope compared with only one gland from nine possums studied by Adams (1955). Cysts and follicles in parathyroid glands are discussed in more detail in chap 11, General Discussion, section 11.3.

Compared with the other dasyurid species examined in this current study, the number of mast cells in the capsule and septa of the parathyroid glands in *S. crassicaudata* was an unusual feature (Fig. 4.6a). Similar cells were extremely common in the adjacent cervical lymph nodes (Haynes, 1991). Like *Didelphis azarae* (de Campos Soares et al., 1987), *Sminthopsis* has comparatively high levels of histamine in various tissues (Haynes, 1991). Since histamine has been shown to affect the secretion of PTH from principal cells (Kemper, 1984) then maybe the numerous mast cells that occur in *S. crassicaudata* reflect a greater importance between histamine and PTH release in this animal.

From the extrapolation of data available on other marsupials and eutherians it was assumed that the round patch of lymphoid tissue observed in one parathyroid gland (Fig. 4.6c) was thymic tissue even though no Hassall's corpuscles were present . It is quite common for thymic tissue to be present in parathyroid glands of many eutherian species (Roth and

Schiller, 1976) and the possum, *T. vulpecula* (Adams, 1955). Thymus and parathyroid III develop from the third branchial pouch and abnormal cleavage and migration of the anlagen may result in aberrant thymic tissue within parathyroid III (Yadav, 1973; Roth and Schiller, 1976).

4.3.2.2. Light Microscopy - *S. harrisii*

For histological descriptions of the parathyroid gland in *S. harrisii* only formalin fixed, paraffin embedded tissue was available and so a special light microscopic technique, i.e. Altmann's stain for mitochondria, was used instead of electron microscopy to detect oxyphil cells. Oxyphil cells are known to accumulate in older individuals of some species (Roth and Schiller, 1976) and since the Tasmanian devil used was old (nine years), then it was not unreasonable to expect oxyphil cells to be present if they were typical of the parathyroids of older individuals in this species. It was concluded that oxyphil cells do not occur in *S. harrisii* but these generalisations are based on observations of only one individual.

Compared with *S. crassicaudata*, mast cells were quite sparse in the parathyroid gland of *S. harrisii*. and did not display the staining properties of mast cells in the former species.

4.3.2.3. Light Microscopy - *Antechinus* spp.

The light microscopic structure of the parathyroid glands of *A. flavipes* and *A. stuartii* showed features typical of parathyroids from many animals (Roth and Schiller, 1976). Glandular structure was more similar to that in *S. harrisii* than that in *S. crassicaudata*. For example, follicles, cysts, thymic tissue and numerous mast cells were all absent in parathyroids of *Antechinus* (Figs. 4.8a, b, & c) and *S. harrisii* (Fig. 4.7) but present in *S. crassicaudata* (Figs. 4.6a, b, & c).

4.3.3.1. Electron Microscopy - *S. crassicaudata*

In specimens either immersed or perfused with fixative, principal cells could be placed in three categories, viz: light, dark and intermediate, and the proportion of cells in each classification appeared to be independent of the fixation technique. This lack of correlation observed between cytoplasmic densities of the principal cells and modes of fixation supports a morphometric study by Wild (1980). However other studies have suggested that light and dark variants are a result of fixation artefacts and that after fixation by perfusion, differences in cytoplasmic densities disappear (Setoguti, 1977). The effect of fixation on the ultrastructural appearance of the parathyroid gland is discussed in chap. 11, General Discussion, section 11.4.

Light and dark cells have also been considered to represent different stages in the secretory cycle of principal cells (See chap. 2, Literature Review, section 2.6). Light cells represent inactive cells and dark, active. In the current study evidence to support this suggestion was

seen in the greater amount of glycogen and free ribosomes in light cells and the more obvious RER with dilated lumina in dark cells. Widespread RER and RER with dilated lumina have been interpreted as indicating sites of active translation and initial storage of newly formed protein (Cohn and Elting, 1983; Kendall et al., 1993). The apparent equal distribution of secretory and other vesicles in the light and dark variants of the principal cells has also been noticed previously (MacGregor et al., 1975) and supports their findings that no correlations exist between cell type and the number of granules.

The ultrastructure of the parathyroid glands in *S. crassicaudata* is similar to that of other animals described elsewhere (Roth and Schiller, 1976; Wild and Setoguti, 1995). Oxyphil cells were not identified, and in many other small animals, e.g. rat (Lever, 1957), these cells have been noted to be lacking (Roth and Schiller, 1976). The two common types of vesicles viz: electron dense and the other with more granular contents, that were common in the parathyroid cells, may represent the secretory and storage granules respectively that have been described in the rat (Setoguti et al., 1995). Furthermore, perhaps some of the vacuolated structures (See Fig. 4.10b) represent degraded storage granules.

4.3.3.2. Electron Microscopy - *A. flavipes*

The ultrastructure that was described for *S. crassicaudata* above was also present in parathyroid glands in *A. flavipes*. In *A. flavipes* light and dark cells were present in tissue either perfused with or immersed in fixative and there were only minor differences between the contents of light and dark cells (Figs. 4.12a & b). Granules and vesicles similar to those found in *S. crassicaudata* were also present in *A. flavipes*. Noticeable differences between the two species were the outlines of nuclei and cells in *A. flavipes* were more irregular than *S. crassicaudata* and in the former species there were many more non-principal cells in the gland. The inclusion of the non-principal cells was thought to be related to the chronic stress of the animals at the time of death. These findings are discussed below.

4.3.4. Chronic Stress and Parathyroid Ultrastructure

The greater number of non-principal cells (Figs. 4.13a & b), i.e. leukocytes, seen in the parathyroid glands of *A. flavipes* compared with those of *S. crassicaudata* may relate to the condition of chronic stress experienced by *A. flavipes* males at the time of death. The animals were captured in early August towards the end of the mating season when the highly stressed state of the males leads to their death within a few weeks (Bradley et al., 1980). During this period neutrophilia and lymphopenia occur (Cheal et al., 1976) and the presence of neutrophils and lymphocytes in amongst the parathyroid cells may be a reflection of the altered haematological condition.

Apart from irregular nuclear and cellular outlines, the principal cells of the parathyroid glands of *A. flavipes* appeared not to be altered by chronic stress. Renal impairment and failure can result from chronic stress and often linked to renal insufficiencies is hyperparathyroidism (Malmaeus et al., 1984). Enlarged principal cells with increased Golgi complexes and abundant RER and sometimes the presence of oxyphil cells and water-clear cells are characteristic of hyperparathyroidism (Cinti and Sbarbati, 1995). Since no changes in the ultrastructure of the parathyroid principal cells were seen in the animals known to be suffering from chronic stress a suggestion is given that hyperparathyroidism caused by renal impairment was not present in the male antechinuses.

Fig. 4.1. Location of parathyroid III in *S. crassicaudata*

Fig. 4.1a. Ventral view of a superficial dissection of the neck of *S. crassicaudata*. The deeper locations of the carotid bifurcations, parathyroids III (P), and thyroid glands (T) are represented by broken lines.

D	- digastric muscle	Pe	- pectoralis major
I	- infrahyoid muscles	S	- sublingual salivary gland
L	- lymph node	SM	- submandibular sal. gland
m	- mandible	St	- sternomastoid muscle
M	- masseter	v	- transverse neck vein

Bar: 3 mm.

Fig. 4.1b. Zone diagram of section from animal S8. Shows parathyroid III (P) is medial to the carotid bifurcation (C) which is dorso-lateral to the distal pharynx (O) and larynx (L). The laryngeal cartilages have vertical lines; the ossified components have horizontal lines. Ventral to the parathyroid is the posterior belly of the digastric muscle (pm) and the infrahyoids (im). The submandibular salivary gland (S) and lymph nodes (LN) are more superficial.

b - carotid body m - muscle n - nerve

Bar: 0.5 mm.

4.1a

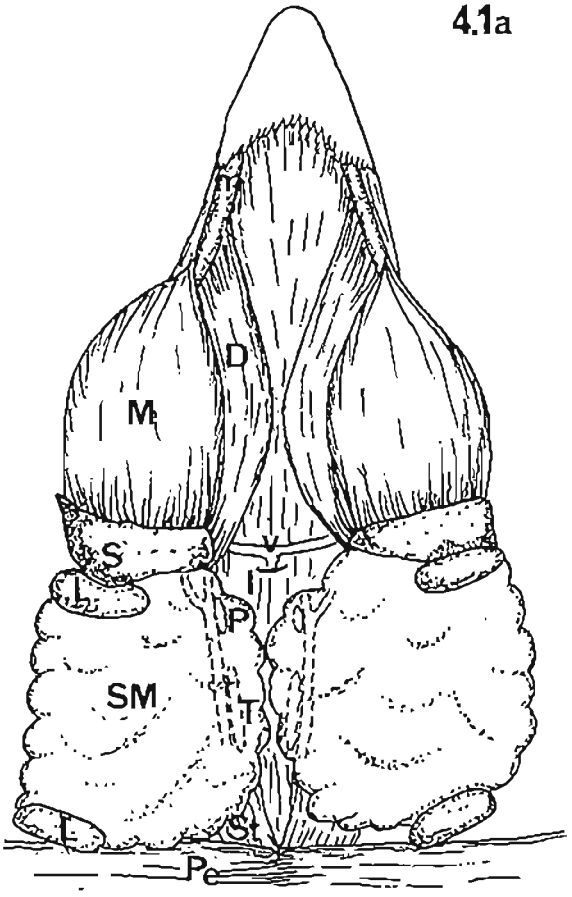
n
D
M
S
V
L
P
SM
T
L
St
Pe

4.1b

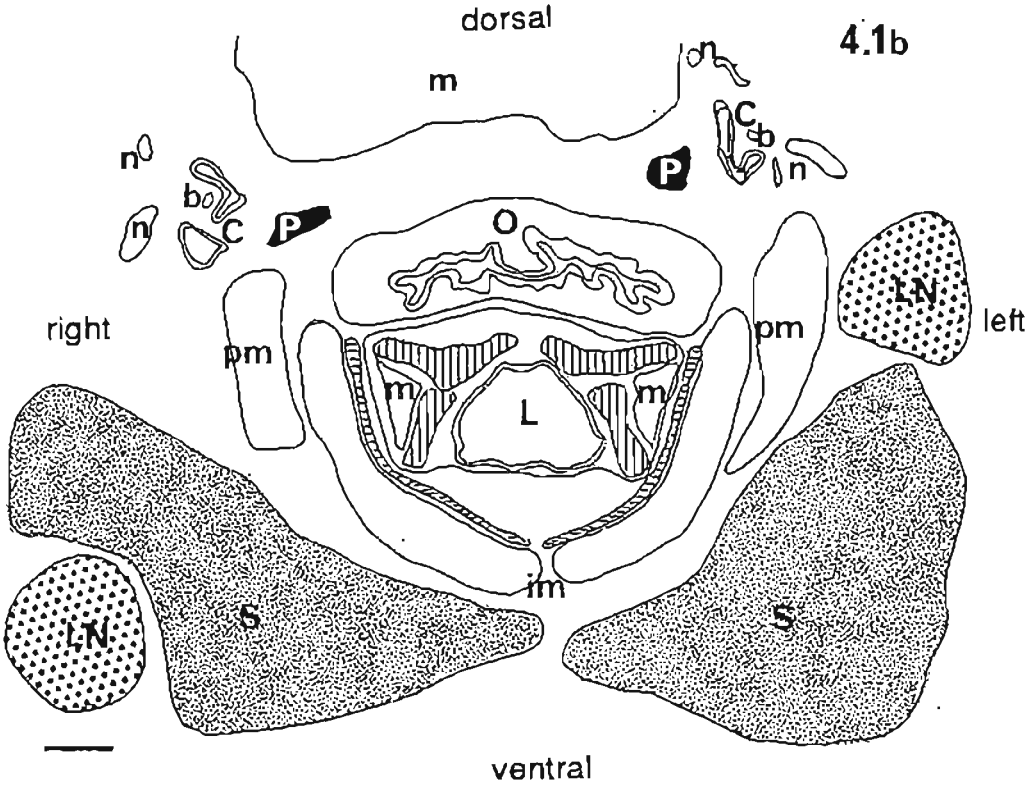
dorsal
m
n
C
b
n
n
b
C
P
P
O
LN
right
pm
pm
left
m
L
m
im
LN
S
S
ventral

Plate 4.2. Structures found near the carotid bifurcation in *S. crassicaudata*

Fig. 4.2a. Shows a ventral view of the right carotid bifurcation (B) and adjoining structures which have been teased apart from each other. The thyroid gland (T) has been separated from the superficial tissues of the trachea. The parathyroid gland (P) occurs dorsal to the bifurcation.

G - ganglion LN - lymph node NX - vagus nerve
NIX - glossopharyngeal nerve
Bar: 0.4 mm.

Figs. 4.2b, 4.2c, and 4.2d confirm the identification of the structures labelled in Figure 4.2a.

Fig. 4.2b. Plastic section, toluidine blue. Shows a parathyroid gland with a follicle (F).
Bar: 50 μm.

Fig. 4.2c. Plastic section, toluidine blue. Shows the cortical region of a lymph node.
Bar: 100 μm.

Fig. 4.2d. Plastic section, toluidine blue. Shows nerve fibres and somata in a ganglion.
Bar: 100 μm.

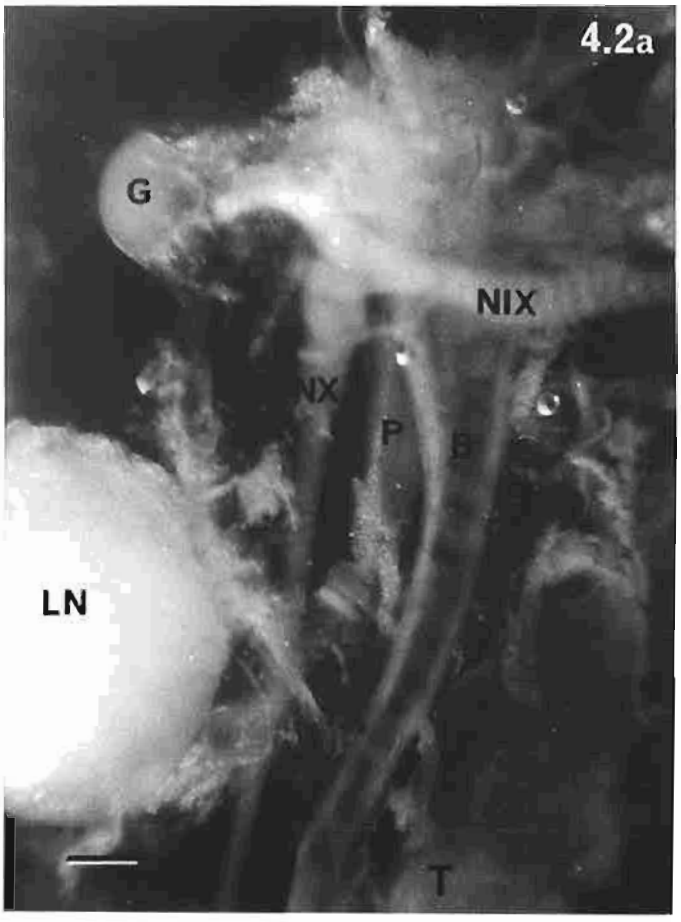
4.2a
G
NIX
NX
P
B
LN
T


4.2b
F

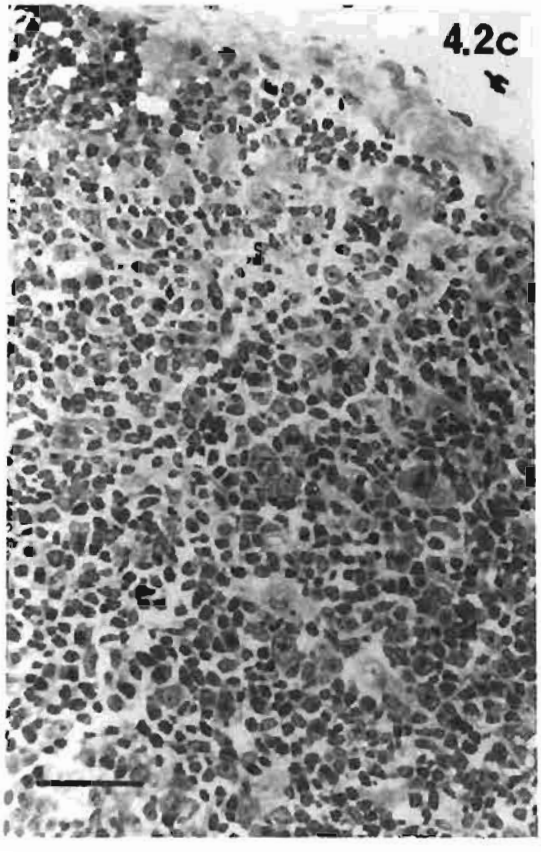
4.2c

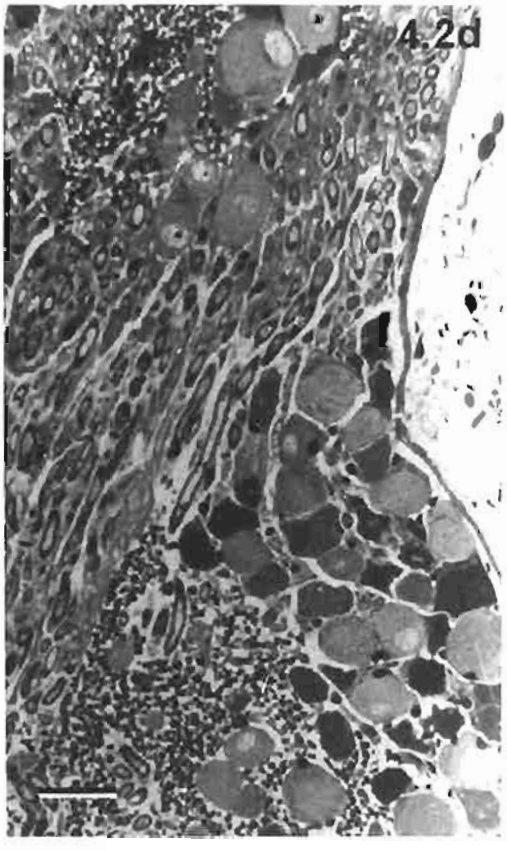
4.2d

Fig. 4.3. Drawing of a serial section showing parathyroid IV in *S. crassicaudata*

Fig. 4.3. Zone diagram of a transverse section of *S. crassicaudata*, dunnart S8, taken at the level of the origins of the right subclavian (B') and brachiocephalic (B) arteries from the aortic arch. Parathyroid IV (P) occurs between the thoracic thymus (Th) and the origins of the right subclavian and brachiocephalic arteries. The trachea and oesophagus have been distorted and displaced slightly during processing and sectioning.

LN	- lymph node	n	- nerve
M	- skeletal muscle	a	- artery
O	- oesophagus	v	- vein
T	- trachea		

Bar: 0.25 mm.

4.3

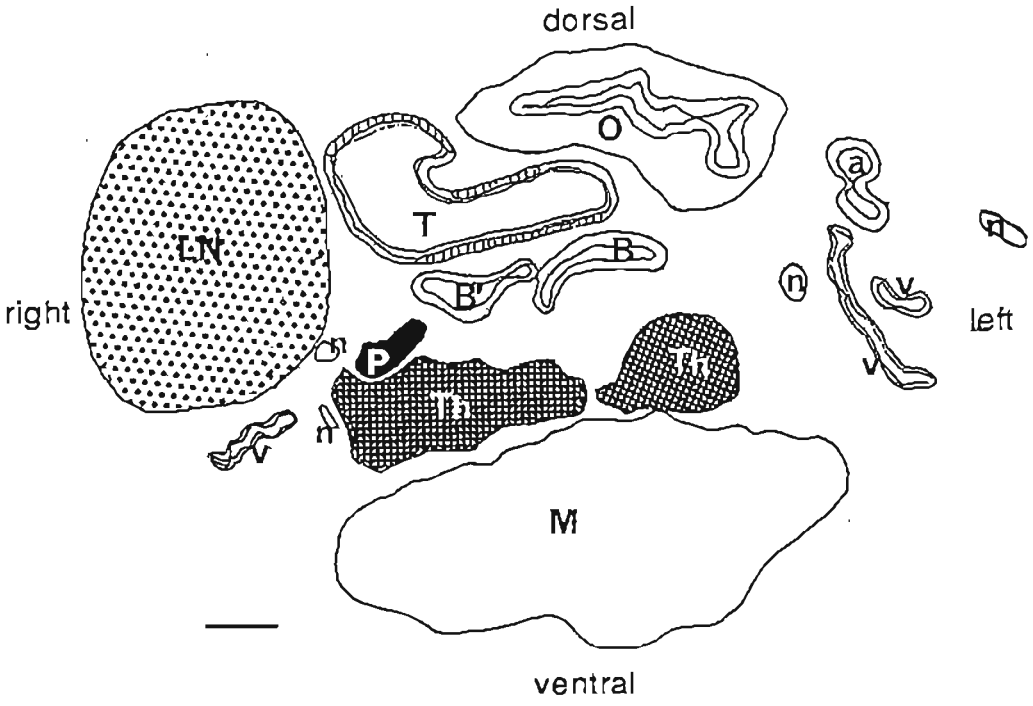

Plate 4.4. Location of parathyroid IV in *S. crassicaudata*

Fig. 4.4a. Shows the position of parathyroid IV (P) in dunnart S9. The gland is ventral to the trachea (T) and adjacent to the commencement of the brachiocephalic artery (BCA). The oesophagus (O) has been dislodged slightly to the left. (The median axis runs horizontally across the middle of the photograph; dorsal is middle left and ventral, middle right).
Paraffin section, H&E
Bar: 120 µm.

Fig. 4.4b. Shows parathyroid IV (P) in dunnart S6. The gland is between the aortic arch (AA), atrial heart muscle (At) and an anterior vena cava (CV). The oesophagus (O) has been dislodged to the left. The median axis runs from the top left corner (dorsal) to the lower right corner (ventral).
Th - thymus; T - trachea; O - oesophagus.
Paraffin section, H&E
Bar: 200 µm.

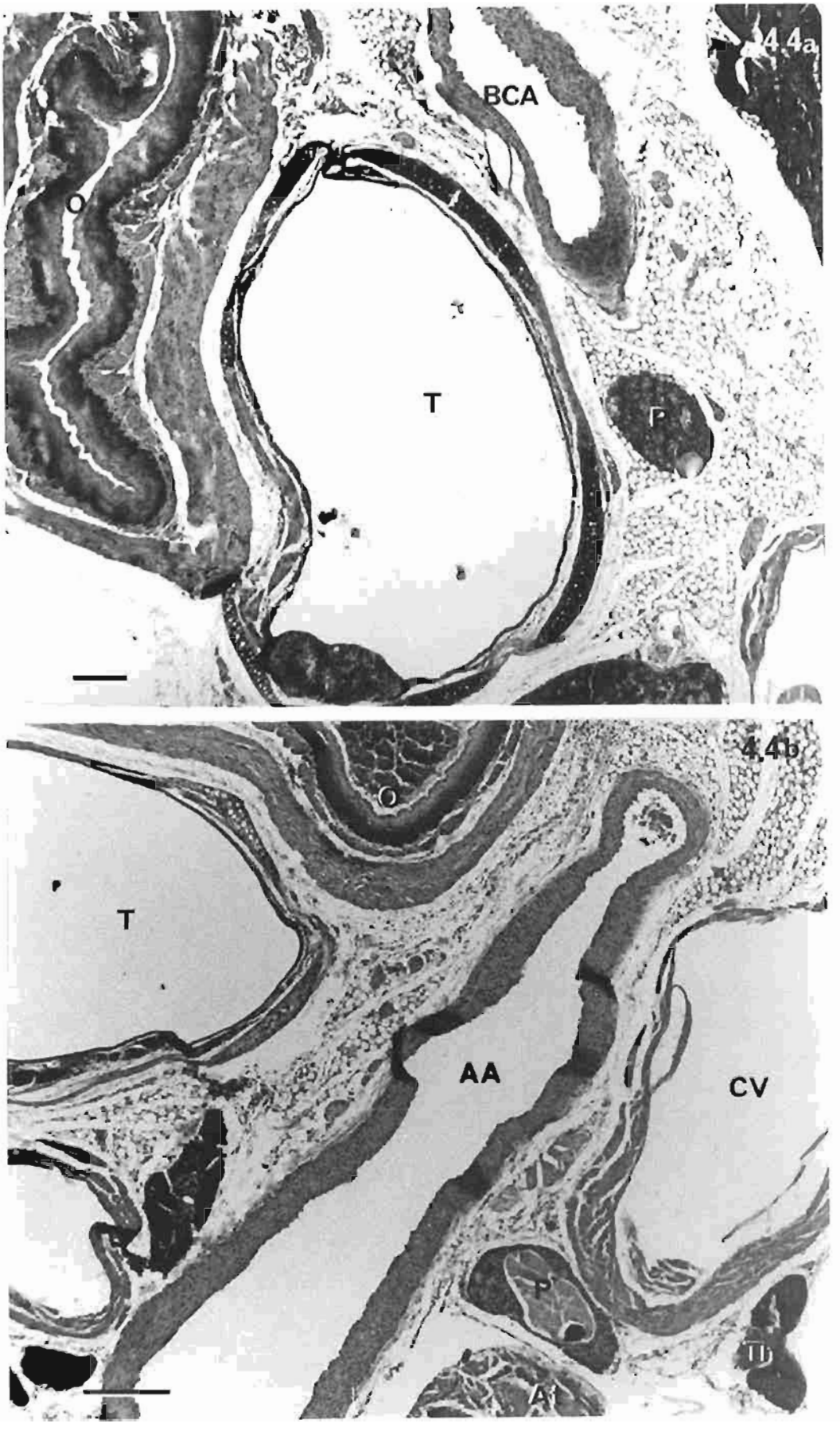
4.4a
BCA
O
T
P
4.4b
O
T
AA
CV
P
Th
Ar

Plate 4.5. Structures found near the carotid bifurcation in *A. stuartii*

Fig. 4.5a. Shows structures of the ventral neck in *A. stuartii* (As8) A right-angled triangle is formed by the laterally coursing glossopharyngeal nerve, sympathetic trunk and common carotid artery.
S - sympathetic trunk
IX - glossopharyngeal nerve
V - small ganglion associated with the vagus nerve

Bar: 0.5mm

Fig. 4.5b. Shows the dorsal view of the dissection in the above figure (Fig. 4.5a.). The parathyroid gland (P) is adjacent to the carotid bifurcation. It has been separated from fatty tissue (F) at the bifurcation. The fine artery supplying blood to the parathyroid gland can be seen branching from the common carotid, just caudal to the bifurcation.

S - sympathetic trunk
V - small ganglion associated with the vagus nerve

Bar: 0.5mm

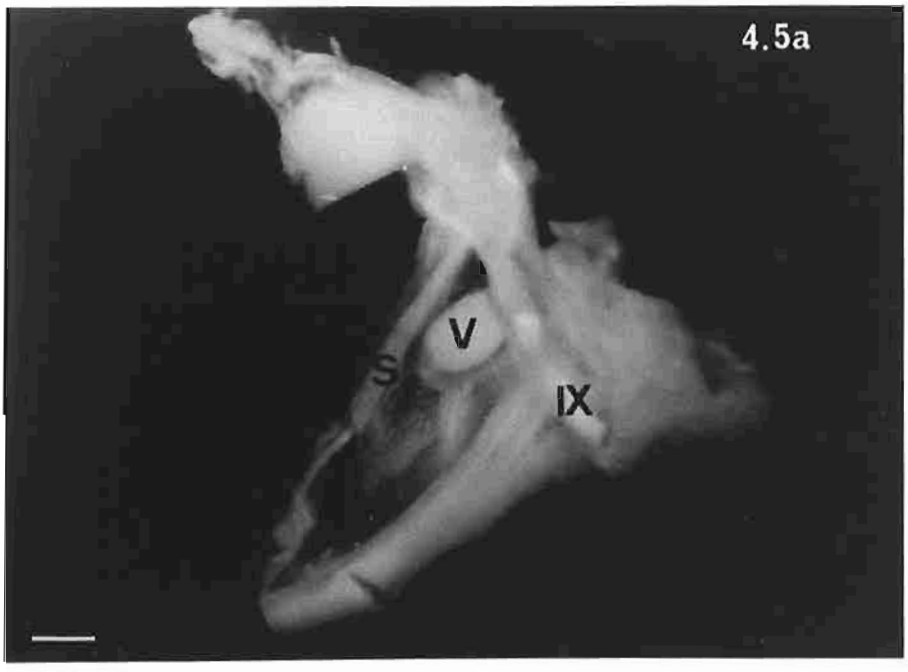
4.5a
V
S
IX

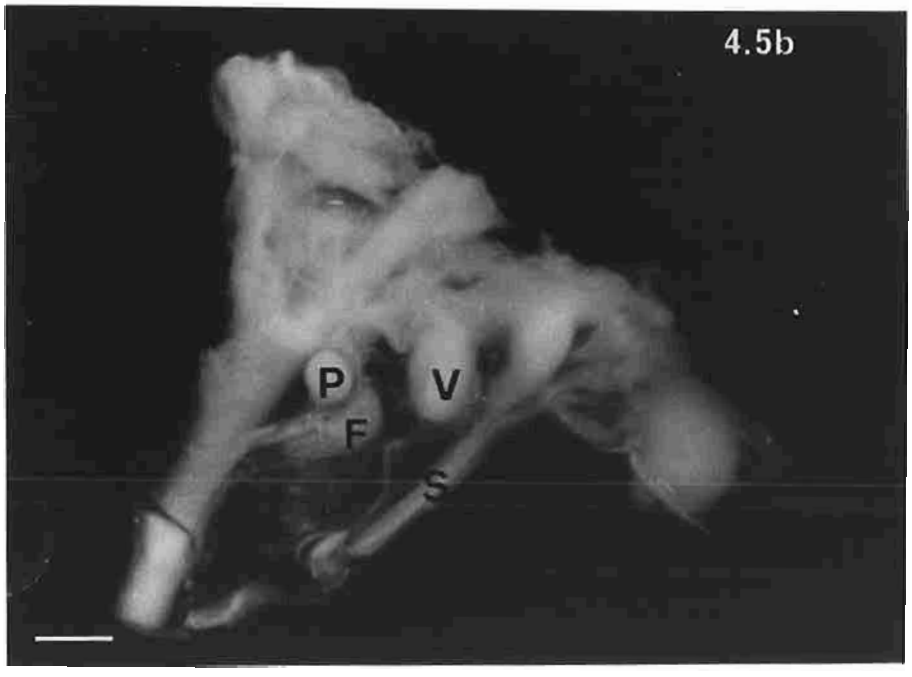
4.5b
P
V
F
S

Plate 4.6. Light microscopy of parathyroid III and carotid body in *S. crassicaudata*.

Fig. 4.6a. Shows the compact arrangement of principal cells with intervening capillaries. Several mast cells (M) are present.
Dunnart S2
Plastic section, toluidine blue.
Bar: 50 µm.

Fig. 4.6b . Shows four follicular structures in a parathyroid gland. Each follicle has pale acidophilic material surrounded by a flattened layer of cells.
Dunnart S5
Paraffin section, H&E.
Bar: 70 µm.

Fig. 4.6c . Shows lymphoid (thymic) tissue within a parathyroid gland.
Dunnart S5
Paraffin section, H&E.
Bar: 30 µm.

Fig. 4.6d . Shows a carotid body nestled between the two branches of the carotid artery just cephalic to its bifurcation.
Dunnart S5
Paraffin section, H&E.
Bar: 150 µm.


4.6a
M
M
M


4.6b

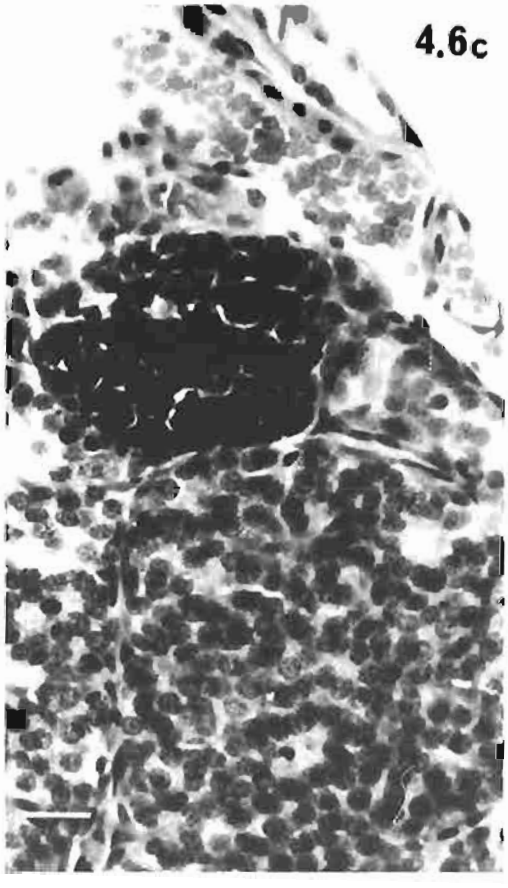
4.6c

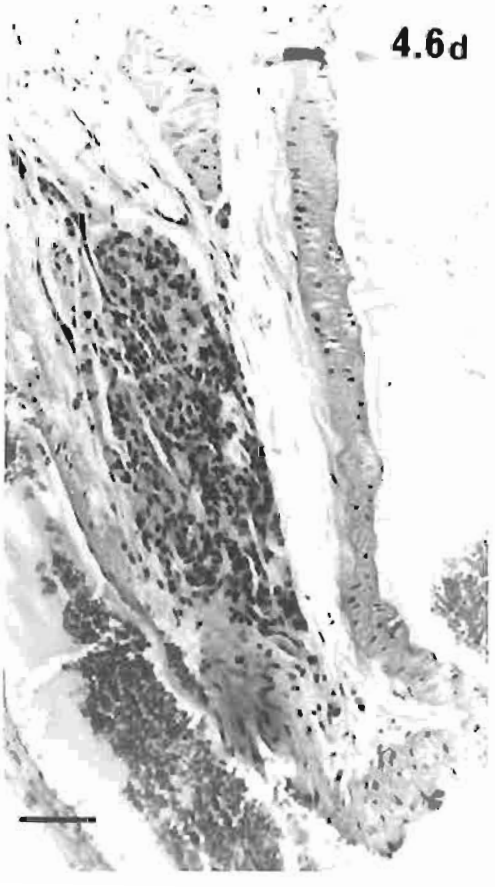
4.6d

Plate 4.7. Light microscopic structure of parathyroid gland in *S. harrisii*

Fig. 4.7 . Paraffin section, H&E. The parathyroid gland from *S. harrisii* has a typical reticulate endocrine structure. Only one kind of principal cell is present.
Paraffin section, H&E.
Bar: 30 μm.

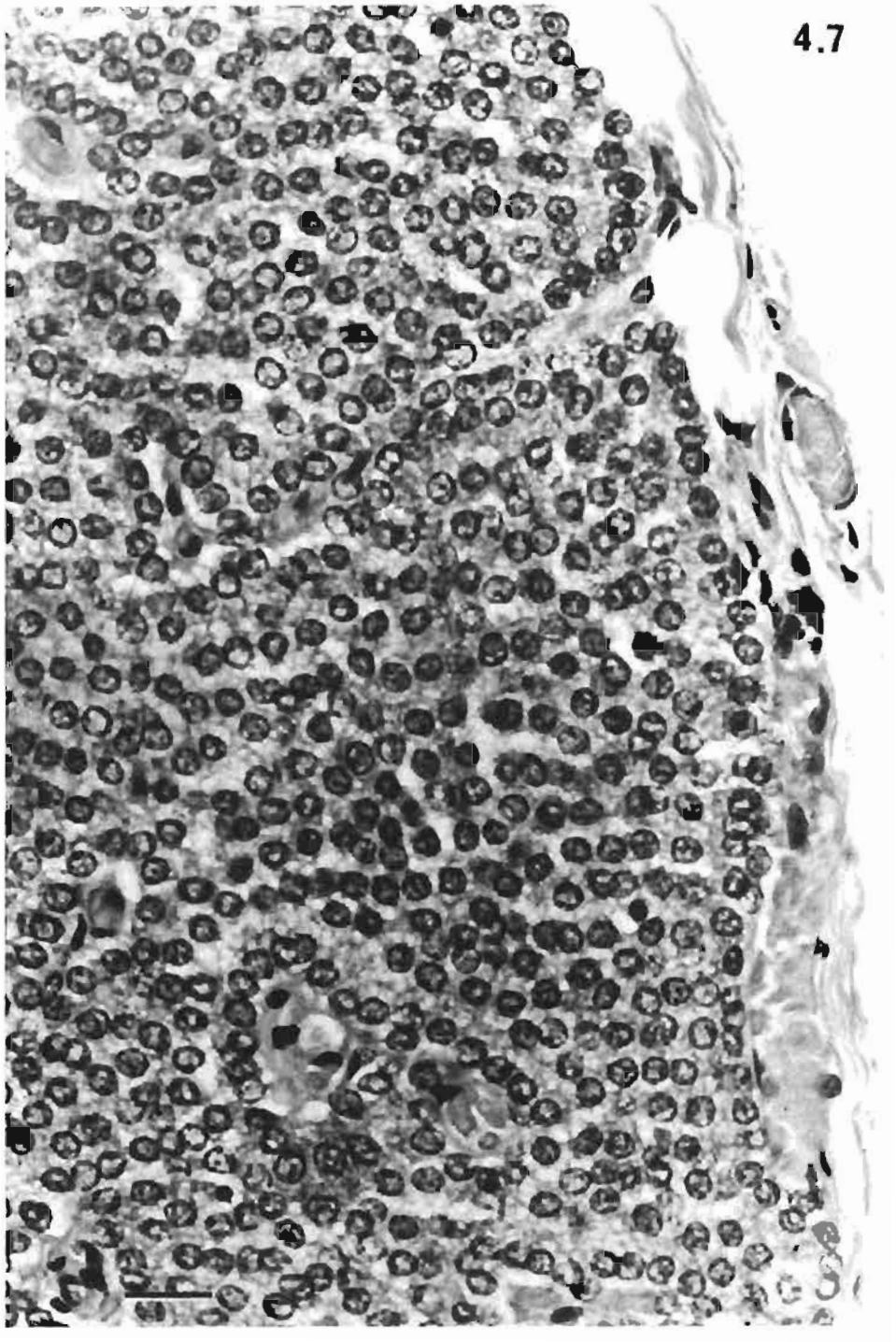
4.7

Plate 4.8. Light microscopy of parathyroid III in *Antechinus* spp.

Fig. 4.8a. Low power view of a parathyroid from *A. flavipes*. Specimen fixed by perfusion. Capillaries are distended, connective tissue sparse and principal cells are compactly arranged. Some cells (arrow) have a scalloped outline.
Antechinus Af1
Resin section, toluidine blue.
Bar: 30µm

Fig. 4.8b. The parathyroid gland from *A. flavipes* was fixed by immersion. Lymphocytes (L) are numerous in the perivascular tissue, contributing to the darker colour of the mesenchymal component.
Antechinus Af2
Resin section, toluidine blue.
Bar: 20µm

Fig. 4. 8c. Shows the typical appearance of the parathyroid from *A. stuartii*. The principal cells have numerous fine cytoplasmic granules.
Antechinus As3
Resin section, toluidine blue.
Bar: 20µm

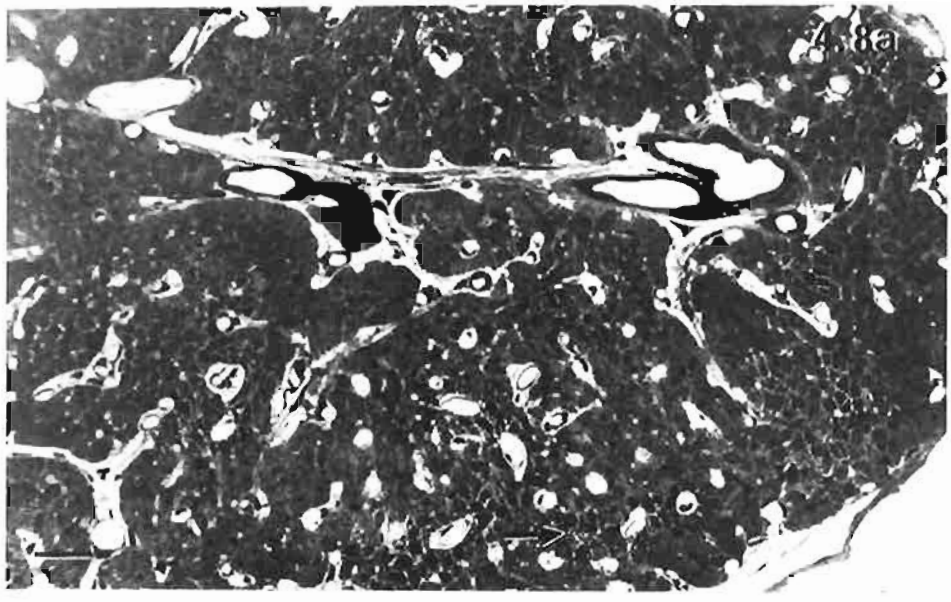

4.8a

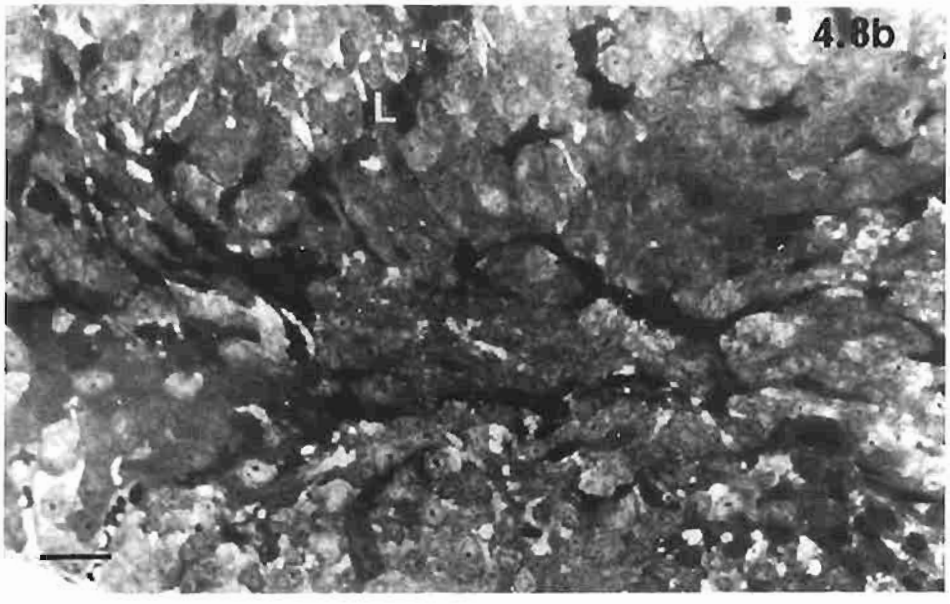

4.8b

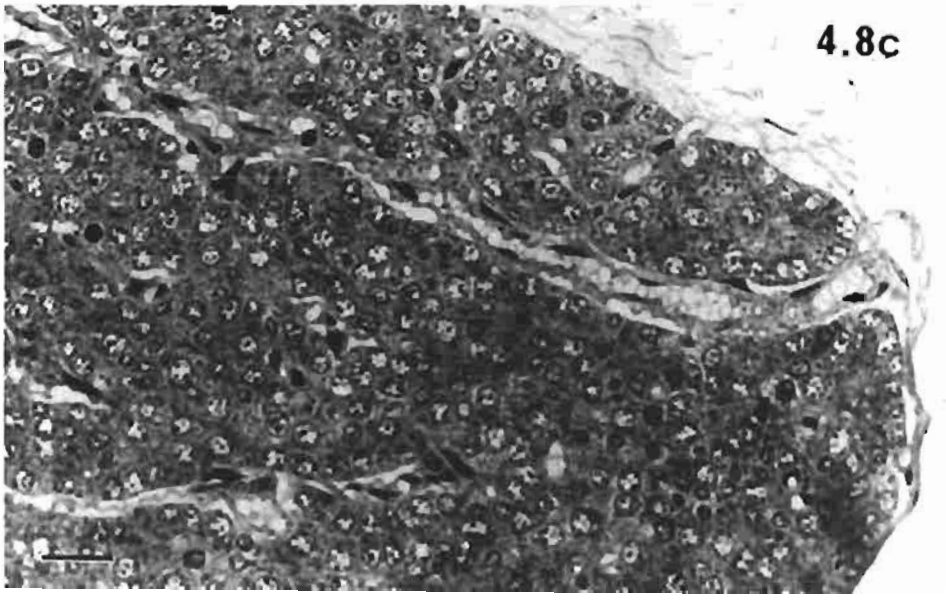

4.8c

Plate 4.9. Ultrastructure of parathyroid glands in *S. crassicaudata* - I

Fig. 4.9a. The electron micrograph shows light and dark cells with irregular outlines. Specimen fixed by perfusion.
Dunnart S15
Bar: 1.5 µm.

Fig. 4.9b . The electron micrograph shows the dilated lumina of RER and a large perinuclear cisterna of a dark cell. The cytoplasmic texture of the light cell is less compact than that of the dark cell. The specimen was fixed by immersion.
Dunnart S19
Bar: 1 µm.

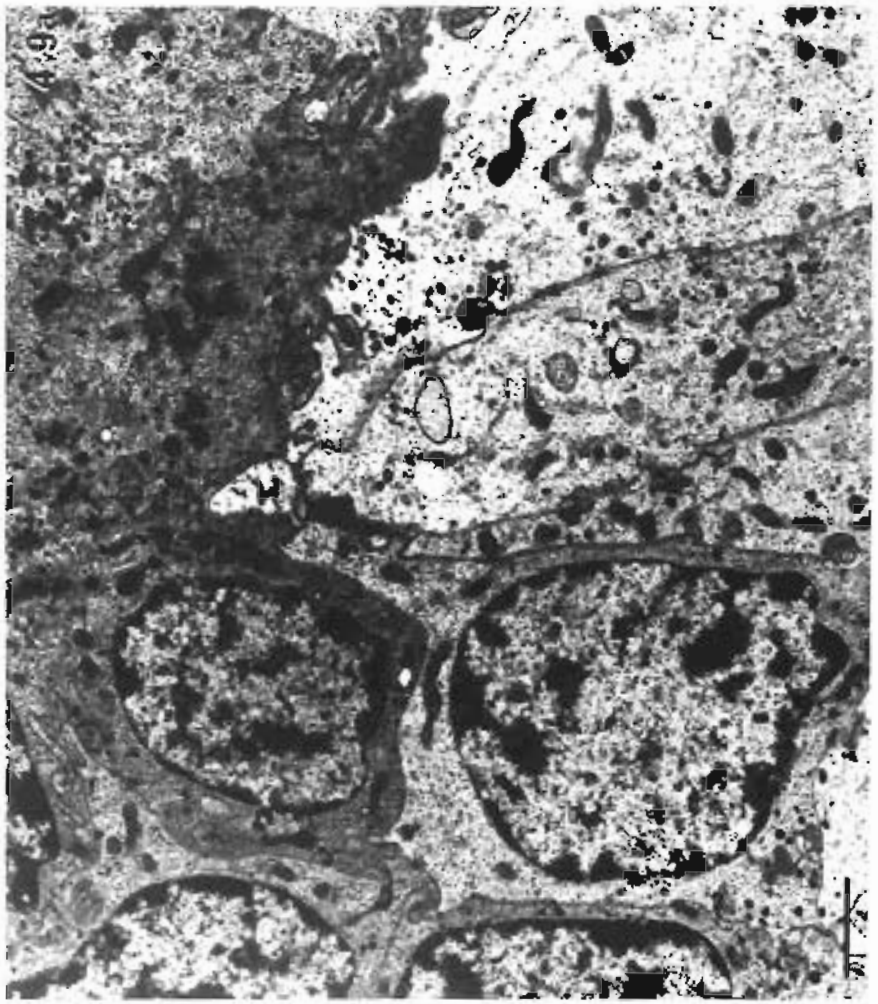

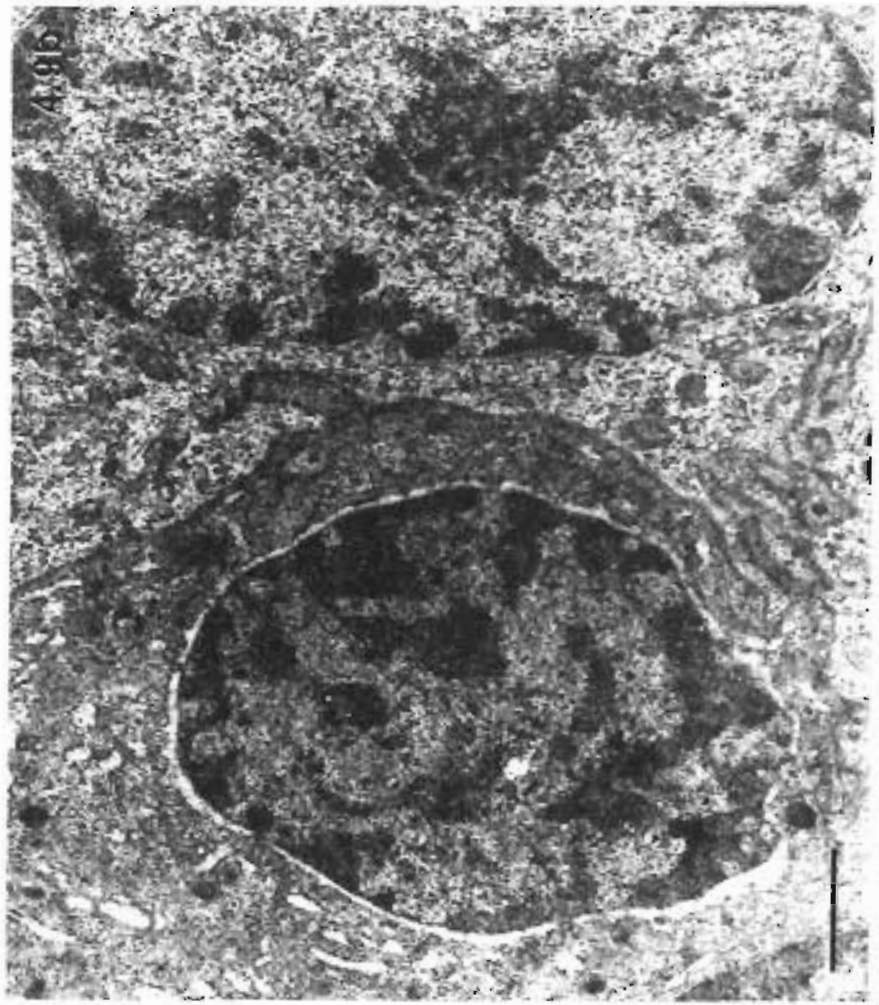

Plate 4.10. Ultrastructure of parathyroid glands in *S. crassicaudata* - II

Fig. 4.10a . The electron micrograph shows several desmosomes (D) between principal cells. Several types of vesicles are present in the cells.
Dunnart S10
Bar: 0.2 µm.

Fig. 4.10b . The electron micrograph shows a lipid inclusion (L) and two types of granules. One is electron dense (A) and the other has a granular texture (B).
Dunnart S27
Bar: 0.2 µm.

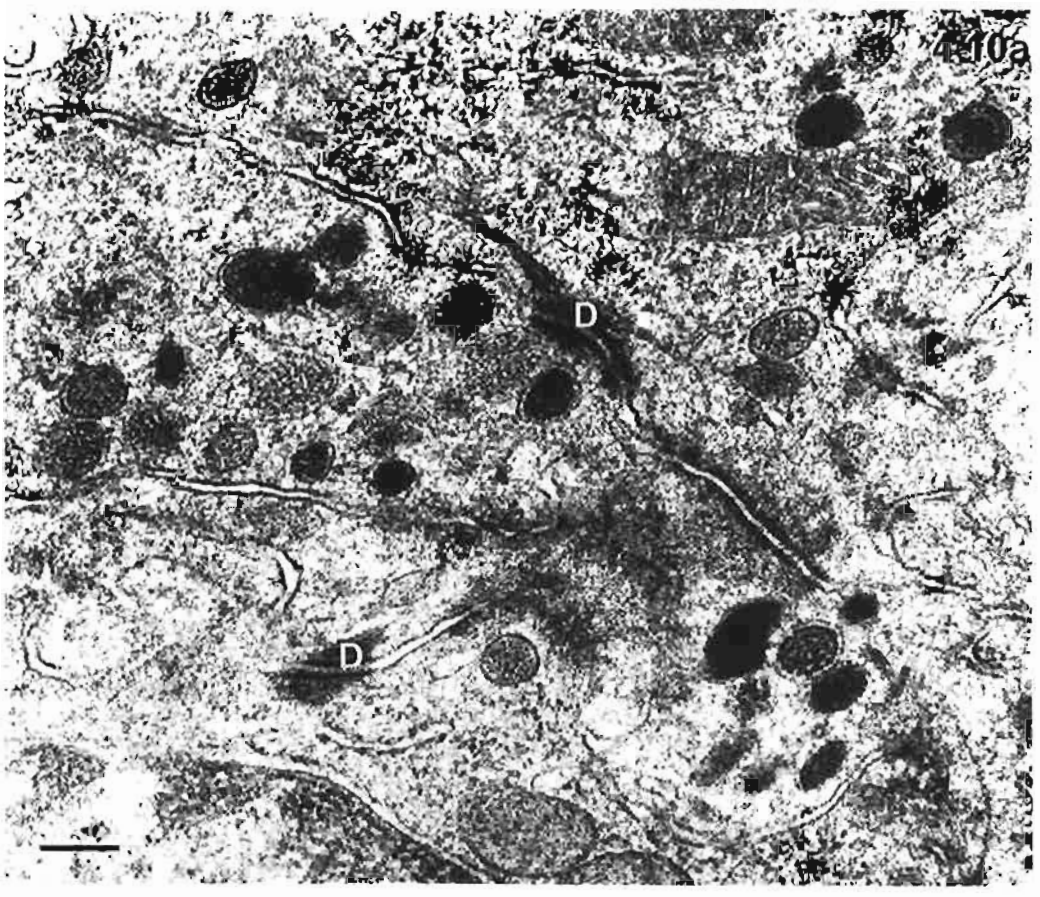
4.10a
D
D

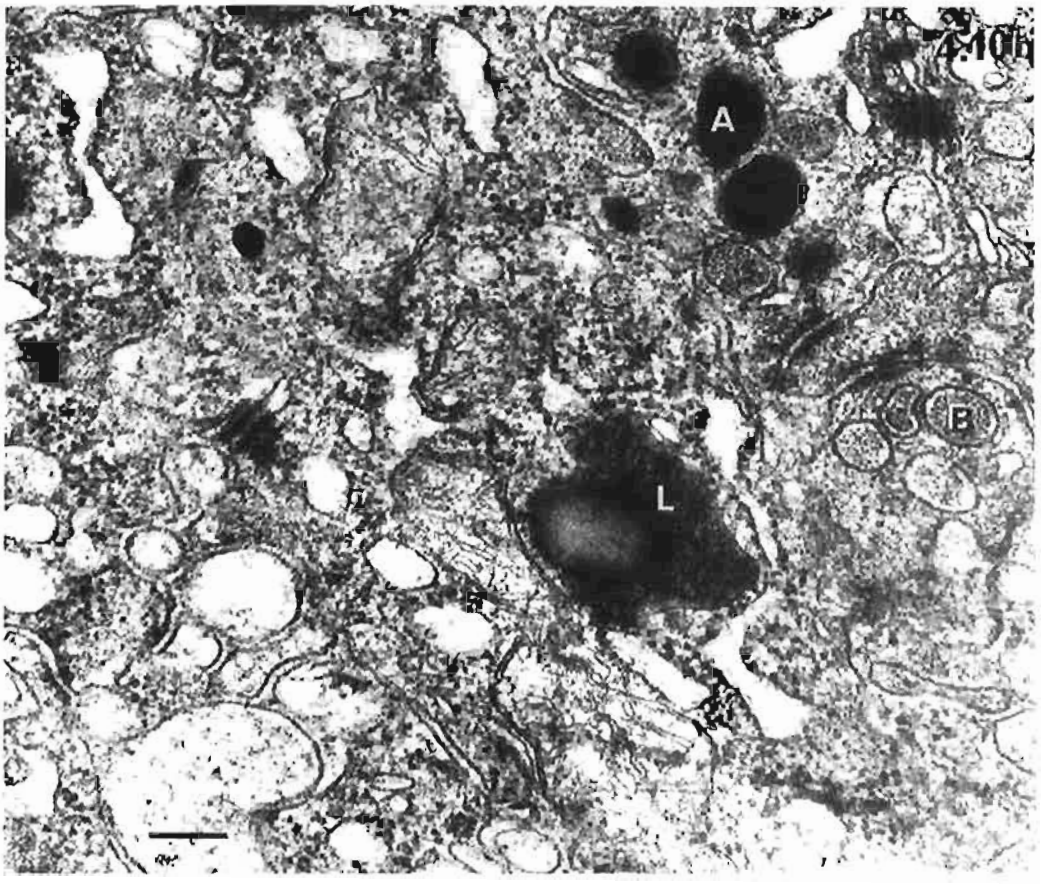
4.10b
A
B
L

Plate 4.11. Ultrastructure of parathyroid glands in *S. crassicaudata* -III

Fig. 4.11a . The electron micrograph shows the typical structure of principal cells, including a Golgi body (G) and elongated, sometimes irregular shaped mitochondria.
Dunnart S30
Bar: 0.5 μm.

Fig. 4.11b . The electron micrograph shows several U-shaped and annular sections of mitochondria (M) and different densities of granules in the cells.
Dunnart S10
Bar: 1 μm.

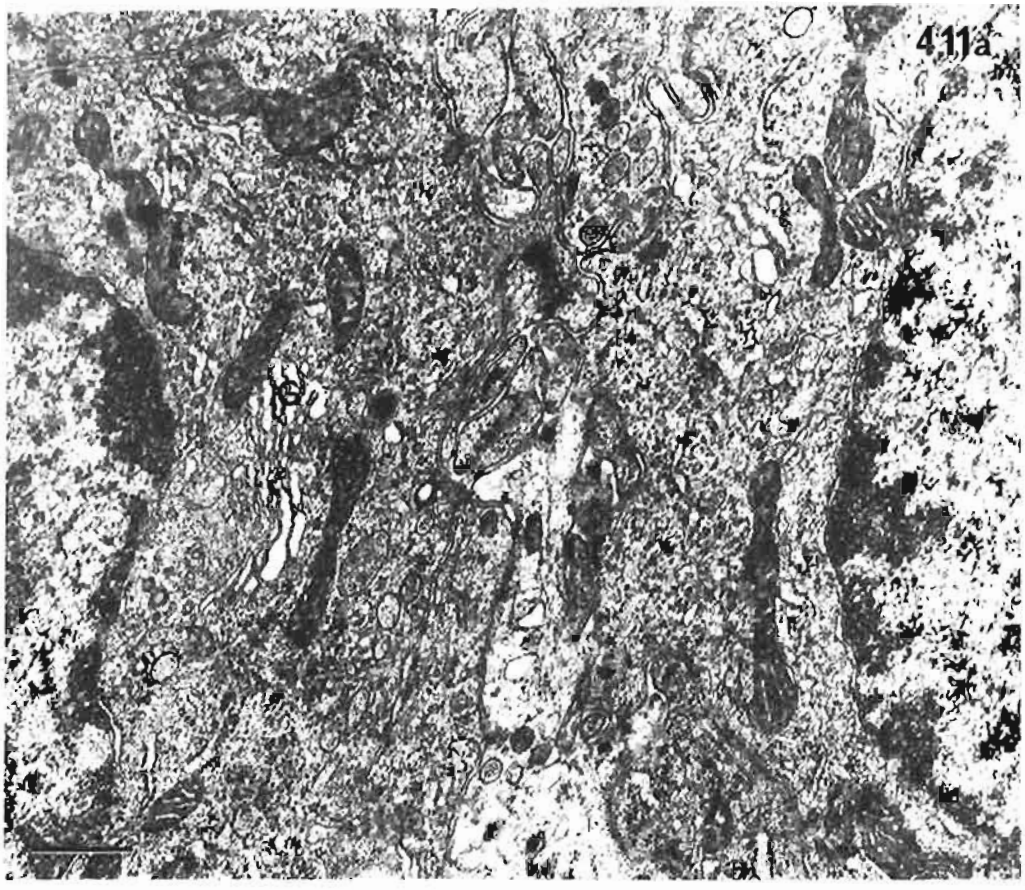
4.11a

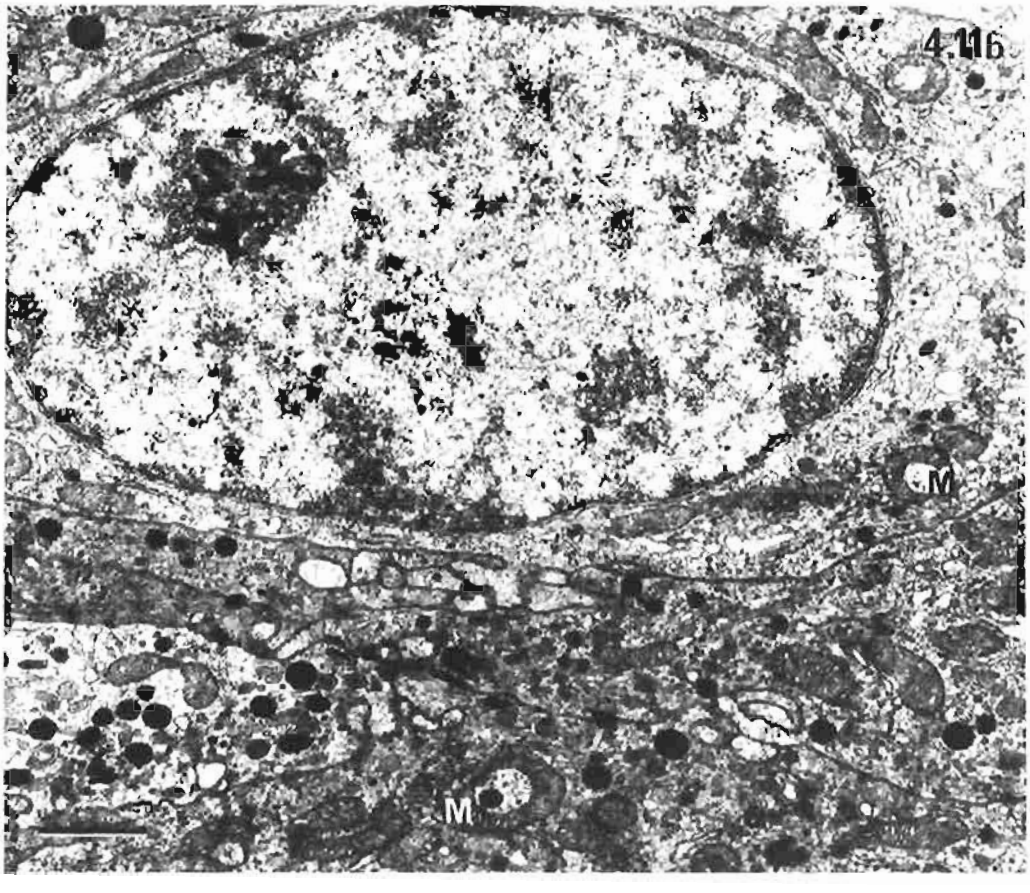
4.11b
M
M

Plate 4.12. Ultrastructure of parathyroid glands in *A. flavipes*.

Fig. 4.12a. Shows parathyroid gland, perfusion fixed. Principal cells vary in staining intensity. Depending on the plane of the section, mitochondria and secretory granules are abundant in some cells and scarce in others. The capillary in the top left corner has a pericyte within the basal lamina of the endothelial cell. The perivascular space appears to be artefactually enlarged.
Antechinus Af1
Bar: 2μm.

Fig. 4.12b. Shows the ultrastructure of the parathyroid gland fixed by immersion. Principal cells have different cytoplasmic densities. Some mitochondrial profiles appear to be annular or U-tube shaped. Several leukocytes (L) are interspersed among the principal cells. The leukocyte in the lower left corner of the micrograph appears to be a pyknotic lymphocyte. Note the irregular processes extending in between the adjacent principal cells.
Antechinus Af2
Bar: 2μm.

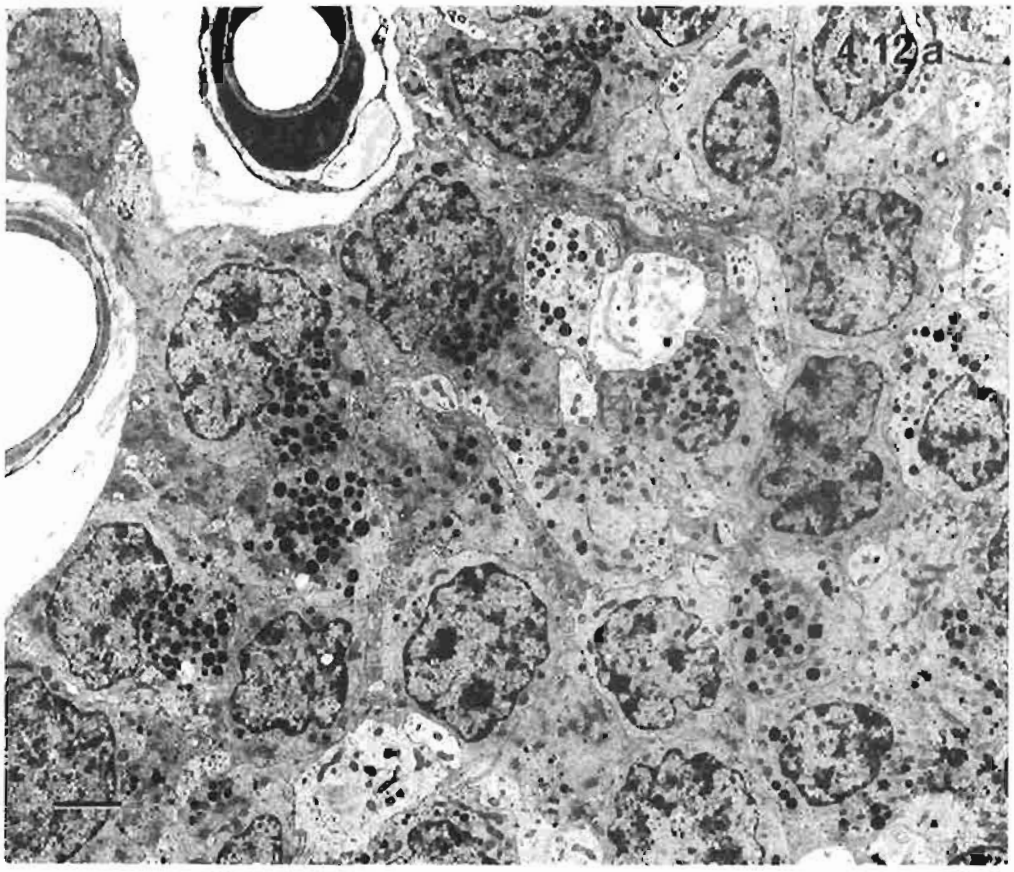
4.12a

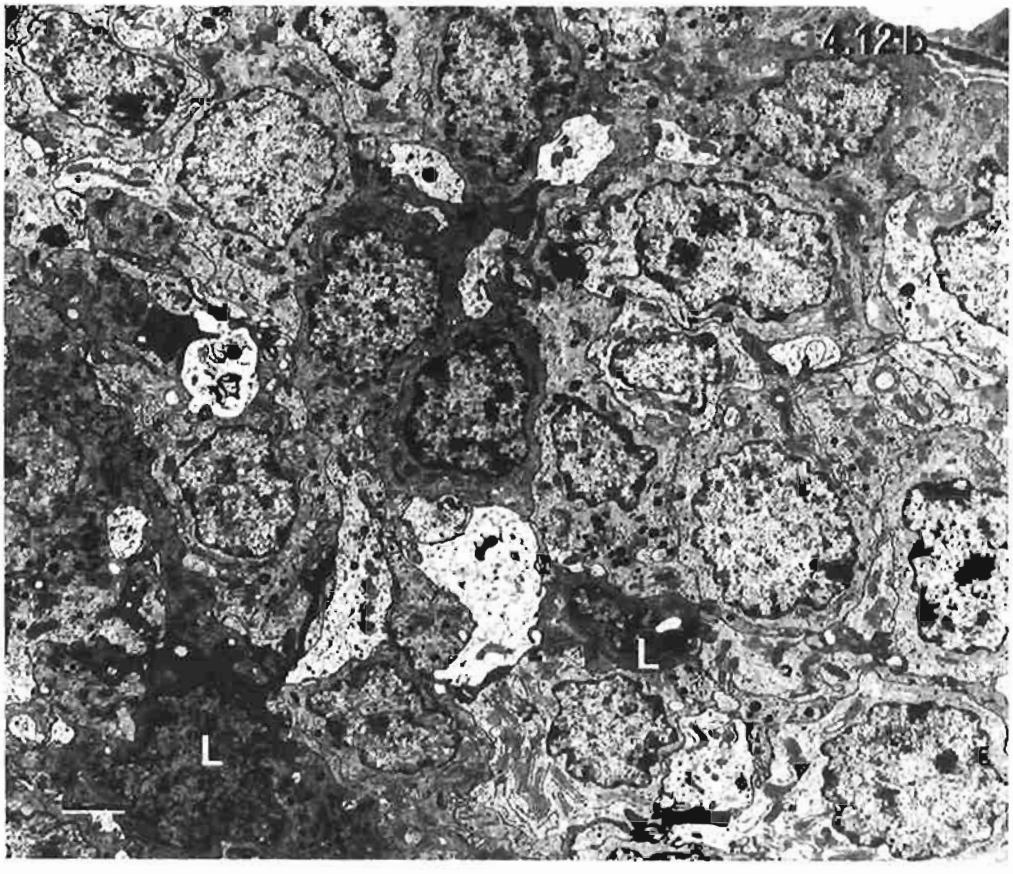
4.12b
L
L

Plate 4.13. Leukocytic infiltration of parathyroids in *A. flavipes*.

Fig. 4.13a. Three dark staining leukocytes, presumably neutrophils, have many cytoplasmic invaginations, phagosomes and vesicles. Other leukocytes (L) with more ribosomes and fewer granules appear to be lymphocytes.
Antechinus Af2
Bar: 2μm

Fig. 4.13b. Shows the enlarged perinuclear space and dilated endoplasmic reticulum of leukocytes identified as neutrophils (N). A variety of vesicles is present in the electron dense cytoplasm.
Antechinus Af2
Bar: 2μm

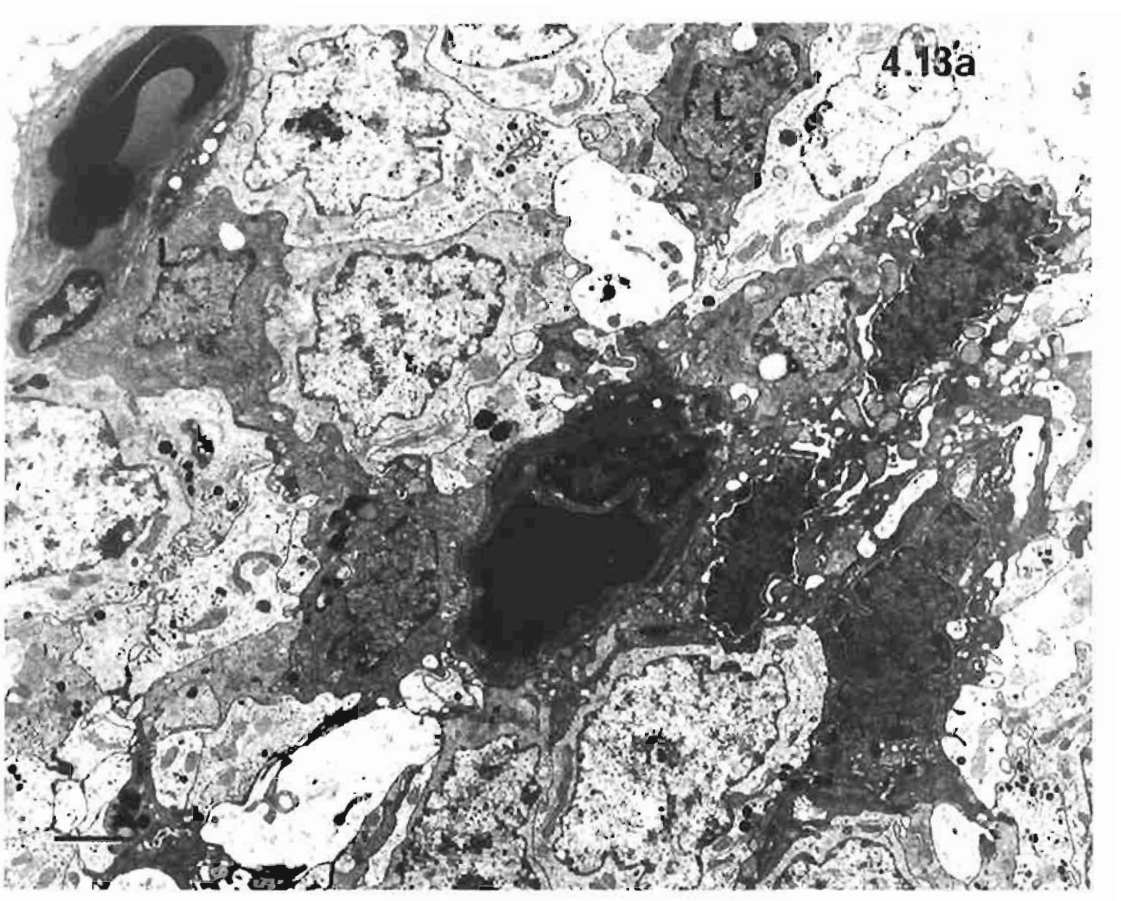
4.13a

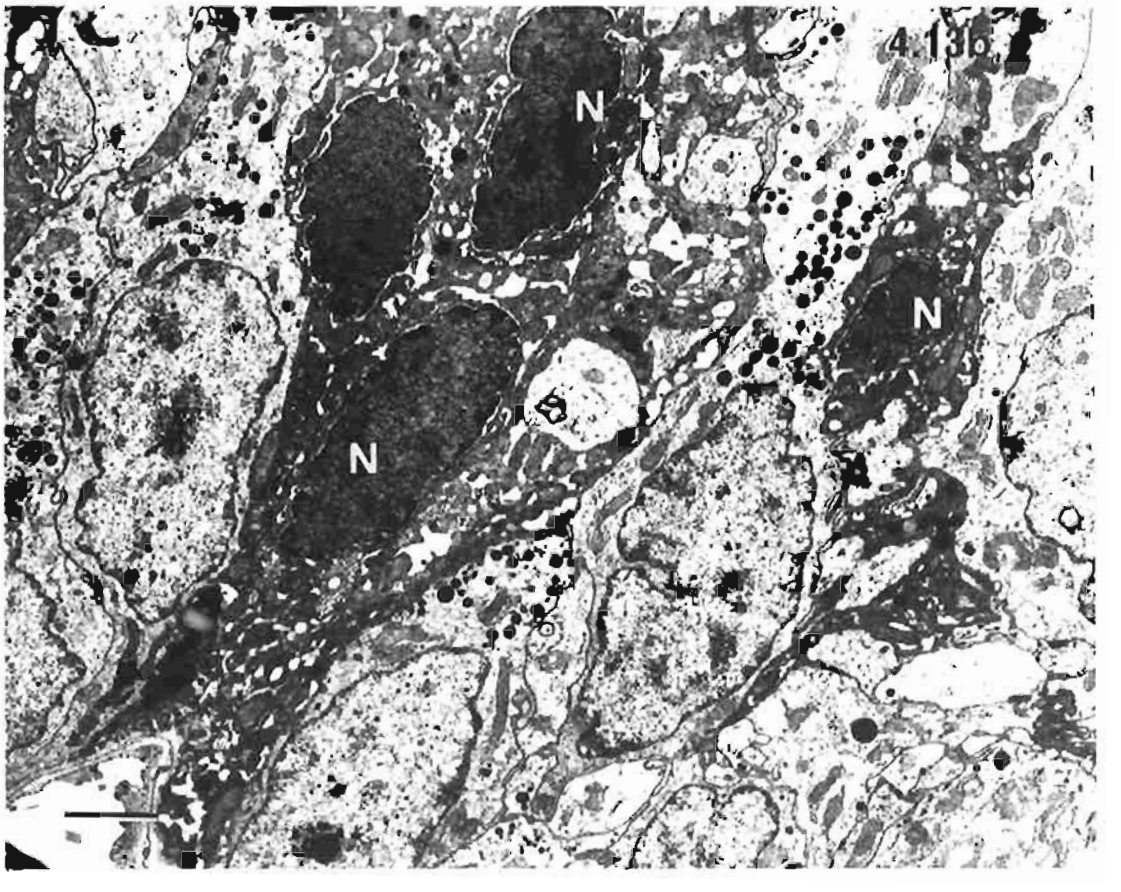
4.13b
N
N
N

Chapter 5

Parathyroid Glands in Peramelid Marsupials

5.1 Introduction

The peramelid marsupials, bandicoots, form an unusual family because they have both polyprotodont and diprotodont characteristics. The structure of the skull and teeth and serology link them with polyprotodonts but the hind feet are syndactylous which is an anatomical characteristic of diprotodonts (Dawson, 1983). Bandicoots have a widespread distribution and are found in most areas that have good ground cover where they can dig for invertebrates. The bandicoot is about the size of a small rabbit and has a conical shaped nose and a thin tail (Strahan, 1983). The two species that were examined in this study were *Isoodon macrourus*, the northern short-nosed bandicoot and *Isoodon obesulus*, the southern brown bandicoot. Animals of the former species are larger (average male weight - 2100g, average female weight - 1100g) than the southern species (average male weight - 850g, average female weight - 700g) (Strahan, 1983).

Descriptions of the parathyroid glands in *Peramelidae* were derived from the examination of two adult female northern short-nosed bandicoots and an adult male southern brown bandicoot. The animals were used initially in fertilization research by Dr W.G. Breed and Dr. D Taggart in the Department of Anatomical Sciences, University of Adelaide (Taggart et al., 1995). They were killed by an overdose of pentobarbital sodium and the reproductive tracts were removed before dissection of the cervical and upper thoracic regions was commenced. Only specimens from *I. obesulus* were suitable for ultrastructural investigations.

A large, reasonably intact piece of tissue, about 6cm long, was removed from one female animal, transversely bisected, fixed in buffered formalin and hand-processed. The tissue specimen extended from a plane just cephalic to the larynx to a plane caudal to the aortic arch. Serial paraffin sections, 10μm in thickness were cut and every tenth section was mounted and stained with haematoxylin and eosin. To assist with the three-dimensional visualisation of the structures, outline diagrams of selected sections were made by placing the histological sections in a small personal viewing 35mm slide projector and outlining the images on a piece of paper placed over the screen.

Tissue around the bifurcations of the common carotid arteries were removed from the second female bandicoot, placed in buffered formalin, processed and embedded in paraffin. Serial sections were cut and stained with haematoxylin and eosin (See chap. 3, Materials and Methods for details).

The parathyroid glands located adjacent to the carotid bifurcations (parathyroid III) were dissected out of the male southern brown bandicoot, fixed in a 3% glutaraldehyde, 3% paraformaldehyde solution, and processed for electron microscopy (See chap. 3, Materials and Methods for details).

5.2. Results

5.2.1. Anatomy

Serial sections revealed parathyroid tissue in four locations in *I. macrourus*. The more cephalic gland, parathyroid III, was located bilaterally in the vicinity of the carotid bifurcation that occurred at the level of the ossified caudal cornu of the thyroid cartilage (Fig. 5.1a). Parathyroid III was not associated with the thyroid. Parathyroid III was adjacent to the ventral aspect of the carotid bifurcation and extended rostrally, just ventral to the initial part of the external carotid. The glands were separate from the carotid body and appeared not to be associated with the small amount of thymic tissue present at the same level of the neck (Fig. 5.1a). The thymic tissue was positively identified by the presence of Hassall's corpuscles and the lack of cortical nodules, subcapsular sinus, and medullary sinuses. From examination of the serial sections, the dimensions of the flattened, diamond-shaped parathyroid III were estimated to be approximately 1.3 x 1.3 x 0.3mm.

Parathyroid IV was a minute structure. The right gland was situated in a more cephalic plane to the left. The former was located in fatty tissue between the brachiocephalic artery and the caudal part of the trachea. The left parathyroid IV was near involuted thymic tissue in sections cut at a level of the caudal limit of the aortic arch and the termination of the trachea (Figs 5.1b and 5.1c). Both glands were spherical to ovoid bodies with approximate diameters not exceeding 0.5mm.

5.2.2. Light Microscopy

In *I. macrourus*, parathyroid III had a typical reticulate, endocrine structure. From a fairly thick capsule of dense connective tissue septa penetrated the gland and divided it into incomplete lobules (Figs. 5.2a & b). The parenchymal cells were small, each with a moderate to dense nucleus (Fig 5.2c) and pale acidophilic cytoplasm; no distinction between light and dark cells could be seen. The cells were arranged in strands and clumps with no follicular structures observed in the paraffin sections.

In *I. obesulus*, thin plastic sections, stained with toluidine blue, showed that the parenchymal cells had a similar staining intensity to their cytoplasm and they were compactly arranged. Several clumps of cells appeared to form small spherical structures with nuclei located peripherally and central regions homogeneously stained but no definite no follicular lumen was discernible with the light microscope.

The histology of parathyroid IV was similar to that of parathyroid III in *I. macrourus* except the capsule was not prominent and septa were absent. One gland contained a small cyst with a diameter of approximately 175µm. On the periphery were two indistinct layers of presumably parenchymal cells enclosing an interior with several acidophilic globules (Fig 5.2d).

5.2.3. Electron Microscopy

Electron microscopic studies confirmed that parathyroid III in *I. obesulus* had a typical reticulate endocrine structure. Parenchymal cells were close together and showed little interdigitation of the cell membranes. Desmosomes were common between cells. Connective tissue in the glands was minimal and mainly confined to perivascular regions. Components including collagen fibrils, fibroblasts, and occasional mast cells (Fig. 5.3). The cells appeared to be all principal cells; the majority had a moderately electron-dense cytosol and light cells were rare (Fig. 5.4a.) No oxyphil cells were observed. Most nuclei appeared similar and contained abundant euchromatin, peripheral heterochromatin and a nucleolus (Figs. 5.3 & 5.4b.). In the cytosol were numerous free ribosomes, mitochondria, glycogen deposits and small secretory granules with electron-dense contents (Figs. 5.4a &b, 5.5a.). Many cells had at least one lipid inclusion (Figs. 5.4b & 5.5a.). Occasionally, structures that were identified as small follicles (Figs. 5.5a & b) were found. The fine granular and fibrillar contents of these follicles were pale and the adjacent plasmalemma had a cytoplasmic layer of dense material associated with it (Figs. 5.5a &b.). At the edge of one follicle, the contour of the plasmalemma (Fig. 5.5a) suggested that exocytosis or endocytosis was occurring.

5.3. Discussion

5.3.1. Anatomy.

In order to minimize artefactual separation of tissues during processing of the two large tissue blocks from one bandicoot, the specimen was secured in an elastic bandage which unfortunately caused some compression and distortion resulting in the asymmetric arrangement of muscles and salivary glands about the median sagittal axis. Slightly oblique rather than true transverse sectioning also contributed to the asymmetry noticeable in the zone diagrams of Figure 1.

The ossification that was observed in parts of the thyroid cartilage has also been noticed in other marsupials including the possum, *T. vulpecula* (Barbour, 1963). The identification of the artery adjacent to the right parathyroid VI as the brachiocephalic artery is based on previous studies of the major blood vessels in the thorax and neck of bandicoots (Tedman, 1990). In *I. macrourus* a single brachiocephalic artery arises from the aortic arch and extends cephalically, ventral to the trachea. The right subclavian artery is the first branch and the right and left common carotid arteries arise a considerable distance cephalically.

The adult locations of the parathyroid glands in the bandicoot, *I. macrourus* are consistent with previous descriptions given for embryonic and foetal specimens of the bandicoots, *Perameles nasuta* and *Isoodon obesulus* (Fraser, 1915). Fraser (1915) postulated that the development of parathyroid IV ceased early and concluded it was not present in the adult, but the current studies have shown that parathyroid IV, albeit tiny, persists in the mature adult. The differences in size between parathyroid III and parathyroid IV not only occurs in the adult but also in the developing bandicoot (Fraser, 1915).

In the current study, specimens from the two female specimens (*I. macrourus*) showed small patches of thymic tissue near the carotid bifurcations (Fig. 5.1a). The lymphoid tissue was identified as thymus by the presence of Hassall's corpuscles, lack of a subcapsular sinus, and a lack of lymph nodules. This thymic tissue was either the cervical thymus or thymus III. It seems unlikely to be the former because its position was deep instead of superficial to the ventral neck muscles (Fig. 5.1a) and a cervical thymus is thought not to occur in bandicoots (Johnstone, 1898; Fraser, 1915; Yadav, 1973). Alternatively, the thymic tissue could have arisen from a developmental anomaly where an abnormal cleavage and migration of the embryonic tissue in the third pharyngeal pouch led to some thymic tissue migrating to the neck instead of the thorax. However the constant presence of thymus III bilaterally in the two bandicoots indicates that in *I. macrourus*, part of thymus III is normally found in the ventral neck and part in the thorax.

5.3.2. Light Microscopy

Lobulation of parathyroid III was observed in the two female specimens (*I. macrourus*) but not in the male specimen (*I. obesulus*). However as only three animals were used in this study, then it is not possible to draw conclusions about morphological differences relating to species or sex. The presence of a cyst in parathyroid IV of bandicoot 2 was unusual. Parathyroid IV glands of other marsupials examined in this study have shown a typical reticulate endocrine structure in spite of cysts, follicles and/or lobulation being present in parathyroid III glands. However in many non-marsupial species (Roth and Schiller, 1976) the structure of parathyroid III and IV has been shown to be identical, with cysts and follicles present in both.

5.3.3. Electron Microscopy

The ultrastructure of parathyroids in bandicoots appears to be similar to that in many other animals (Roth and Schiller, 1976) except for the paucity of light cells. In parathyroid specimens, the number of light cells present may be influenced partly by fixation methods where maximum numbers occur after prompt fixation by immersion and minimal distinction between light and dark cells is evident after fixation by perfusion (Clark and Khairallah, 1972; Setoguti, 1977). The effects of fixation on the morphology of parathyroid glands is discussed in more detail in chap. 11, General Discussion, section 11.4. In this current study of marsupial parathyroid glands, an almost total lack of principal cell variants, i.e. dark and light cell categories, has been observed only in bandicoots and koalas (see chap. 6). However, as the evidence in bandicoots is based on only three specimens, the results are inconclusive.

Follicles are not uncommon in the parathyroid gland (DeLellis, 1993) and have also been observed in other marsupial glands in this study. They are discussed in more detail in chap. 11, General Discussion, section 11.3.

Fig. 5.1a. Drawing of a serial section showing parathyroid III in *I. macrourus*

Fig. 5 1a Zone diagram of a section through the neck of *I. macrourus* at the level of the bifurcation of the right common carotid where the caudal tip of the right parathyroid gland (PTG) can be seen to be separate from the carotid body (CB) and the thymic tissue (thm). The ossified caudal cornua (areas of vertical stripes) of the thyroid cartilage are surrounded by the infrahyoid muscles of the neck. Cartilage is shown as areas of horizontal stripes
Bandicoot 1
Bar - 2mm.

Abbreviations :- C Art - common carotid artery; CB - carotid body; cornu - ossified cornu of thyroid cartilage; EC - external carotid artery; IC - internal carotid artery; muscle - infrahyoid muscles; N - nerve; NIX - glossopharyngeal nerve; NX - vagus nerve; oes - oesophagus; PTG - parathyroid gland; SLSG - sublingual salivary gland; SMSG - submandibular salivary gland; thm - thymus.

5.1a

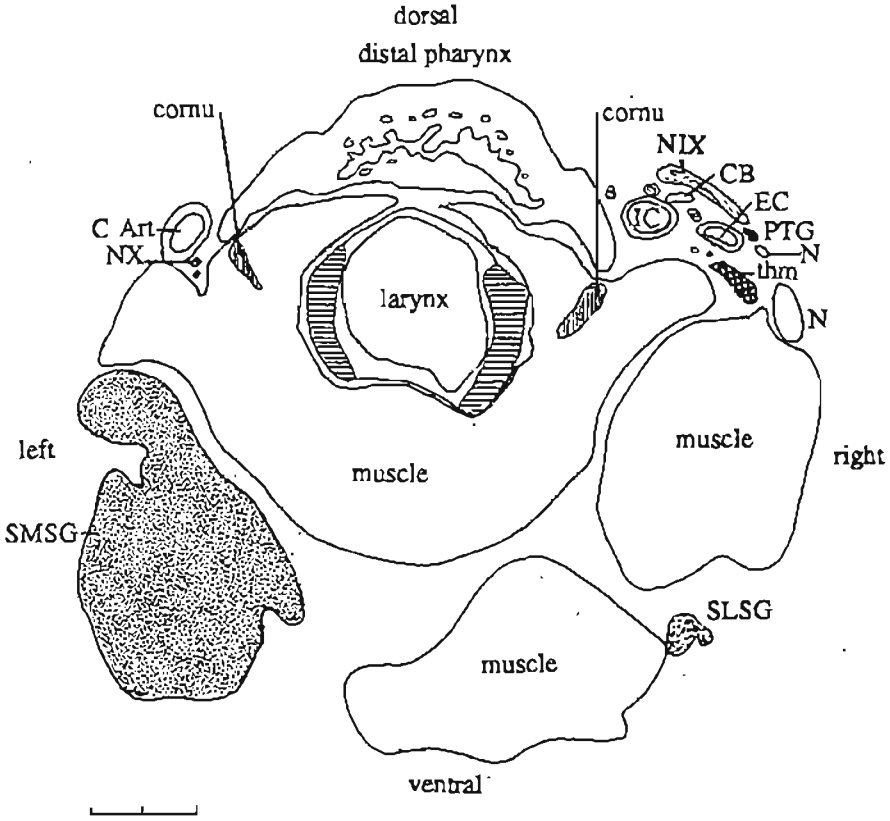
dorsal
distal pharynx
cornu
cornu
NIX
CB
EC
PTG
N
thm
C Art
NX
larynx
N
left
muscle
muscle
right
SMSG
SLSG
muscle
ventral

Fig. 5.1, b&c. Drawing of a serial section showing parathyroid IV in *I. macrourus*

Fig. 5.1b. Zone diagram of a section of mediastinal tissue from *I. macrourus* at the lower level of the trachea. On the right side, parathyroid IV (PTG) is located between the trachea and the brachiocephalic artery (BCA). Locations of the trachea and oesophagus have been distorted slightly during processing and section cutting. Cartilage is shown as striped areas.
Bandicoot 1
Bar - 2mm.

Fig. 5.1c. Zone diagram of a section of mediastinum from *I. macrourus* cut at the level of the caudal border of the aortic arch (AA). On the left side, parathyroid IV (PTG) occurs near the involuting thymus (thm) within fibrofatty tissue. Locations of the trachea and oesophagus have been distorted slightly during processing and section cutting. Cartilage is shown as striped areas.
Bandicoot 1
Bar - 2mm.

Abbreviations:- A - artery; AA - aortic arch; AVC - anterior vena cava; BCA - brachiocephalic artery; eos - oesophagus; LN - lymph node; N - nerve; PC - pericardial sac; PTG - parathyroid gland; thm - thymus; V - vein.

5.1b

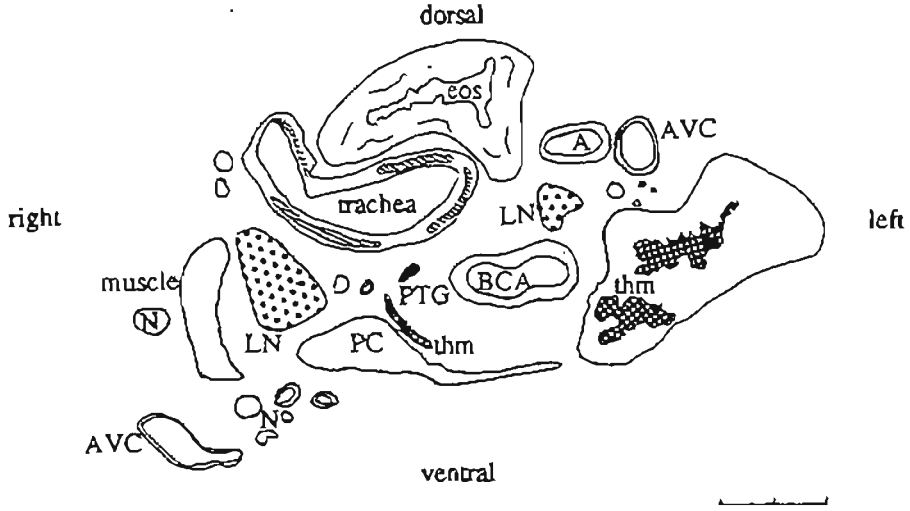
dorsal
oes
A
AVC
trachea
LN
right
left
muscle
N
BCA
thm
PTG
LN
PC
thm
N
AVC
ventral

5.1c

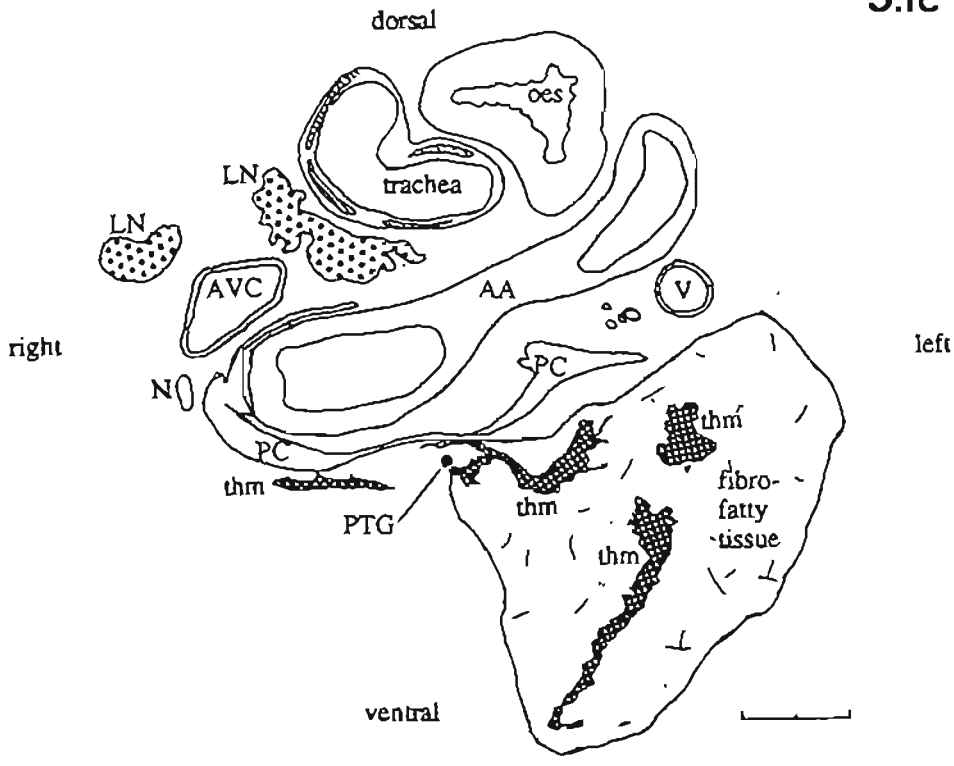
dorsal
oes
LN
trachea
LN
AVC
AA
V
right
left
PC
N
thm
PC
thm
PTG
thm
fibro-
fatty
tissue
thm
ventral

Plate 5.2. Light Microscopy of Parathyroid Glands in *I. macrourus*.

Fig. 5.2a. Low power view of the carotid bifurcation showing the proximity of parathyroid III (PTG) to the carotid branches. The parathyroid gland is separate from the carotid body (CB).
EC - external carotid; IC - media of the internal carotid.
Bandicoot 2
Paraffin section, H&E.
Bar - 0.2mm.

Fig. 5. 2b. Shows the histology of parathyroid III. Note the clumps and strands of principal cells with the relatively thick septa (S) and capsule of connective tissue. No fat cells occur in the gland.
Bandicoot 2
Paraffin section, H&E.
Bar - 100µm.

Fig. 5.2c. High power view of parathyroid III showing all principal cells appear similar.
Bandicoot 2
Paraffin section, H&E.
Bar - 20µm.

Fig. 5.2d. Low power view of parathyroid IV. Shows a cyst lined by two indistinct layers of cells and several acidophilic globules (G) in the lumen.
Bandicoot 2
Paraffin section, H&E.
Bar - 50µm.

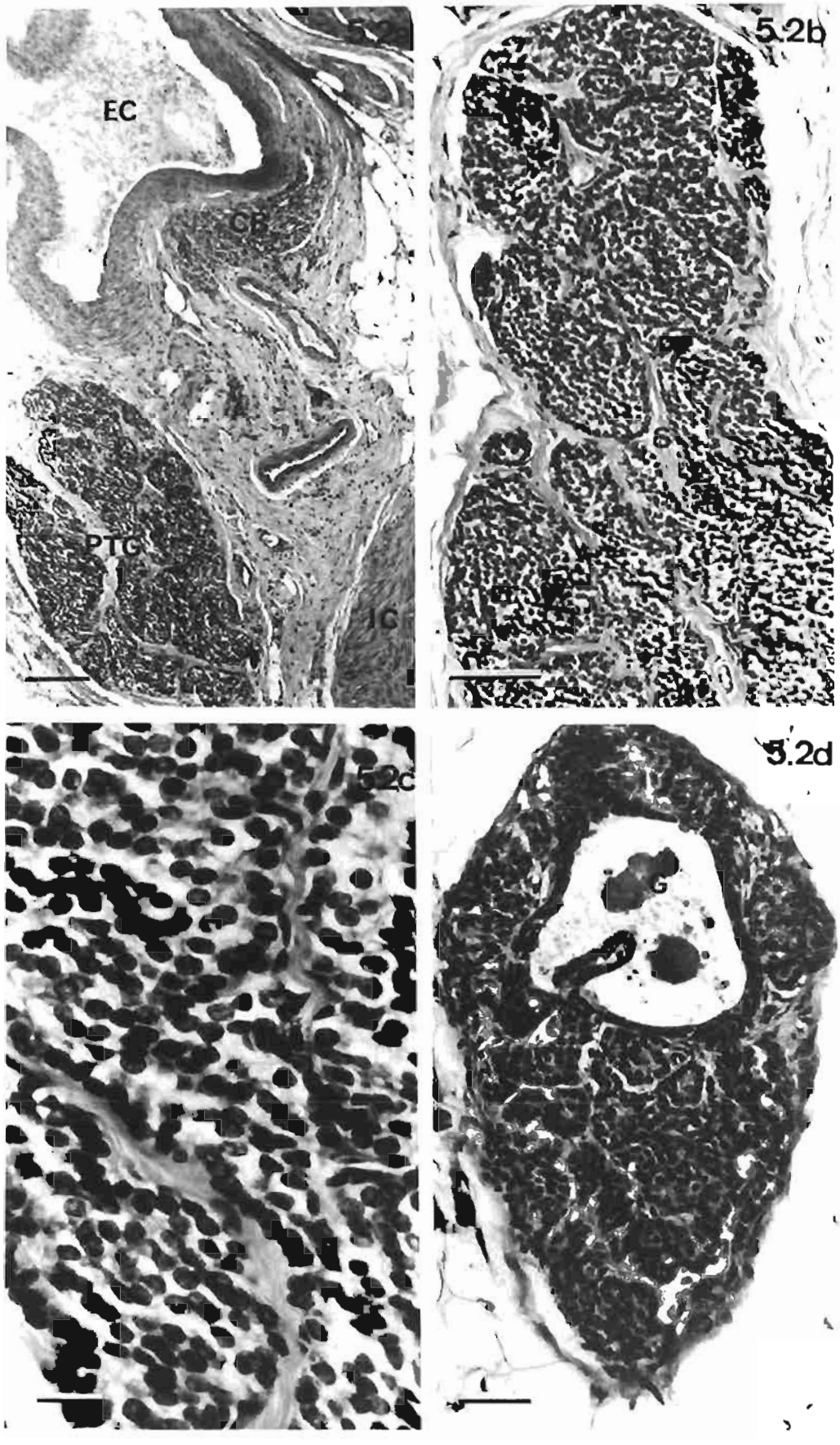
EC
CB
PTG
IC
5.2b
5.2c
5.2d

Plate 5.3. Ultrastructure of parathyroid III in *I. obesulus* - I

Fig. 5.3. Shows the compact arrangement of the parenchymal cells in parathyroid III (*I. obesulus*). Connective tissue is mainly confined to the to the perivascular areas. A mast cell (M) is present adjacent to the capillary.
Bandicoot 3
Bar: 2.5μm.

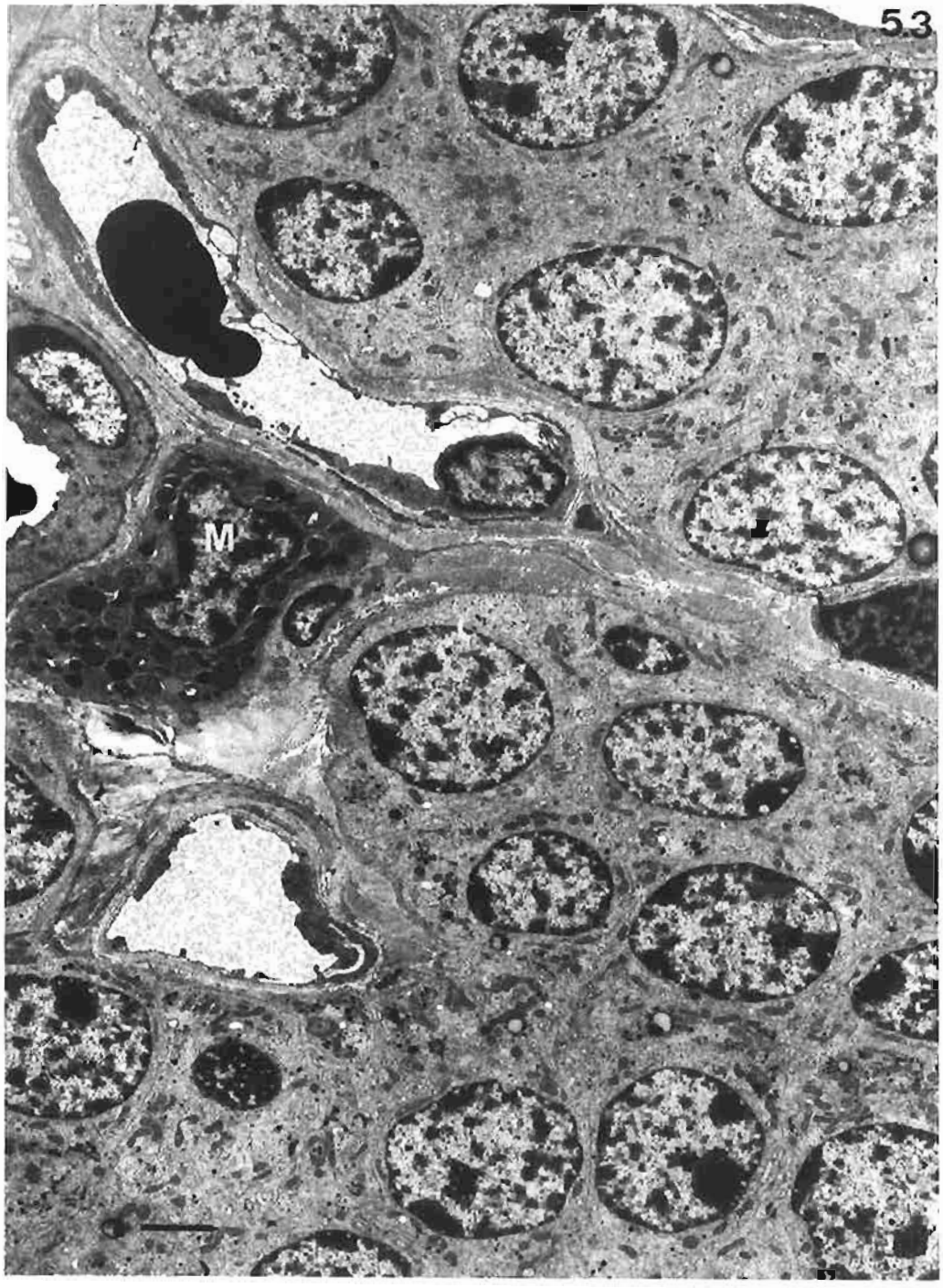
5.3
M

Plate 5.4. Ultrastructure of Parathyroid III in *I. obesulus* - II

Fig. 5.4a. Shows a rare light cell surrounded by dark cells which predominated in the parathyroid. The number of organelles and inclusions in the light and dark cells appears similar. In the light cell a Golgi apparatus (arrow) with associated granules are present to the right of the nucleus.
Bar: 1µm.

Fig. 5.4b. Shows the general ultrastructure of parathyroid III. Various small granules, ribosomes, RER are widespread. A Golgi apparatus (G) can be distinguished in the central cell and lipid inclusions are in the cells on the upper left of the micrograph.
Bar: 1µm.

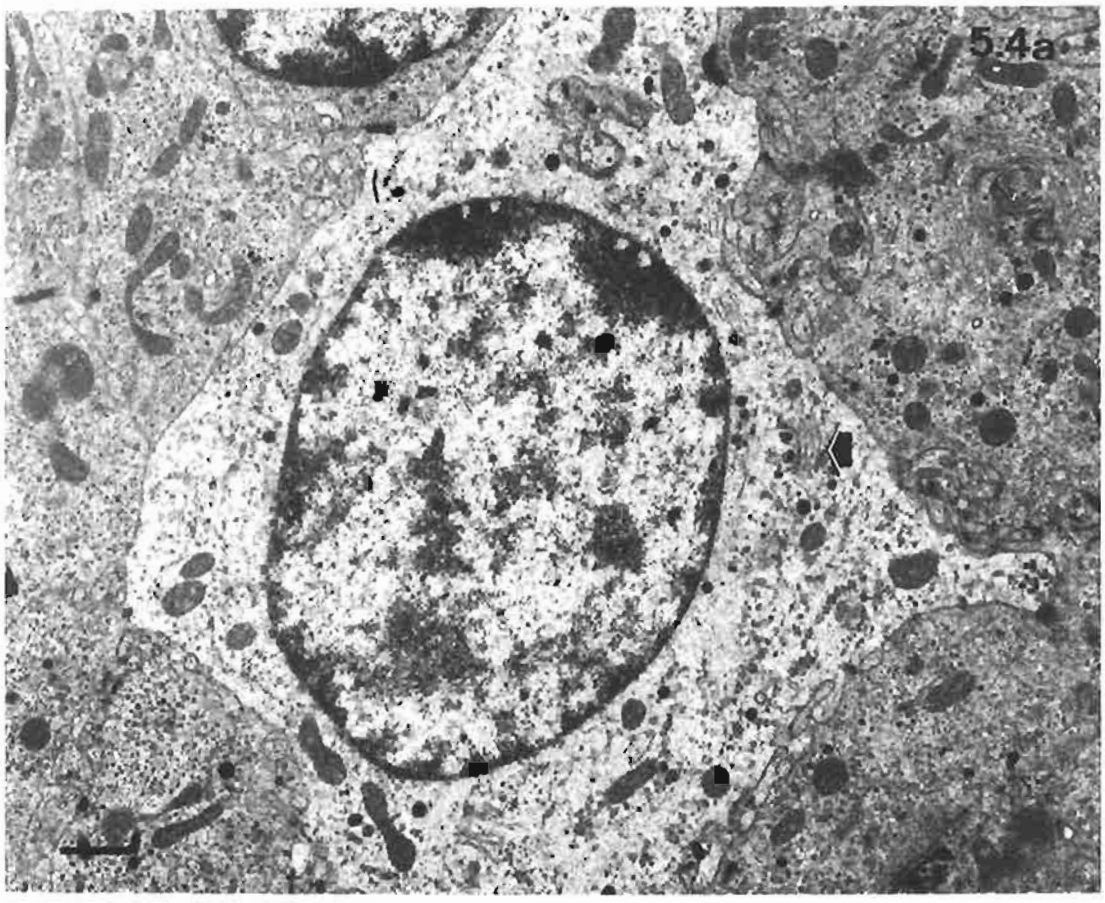
5.4a

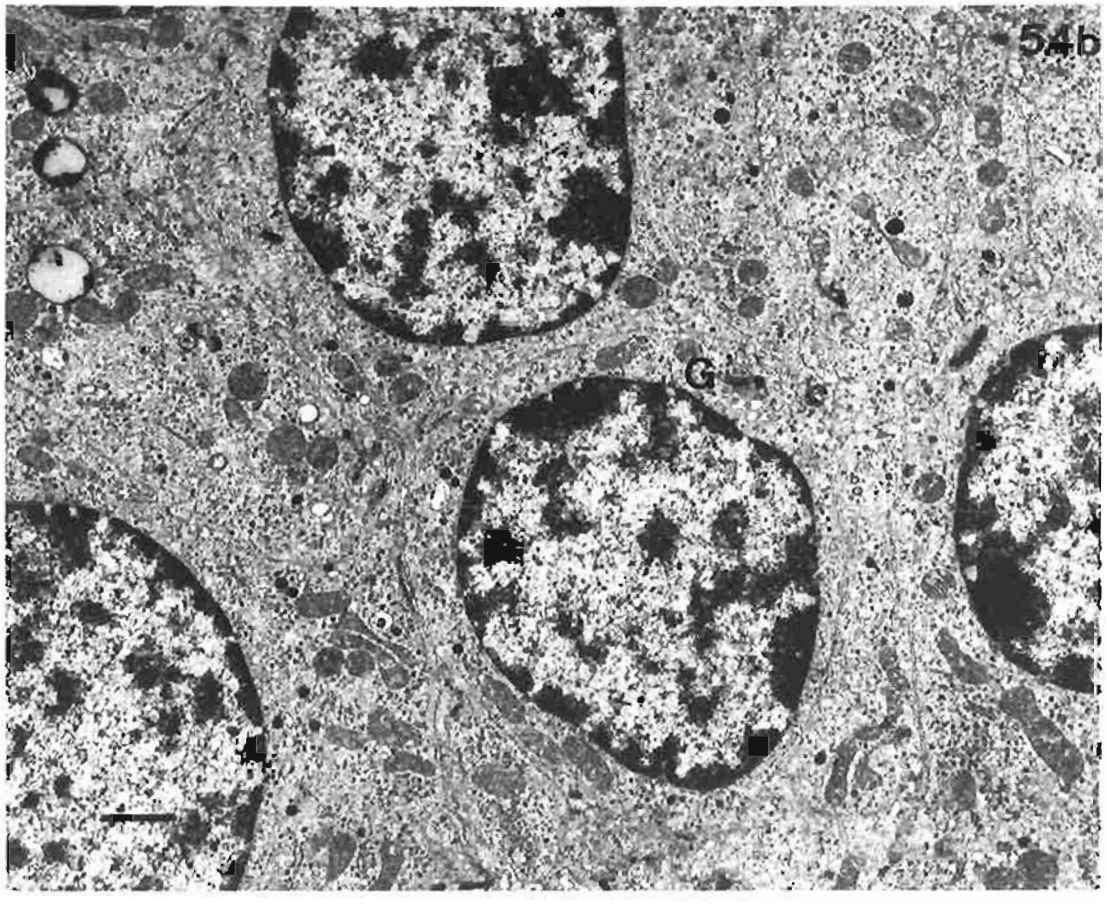
5.4b
G

Plate 5.5. Ultrastructure of Follicles in *I. obesulus*

Fig. 5.5a. Shows the central region of a follicle. Numerous mitochondria, ribosomes, and lipid inclusions are present in the cells. The cell membranes bordering the follicular contents have a cytoplasmic deposition of electron-dense material. The arrow indicates possible exocytosis or endocytosis.
Bandicoot 3
Bar: 0.5µm

Fig. 5.5b. Shows details of the follicular contents. Fine granular and fibrillar material is set in an electron-lucent medium. Electron-dense material is associated with the plasmalemma bordering the follicular contents; it is lacking from cell membranes between adjacent principal cells (upper right of micrograph).
Bandicoot 3
Bar: 0.3µm.

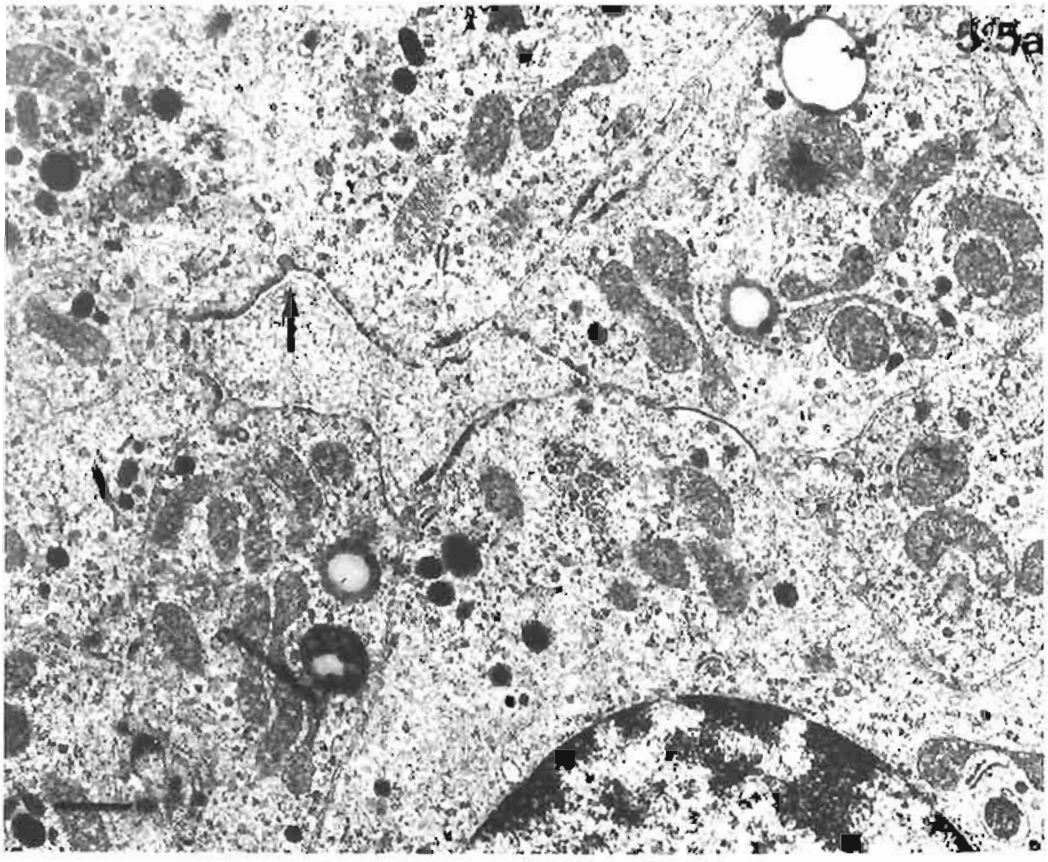

5.5a

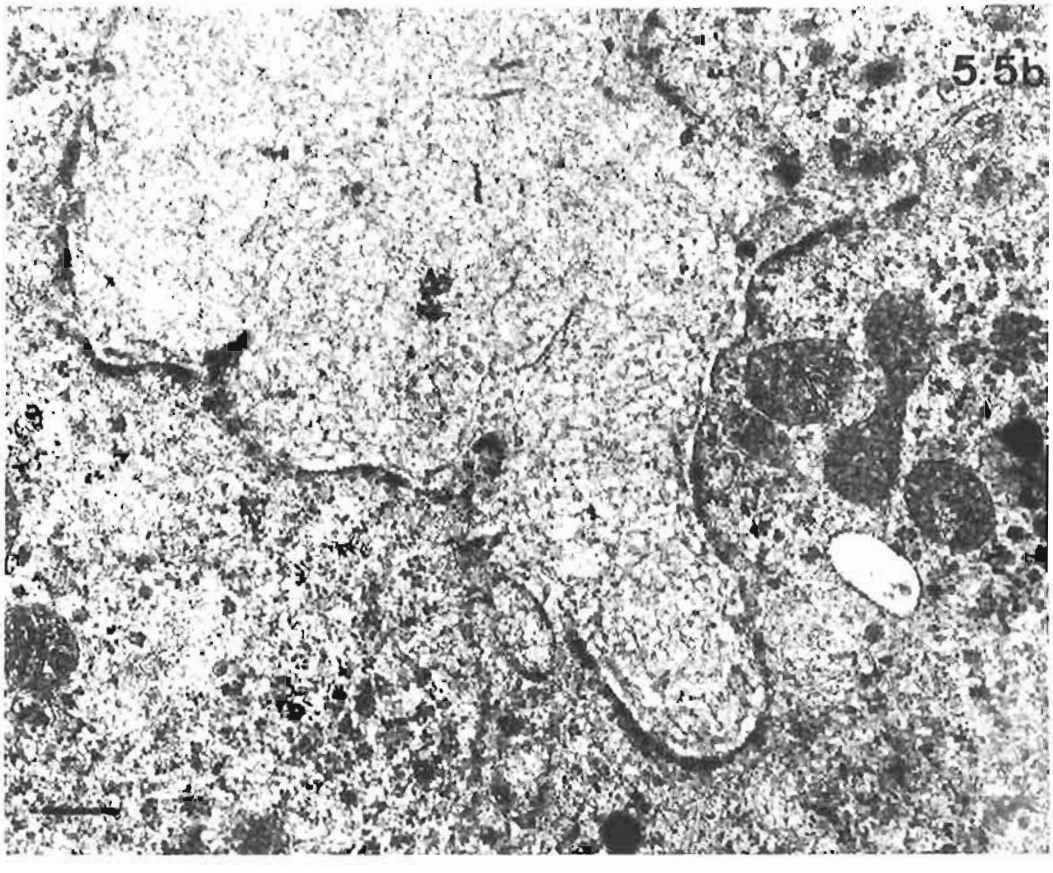

5.5b

Chapter 6

Parathyroid glands in Vombatoidea: *Lasiorhinus latifrons* and *Phascolarctos cinereus*

6.1.1. Introduction - Wombat

Only one reference on the parathyroid glands in wombats and koalas (Fraser, 1915) was found in the scientific literature and that study focused on the embryology and anatomy of the parathyroids in five wombats and ten koalas, all of which were either embryos or pouch young. No detailed study has been recorded of the anatomy and histology of these glands in mature animals.

In the current study, specimens from 13 southern hairy-nosed wombats, *Lasiorhinus latifrons*, were examined, whereas the common wombat, *Vombatus ursinus*, was used in the studies by Fraser (1915) where it was referred to as *Phascolomys mitchelli*. The former species inhabits arid and semi-arid areas of South Australia; the latter is found in forested regions of Tasmania, Victoria and eastern New South Wales. Both species are large, heavy-set with short powerful limbs. Adult body weight and length range from 20 to 40 kg and from 80 to 120 cm respectively with the common wombat being slightly larger and longer than the southern hairy-nosed species. From an overview of a wide range of anatomical studies done on *L. latifrons* and *V. ursinus* there appear to be few differences between the two species (Wells, 1989).

Tissue samples were obtained from ten wombats which had been killed as part of a culling program in farming areas 150 Km north-east of Adelaide, South Australia. Specimens for various research studies (Taggart et al., 1996) had been taken from the dead wombats before each common carotid artery and its bifurcation were exposed. Tissue in this area was excised and placed in electron microscopy fixative with low (0.25%) glutaraldehyde concentration (Appendix B). Approximately 24 hours later, in the Department of Anatomical Sciences, parathyroids (and inadvertently, ganglia etc.) were removed from the larger tissue specimens and processed for electron microscopy. Details are given in chap. 3, Materials and Methods, section 3.5. One wombat, W11, was frozen approximately four hours after death and then later thawed for dissection of the ventral neck.

To investigate the status of parathyroid IV in the wombat, tissue from the entire length of the ventral neck and mediastinum were removed from two wombats W12 and W13, fixed in 10% formalin, and later dissected with the aid of a microscope. Samples from these three animals were processed for light microscopy and sections stained with haematoxylin and eosin (see chap. 3, Materials and Methods, section 3.4).

Examination of parathyroid glands from wombats revealed considerable intercellular material of unknown identity in perivascular areas (See Fig. 6.1b). In order to identify this substance, paraffin sections from wombat W11 and appropriate positive controls (described below) were subjected to the following techniques:

a. Periodic Acid, Schiff's (PAS) (see Appendix H),
b. Toluidine Blue (see Appendix I),
c. Alcian Blue, pH 2.5 and pH 1.0 (see Appendix J).

The following techniques were used to clarify the components of the parenchymal cells and follicles in paraffin sections from wombats W11, W12, and W13. Carbohydrate-rich substances and glycogen were shown by the first technique and oxyphil cells by the second technique.

a. PAS, amylase and PAS, (see Appendix H)
(positive control was rat liver)
b. Altmann's technique for mitochondria (see Appendix G).
(positive control was parathyroid gland with oxyphil cells
from a 72-year old man).

6.1.2. Introduction - Koala

The koala, *Phascolarctos cinereus* is, one of the best known Australian marsupial species and needs little introductory description. The natural distribution of koalas is the eastern coastal and forest areas from north Queensland to Victoria. They have also been successfully introduced to the Mt Lofty ranges and Kangaroo Island in South Australia. Adults range in size from 70 to 82 cm and in weight from 4 to 14 kg with males being larger than females (Taylor, 1984).

In the current study, specimens from six koalas were obtained from post-mortem examinations (see chap. 3, Materials and Methods, section 3.2) and placed in either 10% formalin or electron microscopic fixative. The latter fixative was used if the length of time between death and fixation was less than 20 minutes. A dissection microscope was used to locate tissues of interest and then tissue processing done as previously described (see chap. 3, Materials and Methods, sections 3.4 and 3.5).

Paraffin sections from koalas #3, #4, and #6 were treated with PAS, amylase and PAS, and Altmann's stain in the same ways, for the same reasons, and using the same positive controls as wombat specimens, the details of which were given in the preceding section 6.1.1.

6.2. Results

6.2.1.1. Anatomy - Wombat

Parathyroid glands were found in 16 of the 20 specimens of carotid bifurcations removed from ten wombats and two glands were found in all neck dissections of wombats, W11, W12 and W13. In nine wombats, one parathyroid gland was found in the vicinity of both carotid bifurcations; in three animals a parathyroid was located near the right bifurcation but not the left, while in wombat W1, two separate glands were found on the left but none on the right bifurcation. The lack of bilateral glands in four animals was possibly because of the difficulties associated with the collection of specimens leading to insufficient tissue being removed. Parathyroid III was either on the dorsolateral aspect, very near the adventitia of the common carotid, or adjacent to the bifurcation where it was loosely associated with the origins of the external or internal carotid arteries. It was never found in the interarterial tissue where the carotid body was located. In fact, the carotid body in the wombat did not form a discrete, nodular body and could not be detected with a dissecting microscope. The parathyroid glands were flattened, ovoid structures with dimensions approximately 6 x 4 x 1.5 mm. In wombat W1, the two glands on the left bifurcation were separate structures, one mm caudal to the bifurcation and the other at the origin of the external carotid.

In the dissection of the neck of three wombats (W11, W12, W13), the carotid bifurcation was at a level just cephalic to the thyroid gland. The origins of the internal and external branches were covered superficially by the caudal margin of the posterior belly of the digastric muscle and the diagonally placed omohyoid muscle. Ventral to these structures were the submandibular salivary gland and the cervical thymus. The anatomy of the carotid bifurcation and muscles of the ventral neck was similar to that of the possum (Figs. 7.2a & b).

Examination of sections from mediastinal tissue from wombats W12 and W13 revealed two parathyroid glands (parathyroid IV) and two separate thymic lobes in wombat W12 and one thymic lobe in wombat W13. The dimensions of the roughly ovoid glands and thymic lobes were approximately 2 x 3 mm and 4 x 3 mm respectively. The structures were embedded in fibrofatty tissue where fat cells were clustered together to form globular structures about the same size as the thymic and parathyroid elements.

6.2.1.2 Anatomy - Koala

Examination of neck and mediastinal tissues in the six koalas revealed the presence of parathyroid glands only in the vicinity of the carotid bifurcations and in four of these animals two parathyroids were associated with a carotid bifurcation. The most cephalic position was approximately 2 mm beyond the bifurcation and the most caudal, 4 mm before the same reference point. The carotid bifurcation occurred at the level of the lateral process of the hyoid bone. The caudal part of the digastric and the omohyoid muscles were ventral to the bifurcation with the cervical thymus superficial to them. Of the twelve carotid bifurcations examined, at least one parathyroid gland was found in eight specimens with an additional gland present in five of these eight bifurcations. Table 6.1 shows the animals and number of glands associated with each carotid bifurcation.

Table 6.1. - Anatomy of Parathyroid Glands in the Koala

Koala number	site	number of glands
1	LCB	1
	RCB	1
2	LCB	2
	RCB	2
3	LCB	0
	RCB	2
4	LCB	2
	RCB	0
5	LCB	0
	RCB	2
6	LCB	1
	RCB	0

Abbreviations: LCB - left carotid bifurcation; RCB - right carotid bifurcation

Glands were round to oval except for a specimen from the right carotid bifurcation of koala #2 where two small nodular structures were attached to a larger structure. Ovoid glands measured approximately 3 x 2 x 2 mm. In the four samples of carotid bifurcation where no parathyroid gland was detected, probably insufficient tissue had been excised at the post-mortem. Careful dissection (koalas #4, #6) and serial sectioning (koala #2) of the caudal regions of the neck and mediastinum failed to reveal parathyroid tissue. Furthermore, no thoracic thymus was detected.

6.2.2.1 Light Microscopy - Wombat

Twenty-five parathyroid glands from thirteen wombats were examined with the light microscope. Apart from paraffin sections of eight parathyroid glands from animals W11, W12, and W13, resin sections stained with toluidine blue were used in the study. Twenty-three specimens were from neck dissections and two were from mediastinal tissues; the former were assumed to be samples of parathyroid III and the latter, parathyroid IV.

The round to oval glands were encapsulated with a thin layer of dense connective tissue. Mast cells, obvious by their metachromatic staining with toluidine blue in resin sections (Fig. 6.1a), and some leukocytes, were present in the capsule and pericapillary tissues. Parenchymal cells were tightly clustered into clumps separated by capillaries and other blood vessels with accompanying tissue (Fig. 6.1a). In all specimens there was pale staining material in the pericapillary area (Fig. 6.1b). Often it was acellular with a flocculent appearance suggestive of a glycan composition. The results of the staining of this substance with PAS, toluidine blue, alcian blue pH 2.5, and alcian blue pH 1.0 are shown in Table 6.2. Human liver and possum colon were used as positive controls.

Table 6.2. - Characteristics of Intercellular Perivascular Substance in Parathyroid Gland of the Wombat.

tissue	Tol. Blue	PAS	AB pH 2.5	AB pH 1.0
intercellular substance	pale purple	-ve	-ve	-ve
follicular contents	blue	+ve	-ve	-ve
principal cells	blue	+ve*	-ve	-ve
mast cells	blue	-ve	-ve	-ve
hepatocytes (+ve control)	blue	+ve	-ve	-ve
colonic goblet cells (+ve control)	pale purple	+ve	+ve	+ve
mucosal mast cells (+ve control)	purple-red	-ve	-ve	-ve

Abbreviations: Tol. Blue - Toluidine blue, PAS - Periodic Acid, Schiff's, AB - Alcian Blue.
+ve* - Fine PAS positive granules were present in some cells.

Cysts and follicles, as defined in chap. 2, Literature Review, section 2.5.1, were common in many specimens. Cysts and follicles were present in twelve glands (Fig. 6.2) and two glands from animals W8 and W11 had follicles but not cysts. Some cysts were very large with very irregular profiles and lined by several different types of cells. The lumen of each cyst was filled with evenly stained material in which macrophage-like cells, leukocytes and lipid droplets were present (Fig. 6.2). The smaller follicles were lined by cells similar to parathyroid principal cells and luminal contents were acellular and homogeneous (Fig. 6.1b). The colloid-like material in follicles and cysts was PAS positive, didn't display metachromasia with toluidine blue, and was negative with alcian blue at pH 2.5 and pH 1.0 (see Table 6.2).

In routine paraffin sections, the cytoplasm of the parenchymal cells was pale and acidophilic; intensely acidophilic cells indicative of oxyphil cells were not present. Altmann's technique for mitochondria clearly demonstrated oxyphil cells in the positive control but no mitochondria-rich cell was revealed in wombats W11, W12, and W13. Sections stained with PAS had fine, bright pink granules that were slightly fewer in number in amylase/PAS sections. Several types of parenchymal cells were noticed in the toluidine blue stained resin sections. Although all sections had light and dark parenchymal cells, many cells had a medium staining intensity to their cytoplasm. Dark osmiophilic granules featured in some cells (Figs. 6.1a & 6.3a). Oxyphil cells were larger than principal cells, with a coarse granular cytoplasm (Fig. 6.3a). In several glands, dark staining cells with elongated shapes (Fig. 6.3a) were interspersed among the other cells. Their nuclei were smaller and more hyperchromatic than those of surrounding principal cells and some cells showed cytoplasmic granules.

Thymic tissue was included in the parathyroid gland of wombats, W6 and W12. In the former animal, the rounded mass of thymus, measured 0.9 mm in diameter, and was positively identified by the presence of Hassall's corpuscles and the lack of nodules or subcapsular sinus. Vascular connective tissue partially separated the two tissues but in several places thymic cells appeared to mingle with parathyroid cells without any obvious intervening connective tissue (Fig. 6.3b). In wombat W12, adjacent to the parathyroid, was a thymic lobe only slightly smaller than the gland; intermingling of the two tissues appeared in one location.

In a specimen from wombat, W1, there was an unusual encapsulated, nodular structure on the surface of the otherwise normal parathyroid gland (Fig. 6.4). In the nodule parenchymal cells were larger and more variable in appearance than those in the other parts of the gland. The large pale staining cells, many of which had a large vesicular nucleus, were arranged in a reticulate endocrine manner. Some cells had large unstained cytoplasmic inclusions; others had a granular appearance (Fig. 6.4). Compared with the

rest of the parathyroid gland the nodule had more connective tissue cells and possibly leukocytes accompanying the capillaries.

6.2.2.2 Light Microscopy - Koala

Thirteen parathyroid glands from six koalas were examined with the light microscope. Resin sections (eight glands) stained with toluidine blue and paraffin sections (five glands) were used. Glands were encapsulated but not lobulated. Minimal amounts of connective tissue accompanied the numerous capillaries and surrounded clumps and strands of principal cells. Mast cells were not conspicuous and failed to show intense metachromasia with toluidine blue staining. In resin sections, most principal cells had a similar intensity of cytoplasmic staining; light and dark cells were not generally distinguishable (Fig. 6.5a). Cells in clumps were oval or elongated with vesicular nuclei placed towards the periphery of the clump. Perinuclear cytoplasm was often pale staining or showed collections of vacuoles. Occasionally parenchymal cells with very pale staining cytoplasm or with numerous unstained vesicles were present (Figs. 6.5a & 6.5b), either scattered in amongst principal cells or in small clusters (Fig. 6.5b). In paraffin sections the cytoplasmic staining of parenchymal cells ranged from quite intensely acidophilic to pale, patchy acidophilic. No oxyphil cells were detected in the three glands stained with Altmann's technique for mitochondria. Sections stained with PAS and amylase/PAS showed positively stained granules in some principal cells. Staining was slightly less in sections treated with amylase prior to PAS staining.

Follicles were observed in ten glands. Follicular content was homogeneous, PAS positive, and acellular. It was surrounded by a single layer of cells varying from low cuboidal to high columnar. Cells in the latter category displayed partial polarity with eccentric nuclei located towards the periphery of the follicle (Figs. 6.5a & 6.5b).

6.2.3.1 Electron Microscopy - Wombat

Electron microscopy confirmed the light microscopic observations of a compact arrangement of parenchymal cells. A thin capsule surrounded the gland and although septa were absent, small blood vessels and even capillaries were accompanied by broad bands of quite dense connective tissue (Fig. 6.6a). The unidentified intercellular substance described in light microscopy (see section 6.2.2.1) had the ultrastructure of collagen fibres set in a meshwork of fine, short, fibrils of unknown identity. (Fig. 6.6b). The fibrils and collagen fibres were densely arranged with a notable paucity of fibrocytes and such wide tracts of dense connective tissue were unexpected to be along side small, fenestrated capillaries. The fine fibrils appeared to extend from the basal lamina into the band of collagen fibres (Fig. 6.6a). Patches of connective tissue cells, including mast cells, and leukocytes were also present in the perivascular spaces (Fig. 6.7a); a basal lamina separated parenchymal cells from perivascular components (Fig. 6.7a). Some

glands appeared to show an infiltration of phagocytic cells where very irregularly shaped cells were squeezed in between parenchymal cells (Fig. 6.7b). They had many short processes with many vesicles featured in the cytoplasm which was more electron dense compared with that of parenchymal cells. Nuclei were hyperchromatic, not lobulated and similar sizes to nuclei of parenchymal cells (Fig. 6.7b).

Principal, oxyphil and transitional cells made up the parenchymal cell population. Cell membranes occurred close together with desmosomes present between principal, transitional and oxyphil cells (Fig. 6.8a). In certain regions around the cells the membranes separated slightly forming small canaliculus-like structures (Fig. 6.8b). These canaliculi were distinguished easily from the apparent artefactual shrinkage that was present between some parenchymal cells in the central regions of the specimen block as a result of inferior preservation (Fig. 6.9b).

Most specimens had both light and dark principal cells (Fig. 6.8b) but the majority of cells showed medium density to the staining of the cytoplasm. Cell shape varied from polygonal to spindle (Figs. 6.7b & 6.8b); the round to oval nuclei were mainly vesicular and there appeared to be no correlation between cytoplasmic density and the amount of nuclear heterochromatin. Principal cells showed scant RER with narrow cisternae (Fig. 6.8b) sometimes arranged in a whorl (Fig. 6.9a). Golgi bodies were seldom seen and were quite small. Electron dense granules, identified as secretory vesicles, had an estimated diameter 600 nm. They were in both light and dark cells and often occurred in clusters (Fig. 6.8b & 6.9a). In some cells there were very large (3.4μm), membrane-bound, electron dense inclusions that occupied most of the cytoplasm (Fig. 6.9b). Lipid droplets were not uncommon, appearing osmicated in some preparations and electron light in others (Fig. 6.7a). The homogeneity of the lipid inclusions and the lack of unit membrane distinguished them from rarely seen lipofuscin granules. Mitochondria were oval or tubular. Apart from some being very long (one estimated to be 10μm), the morphology was unremarkable.

Oxyphil cells were seen in parathyroid glands from three wombats, W1, W2, and W3. Unfortunately the fixation of these specimens was not perfect resulting in some fine structural details not being preserved. Oxyphil cells were scattered singly among principal cells. The central, round nucleus contained perhaps more heterochromatin than principal cells. The cytoplasm was packed with mitochondria with a similar appearance to those in principal cells. No extra large, misshapen or tortuous mitochondria were seen. Few other organelles and inclusions were present apart from some peripheral granular structures (Fig. 6.10a).

Transitional cells were characterized by the presence of many mitochondria but not as densely packed as those in oxyphil cells. The increased number of mitochondria occurred

with a diminished amount of cytoplasmic matrix, organelles, and inclusions compared with a principal cell (Fig. 6.10b). Ribosomes, RER, and small secretory granules were scattered in amongst the mitochondria.

Ultrastructural examination of follicles confirmed light microscopic observations that the cells lining the follicle were similar to parenchymal cells and luminal contents had a fine granular homogeneity. Cysts (Fig. 6.11a) were lined by one or two layers of cuboidal to columnar cells, some of which showed polarity with the nucleus at the end of the cell further from the lumen. Generally cells were similar to principal cells apart from perhaps having fewer secretory granules and the presence of large cytoplasmic inclusions. Interspersed among the lining cells were irregular, electron dense leukocytes and/or macrophages (Fig. 6.11a) that appeared to be migrating to the lumen where similar cells in varying states of phagocytosis and degeneration were observed (Fig. 6.11b). Cell membranes abutting onto the follicular lumen had short microvillous projections. At the periphery, the colloid-like contents of the cysts often had round electron lucent components that had similar appearances to the large cytoplasmic inclusions of the lining cells (Fig. 6.11b). The intraluminal leukocytes and/or macrophages showed many large phagosomes, the contents of which were identical in appearance to that of the surrounding "colloid" (Fig. 6.11b). Cells with lobulated nuclei were identified as neutrophils and those with a single, comparatively larger nucleus were identified as macrophages. The cytoplasm of both cell types showed slender microvilli or pseudopodia associated with phagocytosis. Many cells appeared to be degenerative because nuclei were hyperchromatic and phagosomes appeared to be fusing or losing encasing membranes.

The nodule in a parathyroid gland from wombat W1 had a very unusual ultrastructure (Fig. 6.12a). Many cells featured an electron-lucent cytoplasmic matrix with tiny electron dense granules, approximately 140 nm in diameter and no more than a quarter the size of secretory granules (600 nm) in the adjacent "normal" parathyroid tissue. Interspersed amongst the myriad of small granules were large empty vacuoles, lipid droplets, patches of fine fibrillar material, and mitochondria that lacked normal structural organisation (Figs. 6.12a & 6.12b). Most cells had nuclei with more heterochromatin than parathyroid principal cells but some nuclei appeared very active with abundant euchromatin (Fig. 6.12b).

Electron microscopic examination of the parathyroid gland from wombat, W6, confirmed the light microscopic observation that thymic and parathyroid tissues were intermingled without intervening basal laminae. A definite junction between the two tissues was difficult to locate because of the inclusion of lymphocytes in amongst parathyroid principal cells but long, thin cytoplasmic processes of presumably epithelial reticular cells could be identified with mainly one tissue type on either side (Fig. 6.13). The thymic tissue appeared to be functional judging by the appearance of macrophages actively

engaged in phagocytosis of presumably defective thymocytes (Fig. 6.13) and the typical arrangement of thymocytes, epithelial reticular cells and Hassall's bodies.

6.2.3.2 Electron Microscopy - Koala

The ultrastructure of the koala parathyroid gland was compiled from viewing sections of five glands from three animals (koalas #1, #2, and #5). The parenchymal cells were compactly arranged with relatively straight boundaries and few interdigitations. The cytoplasm of most cells showed similar light to medium staining intensity making light and dark cells indistinguishable (Fig. 6.14a).

Cells often expressed limited polarisation with the vesicular nucleus being eccentric and vesicles clustering towards the other end (Fig. 6.14b). Granules and inclusions presented a variety of appearances ranging from small electron dense secretory granules (200 - 400 nm) (Fig. 6.15a), to larger heterogeneous lysosomes (Fig. 6.15a), lipid inclusions and finally to the very large vesicles that were 4.5µm in diameter and dominated the cytoplasm (Fig. 6.15b). The large vesicles were either unstained or had fine granular contents; cells with single, large vesicles usually had no or few smaller granules (Fig. 6.15b). Cells with large vesicles were usually part of follicles.

Other organelles and inclusions besides granules and vesicles did not have unusual features. The Golgi bodies were small and poorly developed and rough and smooth endoplasmic reticulum were relatively sparse. Occasionally the lumina of the endoplasmic reticulum were distended (Fig. 6.16a). The number of mitochondria per cell was variable but no cell with the appearance of an oxyphil cell packed with mitochondria was present. Apart from mitochondrial inclusions seen in one gland (Fig. 6.16b), mitochondria were unremarkable in appearance.

Follicles were present in four of the five glands examined with the electron microscope. They were lined by one or two layers of parenchymal cells and some cells had short microvillous processes projecting into the centre. The fine granular contents of the follicles were similar in appearance to the large vesicles in some parenchymal cells (Figs. 6.15b & 6.17). This material was a colloid-like product. Canaliculus-like structures were present between adjacent lining cells and the follicular cells appeared perhaps to have fewer secretory granules than other parenchymal cells. The presence of the intercellular canaliculi and the similarity in the appearance between the contents of the follicles and large intracellular vesicles suggests the follicular cells produce and store the colloid-like material of the follicles before secreting it into the tiny intercellular canaliculi and then storing it extracellularly.

6.3. Discussion

6.3.1.1. Anatomy - Wombat

From the current study it appears that in the wombat, *L. latifrons*, parathyroid III is located in the vicinity of the carotid bifurcation and parathyroid IV is in the mediastinum. Failure to locate parathyroid III in some specimens was probably because insufficient tissue was sampled. Due to the diverse interests of the researchers who took specimens from the culled wombats, there were some limitations associated with obtaining suitable tissue samples. Also difficulties were encountered by the presence of blood haemorrhaging from the major vessels in the area of interest. The location of parathyroid III in the adult wombat is similar to that in the embryo where the anlage of the gland migrates from the third pharyngeal pouch to the carotid bifurcation (Fraser, 1915).

The finding of a thoracic thymus in the wombat is contrary to previous studies (Symington, 1898; Fraser, 1915; Yadav, 1973) where its absence has been recorded in thirteen out of sixteen animals. Fraser (1915) examined serial sections of embryos whereas Symington (1898) and Yadav (1973) viewed histological specimens selected from dissections of the mediastinum. It is quite possible that in the latter method, small thymic structures may have been overlooked. When the results of the current study are added to the existing information then it can be stated that a thoracic thymus has been detected in five out of eighteen (28%) wombats examined. Thus the current study does not strengthen the hypothesis, proposed by Yadav (1973) that a thoracic thymus is absent in wombats.

The presence of parathyroid IV in one of the two mediastinal samples dissected reflects a similar frequency of occurrence noted by Fraser (1915) where parathyroid IV was detected in three of five embryos. However the absence of the gland in one specimen in the current study may be because it was overlooked in dissection.

6.3.1.2. Anatomy - Koala

The examination of six koalas has shown that there appear to be four parathyroid glands located in the neck of the koala. Presumably parathyroid III and parathyroid IV occur on either side with the former gland more cephalic in location. Failure to find glands in some animals was possibly related to insufficient tissue sampling at the post-mortems although it may reflect either failure of development of parathyroid IV or a caudal location of parathyroid IV in the mediastinum. Studies on the development and migration of parathyroid IV in koala embryos and pouch young showed that it failed to develop in five out of nine specimens and had a variable location from near the thyroid to the origin of the carotid arteries (Fraser, 1915). The current study revealed a higher incidence of parathyroid IV in the koala, i.e. two glands were found on one or both sides in four out of

six animals (67%), compared with the earlier study by Fraser (1915) where parathyroid IV was identified in four out of nine (44%) specimens.

The lack of a thoracic thymus in all three mediastinal specimens examined in the current study supports the earlier observations that have been made by Johnstone (1898), Symington (1900) and Fraser (1915), but is in disagreement with Yadav (1973) (see chap. 2, Literature Review, section 2.4.2). In summarising the current and previous studies, a thoracic thymus has been found in only three out of twenty (15%) specimens examined, suggesting that it is usually absent in the koala.

6.3.2.1. Light Microscopy - Wombat

The intercellular material that was seen in the pericapillary regions of the parathyroid gland was negative with PAS and alcian blue staining but slightly metachromatic with toluidine blue (See Table 6.2). These results suggest glycans were probably not a major component of the intercellular material. Mast cells were metachromatic in resin sections stained with toluidine blue but failed to give positive reactions to all the glycan staining tests applied to paraffin sections (See Table 6.2). This variability in staining can partly be explained by the methods of tissue fixation and preparation. Most specimens embedded in resin, were fixed promptly after death, whereas autolysis occurred during the time elapsed between death and fixation of paraffin embedded tissue samples. Hence mast cells were well preserved in resin sections, but poorly in paraffin sections. The fixation of mast cells may have been better with formaldehyde/glutaraldehyde electron microscopic fixative than with formalin.

The results of staining principal cells with PAS and amylase/PAS suggested that a small proportion of PAS positive granules were glycogen but most contained glycans resistant to amylase digestion. The lack of staining with PAS after amylase treatment in the positive control section of liver demonstrated the validity of the technique. The luminal contents of follicles and cysts contained glycans with a similar staining pattern to that of the majority of granules in the principal cells suggesting a link between the two. The colloidal substance may be a product of the principal cells lining the follicles and cysts. Follicles and cysts are discussed in more detail in chap. 11., General Discussion, section 11.3.

With the light microscope, oxyphil cells were relatively inconspicuous in the wombat compared with their distinct appearance in other mammals including humans (Roth and Schiller, 1976; DeLellis, 1993). In fact their presence in resin sections was realised only after they had been detected with the electron microscope. In human parathyroid glands, oxyphil cells are larger and have a more hyperchromatic nucleus compared with principal cells and often form large clumps. In routine paraffin sections they stain with intense

acidophilia (DeLellis, 1993; personal observations) whereas in resin sections, stained with toluidine blue, oxyphil cells are darker staining than principal cells and have a fine, compact, granular appearance to the cytoplasm (personal observations). In the wombat, oxyphil cells were only detected in animals from which resin sections were prepared. In these sections, stained with toluidine blue, oxyphil cells were scattered amongst the principal cells, not in clumps and differed from human oxyphil cells in that the cytoplasm was filled with fine vesicles instead of dark staining compact granules. No suggestion for this difference in staining of the mitochondria with toluidine blue can be offered.

The appearance of the nodular structure in wombat W1 is discussed below in section 6.3.3.1.

Thymic tissue associated with the parathyroid gland in wombats W6 and W12 was presumably derived from the third pharyngeal pouch, the same embryonic site as parathyroid III. If intermingling of the two cell types occurred early in development, then thymic tissue would migrate with the parathyroid III anlage to the observed location near the carotid bifurcation (Fraser, 1915; Fraser and Hill, 1915; Adams, 1955). The fact that thymic tissue was found in only two of twenty-three specimens reflects the general consensus that, in the wombat, the third pouch has little or no input to thymus III (Fraser, 1915; Yadav, 1973).

6.3.2.2. Light Microscopy - Koala

The light microscopic structure of the parathyroid glands of koalas was similar to that of many other animals (Roth and Schiller, 1976) except for the frequency of follicles (ten of thirteen glands) and the numerous unstained vesicles in the principal cells. Follicles are discussed in more detail in chap. 11, General Discussion, section 11.3 and the unstained vesicles are discussed below in section 6.3.3.2.

Subtle differences were present in the light microscopic structure of the parathyroid glands from wombats and koalas. For example, the wide tracts of dense connective tissue in the wombat gland were absent in the koala where minimal connective tissue elements were present. Cysts were quite common in the wombat but not found in the koala. Similarly no thymic tissue was associated with the koala parathyroid. In fact, of the marsupials studied in the current project, the bandicoot (see chapter 5) and the koala were the only species in which thymic and parathyroid tissues were not occasionally mingled. Finally the presence of oxyphil cells in the wombat was a feature not shared by other marsupials. These differences suggest that perhaps the closeness of the two phascolomid species in the phylogenetic scale is of less consequence in determining structure of the parathyroid gland than the diverse influences of diet, habitat and other factors. Similar conclusions have been reached in the reptilian families, Chelonia (turtles and tortoises)

and Lacertilia (lizards) where correlations between parathyroid structure and phylogenetic homologies are less apparent than the correlations between parathyroid structure and diet and habitat (Srivastav et al., 1995).

6.3.3.1. Electron Microscopy - Wombat

Ultrastructural studies revealed imperfect fixation in some animals. Again the circumstances under which the specimens were obtained sometimes imposed delays between the death of the animal and immersion of tissue in fixative. Also if fibrofatty tissue covered the parathyroid gland then the penetration of the fixative was impaired and autolysis present. The lack of prompt fixation possibly contributed to the crenated appearance of the parenchymal cells in W9 and the lack of mitochondrial detail in animals W1, W2, and W3.

The wide tracts of dense connective tissue that accompanied the vascular supply in the wombat parathyroid gland were unusual. The presence of many fine electron dense fibrils in amongst the collagen fibres may have accounted for the unusual flocculent appearance of the connective tissue in light microscopy. The composition of these fibrils was not identified but from their morphology and staining characteristics, they probably belonged to the collagen family of proteins rather than connective tissue proteoglycans.

The identity of the numerous phagocytic cells which were seen in some parathyroid glands remains an enigma although the suggestion of macrophages was made in the results (section 6.2.3.1). Cells with these characteristics were confined to the parathyroid gland; they were not present in the adjacent tissue samples, suggesting their presence was related to an localised intraglandular condition. Other possible identities that were considered for these cells included mast cells, neutrophils and pyknotic principal cells. They were identified as macrophages because of their long cytoplasmic processes and numerous granules that, unlike mast cell granules in the same sections, were not metachromatic with toluidine blue. The large, non-lobulated nuclei were also more characteristic of macrophages rather than neutrophils. Similar cells appeared to be migrating into the lumina of cysts. Numerous macrophages have not featured in descriptions of parathyroid glands in health or disease (Nilsson, 1977; DeLellis, 1993; Cinti and Sbarbati, 1995). Perhaps they have a phagocytic role in the lumen of cysts and move through the parenchymal cells in their passage from the vascular system to the cysts. However structural evidence for this function was lacking because areas adjacent to cysts did not appear to have higher densities of these cells.

Another explanation for the presence of these electron dense, irregular shaped cells is that they do not have a haemopoietic origin at all. Instead, they represent dying parenchymal cells. The very hyperchromatic nucleus is consistent with pyknosis but not the long

cytoplasmic processes and numerous, intact vesicles. If the cells were pyknotic then, assuming the tissue is normal, a small number of mitotic cells would be expected to be seen so that cell population numbers can be maintained. Of course the number of cells seen in mitosis will be far less than pyknotic cells because the mitotic phase for cells is much shorter than pyknosis (Alberts et al., 1994). However no mitotic cells were seen in any section of parathyroid tissue. Although information pertaining to the rate of turnover of parathyroid principal cells has not been found in the literature the mitotic index indicates a long lifespan. In the rat parathyroid gland, the mitotic index, i.e. the mean number of cells in mitosis per mm^3 of parenchymal tissue, has been estimated as 1.2 ± 0.3 (Hansson et al., 1971).

In the current study of marsupials and monotremes, oxyphil cells have been detected in the parathyroid glands of only wombats. Many hypotheses have been proposed for the formation of oxyphil cells in parathyroid glands and these have been reviewed in chap. 2, Literature Review, section 2.8. Whether the occurrence of oxyphil cells in *L. latifrons* is related to increasing age or results from its unique physiology is not known. Unfortunately the increased incidence of oxyphil cells in elderly wombats cannot be investigated because no known method exists for determining the age of mature wombats. The dentition does not show specific age-related patterns due to both the incisors and molars being open-rooted and growing continuously throughout life (Wells, 1989). Captive wombats have an average life expectancy of about 20 years (Triggs, 1988) that is similar to the lifespan of other herbivorous mammals (cows, horses) in which oxyphil cell numbers have been related to increasing age (Roth and Schiller, 1976). However, the western grey kangaroo, *Macropus fuliginosus*, is a herbivore with a similar life-span to *L. latifrons* and no oxyphil cells were found in this marsupial (see chapter 8). This raises questions into what is different in the physiology of *L. latifrons* compared with *M. fuliginosus* to account for the unique presence of oxyphil cells in the former species. Compared with the kangaroo, the wombat has a much better water conservation mechanism and is able to exist without drinking water. Hot, low humidity conditions of day-time are avoided in the protection of cool, moist burrows and water loss is minimal due to reabsorption of water from the kidney tubules and distal colon. Of all mammals, the hairy-nosed wombat produces the driest faecal pellets (Wells, 1989). A suggestion is made that the exceedingly low water turnover rate and the relative longevity of *L. latifrons* impose certain demands on the parathyroid glands that result in the manifestation of oxyphil cells.

The unusual nodular structure (Figs. 6.4, 6.12a & b) that was present in a parathyroid gland from wombat W1 was probably pathological and not representative of the normal histology. Cellular ultrastructure was distinctly different from the surrounding parathyroid principal cells and there was increased leukocytic infiltration. The patches of tonofilaments and increased number of secretory(?) granules that were observed in the

current study have previously been described as features found in primary hyperparathyroidism and parathyroid adenomas in humans (DeLellis, 1993; Cinti and Sbarbati, 1995).

The apparent mingling of thymic and parathyroid tissues has been noticed in many marsupials, not just wombats, in this current study and consequently is discussed in chap. 11, General Discussion, section 11.5.

6.3.3.2. Electron Microscopy - Koala

The ultrastructure of the parathyroid glands in the koala is similar to that described for many mammals (Roth and Schiller, 1976). The unusual features are the prevalence of follicles and the presence of lipid inclusions and large pale staining vesicles in the parenchymal cells. Lipid inclusions were widespread in the parenchymal cells whereas cells with large vesicles were mainly associated with follicles. Follicles are infrequently encountered in parathyroid histology (Roth and Schiller, 1976; Nilsson, 1977; DeLellis, 1993; Cinti and Sbarbati, 1995). In the current project, of all the marsupial parathyroids examined, follicles were most common in the koala. The possible origin and function of parathyroid follicles are discussed in more detail in chap. 11, General Discussion, section 11.3. The number and size of lipid inclusions in the parenchymal cells were unique to the koala compared with parathyroid glands from other marsupials. Lipid droplets are relatively abundant in the resting phase of principal cells (Roth and Capen, 1974; Nilsson, 1977; DeLellis, 1993; Cinti and Sbarbati, 1995). In the normal human parathyroid gland 80% of principal cells have been shown to contain lipid droplets and the reduced amount of lipid has been used as a criterion to classify hyperplasia and adenoma (Cinti and Sbarbati, 1995). However it is acknowledged that other factors besides secretory activity influence the number of lipid droplets. For example, a study on the effects of insulin deficiency and parathyroid function and morphology in rats showed normal parathyroid functions but increased amounts of lipid in the principal cells (Bertoni et al., 1988). In view of this information on the quantity of lipid droplets in principal cells two explanations are offered for the prominence of lipid in koalas. Either the accumulated lipid represents a peculiarity of the species and is unrelated to secretory cycles or the koala has a high percentage of cells in the resting phase of the secretory cycle, reflecting a low glandular activity.

The link between the colloid-like material of the follicles and the large intracellular vesicles of the lining cells, that was suggested in the results matches similar proposals made for human parathyroid glands (Cinti and Sbarbati, 1995). However these researchers concluded that the colloid-like substance had both a lipid and colloid nature whereas in the current study the total lack of osmiophilia indicated lipids were probably not part of the stored material. Canaliculi were suggested as the means of transport for the

secretion from principal cells to the follicular lumen. A similar mode of intercellular transport has been identified in the parathyroid gland of the rat (Wernerson et al., 1995) where a three-dimensional study revealed an intercellular pathway for secretion released from areas of membranes quite distant from capillaries.

Plate 6.1. Light microscopy of wombat parathyroid - I

Fig. 6.1a. Shows the compact arrangement of light and dark principal cells and quite substantial amounts of connective tissue that accompany the capillaries. Mast cells (arrows) are present in the pericapillary tissue.
1μm resin section, toluidine blue
Wombat W1
Bar: 10μm

Fig. 6.1b. Shows that all parenchymal cells have a similar intensity of cytoplasmic staining and that the abundant extracellular material (E) is compactly arranged in the perivascular areas. Note that the two follicles are lined by cells identical to parenchymal cells.
1μm resin section, toluidine blue
Wombat W1
Bar: 20μm

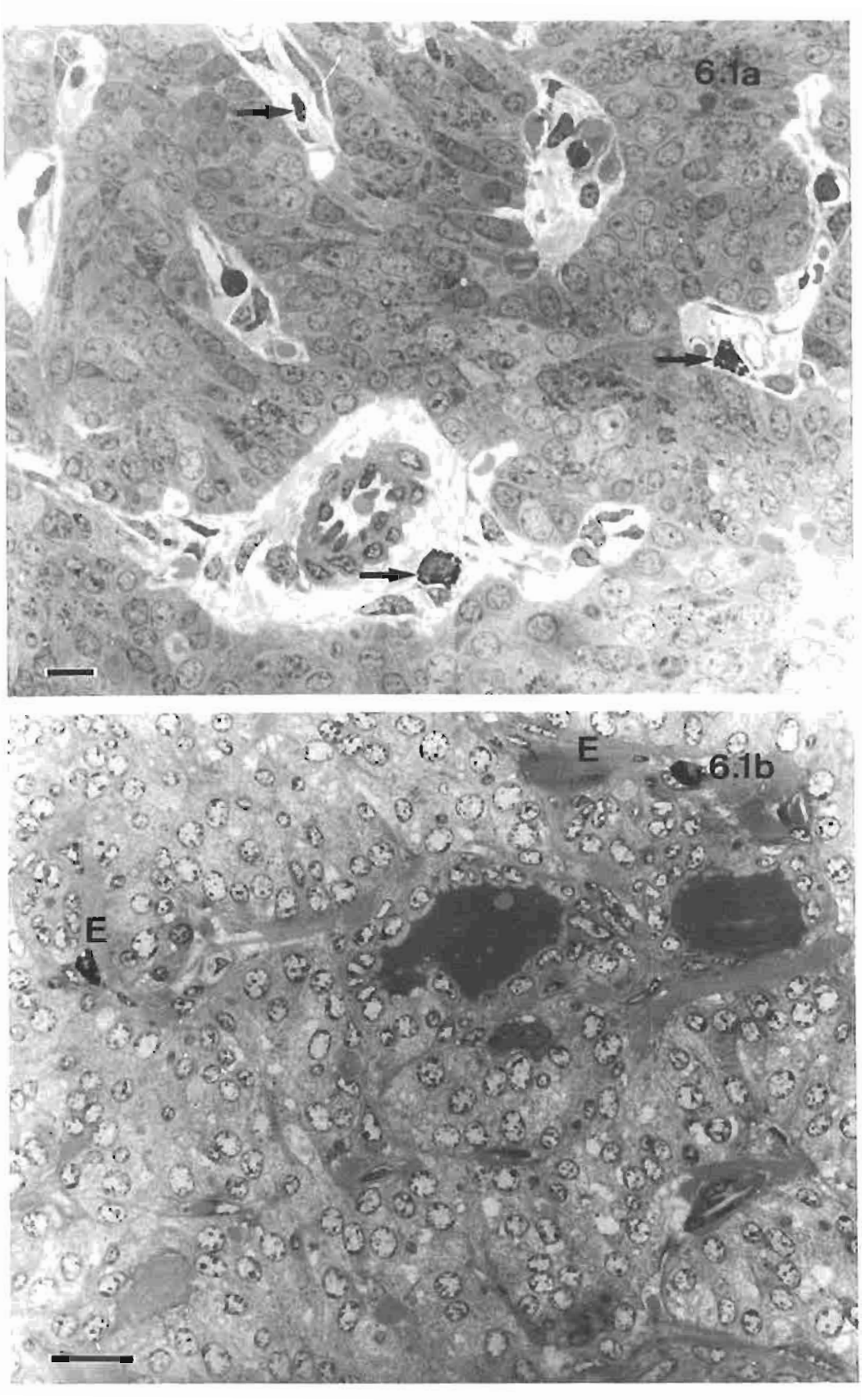
6.1a
E
6.1b
E

Plate 6.2. Light microscopy of wombat parathyroid - II
Follicles and cysts

Fig. 6.2. Shows a follicle and cysts that are common components of parathyroid glands. Note, compared with the follicle, the cysts are larger, have irregular outlines, are lined by cells usually different in appearance to surrounding principal cells and lipid droplets as well as a variety of cells, including leukocytes, are present in the lumen.
1μm resin section, toluidine blue
Wombat W1
Bar: 30μm

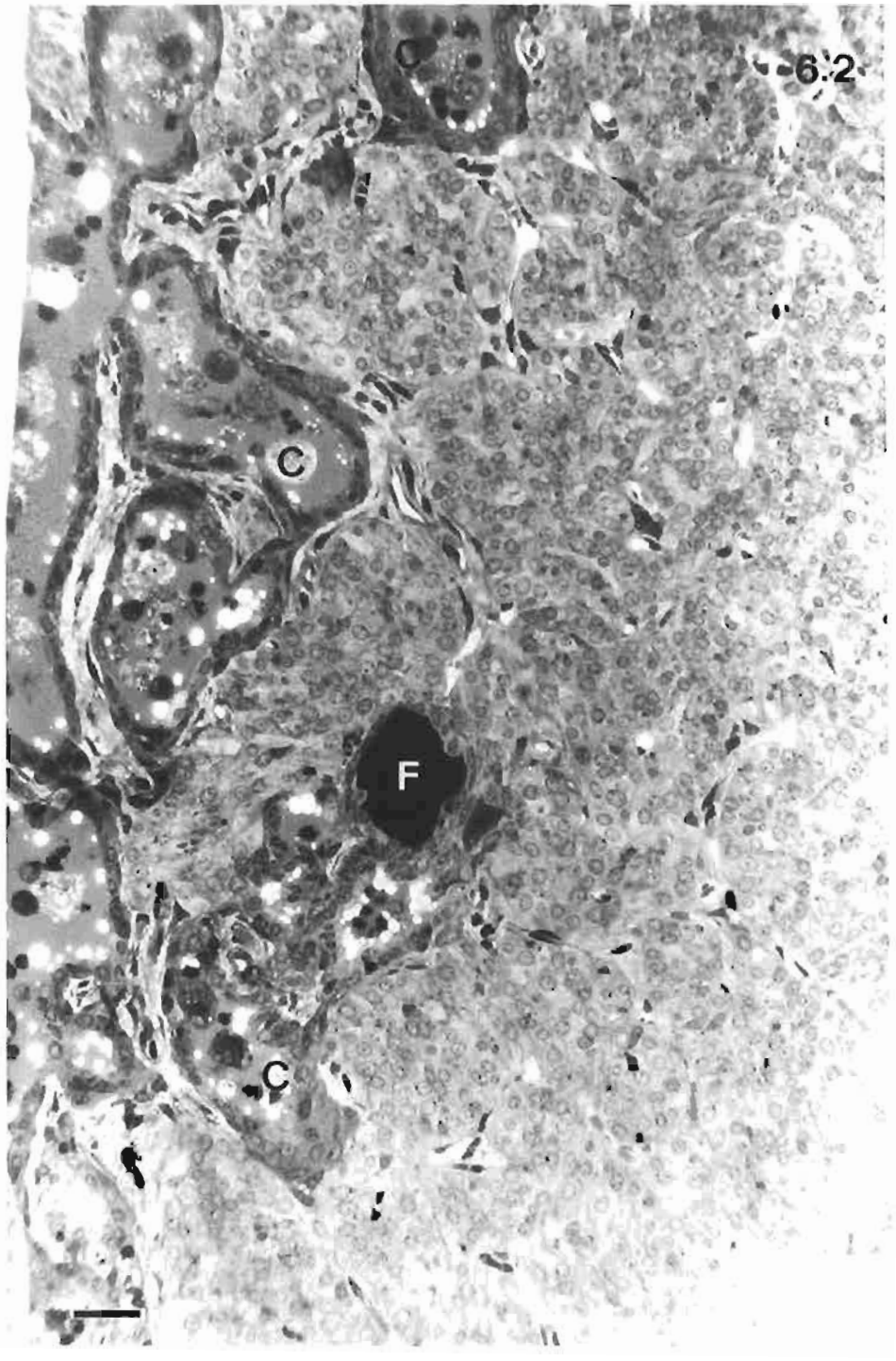
6.2
C
C
F
C

Plate 6.3. Light microscopy of wombat parathyroid - III
Oxyphil cells and thymus

Fig. 6.3a. Shows small, elongated, dark cells (C) interspersed with principal cells and two oxyphil cells (O). Note that compared with principal cells, the oxyphil cells are larger, less elongated in shape and have an even distribution of fine vesicles that are thought to be mitochondria.
1µm resin section, toluidine blue
Wombat W2
Bar: 5µm

Fig. 6.3b. The low power micrograph illustrates the mingling of thymic and parathyroid tissues. In the centre of the micrograph, no obvious connective tissue barriers separate thymus (left) from parathyroid (right).
1µm resin section, toluidine blue
Wombat W6
Bar: 50µm

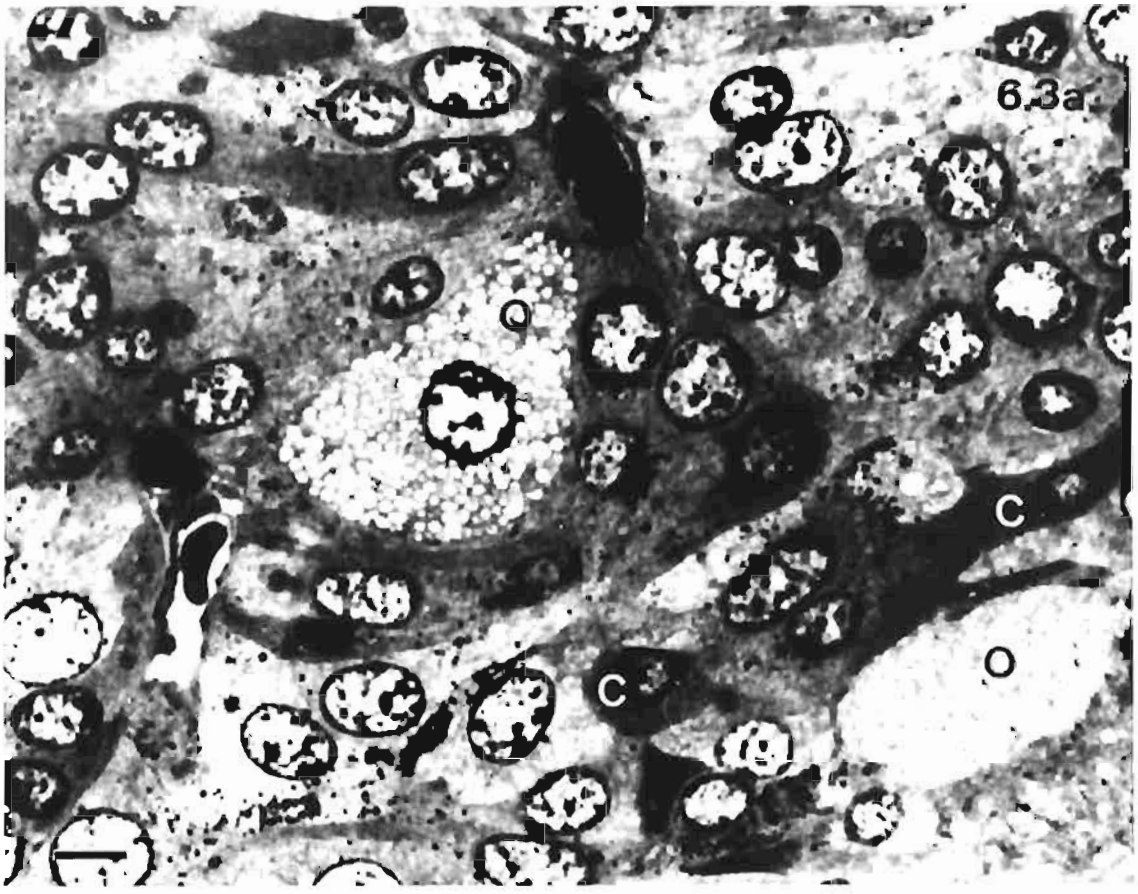
6.3a
C
C
O

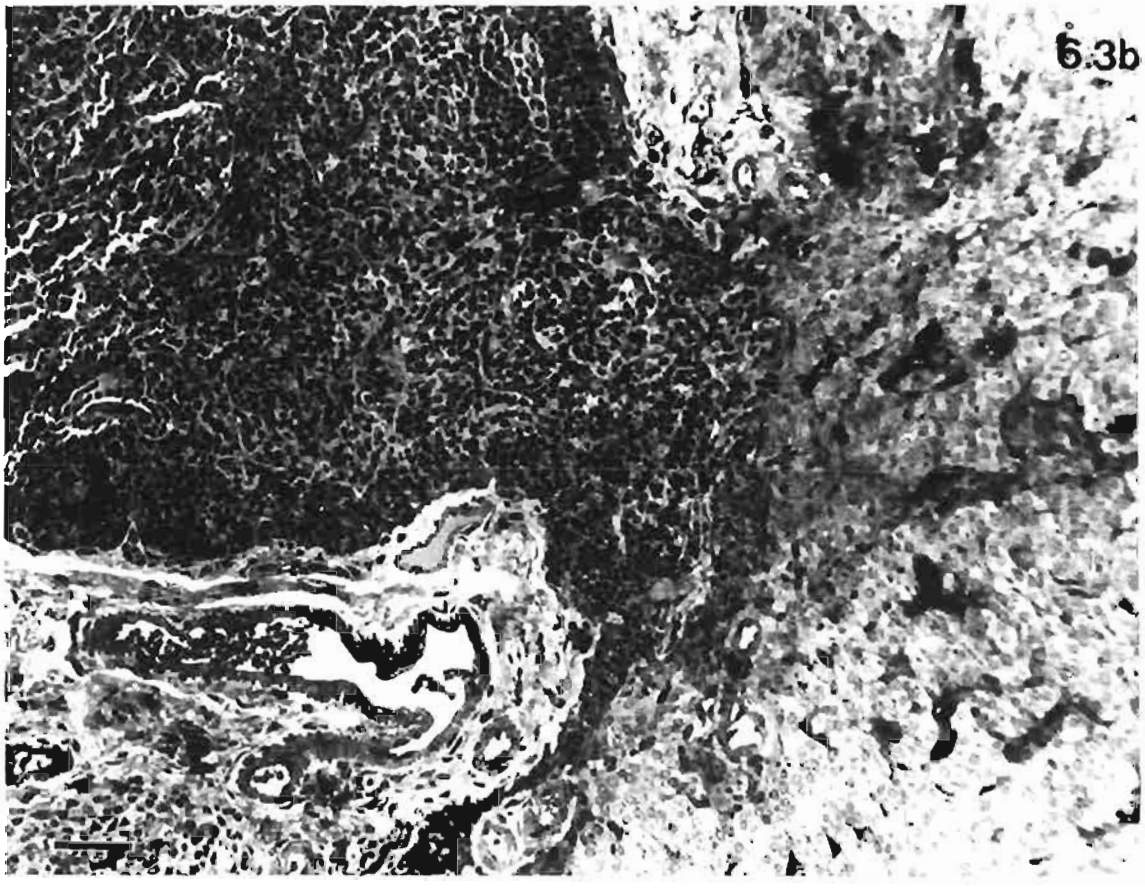
6.3b

Plate 6.4. Light microscopic structure of nodular structure in parathyroid gland in wombat W1

Fig. 6.4. Shows the nodular structure, found associated with a parathyroid gland in wombat, W1. Large, pale vacuolated cells, connective tissue cells and leukocytes form a reticulate endocrine structure in the nodule.
1µm resin section, toluidine blue
Wombat W1
Bar: 20µm

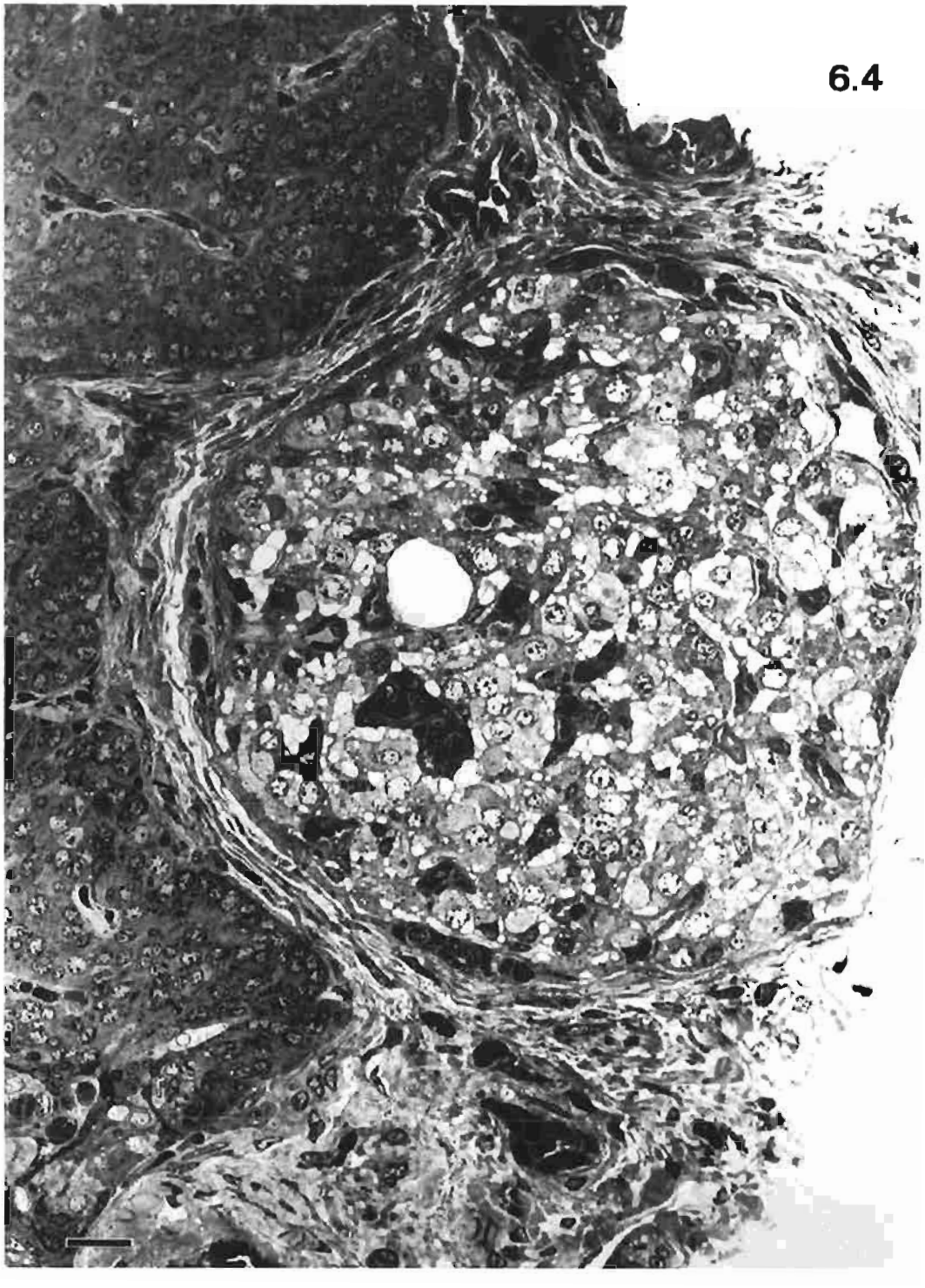

6.4

Plate 6.5. Light microscopy of koala parathyroid

Fig. 6.5a. Shows the typical reticulate endocrine structure of the koala parathyroid gland. Cells arranged in clumps (C) show obvious polarisation with nuclei placed peripherally. Occasional cells are very pale but most have a fine granular cytoplasm. In the centre of the micrograph is a follicle (F) that has been cut through its periphery. The lining cells also show polarisation.
1µm resin section, toluidine blue
Koala #2
Bar: 10µm

Fig. 6.5b. Shows an area where there are numerous pale staining cells with vacuoles and parts of two large follicles lined by low cuboidal cells. Follicular content is homogeneous and acellular.
1µm resin section, toluidine blue
Koala #2
Bar: 10µm

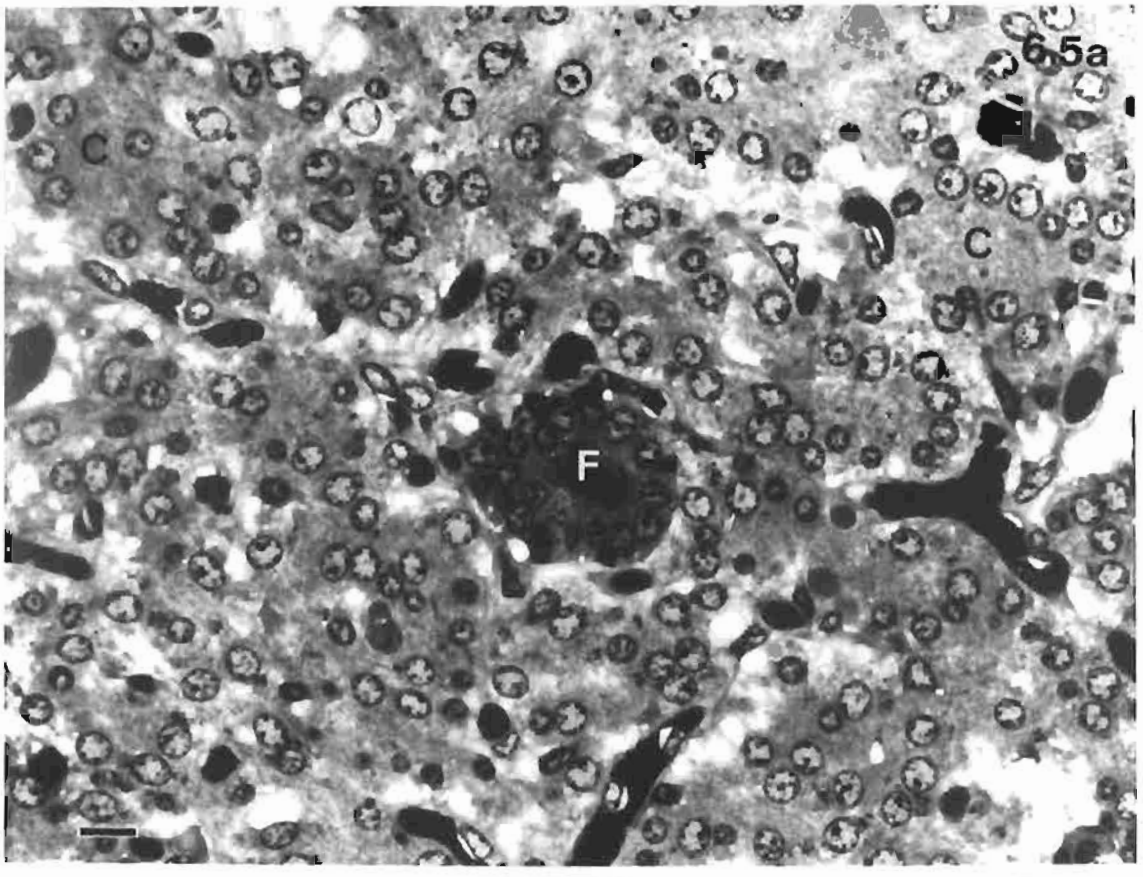
6.5a
C
C
F

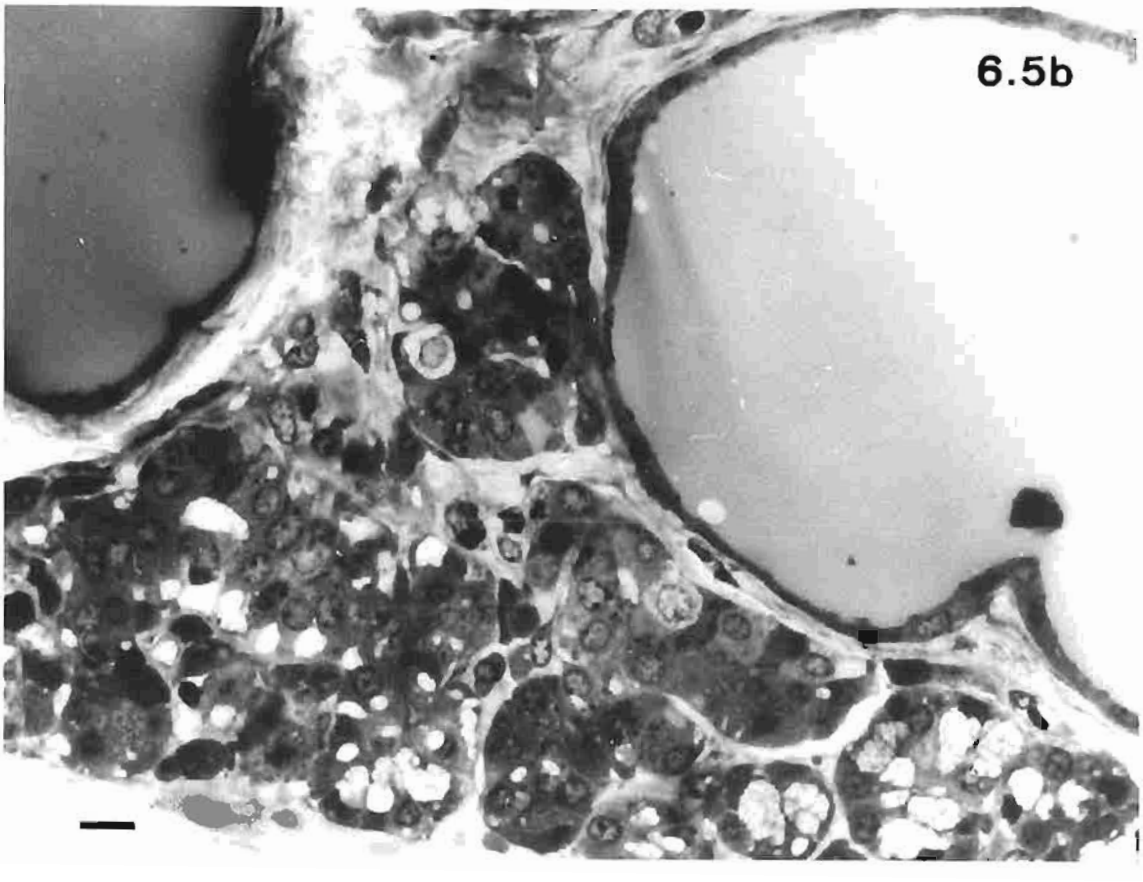
6.5b

Plate 6.6. Ultrastructure of pericapillary tissue in the wombat parathyroid

Figs. 6.6a. & 6.6b. The electron micrographs show the wide pericapillary area packed with a meshwork of collagen and fine interlacing fibrils (F) that appear to be associated with the basal laminae and collagen fibres.
Wombat W8
Bar: 1µm (Fig. 6.6a)
400nm (Fig. 6.6b)

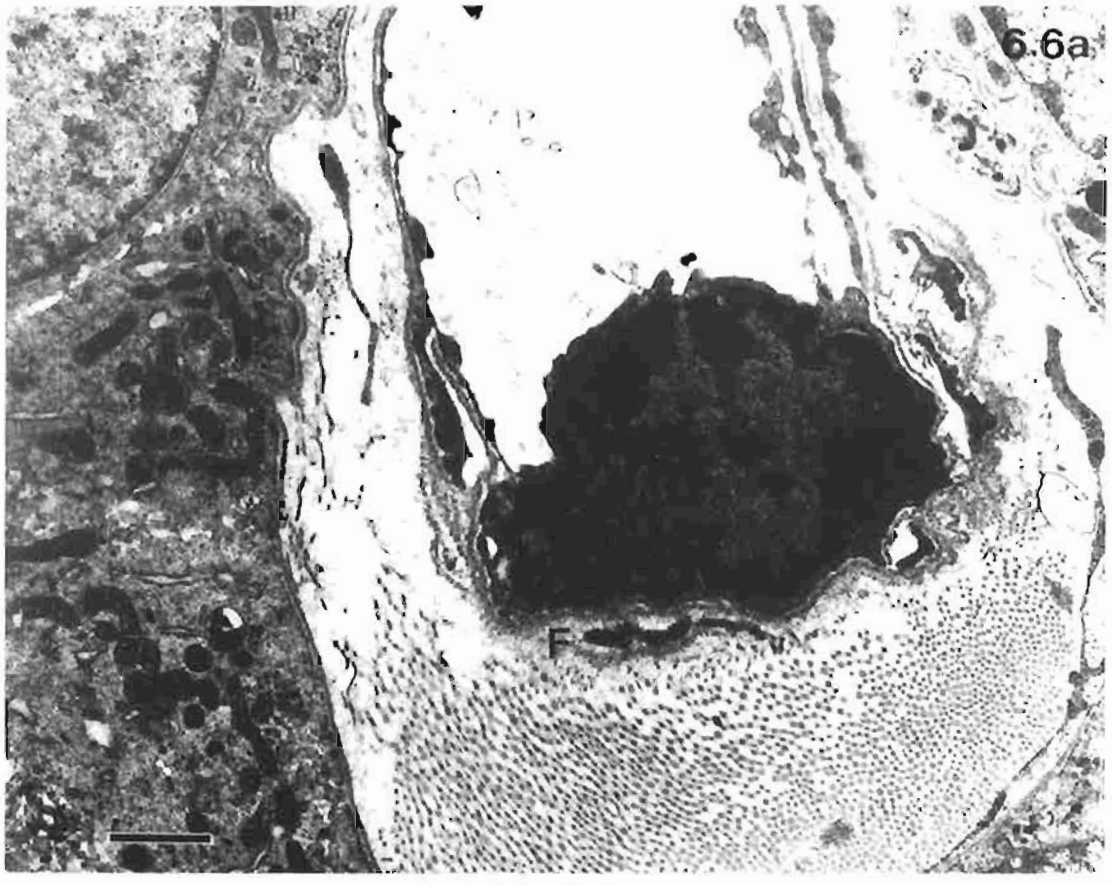
6.6a
F

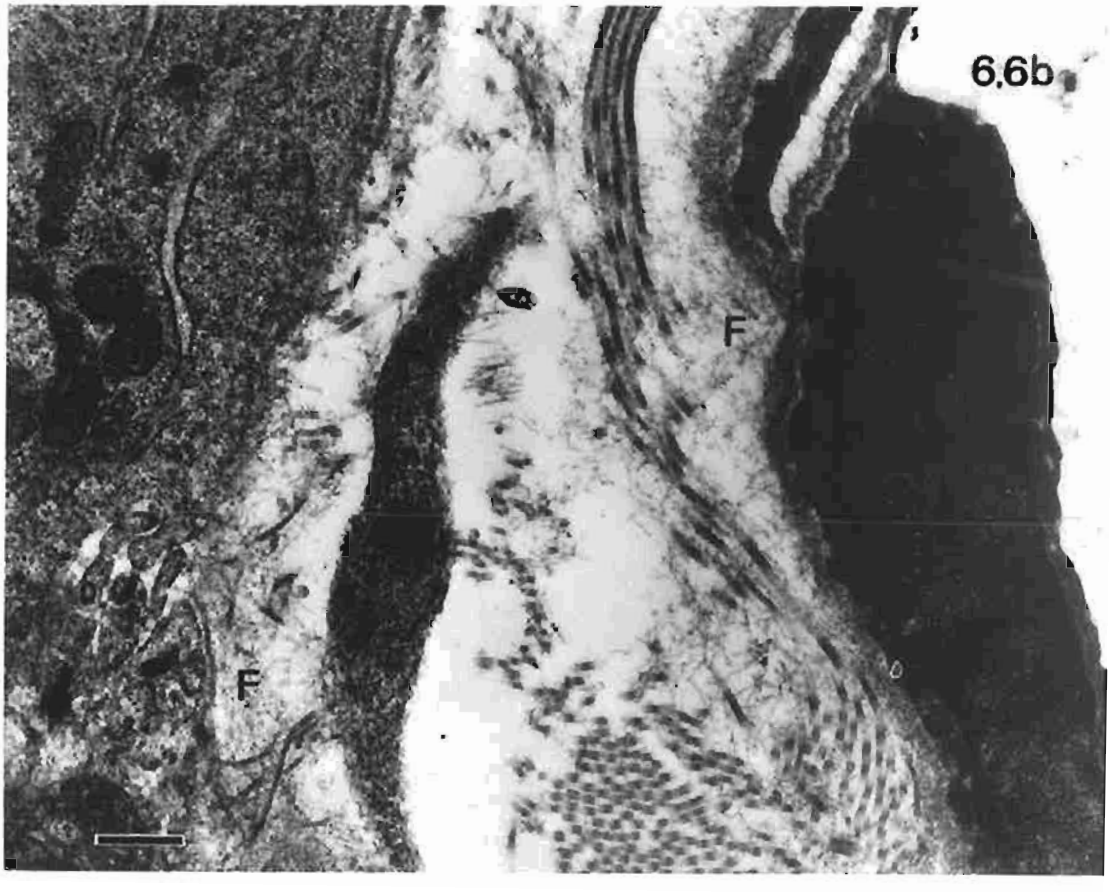
6.6b
F
F

Plate 6.7. Ultrastructure of non parenchymal cells in the wombat parathyroid

Fig. 6.7a. Shows a mast cell (M) in the connective tissue adjacent to a capillary. Most of the granules in the mast cell are large and electron dense. Mast cells are quite numerous in the parathyroid gland.
Wombat W1
Bar: 1μm

Fig. 6.7b. Shows electron dense, irregular shaped cells (C) in amongst parenchymal cells. Note the slender cytoplasmic processes, the single large hyperchromatic nucleus and the many cytoplasmic vesicles, features indicative of macrophages.
Wombat W2
Bar: 3μm

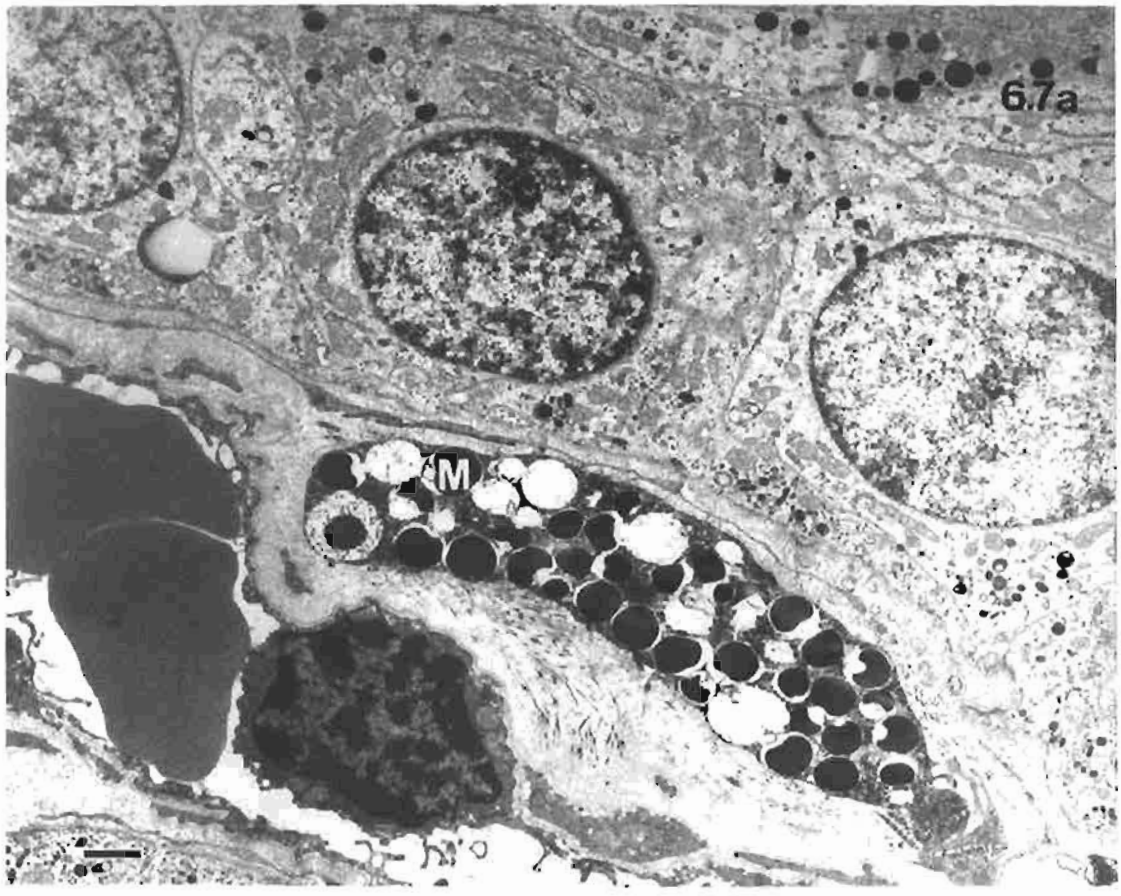
6.7a
M

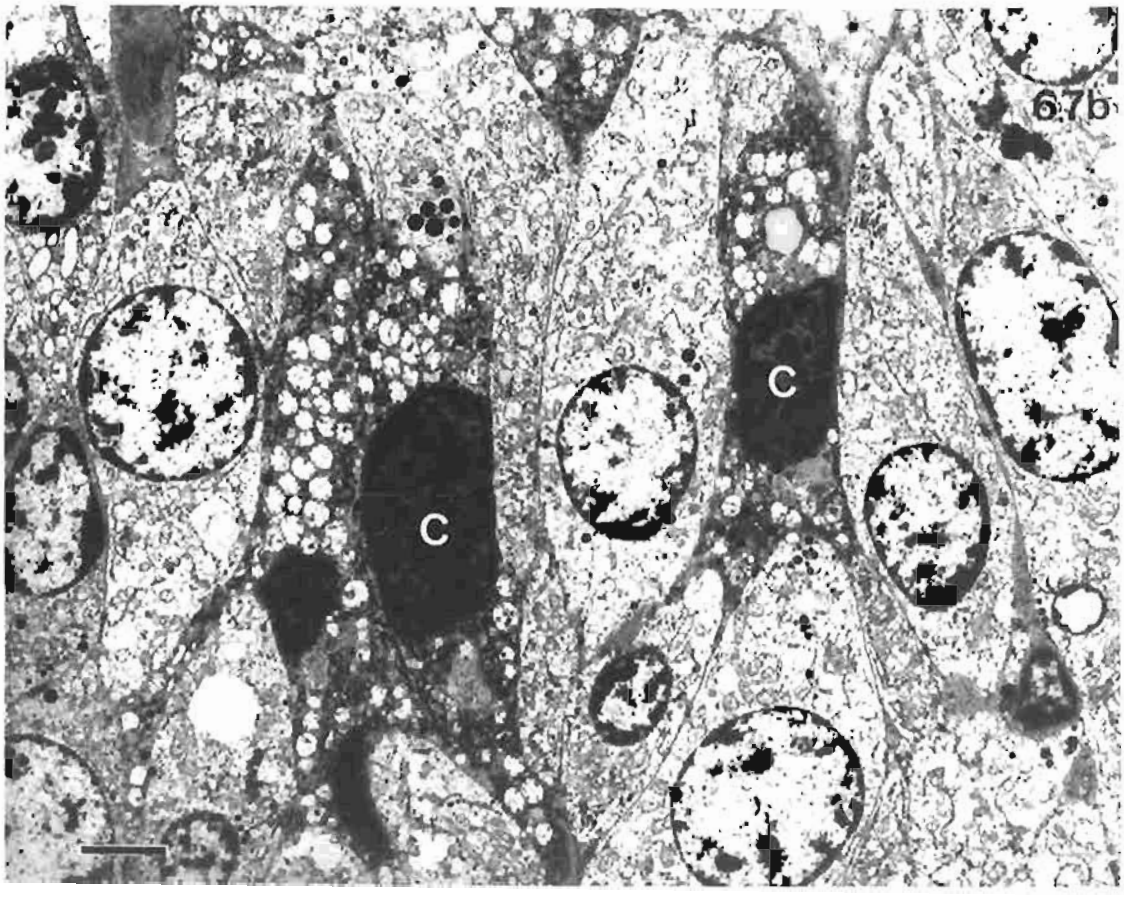
6.7b
C
C

Plate 6.8. Ultrastructure of wombat parathyroid - I
Desmosomes, light and dark cells

Fig. 6.8a. Shows an oxyphil cell packed with mitochondria and closely adhered to an adjacent cell by a desmosome.
Wombat W3
Bar: 0.5µm

Fig. 6.8b. Shows principal cells with different electron densities. Small canaliculus-like structures (C) interrupt the closeness of the adjacent cell membranes. Note electron dense secretory granules are in both light and dark cells and the relative scarcity of RER.
Wombat W6
Bar: 1µm

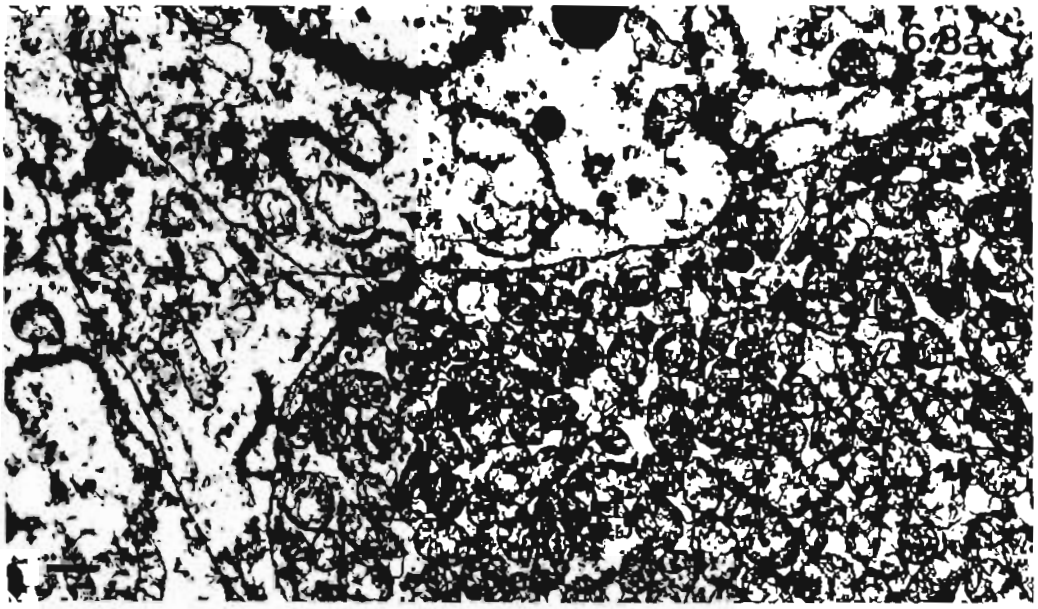
6.8a

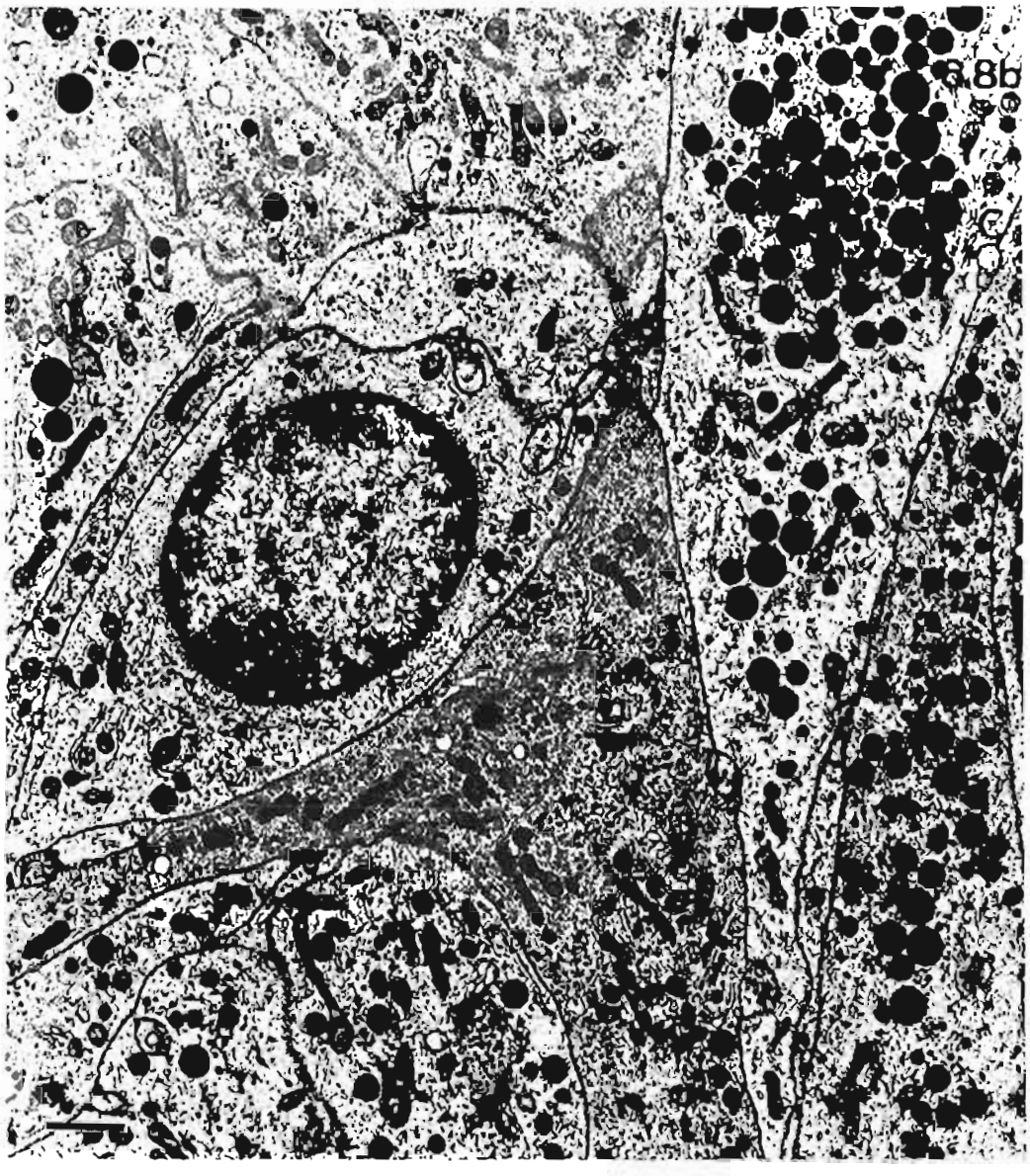
6.8b

Plate 6.9. Ultrastructure of wombat parathyroid - II
Polarity and vesicles

Fig. 6.9a. Shows the elongated principal cells cut transversely. The nucleus occupies most of the cross section area of the cells. Except in the perinuclear area most cells show secretory granules, mitochondria and scant amounts of RER. The central cell has RER arranged in a whorl.
Wombat W3
Bar: 2μm

Fig. 6.9b. Shows cellular shrinkage related to poor fixation. Note three types of inclusions: the small electron dense secretory granules (E), the lipid inclusions (L) and the very large vesicles (V).
Wombat W9
Bar: 1μm

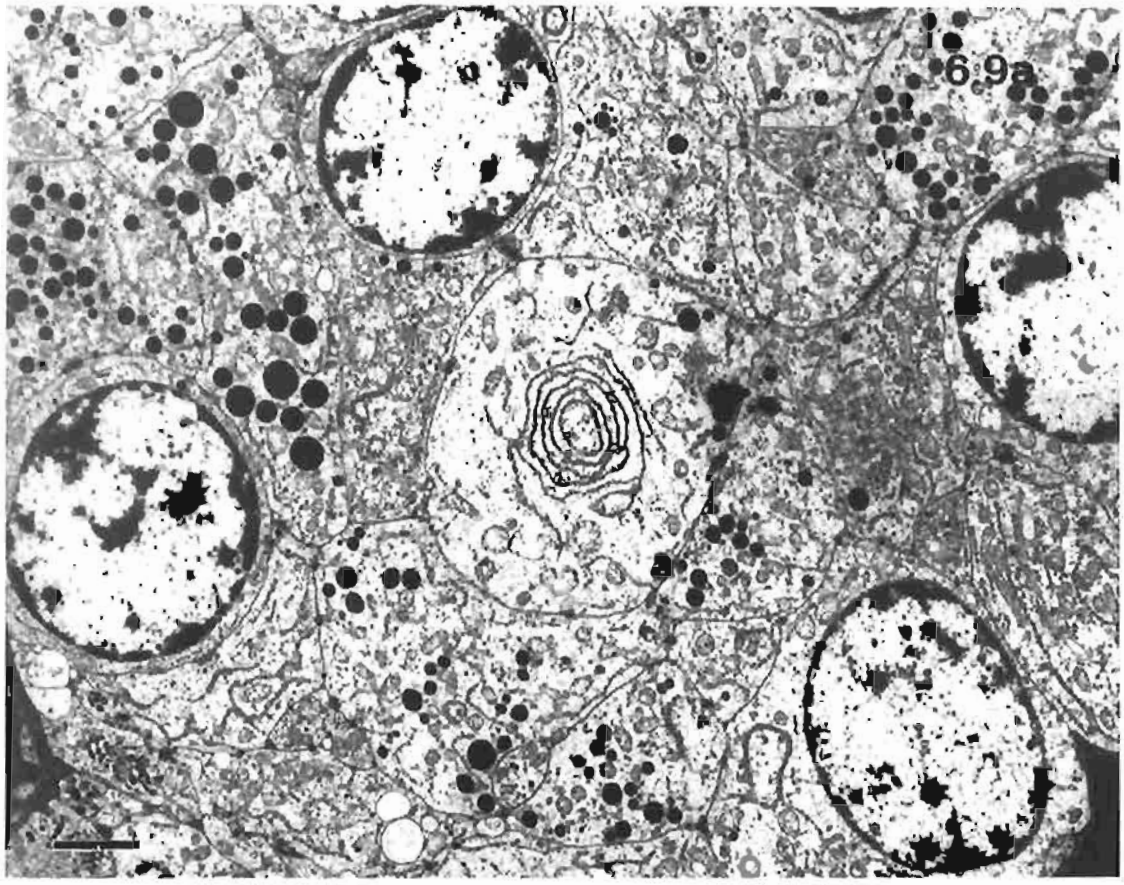
6.9a

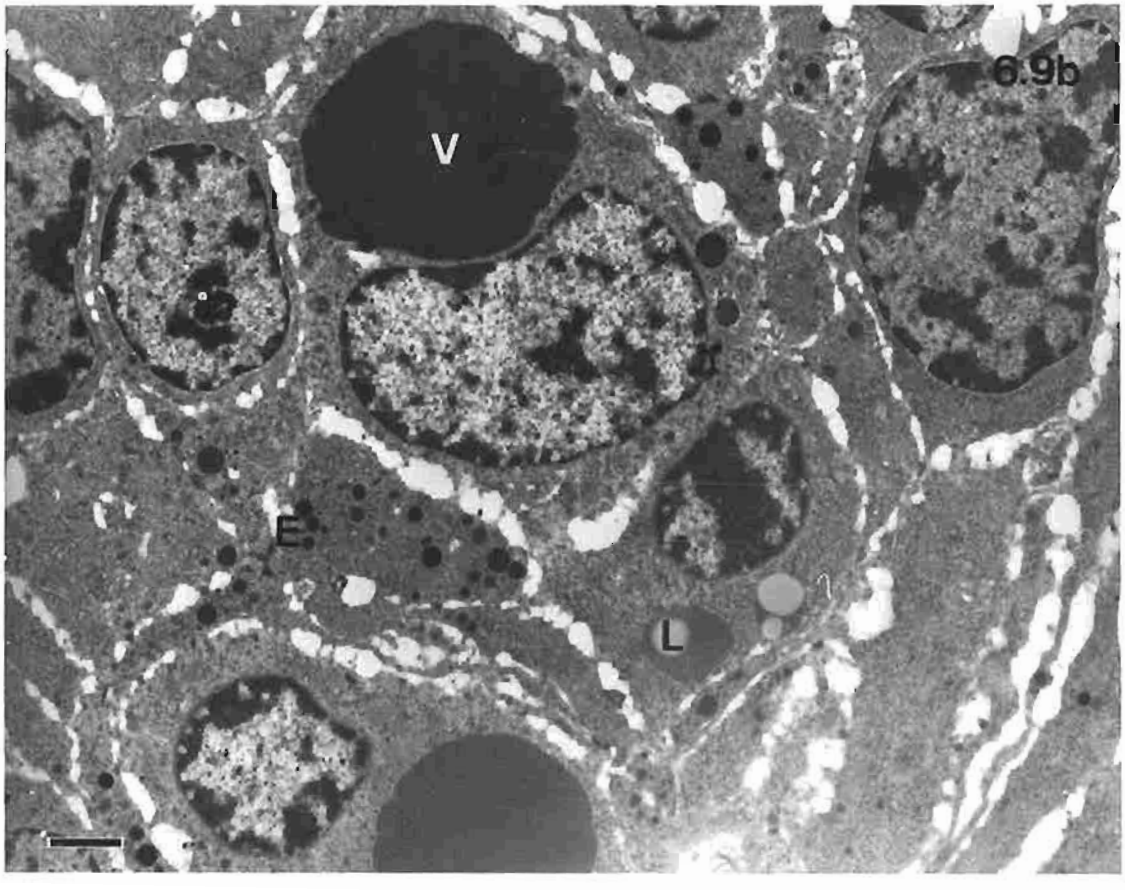
6.9b
V
E
L

Plate 6.10. Ultrastructure of wombat parathyroid - III
Oxyphil and intermediate oxyphil cells

Fig. 6.10a. Shows an oxyphil cell. The cytoplasm is packed with mitochondria, almost to the complete exclusion of other cytoplasmic structures.
Wombat W2
Bar: 1μm

Fig. 6.10b. Shows a transitional oxyphil cell where compared with an oxyphil cell (Fig. 6.10a), mitochondria are less numerous and other organelles and inclusions can be seen in amongst the mitochondria.
Wombat W3
Bar: 2μm

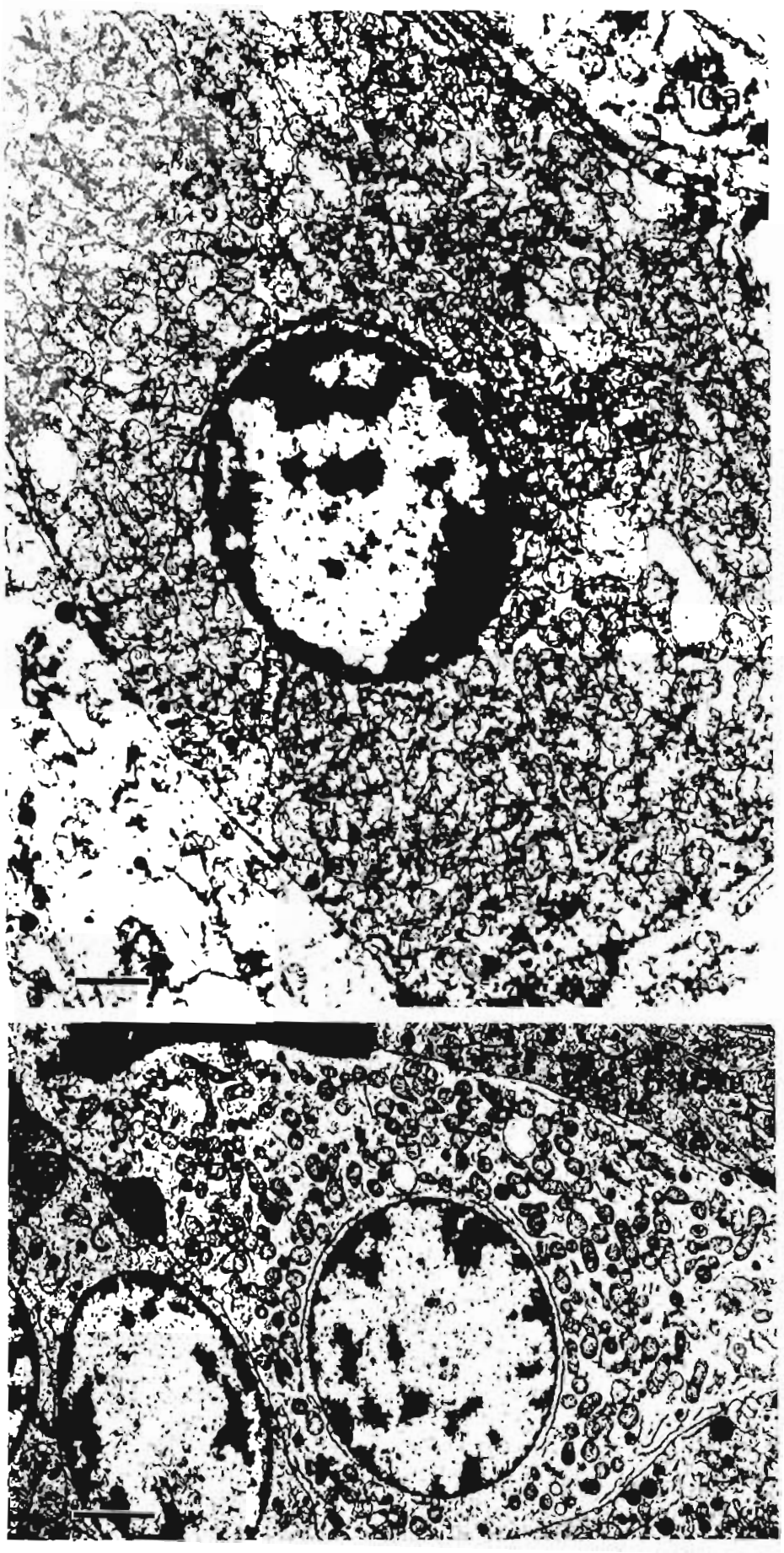
A 10a

Plate 6.11. Ultrastructure of cysts in wombat parathyroid

Fig. 6.11a. Shows a narrow region of a cyst lined by principal cells and dark electron dense cells (D) with numerous vesicles. The dark cells are interpreted as migrating to the lumen.
Wombat W5
Bar: 3μm

Fig. 6.11b. Shows intraluminal cells in a cyst. In the macrophage (M), the nucleus is hyperchromatic, and large phagosomes fill the cytoplasm. Note the contents of the phagosomes (P) are similar to both the round electron lucent area (E) on the edge of the colloid-like contents and to the large cytoplasmic vesicle (V) in the lining epithelial cell. The lower cell (N) in the lumen of the cyst appears to be a neutrophil.
Wombat W5
Bar: 3μm

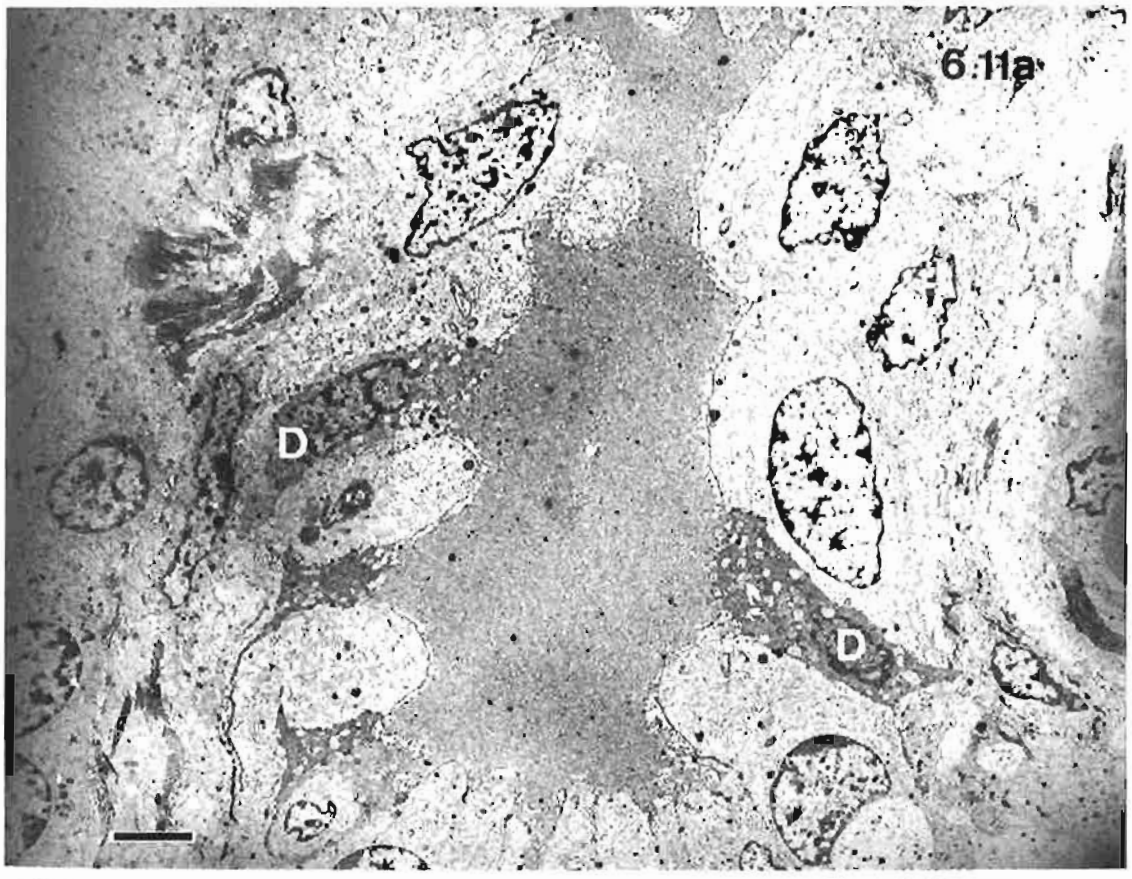
6.11a
D
D

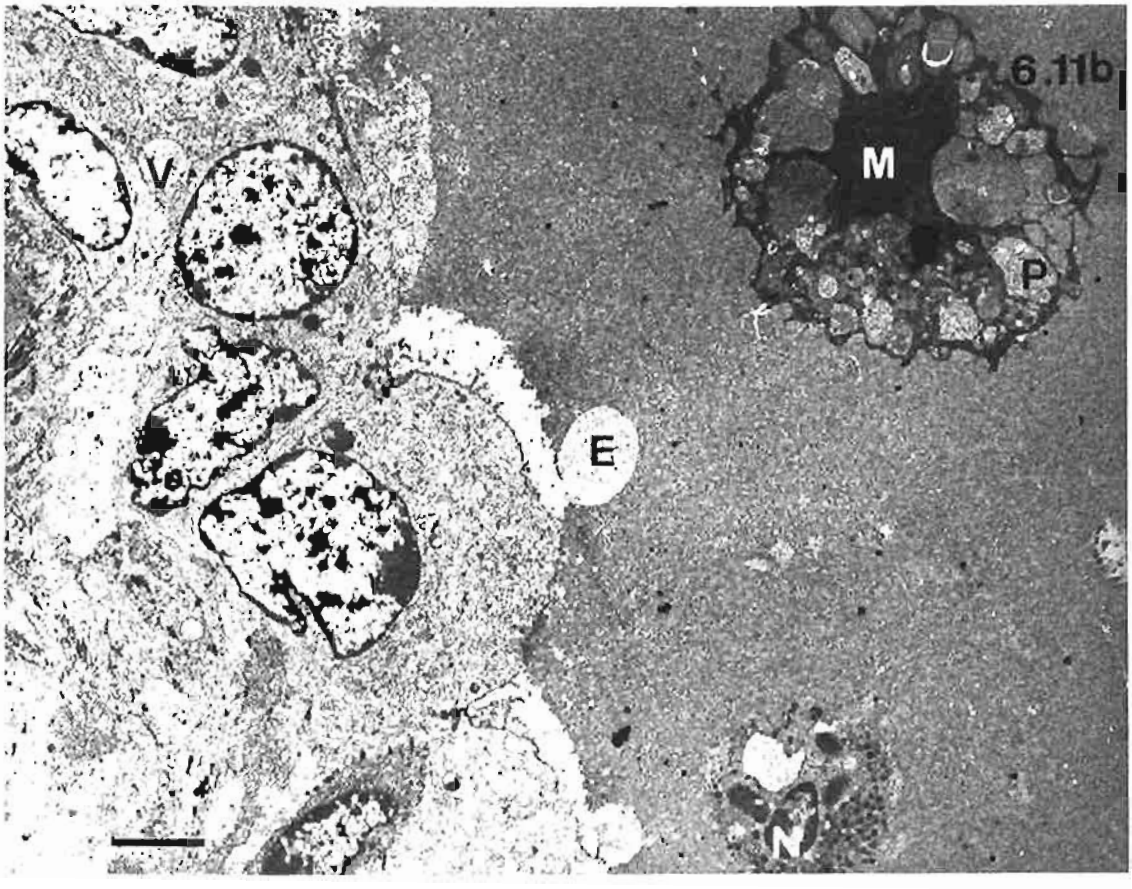
6.11b
M
P
V
E
N

Plate 6.12. Ultrastructure of nodule in parathyroid gland in wombat W1

Figs. 6.12a. & 6.12b. The structure of the unusual nodule found in a parathyroid gland from wombat W1 is shown in the two micrographs. Many cells show an electron lucent cytoplasm with numerous tiny granules, empty vesicles and lipid inclusions. Patches of fibrillar material (T) (tonofilaments ?) are obvious.

Wombat W1

Bar: 3μm (Fig. 6.12a)

1μm (Fig. 6.12b)

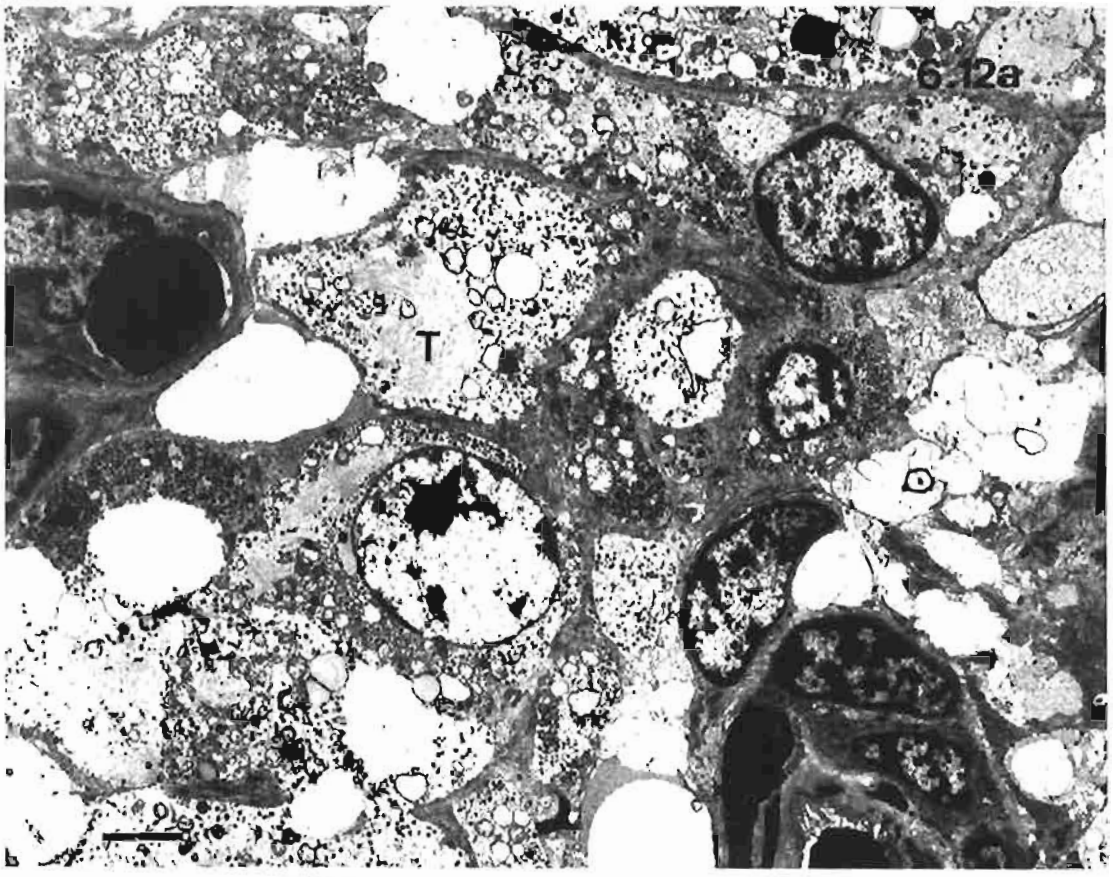
6.12a
T

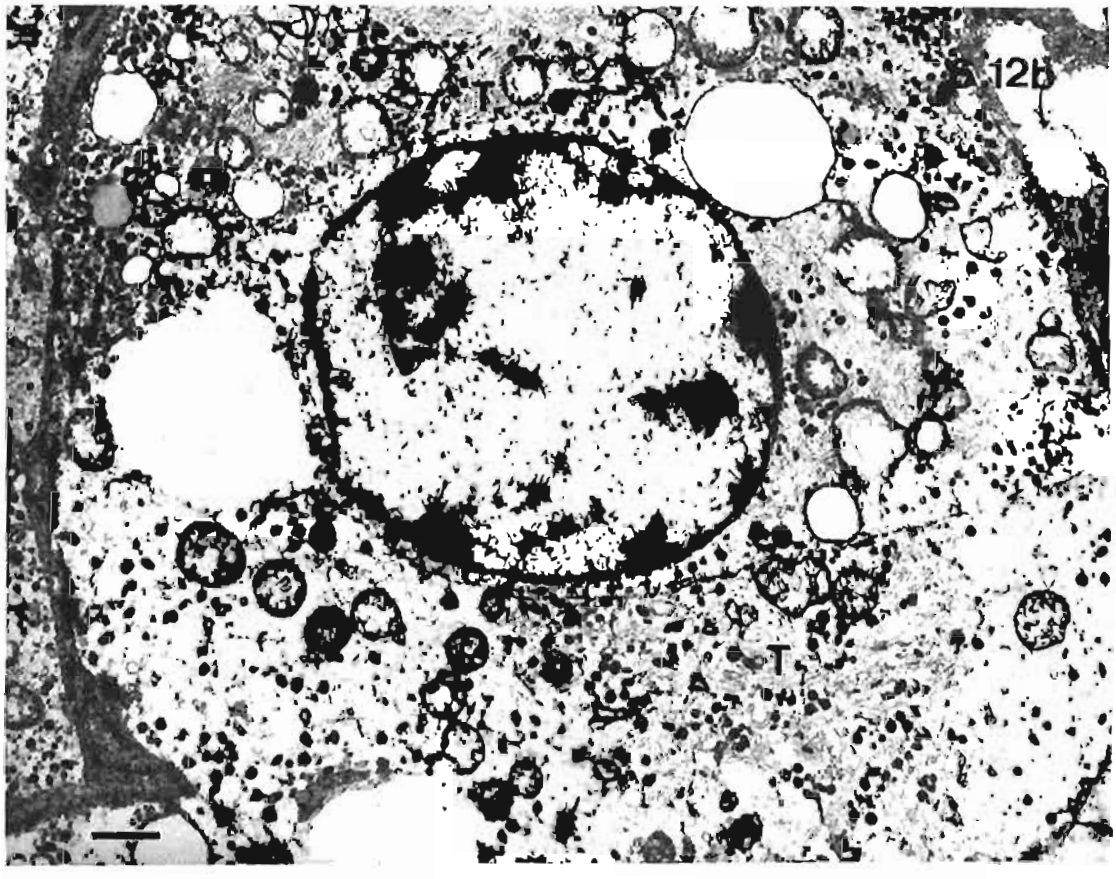
12b
T
T

Plate 6.13. Ultrastructure of parathyroid and thymus junction in wombat W6

Fig. 6.13. Shows thymic tissue (lower) separated from parathyroid tissue (upper) by long thin processes of epithelial reticular cells (ER). A lymphocyte (L) is present in amongst principal cells of the parathyroid gland and in the thymic tissue a thymocyte (T) is enclosed within a macrophage (M).
Wombat W6
Bar: 1µm

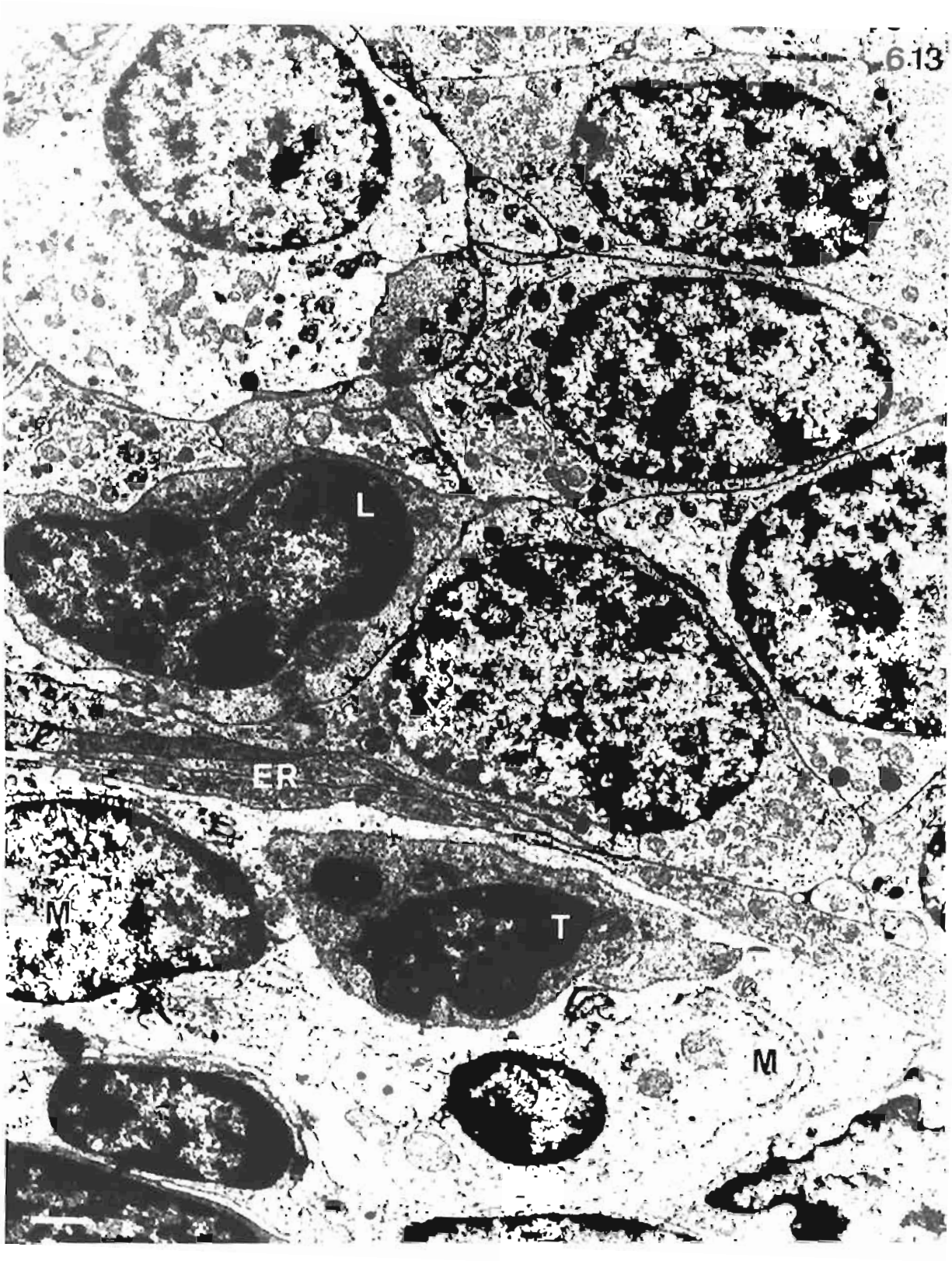
6.13
L
ER
M
T
M

Plate 6.14. Ultrastructure of koala parathyroid gland - I

Fig. 6.14a. Illustrates the compact arrangement of parenchymal cells and the lack of light and dark cell categories. Lipid droplets and secretory granules are clustered within the cells.
Koala #5
Bar: 2.5µm

Fig. 6.14b. Shows partial polarisation of principal cells with concentration of lipid droplets (L) and secretory granules (G) in cytoplasmic areas adjacent to the secretory surface and RER (R) clustered at the opposite ends of the cells. Lateral cell boundaries have interdigitation and canaliculus-like gaps (arrows).
Koala #1
Bar: 1µm

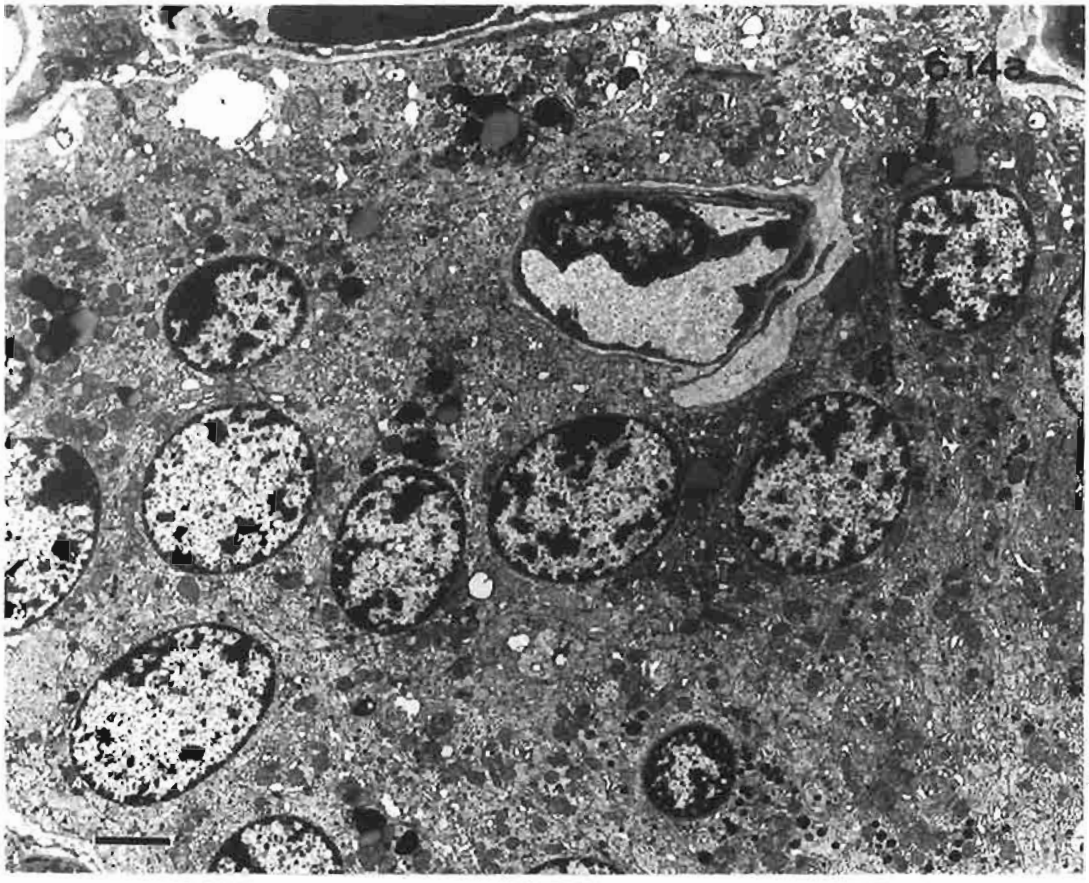
6.14a

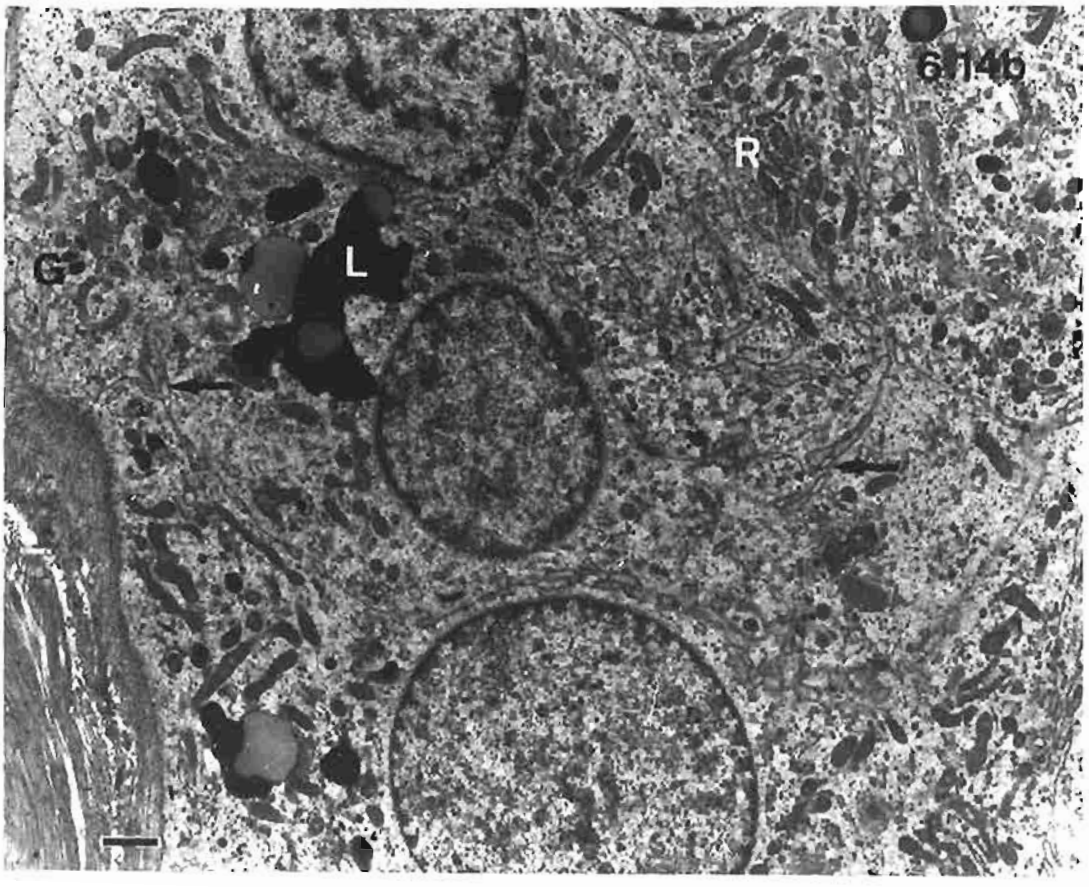
6.14b
R
L
G

Plate 6.15. Ultrastructure of koala parathyroid gland - II
Secretory granules and large vesicles

Figs. 6.15a & 6.15b. Inclusions in the principal cells ranged from the electron dense secretory granules (G) (200 - 400nm diameter) in the upper micrograph to the huge electron lucent inclusions (V) (4.5µm diameter) in the lower micrograph. Large vesicles were found only in cells near to or lining follicles. Well preserved cristae show in the mitochondria of the upper micrograph as well as some RER with dilated lumina, ribosomes and a residual body. Secretory granules are lacking in cells with the large vesicles in the lower micrograph.

Koala #5 (Fig. 6.15a)

Koala #2 (Fig. 6.15b)

Bar: 250nm (Fig. 6.15a)

1µm (Fig. 6.15b)

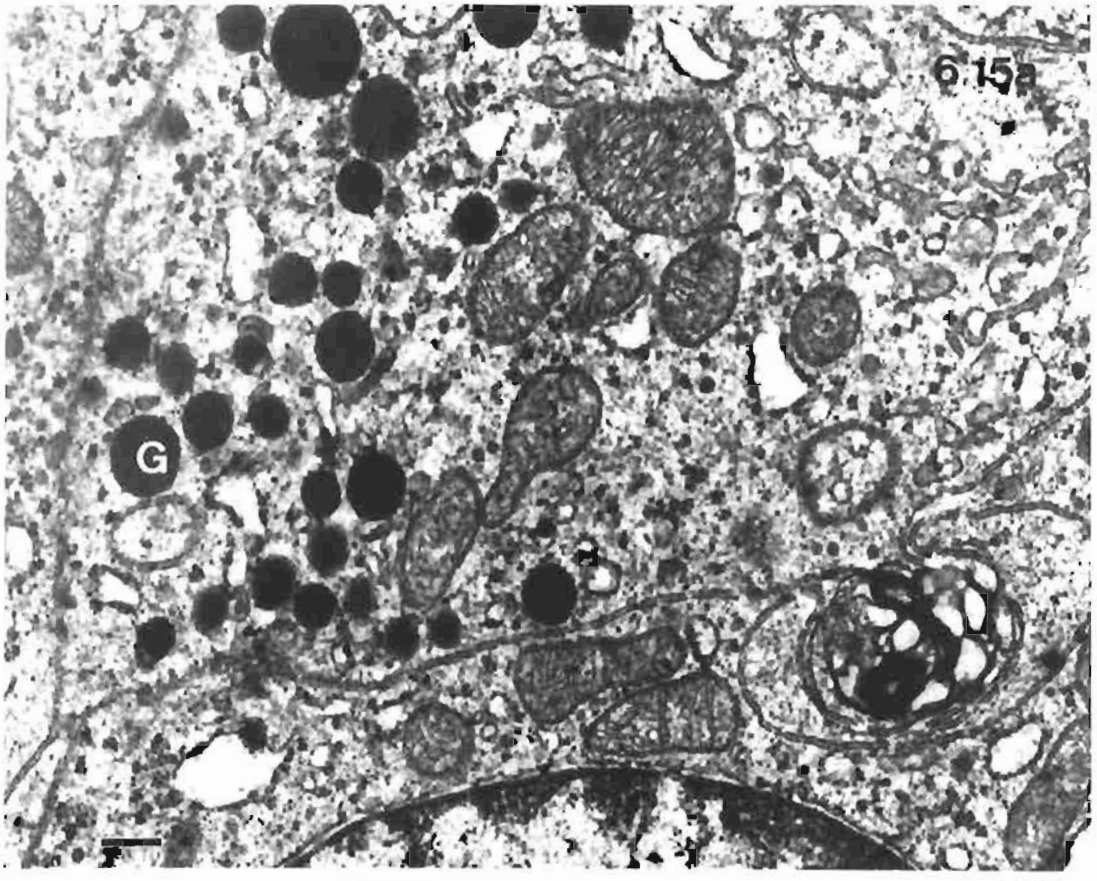
6.15a
G

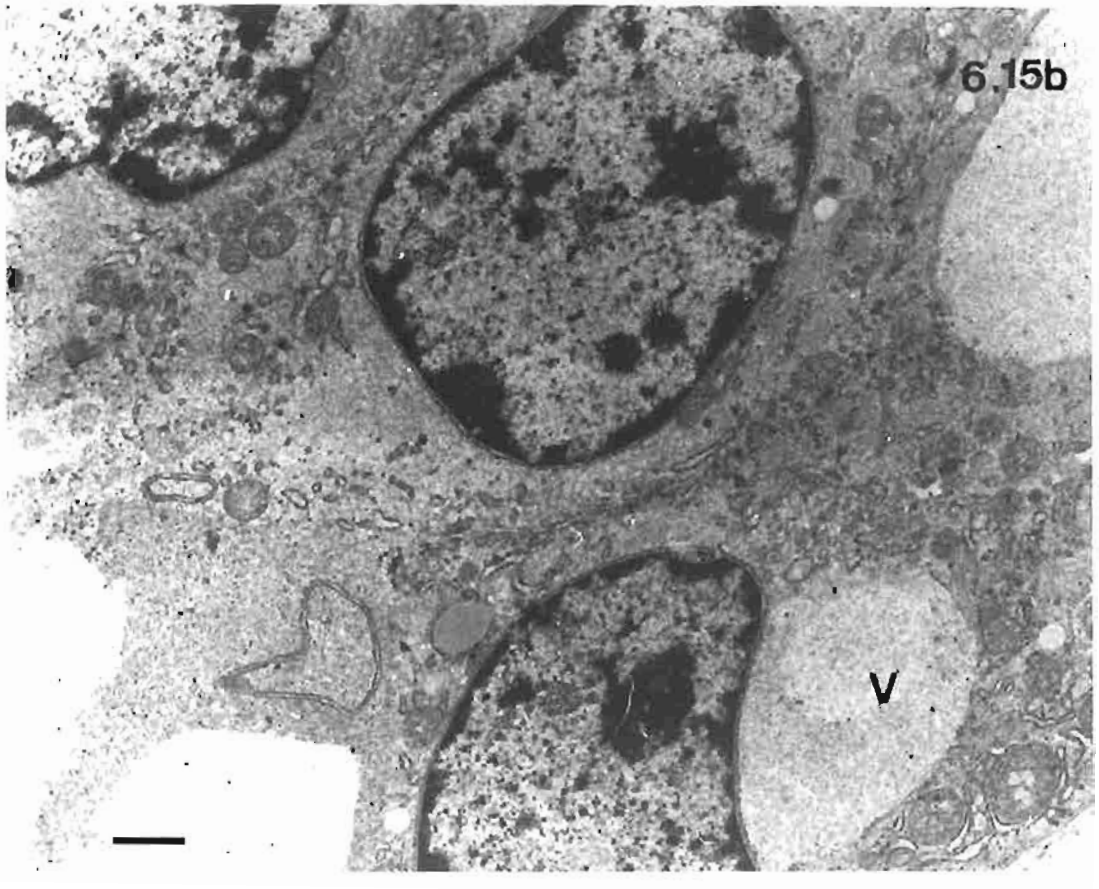
6.15b
V

Plate 6.16. Ultrastructure of koala parathyroid gland - III

Figs. 6.16a. & 6.16b. The micrographs show the main ultrastructural features of the principal cells are the large lipid inclusions (L). The upper micrograph shows a small, undeveloped Golgi body (G), the size of which is typical of the principal cells, and associated dilated endoplasmic reticulum (D). The lower micrograph shows numerous mitochondria; one encloses a granule.

Koala #1 (Fig. 6.16a)

Koala #5 (Fig. 6.16b)

Bar: 0.5μm (Fig. 6.16a)

1μm (Fig. 6.16b)

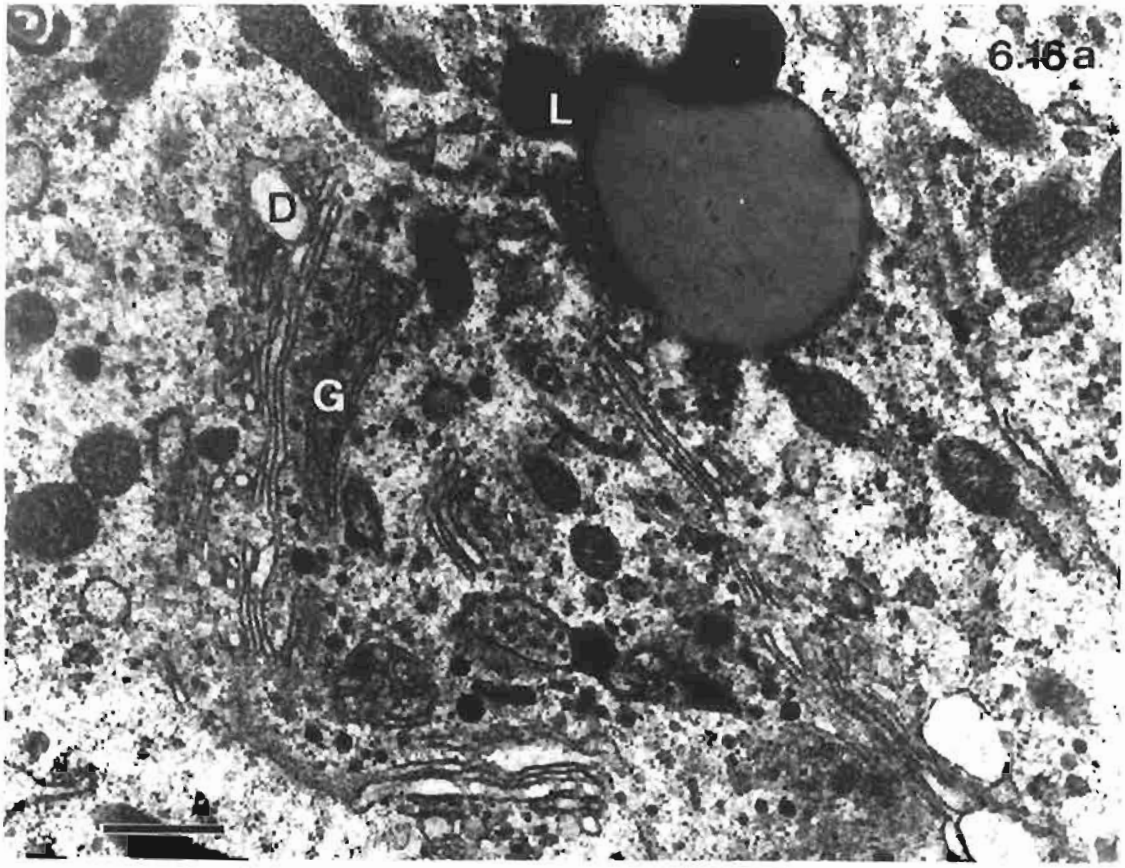
6.16a
L
D
G

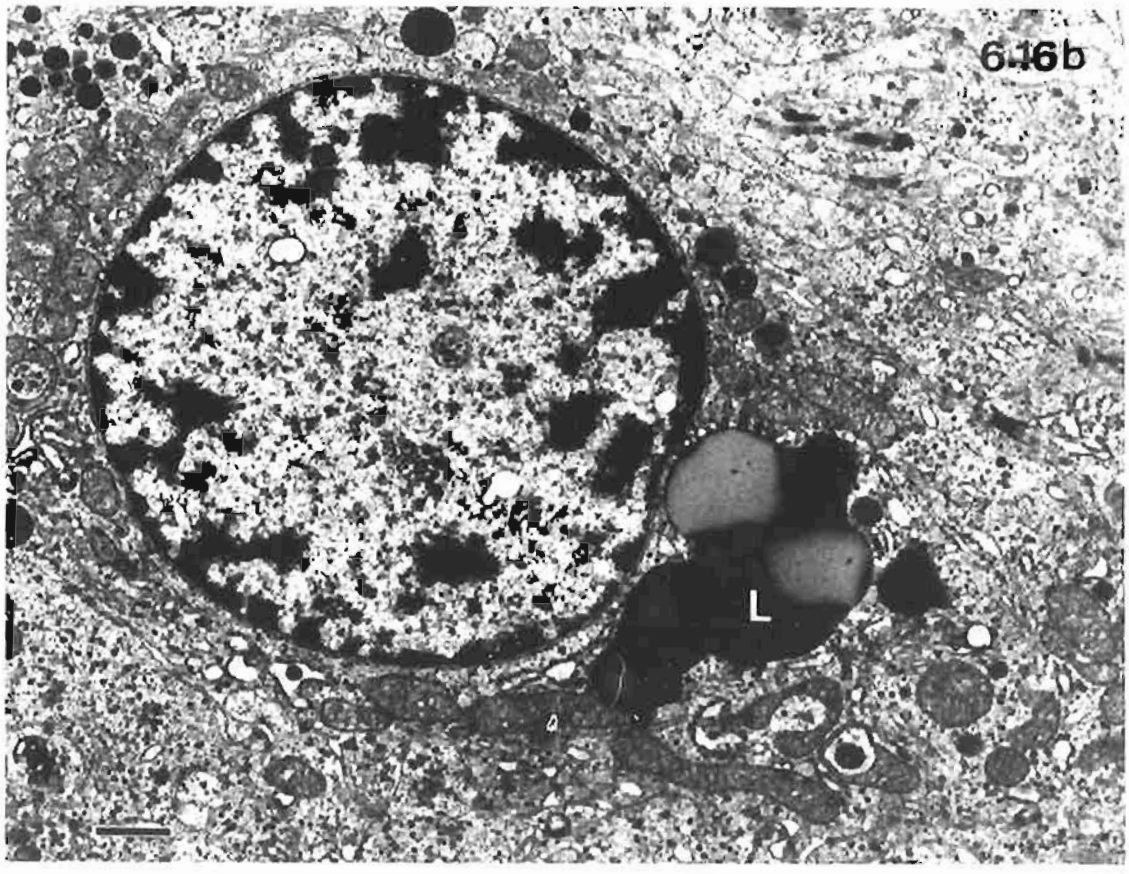
6.16b
L

Plate 6.17. Ultrastructure of follicle in koala parathyroid gland

Fig. 6.17. Shows the ultrastructure of a follicle. The contents of the large electron lucent vesicles (V) of the lining cells are similar to the luminal contents. Note the canaliculus-like gaps (arrows) between the lateral membranes of the cells and the lack of secretory granules.
Koala #2
Bar: 1μm

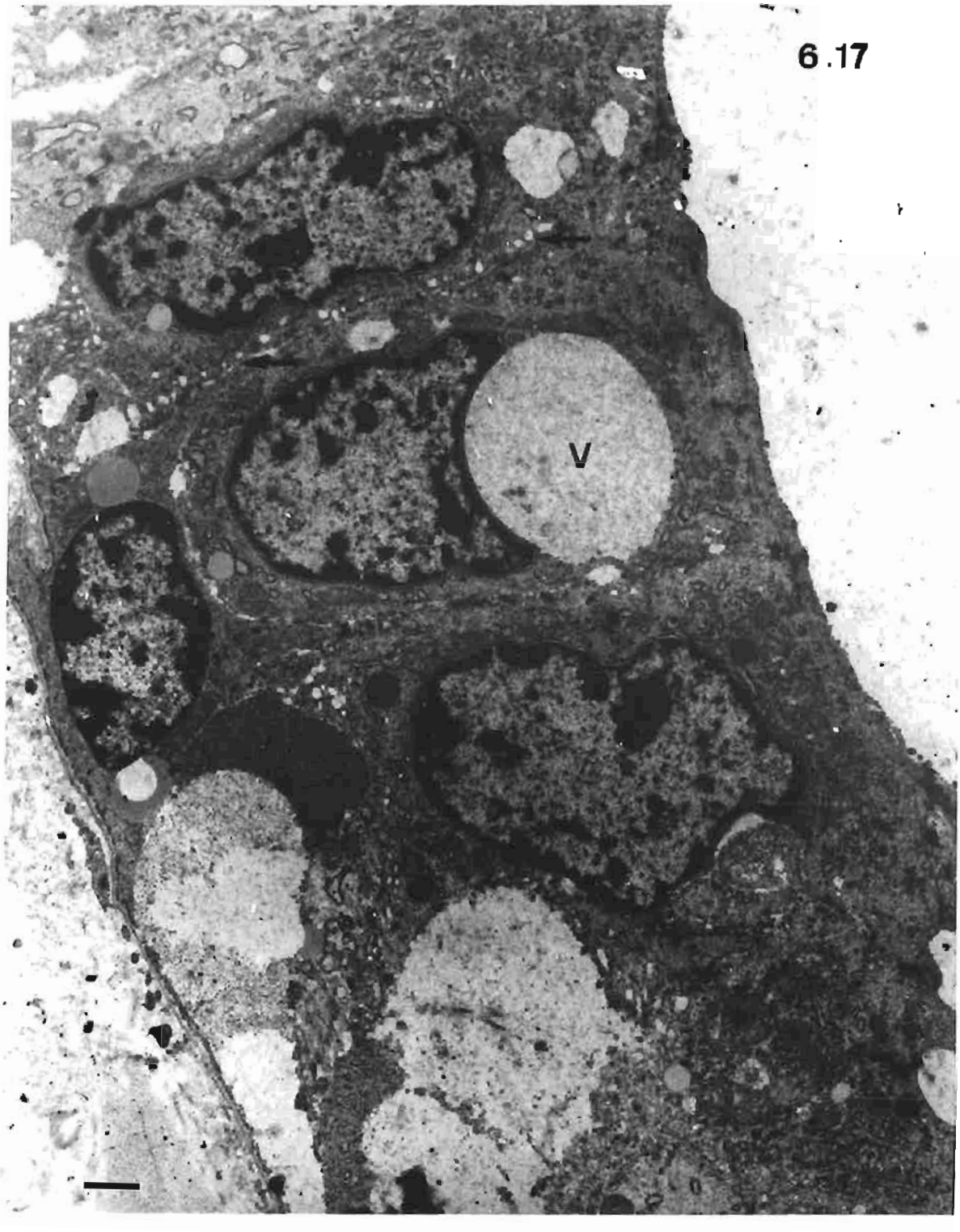
6.17
V

Chapter 7

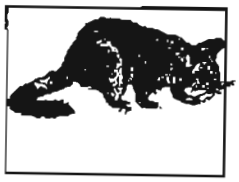

Parathyroid Glands in the Phalangerid Marsupial, *Trichosurus vulpecula*

7.1 Introduction

There is more published information available on the parathyroid glands of the brush-tail possum, *Trichosurus vulpecula*, than on that of any other Australian marsupial. However this information is provided in only two studies. One focused on the embryological development of the parathyroid glands (Fraser and Hill, 1915); the other distinguished the difference in location and structure between the carotid body and parathyroid glands (Adams, 1955).

The brush-tail possum is the most common Australian possum. It is about the size of a domestic cat and its average weight ranges from 1.5 to 3Kg for females and 2 to 4.5Kg for males (Strahan, 1983). Unlike most Australian marsupials, the brush-tail possum has adapted well to urban life. Possums are territorial and in the establishment of territories for juvenile possums, mortality rates can be high due to overcrowding, lack of suitable sites for dens and stress (Green, 1984). Unfortunately tolerance to possums living in urban properties is sometimes lacking and this results in the removal of the animals. The 23 possums used in this study on the parathyroid glands all came from suburban Adelaide where they were caught and relocated to holding cages at the Central Animal House of the University of Adelaide.

Since the conditions of captivity were considered to be potentially influential on the state of health and parathyroid morphology at the time of death then it is necessary to include a brief description of the housing of the possums at the Central Animal House. Prior to 1990, possums that had been trapped were all housed together for unspecified periods in a large cage with several nesting boxes available and the time spent in the wire trapping cages was not recorded for individual animals. Since 1990, each possum is kept in a wire trapping cage for less than 24 hours and is then housed in a separate enclosure with a nesting box for periods not exceeding 4 days. Nineteen possums, P1 to P19 were kept in the former conditions and four possums, P20 to P23, in the latter conditions. Hence before 1990, the unsuitable housing of possums may have led to a state of

chronic stress in some possums and since 1990, possums unhealthy at the time of capture could be identified.

The details of the techniques used for the morphological descriptions in this chapter are given in chap. 3, Materials and Methods. Seven possums were perfused with fixative, and tissue specimens from the remaining 16 animals were immersed in fixative. Thirty parathyroid III specimens were examined with the light microscope. Some histological sections were toluidine blue stained, resin sections; others were paraffin sections, stained with haematoxylin and eosin or PAS. Electron microscopic studies were done on twelve possums, three of which were perfused with a fixative suitable for electron microscopy (See chap. 3, Materials and Methods). Since parathyroid IV could only be located by examining serial sections of large areas of mediastinal tissue, it was not practicable to subject it to ultrastructural study.

7.2. Results

7.2.1. Anatomy

7.2.1.1. Parathyroid III

In *T. vulpecula*, parathyroid III lay deep bilaterally in the ventral region of the neck in the vicinity of the carotid bifurcation adjacent to the larynx. Parathyroid III was ovoid to rectangular in shape. The mean maximum dimension was 2.5mm ± 0.6 and the mean minimum dimension was 1.2mm ± 0.35. Ventrally the gland was covered by infrahyoid and sternomastoid muscles, the cervical thymus and the submandibular salivary gland (Figs. 7.2a & b). Parathyroid III was never found near the thyroid gland. In one possum, P2, a third, small parathyroid gland was found in aberrant thymic tissue near the left carotid bifurcation, and very near but separate from, the common carotid or its external or internal branch (Fig 7.1). Table 7.1 shows the locations of 30 parathyroid glands in possums.

Table 7.1 - Position of Parathyroid III in Possums

Total number of glands - 30.

%age of glands	location
50%	adjacent to the carotid bifurcation
20%	adjacent to the common carotid, just caudal to the bifurcation
14%	adjacent to the external carotid, just cephalic to the bifurcation
13%	just cephalic to the carotid bifurcation, in between the internal and external branches
3%	adjacent to the internal carotid, just cephalic to the bifurcation

In addition to parathyroid III being located near the carotid bifurcation, other structures similar in size and shape by observation with the dissecting microscope also occurred in this vicinity. Thus positive identification from the histological examination of sections was necessary to distinguish small lymph nodes, aberrant thymuses, and ganglia from parathyroid glands. The carotid body was a minute structure and could not be recognized as a separate entity during dissection using a microscope (Fig. 7.3a). When parathyroid III occurred between the internal and external carotid arteries, it was cephalic to the carotid body (Fig. 7.3a) which occurred in the conjoined adventitial layers of the two carotid arteries. Histologically, the carotid body had more abundant sinusoidal capillaries and the epitheloid cells were smaller than the parathyroid parenchymal cells (Fig. 7.3b).

7.2.1.2. Parathyroid IV

The location and number of parathyroid IV in possums were investigated in ten animals. Unlike parathyroid III, parathyroid IV did not occur in a constant position and unless serial sections of the ventrocephalic mediastinum and caudal regions of the neck are examined microscopically, this gland is easily overlooked. Of the ten possums examined, at least one parathyroid IV was found in mediastinal tissue in eight animals. Descriptions of parathyroid IV from the serial sections are summarised in Table 7.2. Two parathyroid IV specimens were found in possums P7 and P8 and three glands were found in possum P2.

Table 7.2 - Parathyroid IV in Possums

animal #	number	description
P2	3	All were present in the same thymic lobe. Each was ovoid and separate from the other glands (see Figs. 7.4a & b). The max. diam. of the glands were 0.2mm, 0.5mm, and 1.2mm.
P3	1	Located in adipose tissue, adjacent to thymus.
P4	1	Located at the periphery of, but separate from, an involuted thymus.
P5	1	Located at the periphery of a thymic lobe.
P7	2	Each gland was in separate lobes of the thoracic thymus. Serial sections revealed no connections between the two structures which were separated by 5mm.
P8	2	The two glands were 6mm apart. One was ovoid in connective tissue (Fig. 7.4c); the other, associated with thymic tissue.
P9	1	The gland was located dorsolaterally to the left common carotid, approximately 7mm cephalic to the origin of this vessel.
P12	1	The gland was within a lobule of an involuting thymus.

7.2.2. Light Microscopy

7.2.2.1. Parathyroid III

The glands displayed a reticulate endocrine structure with epithelial cells present in clumps and strands, separated by numerous capillaries (Fig. 7.5a). A thin capsule surrounded the gland and delicate, PAS-positive reticular fibres supported the parenchymal and vascular tissue (Fig 7.5b). Each gland was devoid of lobulation, had a compact arrangement of its cells and fat cells were absent from the interstitial reticular tissue.

In 16% of 30 parathyroid III specimens, thymic tissue was associated with the endocrine structure. Either fragments of thymic tissue were present at the periphery of the glands (Fig 7.6b) or in one case, possum P2, parathyroid III was completely surrounded by thymic tissue which also intruded into the gland (Fig. 7.6a). The nature of the lymphoid tissue was confirmed as thymus by the presence of Hassall's corpuscles in some situations (Fig. 7.6d). The delineation between parathyroid and thymic tissues was indistinct in several cases and gave the appearance of the intermingling of the two tissues (Fig. 7.6c). The electron microscopic studies that are reported in section 7.2.3., describe the junction between thymic and parathyroid tissue in more detail.

Follicles and cysts were seen in 12.5% and 25% respectively of the parathyroid III samples. (Follicles and cysts were defined in chap. 2, Literary Review, section 2.5.1). The cells of the small, spherical follicles were similar, but sometimes flatter, to principal cells (Figs. 7.7a &b). The luminal diameters were less than 150μm and the structureless, weakly acidophilic contents were PAS-positive.(Fig. 7.5b). Some cysts were large spherical structures; others were irregularly shaped. The minimal diameter of the cysts was 300μm. Although some cysts were empty, they usually contained pale acidophilic, amorphous material in which leukocytes and large frothy cells could be seen (Figs. 7.7c &d). Cysts were lined by cuboidal or columnar cells. In some cysts (Figs 7.7d) the epithelium was pseudostratified columnar ciliated epithelium, reminiscent of respiratory epithelium.

Parenchymal cells appeared to be mainly principal cells. No intensely acidophilic cells, indicative of oxyphil cells were present but some water-clear cells were observed in toluidine blue stained resin sections from possums P11. P12, and P13 (Fig. 7.9a). In resin sections, the water-clear cells contained large vacuoles that were not osmiophilic (Fig. 7.9a). In some but not all resin sections, principal cells could be further subdivided into light and dark cells. The two cell types seemed to be randomly arranged and did not occur in clumps.

7.2.2.2. Parathyroid IV

The histological structure of parathyroid IV was essentially the same as that of parathyroid III, except that the former glands were smaller and devoid of cysts and follicles. Eight of the twelve parathyroid IV glands were associated with thymic tissue (Figs. 7.4a & b).

7.2.3. Electron Microscopy

The ultrastructure of 23 parathyroid III specimens from twelve possums, three of which (P10, P11, P15) were perfused with fixative, revealed that the vast majority of parenchymal cells appeared to be principal cells; oxyphil cells were not present. Water-clear cells were identified in possums P11. P12, and P13. Principal cells showed variations in their cytoplasmic density and light cells (Fig. 7.8a) could be identified in most specimens. However, most principal cells had a moderately dense staining cytoplasm and no light cells could be distinguished in the parathyroid glands from the three possums, P10, P11, and P15, fixed by perfusion (Fig. 7.8b).

The round to polygonal, mono-nucleated principal cells were slightly less than twice the diameter of the nucleus which generally exhibited extensive euchromatin and a prominent nucleolus (Fig. 7.8b). Only one example of a multi-nucleated parenchymal cell was observed in all the sections examined (Fig. 7.9b). The plane of section revealed three nuclei, two of which had nucleoli. The cytoplasmic contents of the very large cell were similar to the adjacent mono-nucleated cells. Light cells appeared to be slightly larger than the other principal cells. Cellular outlines were generally somewhat irregular with the interdigitation of short microvillous processes (Figs. 7.10a & 7.10b). Desmosomes were also numerous between adjacent cells (Fig. 7.10a). In specimens from possums P11 (perfused with fixative), and particularly P12 (immersed in fixative), the intercellular space appeared to be greatly increased, resulting in short microvillous processes becoming attenuated and giving very irregular outlines to the cells (Fig. 7.9b). In specimens from P11, the irregular outline of the cells and the increased interstitial space were more pronounced in the centre of the sections rather than at the periphery (Fig. 7.9c) suggesting a fixation artefact was responsible for the appearance.

Most cells appeared to have moderately electron dense cytoplasm with polyribosomes and glycogen granules (Fig. 7.10a & 7.11b). Mitochondria were evenly distributed throughout the cytoplasm and their matrix was slightly more dense than the cytosol. Cristae formed shelf-like projections. The mitochondria seemed to be quite elongated, sausage shaped structures (Fig. 7.8b); some resembled U-tubes, others were slightly tortuous.

The Golgi apparatus was not pronounced and often it was not seen in the parenchymal cells. It consisted of several flattened cisternae with associated vacuoles, vesicles and immature secretory granules (Fig. 7.10a). The amount of RER and SER varied from cell to cell

(Figs. 7.10b & 7.11a). Some cells showed moderate amounts of RER (Fig. 7.11a), whereas other cells seemed almost totally devoid of this organelle (Fig. 7.8a). Similarly the amount of SER exhibited variations in abundance. Cells where SER was abundant showed it to be present in fine tubular and vesicular components (Fig. 7.10b).

A variety of membrane bound vesicles was seen in the possum parathyroid gland. Sizes ranged from the very small electron dense secretory granules (Figs. 7.10a & 7.10b) to the huge pale inclusions approximately 5μm in diameter (Figs. 7.9b & 7.11b) that occurred in three possums. The most widespread type of granule was small with electron dense contents and occasionally a halo occurred between the granule and the encasing unit membrane (Fig. 7.10b). The average diameter of these granules was estimated to be 130nm. These granules were assumed to be secretory granules and were slightly less common in light cells.

Medium sized granules, ranging from 500nm to 900nm in diameter, included lysosomes, secondary lysosomes, lipofuscin, and other forms of inclusion bodies (Figs. 7.7b, 7.10a, 7.10b). Some granules had electron dense, homogeneous contents and were identified as primary lysosomes (Fig. 7.10a); others had a heterogeneous appearance often with concentric lamellar structures, typical of lipofuscin (Fig. 7.10b). One type of granule had an electron lucent globular component which appeared to displace the electron dense component to one side of the granule, creating an unusual effect (Fig. 7.10a).

In three possums, P11, P12, and P13, large pale unit membrane bound structures dominated the cytoplasm of some principal cells (Figs. 7.9b & 7.11b). These generally rounded inclusions contained very fine granular material of unknown identity. Some of these inclusions consisted of smaller structures that were separated by very thin partitions and in two cells the contents of these inclusions appeared to be in the process of being released from the cells. Apart from these huge cytoplasmic structures, the cells appeared to be healthy and similar to other parenchymal cells. In some cells, the vacuoles seemed to be dilated RER (Fig. 7.11b) with ribosomes on the encasing membrane. The cells with these vacuoles were identified as water-clear cells.

Ultrastructural studies confirmed the presence of minimal connective tissue within the glands. Basal laminae separated the parenchymal cells from connective tissue and vascular components (Fig. 7.11a). The numerous capillaries were typical of fenestrated capillaries found in endocrine glands. They had many pinocytotic vesicles and fenestrations which had diaphragms covering the pores (Fig. 7.11a).

Only one of the specimens that were processed for electron microscopy showed thymic tissue associated with the parathyroid gland. The left parathyroid gland of possum P15 had thymic tissue on the periphery of the section (Fig. 7.12). The thymus showed a typical

mammalian thymic structure with long cytoplasmic processes, presumably belonging to epithelial reticular cells, encompassing lymphocytes. Hassall's corpuscles and macrophages (Fig. 7.13a) were also present. Several macrophages showed morphological evidence of phagocytosis with numerous short microvillous projections and pale staining phagosomes. The gap between the thymus and the parathyroid gland was extremely narrow in some places and an intervening basal lamina was not always present. However, the attenuated processes of the epithelial reticular cells could always be recognized at the periphery of the thymus (Fig. 7.12 & 7.13b).

7.3. Discussion

7.3.1. Anatomy

The usual number of parathyroid glands in *T. vulpecula* appears to be four, arranged as a cephalic pair, parathyroid III and a caudal pair, parathyroid IV. Parathyroid III is found in the vicinity of the carotid bifurcation and parathyroid IV occurs in the mediastinum, often associated with the thoracic thymus. These observations confirm earlier findings by Fraser and Hill (1915) and Adams (1955).

The dimensions given for the parathyroid glands in this study are bound to be slightly variable, depending on whether measurements have been made on fresh or fixed specimens, and on whether fixation was by immersion or perfusion. However, the mean maximum and minimum dimensions of parathyroid III, viz., 2.5mm and 1.2mm respectively, are similar to those previously given by Fraser and Hill (1915): left, 2.25 x 1.5mm; right, 2.0 x 1.0mm, and Adams (1955): 2 to 2.25 x 1 to 1.5mm.

Due to their variable location, the only way the total number of the more caudally located glands, parathyroid IV, can be determined is by cutting serial sections of the entire superior mediastinum, sectioning the major branches from the aortic arch, the thoracic thymus and the intervening fibro-fatty tissue. Perhaps insufficient tissue was taken from the possums in the specimens where no or only one parathyroid IV was found. A possible explanation for the presence of the third parathyroid IV which was observed in one possum, P2, is that during embryological development, one of the caudally migrating parathyroid IV anlage splits into two groups of cells. These groups then continued to develop separately within the thoracic thymus.

The number and location of parathyroid IV in adult possums has been investigated previously only by Fraser and Hill (1915) who examined two adult possums. In one animal, four 'epithelial bodies' were found, two of which were located in between thoracic thymic lobes and measured 0.5 x 0.36mm and 0.72 x 0.67mm. The other 'epithelial bodies' were embedded in the left thymus. In the other animal the left and right thymus both contained two small 'epithelial bodies'. These minute structures were probably

accessory glands formed by division of embryonic anlagen. Accessory glands are quite common in humans; up to eight parathyroid glands have been found in dissections of the neck (Roth and Schiller, 1976).

7.3.2. Light Microscopy

The lack of fat and the compact arrangement of principal cells in the parathyroid glands described in this study on possums are similar to the features of this gland in many other species (Roth and Schiller, 1976). There has been only one other detailed histological study of the parathyroid glands in *T. vulpecula* (Adams, 1955) and compared with the present results, fewer variations in the glandular structure were observed. In a study of nine possums, only two glands had unusual features. One included thymic tissue and a structure described as a 'vesicle or follicle' was observed in the other. This structural uniformity contrasts sharply with the present study where thymic tissue and follicles or cysts were found in 16% and 25% respectively of parathyroid III specimens examined. The positive identification of the thymus was based on the presence of Hassall's corpuscles (Fig. 7.6d) that appear to be a universal feature of the thymus, including the marsupial thymus (Yadav, 1973). Since follicles and cysts and aberrant thymic tissue were found in parathyroids from most other marsupials in the current study, they are discussed collectively in chap. 11, General Discussion.

7.3.3. Electron Microscopy

In possums the presence of light and dark cells appeared to be influenced by the mode of fixation. Parenchymal cells in perfused specimens showed similar cytoplasmic densities whereas in specimens immersed in fixative, light and dark cells could usually be identified. Dark cells are thought to represent the active phase in the secretory cycle (Roth and Schiller, 1976) but in possums it seems that the proportion of light and dark cells in the parathyroid may be artefactual. This finding supports other studies that have shown parathyroid ultrastructure in dogs (Setoguti, 1977) and in rats (Wild and Setoguti, 1995) is influenced by methods of fixation and fixation by perfusion results in a lack of dark and light variants of the principal cells In the current study the mode of fixation was shown to modify the ultrastructure of parathyroids of other marsupials besides possums and hence the factors affecting the proportion of light and dark cells are discussed together in chap. 11, General Discussion, section 11.4.

Descriptions of the ultrastructural changes in cells at different stages of the secretory cycle include irregular outlines of active cells and straight membranes of inactive cells (Roth, 1979). However, these plasmalemmal variations may be partially artefactual and relate to fixation. Faccini (1970) described straight cell membranes after osmium tetroxide fixation and tortuous outlines after fixation by glutaraldehyde. In the present study, as all specimens were first fixed with glutaraldehyde and post-fixed with osmium tetroxide, perhaps the

irregularity of the plasmalemma has been accentuated by glutaraldehyde fixation and does not accurately reflect secretory activity.

The ultrastructure of the parathyroids that were fixed by perfusion, i.e. possums P10, P11, and P15, showed considerable variations in cellular profile and intercellular volume. Compared with the last specimen, the entire parathyroid from P10 had a shrunken appearance to its cells and enlarged intercellular areas whereas in the gland from P11 only centrally located cells were shrunken (See Fig. 7.9c). These features were interpreted as fixation and processing artefacts. The osmolarity of glutaraldehyde solutions used for fixation has been shown to influence ultrastructure with hypertonicity resulting in shrinkage and hypotonicity in swelling (Pearse, 1980). In possum P10 it is suggested that the shrunken appearance of the cells may have been the result of an inadvertent error being made in the preparation of the perfusing and fixative solutions. In possum P11 it is suggested that the duration of post-fixation in osmium tetroxide was too short, inner cells were not exposed to osmium tetroxide and were susceptible to shrinkage in the subsequent dehydrating processes. However this explanation is not entirely satisfactory because osmiophilic lipid inclusions were present in the central region which provided evidence that osmium did penetrate deep into the glands. Thus in conclusion, the shrunken appearance of the centrally located cells in the parathyroid from possum P11 is an artefact, the causes of which are unknown.

The large vacuolated cells that were seen in three possums were labelled water-clear cells and not hyperplastic principal cells because they had greater similarity to the former category. However it is realized that the label 'water-clear cells' may not be appropriate as the vacuolated cells do not share all the classical features of the unusual water-clear cells that are most comprehensively described by DeLellis (1993). Although they appeared to have fewer and larger vacuoles per cell than water-clear cells described elsewhere, the fine granular contents of the vacuoles and the smooth encasing membrane were very characteristic (Sheldon, 1964; Roth, 1970; Hasleton and Ali, 1980; Emura et al., 1990). In resin sections the vacuoles of water-clear cells do not stain with toluidine blue (DeLellis, 1993); the same characteristic was noted in this study. Hyperplastic principal cells are characterised by dilated pale RER cisternae with irregular profiles (Faccini and Care, 1965); in this study only occasional vacuoles were studded with ribosomes and the profile of the vacuoles was mainly spherical. Some cells had a large vacuole with ribosomes as well as 'normal' RER (Fig. 7.11a.). In hyperplastic parathyroid cells, all RER structures appear dilated (Faccini and Care, 1965).

Water-clear cells almost never occur in normal human parathyroid glands (Roth, 1970) or other vertebrate parathyroids except for their occasional presence in the golden hamster (Emura et al., 1990) and rabbit (Wild and Setoguti, 1995). These cells were also found in parathyroid glands from echidna (See chap. 9). In chapter 9 the proposed origins of the

vacuoles are discussed whereas in this chapter the physiological conditions that result in the presence of water-clear cells in the parathyroid gland are considered.

In humans, the presence of water-clear cells in the parathyroids is most commonly associated with secondary hyperparathyroidism due to chronic renal failure (Roth and Marshall, 1969; Malmaeus et al., 1984; Klahr et al., 1985) and rarely with primary hyperparathyroidism (Sheldon, 1964; Roth, 1970). However chronic renal failure doesn't always lead to hyperparathyroidism. A study by Hasleton and Ali (1980) showed that less than 1% of 700 cases of chronic renal failure involved secondary hyperparathyroidism and in these hyperplastic glands no true water-clear cells were seen in the variable ultrastructure. In summary, water-clear cells are rarely seen in the human parathyroid gland and their presence indicates a hyperplasia of the gland often associated with chronic renal failure. However chronic renal failure has a variable effect on parathyroid gland morphology.

In an attempt to explain the presence of water-clear cells in a minority of possums, it is postulated that these cells are not part of the normal histology of the parathyroids in this species but represent hyperplasia of the glands. At the time of death, it was noted that the general condition of five possums, including the three animals whose parathyroids showed water-clear cells, was poor. They appeared to have mange, with their coats in a poor condition; they had muscle wasting and lacked body fat. Unfortunately, no further pathological investigations were deemed necessary at the time but, in retrospect, it seems feasible that these possums were suffering from chronic stress that could have involved impairment of renal function and associated parathyroid abnormalities.

Stress can occur in possums that have been trapped and held in captivity. They are not gregarious animals and an important part of their behaviour in the wild is the establishment of individual dens (Green, 1984). When possums are kept in captivity, particularly if they are in the same enclosure, some individuals will become stressed (Presidente, 1982). Besides the physical signs of stress seen in pelage, weight, and behavioural changes, the immunity of stressed possums is lowered and they become very susceptible to infectious diseases (Speare et al., 1984). Blood-borne bacteria cause widespread infections and, if the kidneys are implicated, renal malfunction may result and lead to secondary hyperparathyroidism. In secondary hyperparathyroidism in humans, the number of oxyphil cells usually increases also (Hasleton and Ali, 1980; Malmaeus et al., 1984). However, no oxyphil cells were seen in specimens from any possum.

In the possum, the tissue components between parathyroid cells and lymphocytes of the thymus appear not always to include a basal lamina. Similar structural relationships were seen in several other marsupial species and these findings are collectively discussed in chap. 11, General Discussion, section 11.4.

Fig. 7.1. Drawing of dissection of possum P13.

Fig. 7.1. Shows the ventral view of the right carotid bifurcation with parathyroid III (P) just cephalic to the origin of the external carotid and completely separate from the thyroid (T). The structures have been slightly teased apart and moved laterally in order to show them more clearly. The omohyoid (O), the sternomastoid (SM) and the cleido-mastoid (CM) have been severed and reflected.

C - right common carotid artery
G - ganglion
J - internal jugular vein
IX - glossopharyngeal nerve
X - vagus nerve and location of sympathetic trunk (dorsal and mainly hidden).

Possum P13
Bar: 4mm.

7.1

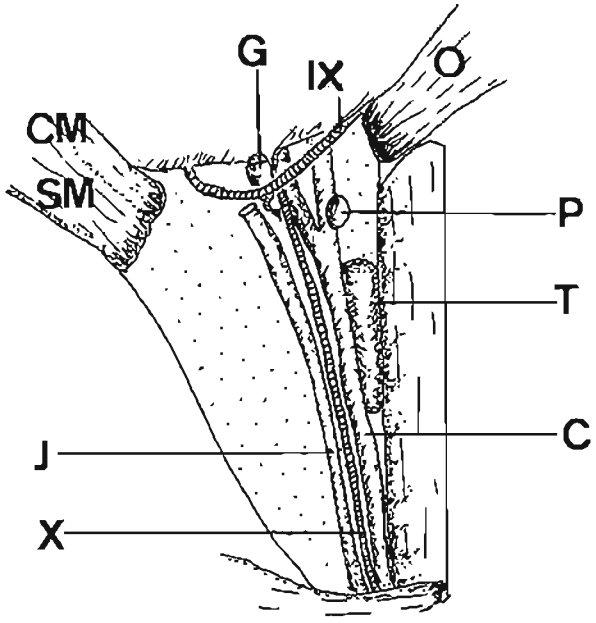

Plate 7.2. Anatomy of the ventral neck in *T. vulpecula*

Fig. 7.2a. Reflection of the skin and the platysma. Shows the right cervical thymus (Th) which has been detached from surrounding connective tissue and the more superficial muscles of the neck.
Bar: 8mm.

Fig. 7.2b. The sternomastoid and cleidomastoid muscles and the cervical thymus have been reflected. The omohyoid muscle (O) overlies the right common carotid artery; the bifurcation is shown by an arrow and it is in this vicinity that parathyroid III is found.
Bar: 5mm.

C - right common carotid
CM - cleidomastoid muscle
D - digastric muscle
L - larynx
M - mastoid muscle
O - omohyoid muscle
SM - sternomastoid muscle
T - trachea
Th - cervical thymus

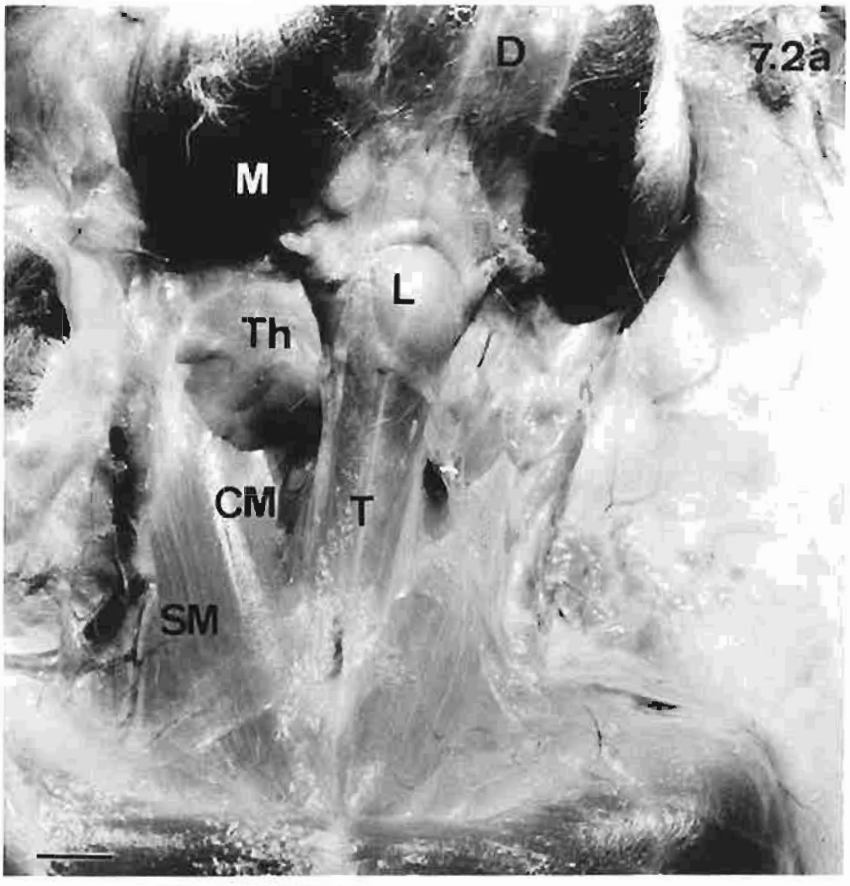
D
7.2a
M
L
Th
CM
T
SM

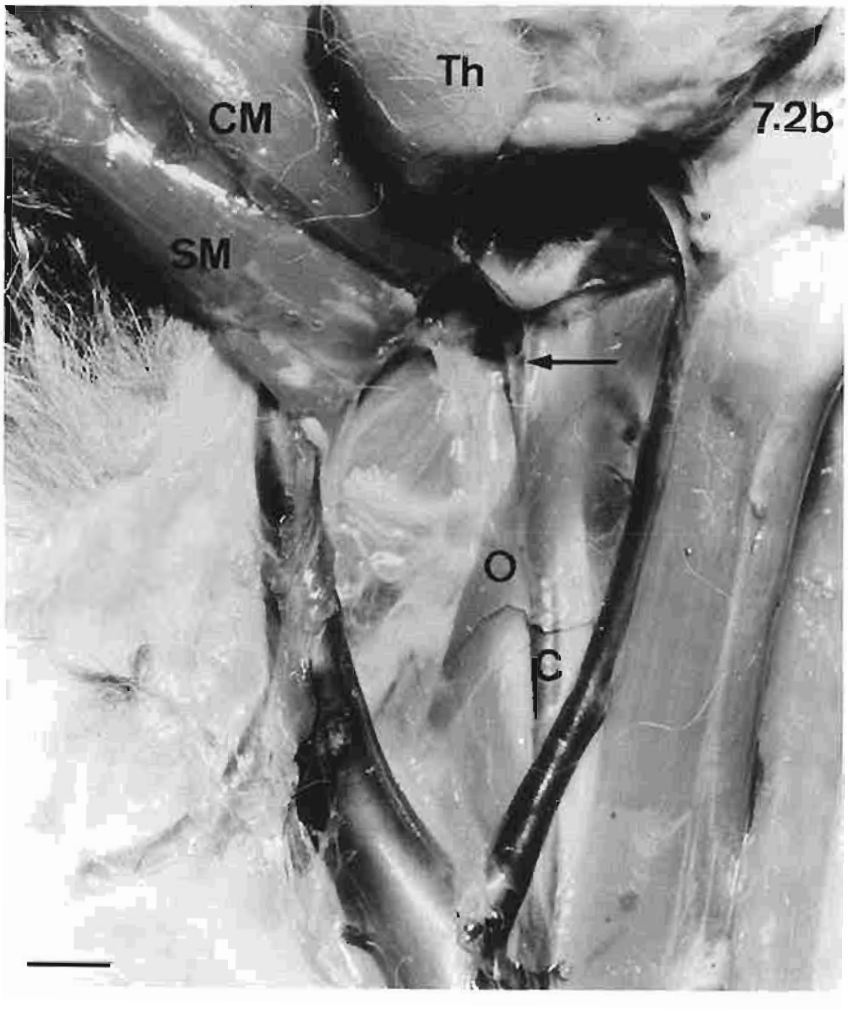
Th
CM
7.2b
SM
O
C

Plate 7.3. The carotid body in *T. vulpecula*

Fig. 7.3a. Low power view of a longitudinal section of the right carotid bifurcation (B). Parathyroid III (P) is rostral to the carotid body (C). The gland is near but separate from the adventitia of the carotid branches, whereas apart from the artefactual tear, the connective tissue around the carotid body is contiguous with the adventitia of the arteries.
Possum P6, paraffin section, H&E.
Bar: 0.3mm.

Fig. 7.3b. Shows the distinctive histological structure of the carotid body in the shared adventitia of the internal and external carotid arteries, just cephalic to the carotid bifurcation. There is a rich network of sinusoids and capillaries amongst the epitheloid cells.
Possum P6, paraffin section, H&E.
Bar: 50μm


7.3a
P
C
B

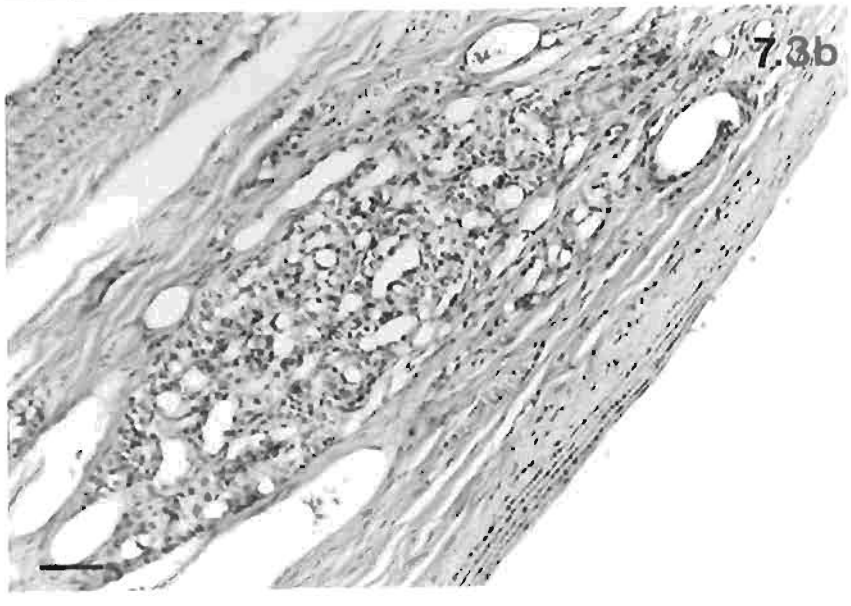
7.3b

Plate 7.4. Parathyroid IV in *T. vulpecula*

Fig. 7.4a. Shows parathyroid IV surrounded by thoracic thymus. The paler staining principal cells of the parathyroid contrast with the small, dark lymphocytes of the surrounding thymus.
Possum P2, paraffin section, H&E.
Bar: 50µm.

Fig. 7.4b. Shows another completely separate part of parathyroid IV gland in the same thymic lobe that appears in Fig. 7.4a. The arrangement of the thymus into cortex and medulla is apparent in the upper part of the micrograph.
Possum P2, paraffin section, H&E.
Bar: 50µm.

Fig. 7.4c. Shows parathyroid IV as a separate structure in the mediastinal connective tissue and not associated with the thoracic thymus. The gland has principal cells arranged in clumps and cords with the elongated nuclei of connective tissue cells and capillaries spread throughout the gland.
Possum P8, paraffin section, H&E.
Bar: 50µm.

7.4a

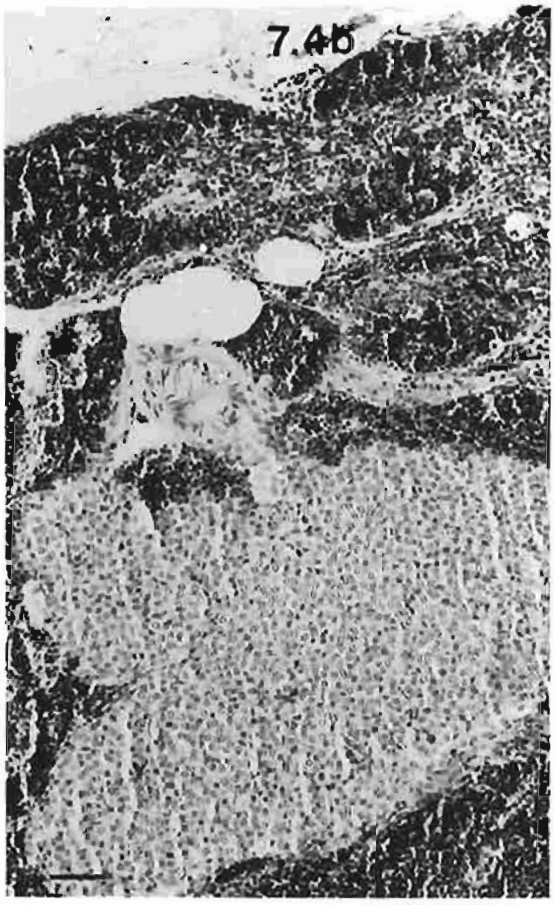

7.4b

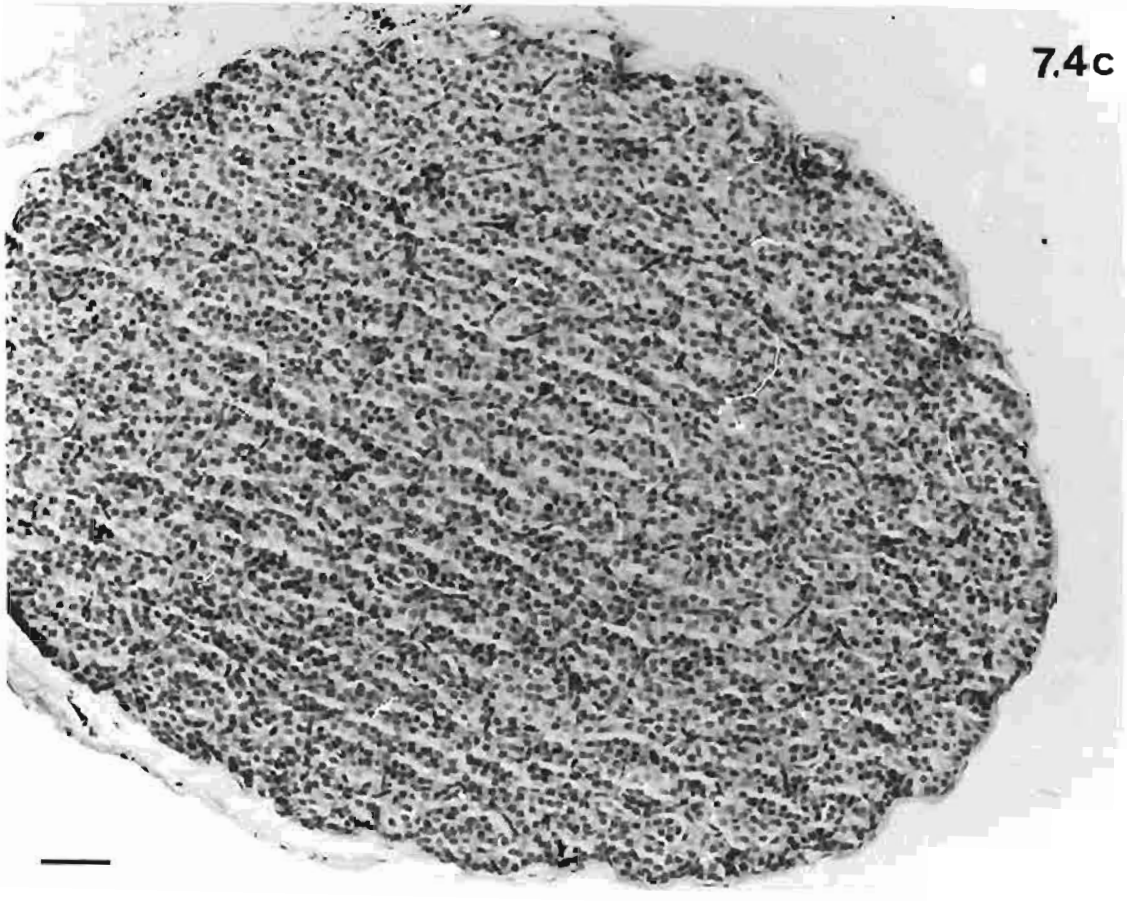

7.4c

Plate 7.5. Light microscopic structure of parathyroid III in *T. vulpecula*

Fig. 7.5a The low power view shows the compact reticulate structure of the parenchymal tissue. The principal cells are in clumps and strands. A thin capsule surrounds the parathyroid.
Possum P9, paraffin section, H&E.
Bar: 50μm.

Fig. 7.5b. Shows the reticular framework (R) of the parathyroid gland with minimal connective tissue supporting the parenchymal cells. The contents of a small follicle (F) are PAS positive.
Possum P7, paraffin section, PAS stain.
Bar: 30μm.

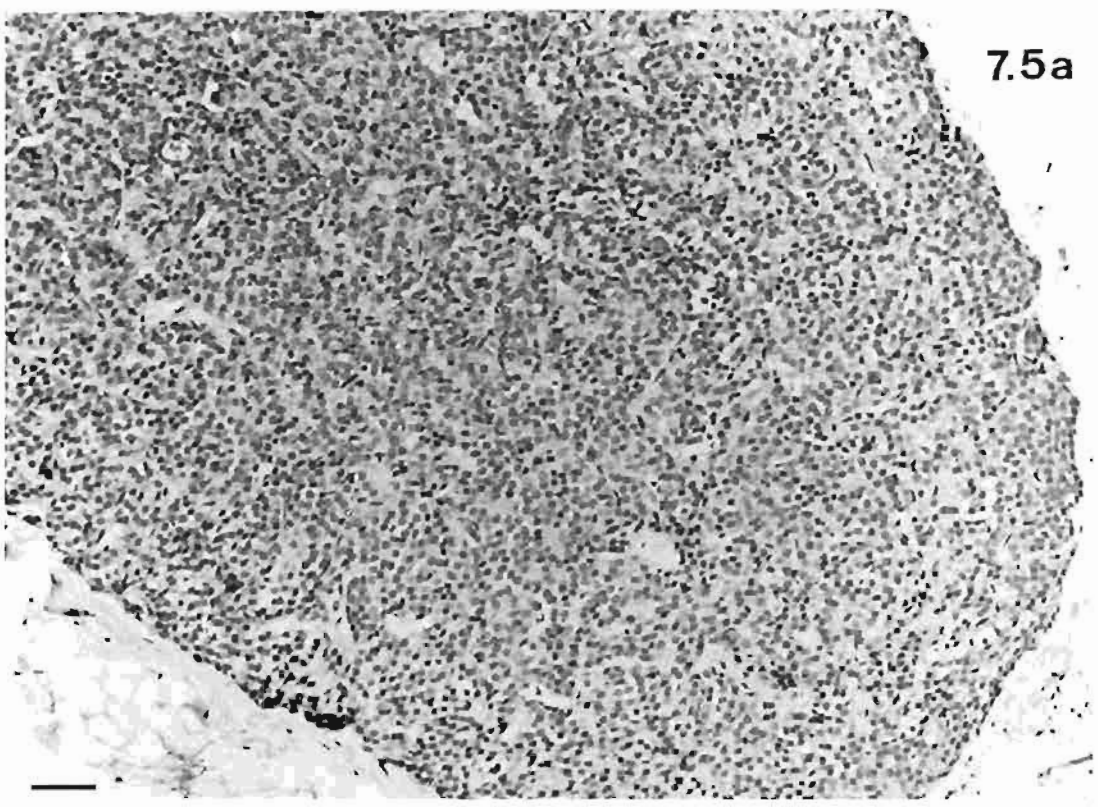

7.5a

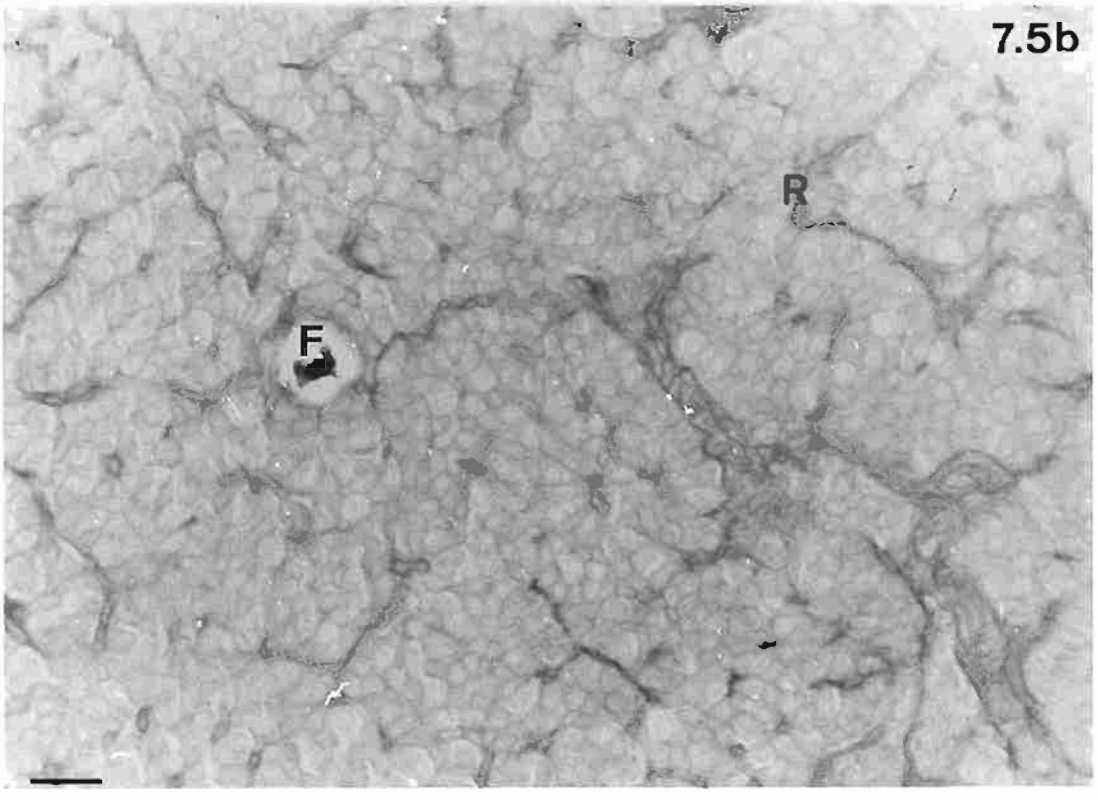

7.5b

Plate 7.6. Thymic tissue in parathyroid III in *T. vulpecula*

Fig. 7.6a. Shows the parathyroid gland completely surrounded by thymic tissue which also penetrates into the gland.
Possum P2, paraffin section, H & E.
Bar: 100µm.

Fig. 7.6b. Shows small fragments of thymic tissue at the periphery of the parathyroid gland inside the capsule of the gland.
Possum P9, H & E.
Bar: 100µm.

Fig. 7.6c. Shows indistinct boundary between the thymic and parathyroid tissues.
Possum P2, paraffin section, H & E section.
Bar: 50µm.

Fig. 7.6d. Shows a small Hassall's corpuscle (H) in lymphoid tissue, thus determining the positive identification of the tissue as thymus.
Possum P1, paraffin section, H & E.
Bar: 30µm.

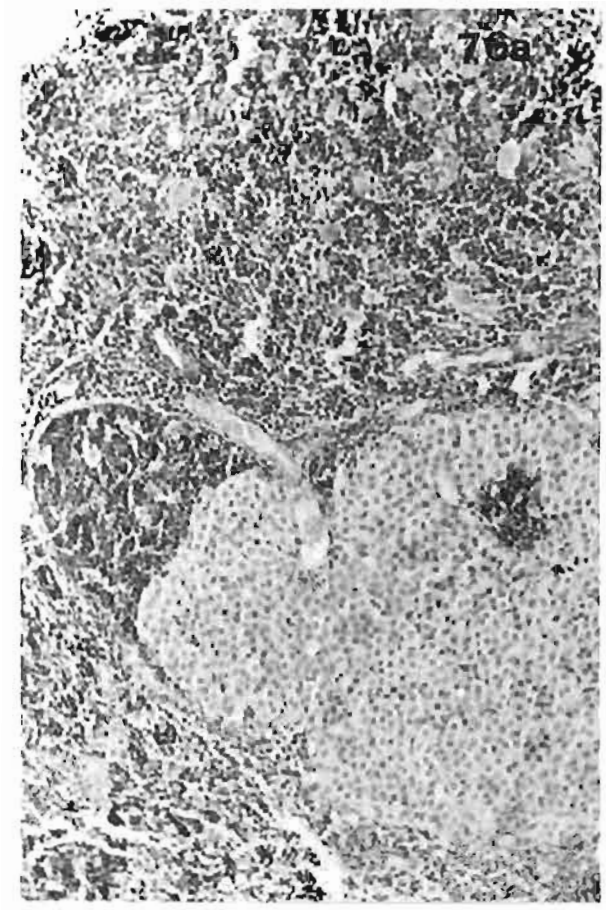
7-6a

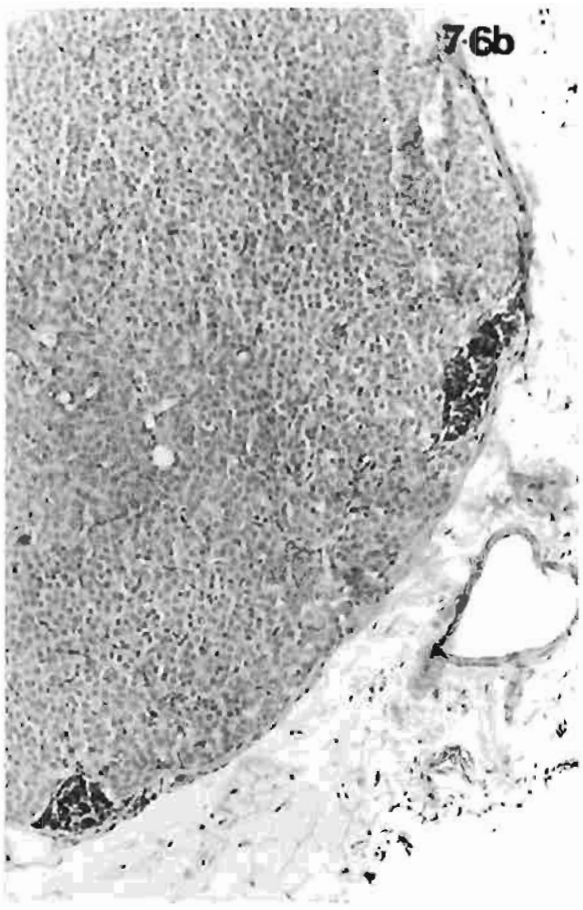
7-6b

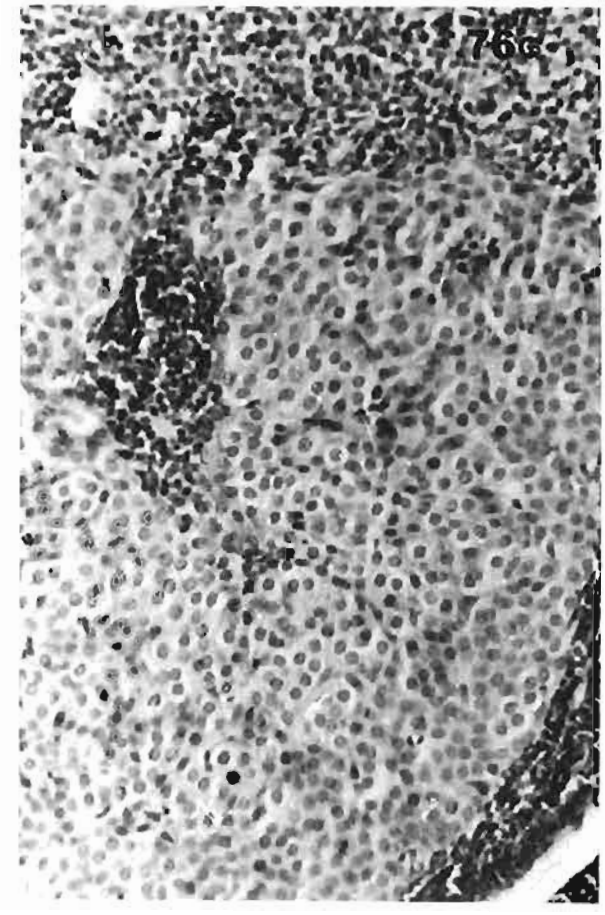
7-6c

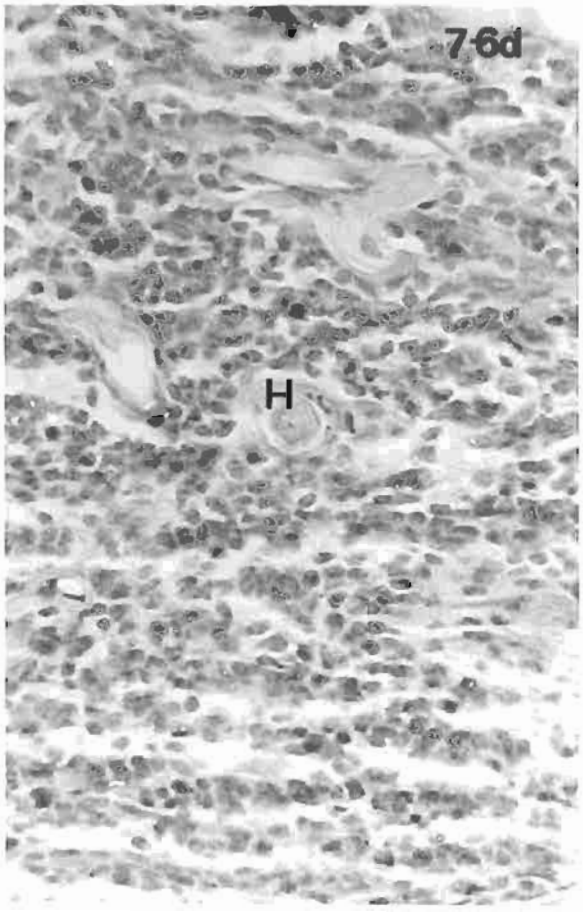
7-6d
H

Plate 7.7. Follicles and cysts in possum parathyroid

Fig. 7.7a. Shows two follicles at the periphery of a parathyroid gland. Both follicles contain a pale acidophilic substance surrounded by principal cells some of which are flattened.
Possum P8, paraffin section, H & E.
Bar: 50μm.

Fig. 7.7b. Shows a small follicle (F) within aberrant thymic tissue at the periphery of a parathyroid gland. The cells around the pale centre of the follicle are similar to parathyroid principal cells. There is apparent mingling of the two tissue types.
Possum P9, paraffin section, H & E.
Bar: 20μm.

Fig. 7.7c. Shows a large cyst on one side of a parathyroid gland.
Possum P7, paraffin section, H & E.
Bar: 100μm.

Fig. 7.7d. Shows a high power view of the cyst in Figure 7.7c. The cyst is lined by a pseudostratified ciliated columnar epithelium and contains neutrophils and degenerating cells.
Possum P7, paraffin section, H & E.
Bar: 20μm.

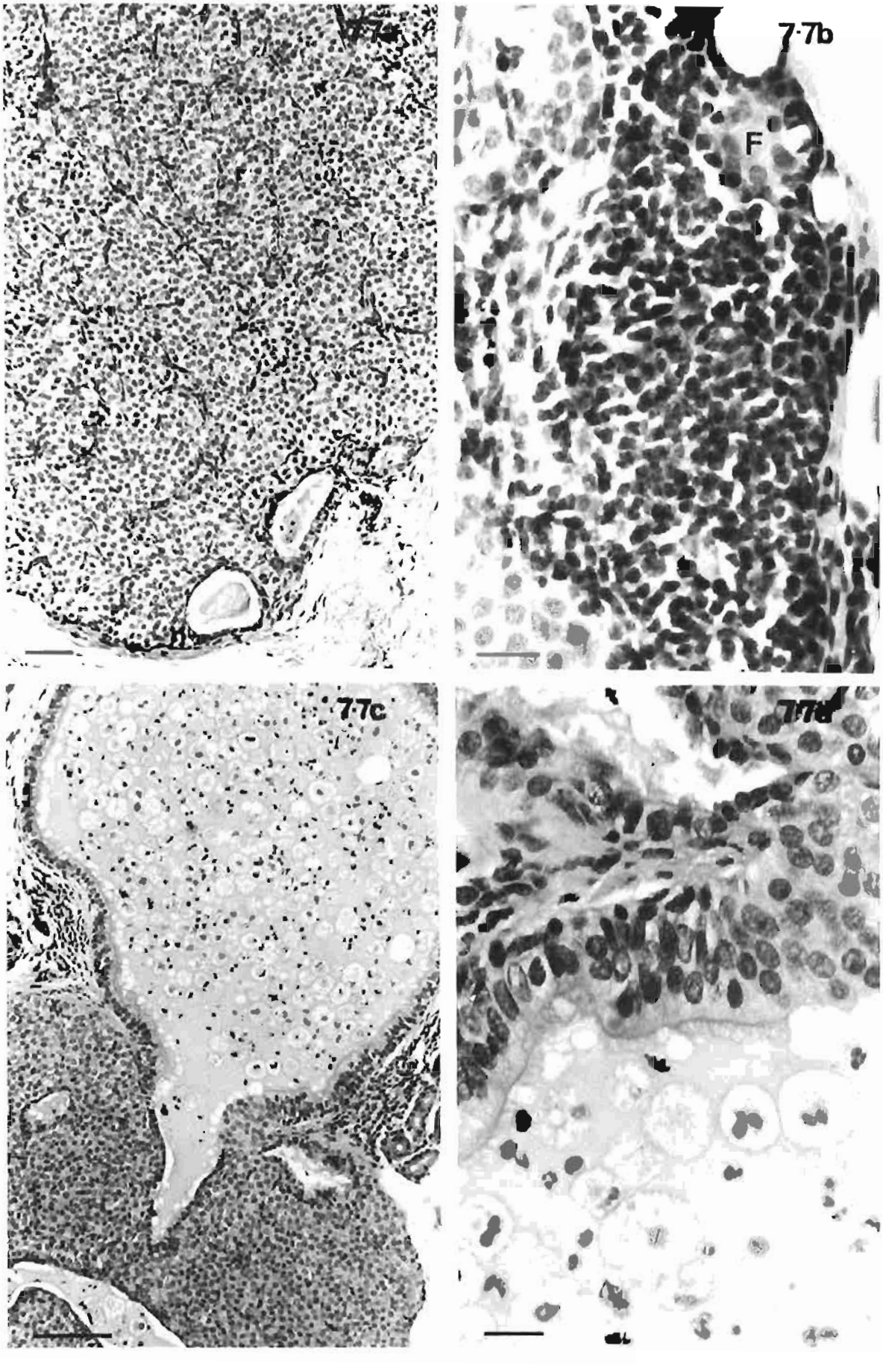
7·7b
F
7·7c
7·7d

Plate 7.8. Ultrastructure of possum parathyroid glands - I
Principal cells

Fig. 7.8a. Shows variation in the cytoplasmic densities of the principal cells in a parathyroid gland fixed by immersion. Light cells (L) can be distinguished from dark cells (D).
Possum P13, fixed by immersion.
Bar: 2μm.

Fig. 7.8b. Shows principal cells of a parathyroid gland fixed by perfusion. The cells have similar cytoplasmic densities.
Possum P10, fixed by perfusion.
Bar: 1μm.

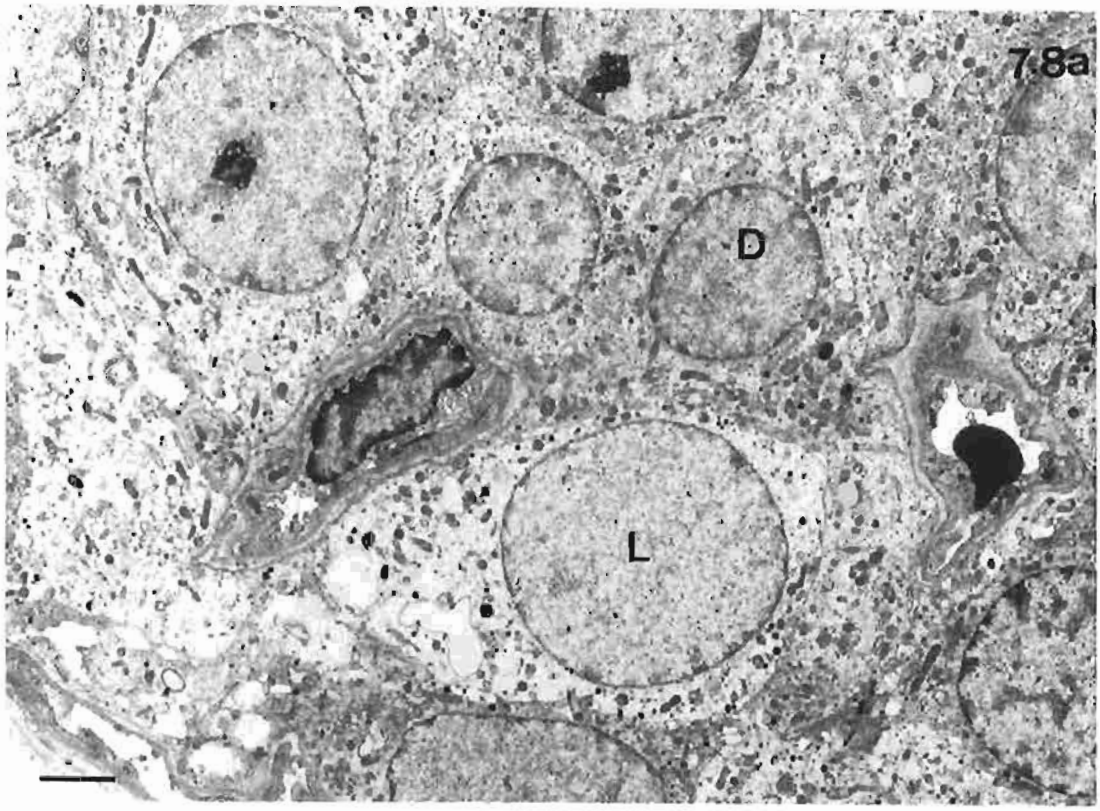
7.8a
D
L

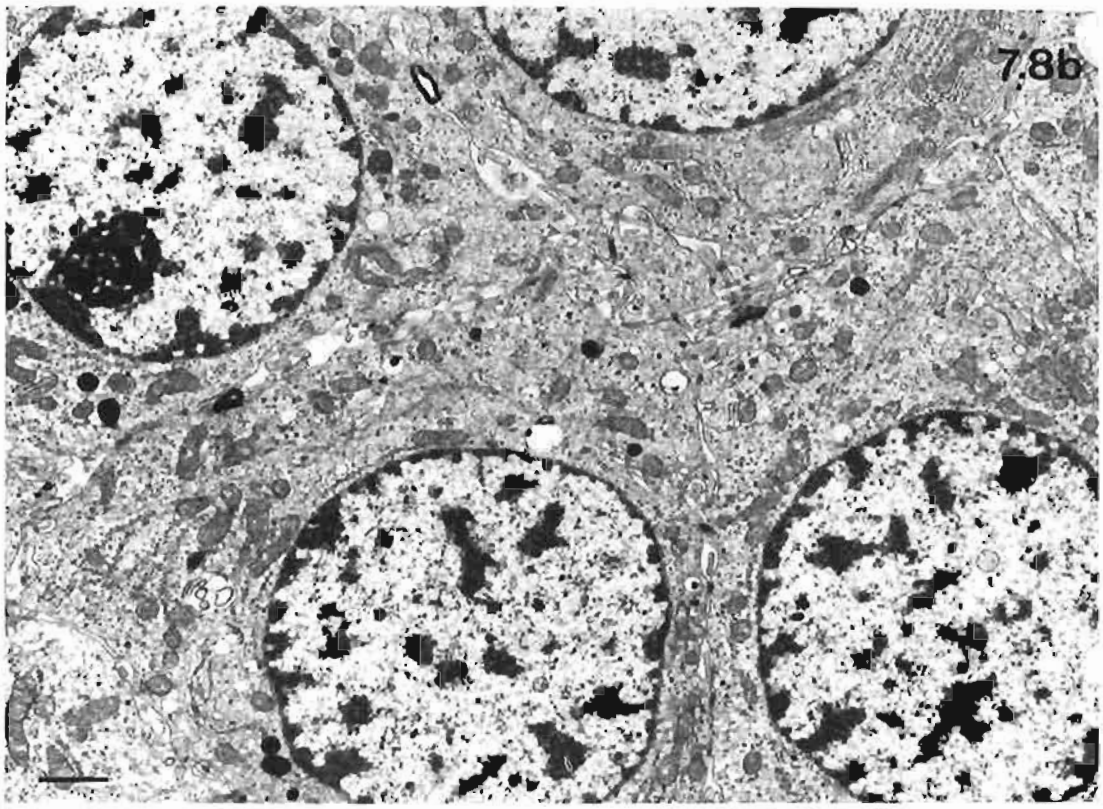
7.8b

Plate 7.9. Water clear cells and the effects of fixation on morphology of the parathyroid in *T. vulpecula*

Fig. 7.9a. Shows the light microscopic appearance of water-clear cells (W). Note the large unstained vacuoles in the water-clear cells and the diffuse glandular arrangement of osmiophilic lipid inclusions.
Possum P12, fixed by immersion, resin section, toluidine blue.
Bar: 5µm.

Fig. 7.9b. Shows very irregular cellular outlines forming microvillous processes that span a large intercellular gap. The cells appear shrunk. Large inclusions or vacuoles (V) are in two cells identified as water-clear cells. One cell is multinucleated.
Possum P11, fixed by perfusion.
Bar: 2µm.

Fig. 7.9c. Shows a difference in cellular outline between peripherally and centrally located cells of a parathyroid gland. Compared with the central cells, note that the peripheral cells show a more compact arrangement with less intercellular spaces.
Possum P11, fixed by perfusion, resin section, toluidine blue.
Bar: 10µm.

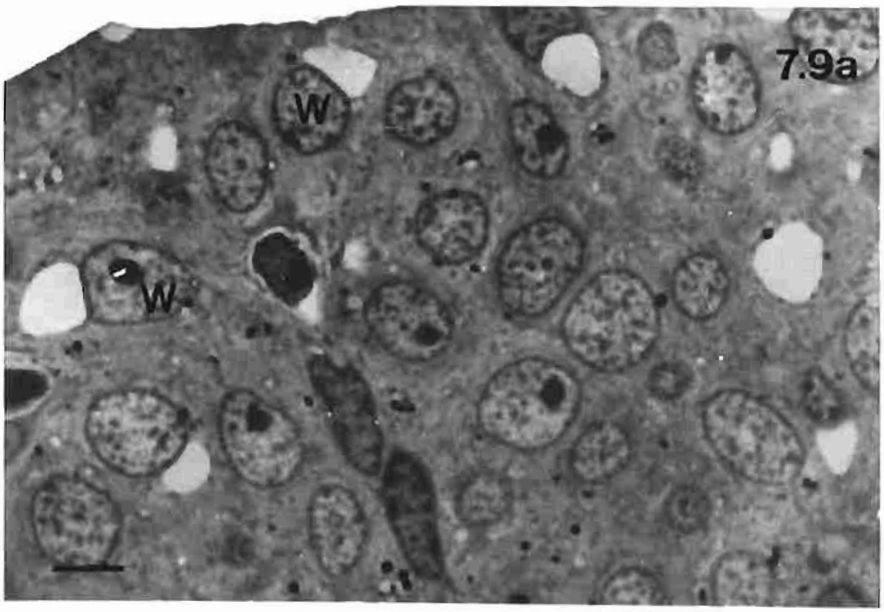
7.9a
W
W

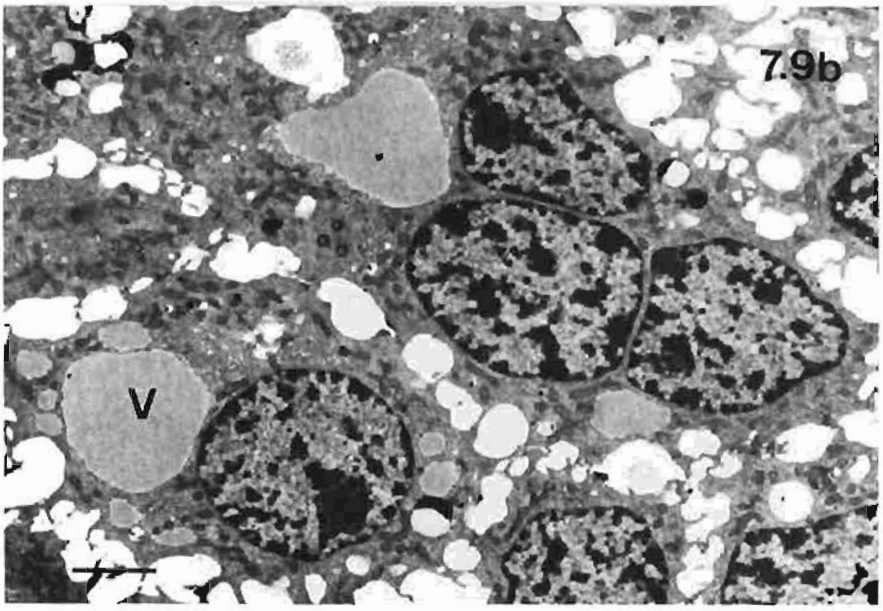
7.9b
V

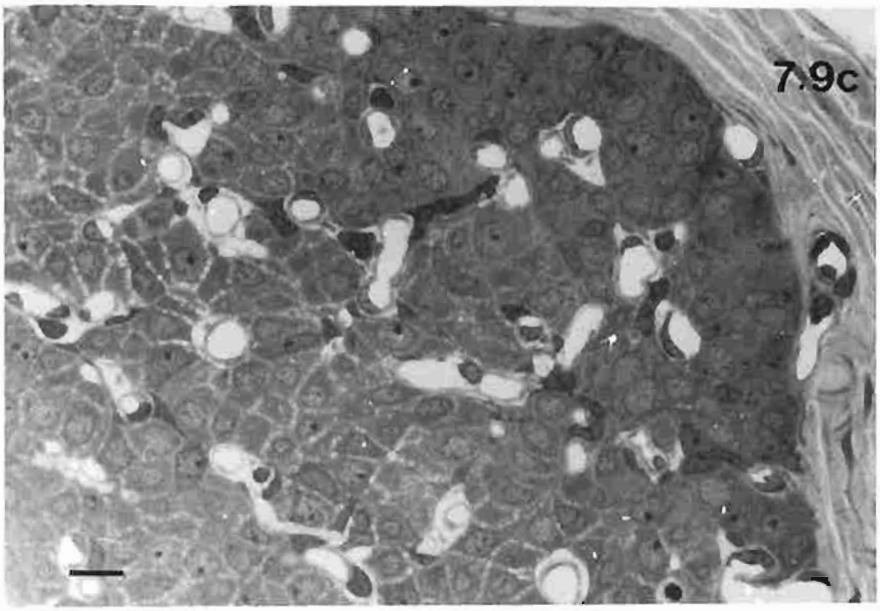
7.9c

Plate 7.10. Ultrastructure of possum parathyroid glands - II
Organelles and inclusions

Fig. 7.10a. Shows the general ultrastructure of the principal cells. There are numerous vesicles of different sizes . Some (V) are associated with the Golgi apparatus (Ga), others (Ve) are much larger. The asterisk shows the unusual appearance of one type of granules. Ribosomes, RER, and mitochondria are spread throughout the cells. A desmosome (D) is present in the lower left of the micrograph and a canaliculus-like space is present between the cells.
Possum P10, fixed by perfusion.
Bar: 500nm.

Fig. 7.10b. Shows vesicles of different sizes (V) and lipofuscin inclusions (L). The black 'V' shows the most common type of vesicles, identified as secretory vesicles. Note the irregular cellular outlines, canaliculus-like areas between cells and the abundant SER in the cell in the upper left of the micrograph.
Possum P10, fixed by perfusion.
Bar: 500nm.

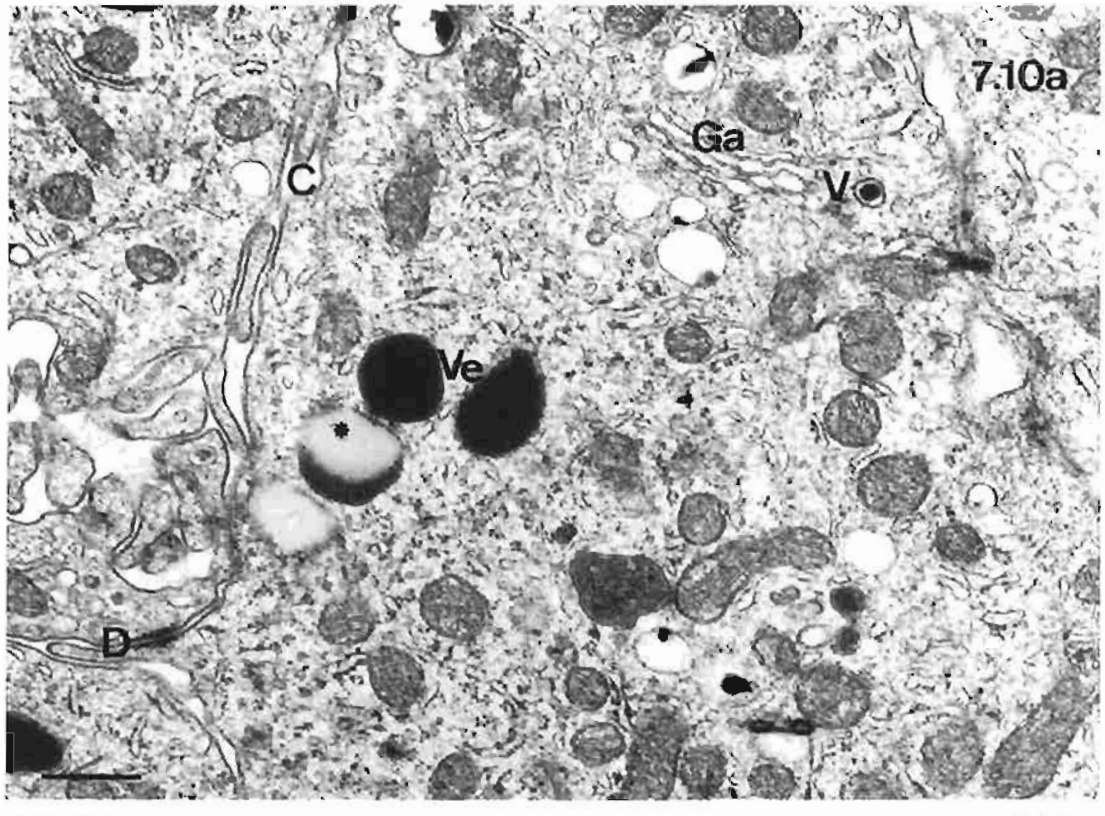
7.10a
C
Ga
V
Ve
D

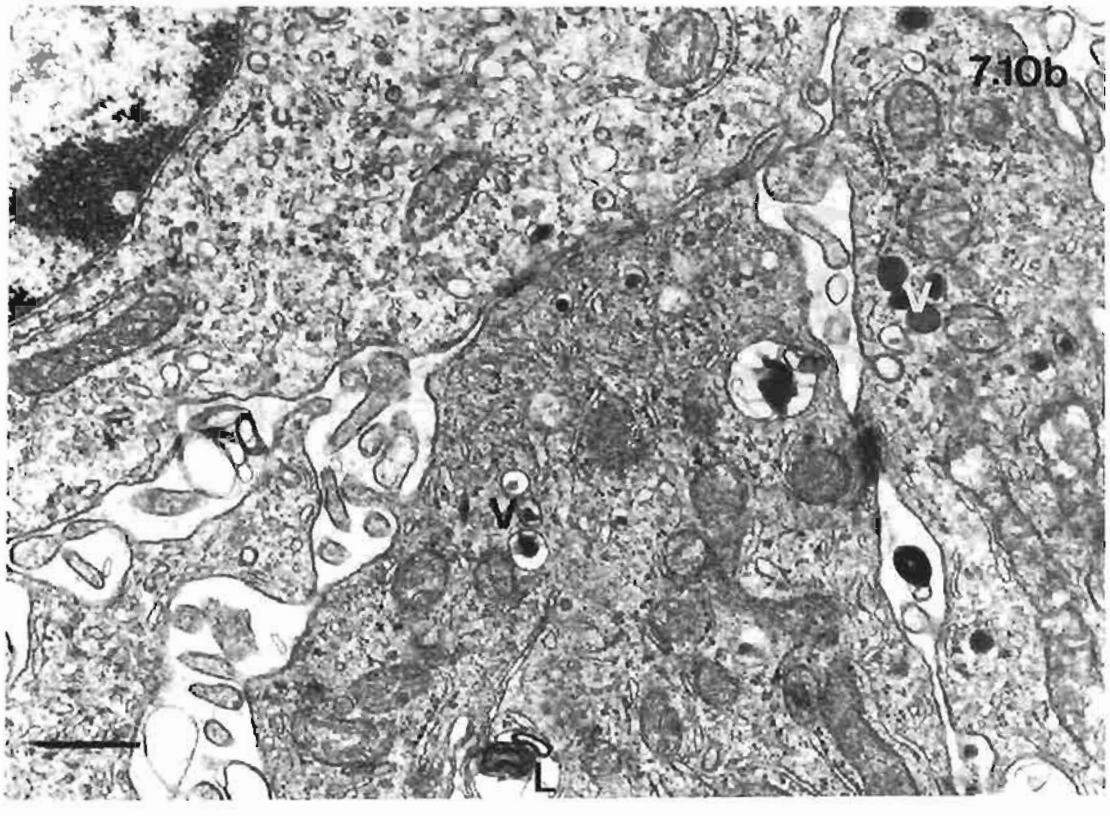
7.10b
V
Ve
L

Plate 7.11. Ultrastructure of possum parathyroid glands - III
Capillaries and Vacuoles

Fig. 7.11a. Shows a fenestrated capillary with diaphragms covering the pores. Part of a pericyte (P) is present within the basal lamina of the endothelial cell. Note the abundant RER in the principal cells, the basal lamina (B) separating them from the pericapillary connective tissue, and the canaliculi (C) between the cells.
Possum P10, fixed by perfusion.
Bar: 500nm.

Fig. 7.11b. Shows a cell with a large pale staining vacuole that appears to be a dilated RER cistern. The cell was identified as a water-clear cell. Several RER with 'normal' profiles are seen in the lower right area of the cell.
Possum P12, fixed by immersion.
Bar: 500nm.

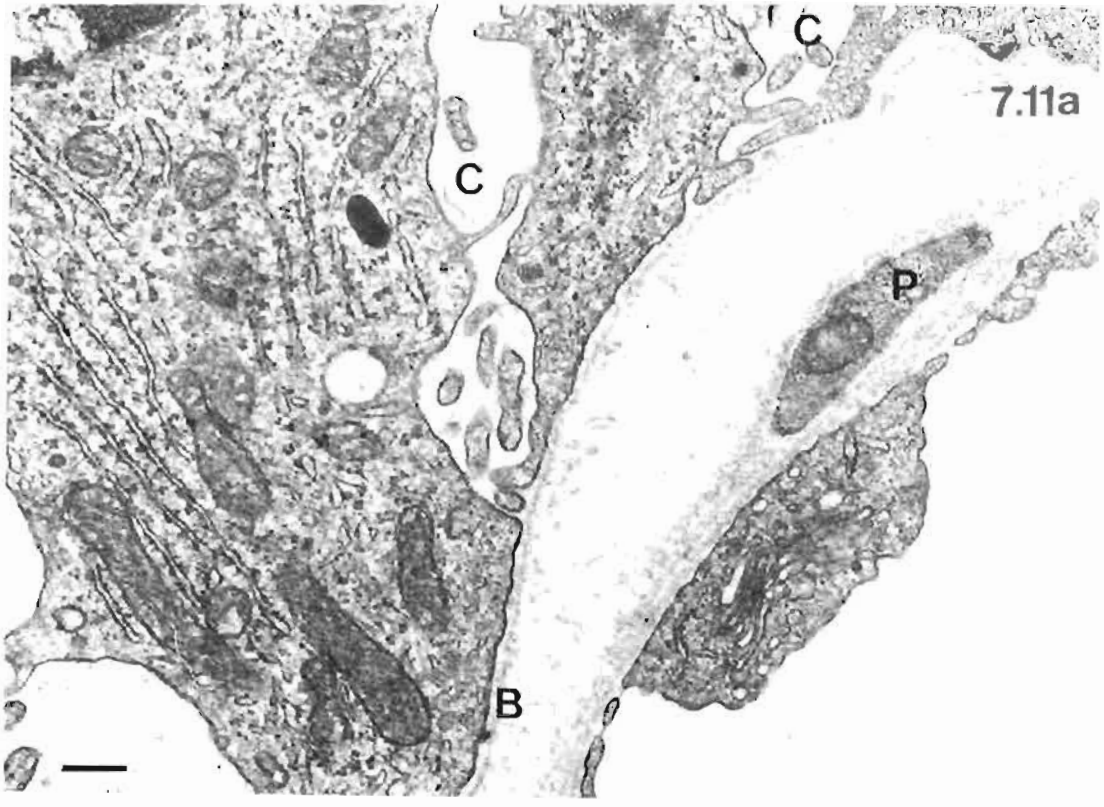
C
C
7.11a
P
B

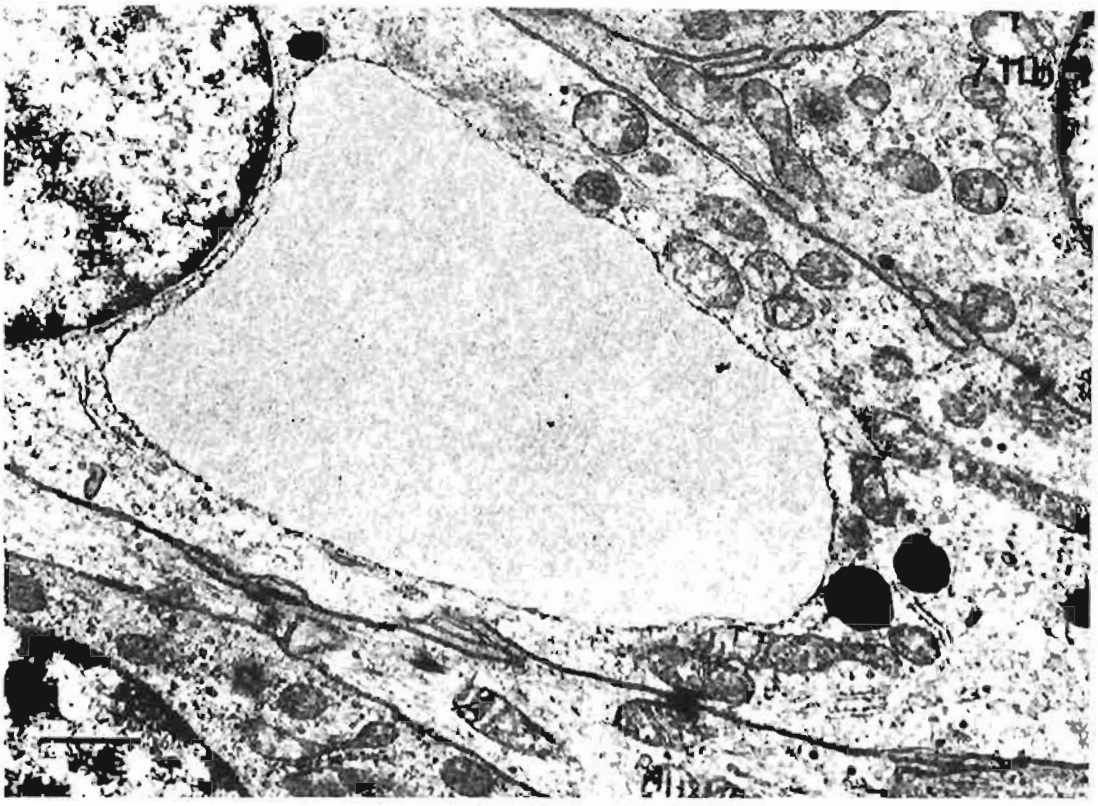
7.11b

Plate 7.12. Ultrastructure of parathyroid and thymus junction in *T. vulpecula* - I

Fig. 7.12. Shows the junction between parathyroid (P) and thymic tissue (T). Epithelial reticular cells (E) separate the two tissues and provide support for the thymus. Note that the basal lamina (arrows) is not present between the thymic and glandular tissues.
Possum 15, fixed by perfusion.
Bar: 1μm.

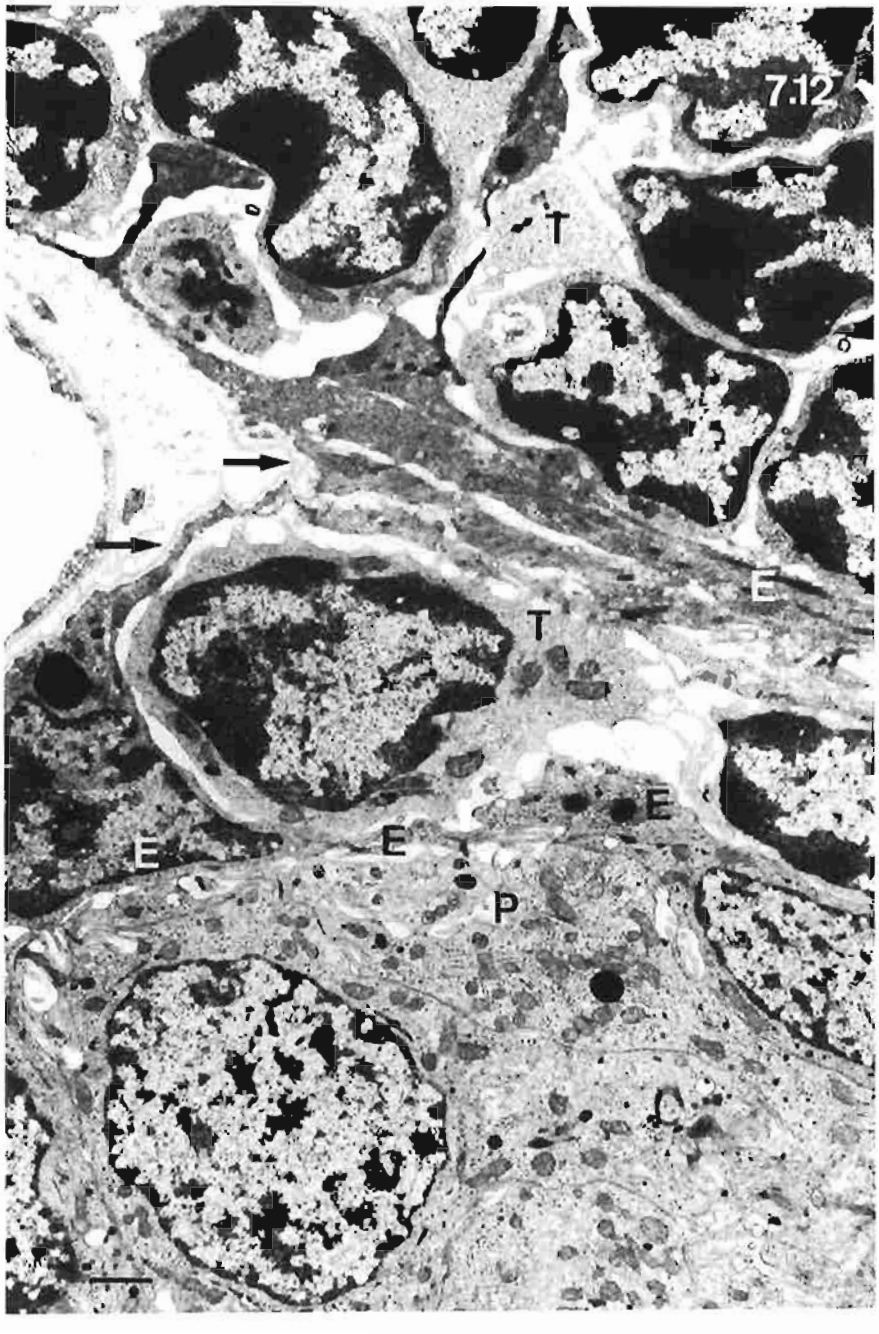
7.12
T
T
E
E
E
E
P

Plate 7.13. Ultrastructure of parathyroid and thymus junction in *T. vulpecula* - II

Fig. 7.13a. Shows the peripheral area of thymic tissue within a parathyroid gland. Processes of epithelial reticular cells (E) surround the thymus and form a framework for lymphocytes (L) and a macrophage (M). Numerous vesicles (V) and short cytoplasmic processes are present in the macrophage.
Possum P15, fixed by perfusion.
Bar:

Fig. 7.13b. Shows the details of the thymus, parathyroid junction. A parathyroid cell (P) in the upper part of the micrograph is separated from a lymphocyte (T) in the thymus (lower right) by epithelial reticular cell processes (E) that contain electron dense tonofilaments.
Possum P15, fixed by perfusion.
Bar: 500nm

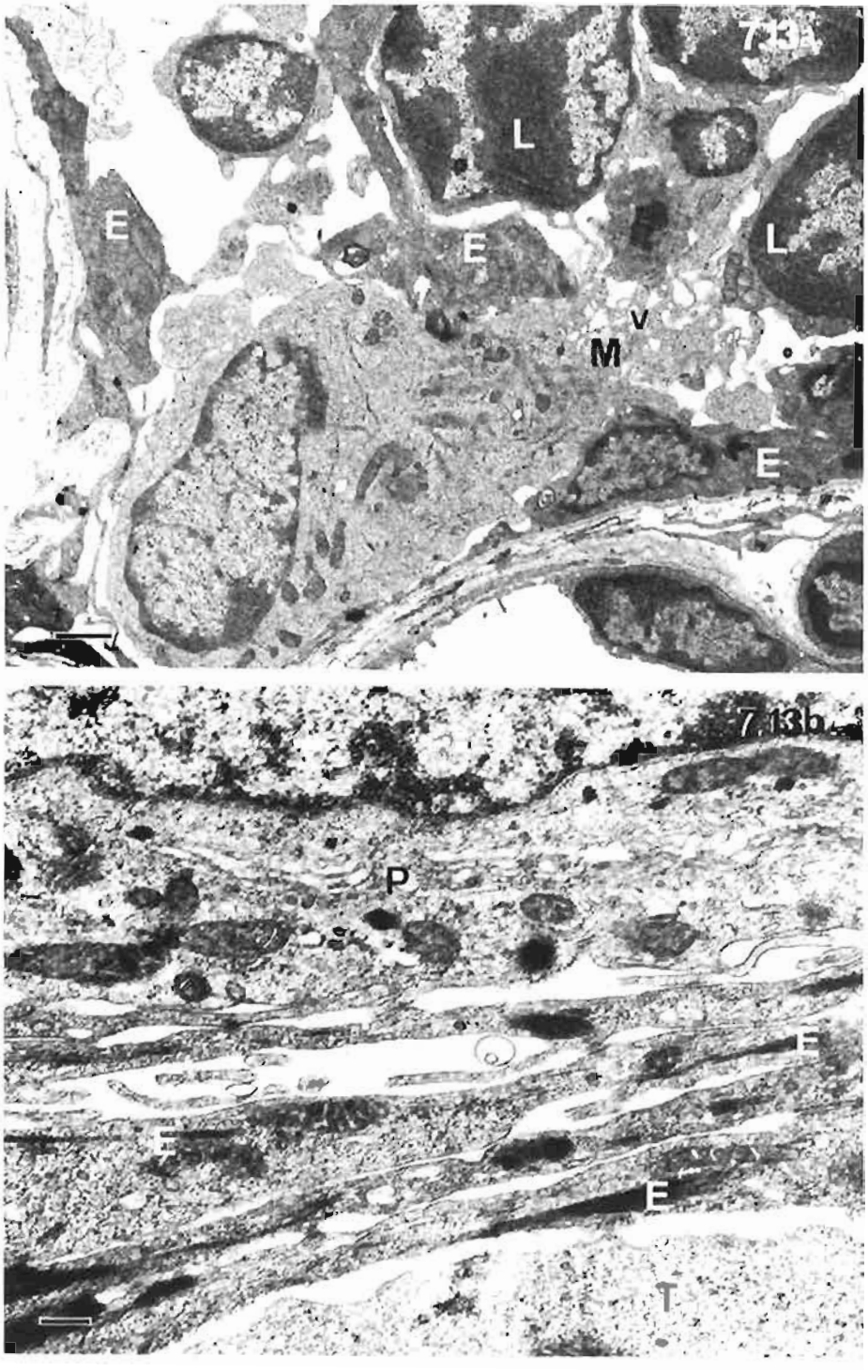
7.13a
L
E
E
L
V
M
E
7.13b
P
E
E
E
T

Chapter 8

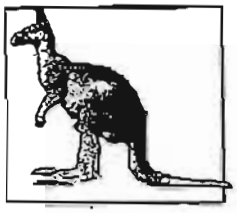

Parathyroid glands in the Macropod marsupial, *Macropus fuliginosus*.

8.1 Introduction

No information on the macropod parathyroid glands has been found in the scientific literature. The descriptions of the macropod parathyroid glands given in this chapter are based on specimens taken from four kangaroos of the subspecies *M. fuliginosus fuliginosus* and 31 kangaroos of the subspecies *M. fuliginosus melanops*. Light microscopic studies were done on 48 glands from 30 kangaroos and ultrathin sections of 40 parathyroids from 25 animals were examined with the electron microscope. In addition to anatomical and histological studies, the relationship between age and ultrastructure was investigated in old and young male kangaroos. The western grey kangaroo, *Macropus fuliginosus*, is one of the larger macropods with old, mature males attaining a maximum weight of more than 55Kg and measuring up to 223cm from head to tail (i.e. tip of nose to tip of tail) (Strahan, 1983). This species, like other large macropod species, shows sexual dimorphism with old females having an average weight of only 28Kg and a head to tail length of 175cm (Strahan, 1983). The subspecies, *M. fuliginosus fuliginosus*, inhabits Kangaroo Island and *M. fuliginosus melanops*, is found in extensive areas of southern Australia, including the Adelaide Hills (Kirsch and Poole, 1972).

The kangaroos used in this study were shot in the field at night as part of culling programs. Except for four kangaroos, the details of the collection and treatment of specimens were the same as those given in chap. 3, Materials and Methods. Briefly, the carotid bifurcations and adjacent tissues and structures were dissected out and placed in either buffered formalin or buffered paraformaldehyde/glutaraldehyde fixative solutions; later, structures thought to be parathyroid glands were identified with the aid of a dissecting microscope, and tissue samples processed for either light or electron microscopy. Tissue from the mediastinum was also collected from three kangaroos, (K5, K6, K15) and processed in a similar manner. In kangaroo K10, the heart, lungs, mediastinal tissue and caudal regions of the ventral neck were removed as a single piece of tissue, placed in buffered formalin and later dissected with the aid of a dissecting microscope.

Three kangaroos (K16, K17, K18) were partially fixed by perfusion in the field. In two kangaroos, K16, K17, immediately after death, the heart was exposed and a cannula inserted into the left ventricle and up into the aorta for perfusion with electron microscopic fixative. The subclavian arteries and the descending aorta were clamped to ensure maximum cephalic flow of the perfusing solutions. The right atrium was punctured to allow the escape of fluid, although most fluids flowed out through the wound made by the bullet entering the head. The duration of the perfusion and the composition of the rinse and fixative solutions were as in descriptions given previously in chapter 3, Materials and Methods. In kangaroo K18, one parathyroid was fixed by immersion; the other was fixed by perfusion. The left carotid was clamped at a level caudal to the larynx and tissue in the vicinity of the bifurcation was excised and immersed in fixative. A cannula was directed into the right carotid and perfused with electron microscopic fixative.

8.2 Age Studies

Since studies done on a variety of animals (Roth and Schiller, 1976) demonstrate that particular histological changes are noticeable in the parathyroid glands of older animals, then a marsupial species with both a reasonable longevity and features that enable a reliable age estimation to be made was selected for this aspect of the research. The western grey kangaroo, *Macropus fuliginosus*, fulfils these requirements with a lifespan of between 10 and 20 years and with extensive, documented information on age determination techniques (Kirkpatrick, 1964; Poole, 1973).

8.2.1. Age Determination Techniques

Kangaroos show several age-dependent dental characteristics including a prolonged, staggered pattern of tooth eruption and loss, as well as molar progression (Kirkpatrick, 1985). The teeth are not fully erupted until about the eleventh year and the molars have a forward progression which continues throughout life (Kirkpatrick, 1985). Data collected from animals of known ages have enabled tables to be constructed which relate molar eruption and/or progression to age (Sharman et al., 1964; Wilson, 1975; Poole, 1976; and Johnston, 1983; Poole et al., 1985). The dental formula of Macropodidae is:

$$I_1^3 C_0^1 P_2^2 M_4^4$$

(Kirkpatrick, 1978). The canine only develops in the upper jaw and does not erupt, being resorbed in pouch life. A diastema thus separates the incisors from the premolars. The anterior premolar, P3, is sectorial and is shed in about the fifth year while the posterior one, dP4, is molariform and deciduous. In the fifth year, dP4 is replaced by a larger premolar, P4 which occupies the space of P3 and dP4; it is later lost at seven or more years (Calaby, 1968). All the

incisors, the premolars, P3 and dP4, and the first molar are fully erupted at 20 months by which time the young kangaroo has left its mother's pouch and is fully independent (Poole, 1973). The second and third molars have fully erupted by three years, and five years nine months respectively. The fourth molar which takes about three years to erupt fully appears at eleven years and over (Calaby, 1968).

Molar eruption values are expressed by the letter M and the molar number written in a Roman numeral for fully erupted teeth and a decimal value from .0 to .4 represents partly erupted teeth. Table 8.1 shows the decimal values given to erupting molars (Sharman et al., 1964). For example, a kangaroo with a dental age MIII.2 would have present in its gums (posterior to the diastema), P4, M1, M2, M3 and the anterior loph of M4.

Table 8.1 Eruption Stages for Molars in Kangaroos (from Sharman et al., 1964)

value	position of anterior loph	position of posterior loph
.4	fully erupted	part way between gum and full eruption
.3	part way between gum and full eruption	just through gum
.2	just through gum	through maxilla, below gum
.1	through maxilla, below gum	below maxilla
.0	below maxilla	

Molar progression commences as soon as each molar erupts. The diastema between the incisors and premolars/molars remains relatively constant and as the molars move forward, they are lost from the front (Calaby, 1968). The progression is recorded as a molar index where a whole number represents the number of the molar anterior to a reference point and a decimal value represents the fraction of the anterior-posterior length of the next molar also anterior to the reference point. The reference point is either the zygomatic process or a line drawn across the anterior rim of the orbits (Kirkpatrick, 1985). For example, in the eastern grey kangaroo, animals with molar indices of 2.75 and 3.77 are five and ten years respectively.

Molar progression gives a more accurate estimation of age than molar eruption, particularly for older animals where all the molars have erupted. However, when animals only need to be grouped into age classes the eruption method is suitable (Kirkpatrick, 1985). In the present study, the age of the kangaroos was estimated by recording the number of molars erupted and

noting the teeth that had been shed and relating these results to data previously determined by Kirkpatrick (1965) and Poole (1976).

8.2.2. Ultrastructural Comparisons of Parathyroid Glands from Young and Old Kangaroos

Quantitative studies comparing ultrastructural components in the parathyroid glands from old and young individuals within several species have consistently shown a significant increase in the number of mitochondria in the parenchymal cells of the older individuals (See chap. 2, Literature Review, section 2.8).

Casual observation of parathyroid cells from old and young kangaroos showed no noticeable differences in the ultrastructure. Hence a quantitative analysis was done to determine if there was a significant increase in the number of mitochondria per $10\mu m^2$ of cytoplasm in the parenchymal cells of old kangaroos compared with young kangaroos. Females were not used in the study in order to avoid the effects of lactation on the parathyroid gland. Three young (less than three years old) and four old kangaroos (at least ten years old) were studied. Although there were other male kangaroos in these two age groups, suitable electron microscopic samples were available from only these seven animals. Ten electron micrographs were taken of random areas of sections and for each micrograph the total area of cytoplasm, the number of mitochondria, and the number of mitochondria per $10\mu m^2$ of cytoplasm were calculated. The total area of cytoplasm photographed for each animal ranged from 400 to 2,500 square μm and total mitochondrial numbers from 350 to 550. Means and standard deviations of the number of mitochondria per $10\mu m^2$ of cytoplasm for each animal were then tabulated. Before comparisons between the old and young groups were made, the homogeneity of both groups of kangaroos was tested using one-way analysis of variance. Next, the variation between the two groups was compared with the variation within groups by the same statistical method.

8.3. Results

8.3.1. Age Estimation of Kangaroos

The approximate age was determined for 29 of the 35 kangaroos used in the study but apart from the two groups of males used for age comparative studies, this information is not central to the research on the kangaroos and the results are presented in Appendix L. Due to time constraints at the time of collecting specimens, the mandibles were not able to be removed from the other 6 kangaroos. The following male kangaroos were classified as juvenile or young adult. The dentition (lower jaw), weights and estimated ages are given in Table 8.2.

Table 8.2. Dentition of juvenile and young adult male kangaroos.

kangaroo	weight (Kg)	dentition	est. age (max)
K9	23	one incisor, two deciduous premolars, 1st molar fully erupted, 2nd molar partially erupted	3yr
K22	12	one incisor, two deciduous premolars, 1st molar	1yr, 8mth
K27	15.5	one incisor, two deciduous premolars, 1st molar	1yr, 8mth

The following male kangaroos were identified as old individuals, being at least ten years old. Table 8.3. shows the dentition of the mandibles of these old kangaroos all of which weighed in excess of 50 Kg. All four kangaroos had a fourth molar and the premolars had been shed. In K26 and K30 the first molar had also been shed.

Table 8.3. Premolars and Molars of Kangaroos at least ten years old.

kangaroo	dentition
K13	one incisor, no deciduous or permanent premolars; 3 molars, 4th molar half erupted
K26	one incisor, no deciduous or permanent premolars; 1st molar shed, 2nd, 3rd and 4th molars present
K30	one incisor, no deciduous or permanent premolars; 1st molar shed, 2nd, 3rd and 4th molars present
K35	one incisor, no deciduous or permanent premolars; four molars present

8.3.2. Anatomy

8.3.2.1. Parathyroid III

The presence of at least one parathyroid gland was recorded for 30 kangaroos; none was found in five. Each parathyroid gland was located in the vicinity of carotid bifurcation which occurs, bilaterally, deep in the ventral region of the neck, dorsolateral to the larynx and deep to the omohyoid and the posterior belly of the digastric muscles. Parathyroid glands were found on both sides in 17 animals, including K27 where three glands were found (two left, one right). In thirteen kangaroos a parathyroid gland was identified only at the right carotid bifurcation. In one of these thirteen animals, kangaroo K35, two glands were located on the same side. One

was 5mm caudal to the bifurcation, loosely associated with the common carotid, and the other was 10mm cephalic to the bifurcation close to the external carotid.

Parathyroid III was generally a flattened ovoid structure with the average dimensions 7 x3 x 1.5 mm. Thirty glands were adjacent to the carotid bifurcation; ten were cephalic to the bifurcation, and nine were caudal. No gland was found cephalic to the glossopharyngeal nerve which runs transversely, about 15mm rostral, across the carotid bifurcation. No gland was found more than 10mm cephalic or 10mm caudal to the carotid bifurcation. Most parathyroid glands were loosely associated with the outer part of the adventitia of the common, internal or external carotid. The glands were surrounded by quite thick fibrous capsules that merged with the surrounding fibro-fatty tissue and, as in other marsupials described in earlier chapters, the kangaroo specimens needed to be examined histologically in order to distinguish parathyroid glands from small lymph nodes, aberrant thymic lobes, and ganglia.

8.3.2.2. Parathyroid IV

The presence of parathyroid IV was sought in four kangaroos. In three kangaroos (K5, K6, K15) serial sections of mediastinal tissue specimens (collected in the field), revealed thoracic thymic tissue but no parathyroid IV. However in kangaroo K10, where the heart, lungs, mediastinal tissue, and the caudal regions of the neck were removed and later dissected with the aid of a dissecting microscope, three discrete parathyroid IV glands were found. A small round gland with a diameter of approximately 1.5 mm was detected on the ventral surface of the brachiocephalic artery at its origin from the aortic arch, and parathyroid tissue was located within two ovoid thymic structures approximately 5 x 3 x 1 mm, one adjacent to the origins of the two common carotids from the brachiocephalic artery and the other 10 mm cephalic to the origin of the left common carotid (See Fig. 8.1.). Both ovoid thymic structures were adjacent to but not part of the adventitia of the arteries.

8.3.3. Light Microscopy

8.3.3.1. Parathyroid III

Forty-nine parathyroid glands from 30 kangaroos were examined with the light microscope. The light microscopic appearance appeared to be basically similar for kangaroos of all ages and both sexes. The parenchymal cells were arranged into groups or lobules separated by quite wide fibrous septa which merged with the surrounding fibro-fatty tissue (Fig. 8.2a). The largest lobule was 1.0 mm x 0.5 mm; others had diameters of 0.3 mm or less. Fat cells (Fig. 8.2a), small blood vessels and nerves (Fig. 8.2b), mast cells (Fig. 8.3) and leukocytes were not uncommon in the septa.

Within a lobule the parenchymal cells were compactly arranged with minimal supporting tissue apparent (Fig. 8.3). No cysts or follicles were seen. Principal cells in routine paraffin sections were either polygonal with a central nucleus or ovoid with an eccentric nucleus. Nuclei showed moderate amounts of heterochromatin and the cytoplasm of the principal cells was generally patchy and acidophilic. Cells with differently staining cytoplasm (i.e. light and dark cells) could only be discerned in thick resin sections stained with toluidine blue. Variation in the staining of the cytoplasm of principal cells was seen in resin sections of most specimens (Figs. 8.2b, 8.3) and evidence indicated that the staining intensity of the cytoplasm was not influenced by the mode of fixation. In kangaroo K18, both glands had similar light microscopic appearances although fixation of the left parathyroid and carotid was by immersion whereas the right gland and artery were fixed by perfusion.

In resin sections the cytoplasm of the principal cells generally had a fine granular appearance. However, parathyroid glands from four kangaroos (K6, K19, K22 and K27) showed cells with large vacuoles or very pale staining, round inclusions (Figs. 8.4a, 8.4b). These features were better seen with the electron microscope (See section 8.3.4).

Specimens taken from eight kangaroos had thymic tissue associated with the parathyroid lobules. In all but two glands, intervening connective tissue could be seen between the parathyroid and thymic tissues (Figs. 8.5a, 8.5b). Electron microscopic examination clarified the nature of the barrier between the two tissue types (See section 8.3.4).

8.3.3.2. Parathyroid IV

The three specimens of parathyroid IV from kangaroo K10 showed a compact arrangement of principal cells. The largest specimen with a diameter of 1.5mm had capillaries and small blood vessels in between clumps of cells without the wide septa seen in the sections of parathyroid III. The more cephalic of the two smaller specimens was an ovoid structure 1.2 x 0.8 mm with a thin but definite capsule separating it from the thymic tissue, identified by the presence of Hassall's corpuscles. The last specimen was thymic tissue with a very small irregular patch of parathyroid cells in amongst the thymocytes. No connective tissue barriers were evident.

8.3.4. Electron Microscopy

The ultrastructure of the glands was derived from looking at ultrathin sections of 40 specimens of parathyroid III from 25 kangaroos; the fine structure of parathyroid IV was not investigated because there no suitably prepared specimens. Electron microscopic examination showed that the parenchymal cells within a lobule were clumped together with minimal supporting tissue visible in between them. In the broad septa, collagen fibrils, capillaries, and connective tissue

cells, including quite numerous mast cells (Fig. 8.6a) were present. A distinct basal lamina separated the clumps of parenchymal cells from the connective tissue (Fig. 8.6a).

All the parenchymal cells were principal cells; no oxyphil or water-clear cells were detected. The cells appeared to vary in shape from a polygon with a central nucleus occupying a significant volume of the cell to an elongated ovoid or rectangle with an eccentric nucleus. Of course, the plane of the section would have influenced the apparent shape of the cells. At intervals along the straight, adjacent cell membranes, the plasmalemma was raised up into very short microvilli or interdigitating processes. In several places these membranous irregularities were the borders of localised, enlarged, intercellular gaps which appeared to be forming canaliculus-like spaces in between the tightly packed cells (Fig. 8.7). Desmosomes (Fig. 8.7) and gap junctions were present between adjacent cells.

Although most sections showed cells with varying intensities of cytoplasmic staining (Fig. 8.7), in many cases the variations were minimal (Fig. 8.6b). In specimens from kangaroo K18 where the right carotid was perfused and the left immersed, the ultrastructure of the cells of the right and left parathyroids appeared to be similar in spite of the different modes of fixation. Similarly the ultrastructure of the parathyroid glands from the other two kangaroos (K16, K17) fixed by perfusion, showed cells with varying cytoplasmic densities (Fig. 8.8a).

Nuclei of most parenchymal cells were indicative of synthetically active cells. Light and dark cells had similar nuclei. Each round to oval nucleus had common features of abundant euchromatin, sparse, peripheral heterochromatin, and a large nucleolus (Fig. 8.7).

Variations in the amount and appearance of RER were noticed in the cells but again, did not correspond to light or dark cell categorisation (Fig. 8.7, 8.8b). Rough endoplasmic reticulum appeared as flattened cisternae (Fig. 8.7, 8.8b), or dilated profiles containing fine particulate matter (Fig. 8.9a). Within the same cell a variety of RER profiles was observed (Fig. 8.9a). Concentric layers of RER were noticed in specimens from K6 (old female), K9 (young male), and K35 (old male) (Fig. 8.10a). In the structures from the first two animals was a small amount of granular cytoplasm; in the last specimen mitochondria were in the centre and closely associated with the outermost layer (Fig. 8.10a).

Mitochondrial numbers appeared similar for light and dark cells (Fig. 8.7). Most mitochondria had round or elongated profiles; some were quite long (Fig. 8.9b), some were curved (Fig. 8.9a), and in some sections, round areas of cytoplasm were enclosed within the mitochondrial profiles (Fig. 8.7). Generally, the mitochondrial matrix was more electron dense than the cytoplasmic matrix. In the matrix small electron dense granules (Figs. 8.7, 8.8b, 8.9a) were

quite common and round, pale inclusions (Fig. 8.7) were sometimes seen. Variations in the size and shape of the mitochondria were observed in glands from both sexes and from all ages. Results of the investigation comparing the age of the kangaroo and mitochondrial numbers in parathyroid glands are given in the next section 8.3.5.

Golgi bodies were reasonably small, each having up to five flattened cisternae, but appeared quite abundant (i.e. two to three bodies) in the principal cells (Fig. 8.10b). Granular structures that were identified as small transfer vesicles and immature secretory vesicles of varying electron densities were associated with the Golgi bodies (Fig. 8.10b).

A wide array of membrane-bound structures, ranging from small electron dense bodies to large electron lucent vacuoles, was present in both light and dark cells and in sections from animals of both sexes and all ages. Small electron dense granules were interpreted as secretory granules. In many cells they were concentrated towards one end, presumably adjacent to the surface from where they were to be secreted (Fig. 8.6b, 8.7, 8.8b). Large granules with heterogeneous contents, often including lamellar structures (Fig. 8.11a), were identified as secondary lysosomes; they were not numerous. Many cells had vacuoles which appeared either empty (Fig. 8.7,8.11a & b), or with granular contents (Fig. 8.11a); some vacuoles were interpreted as dilated RER (Fig. 8.9a) or SER (Fig. 8.11b). Often cells with abundant dilated SER had features consistent with cellular degeneration (Fig. 8.11b); i.e. nuclei had increased heterochromatin and cytoplasm lacked structural integrity.

The thymic tissue that was included in several specimens of parathyroid glands showed a network of epithelial reticular cells, lymphocytes and macrophages (Fig. 8.12a). In most cases the barriers between parathyroid and thymic tissues were distinct consisting of vascular connective tissue and basal laminae (Fig. 8.12a). A continuous layer of epithelial reticular cells was present at the periphery of the thymus adjacent to the basal lamina. A small number of specimens (e.g. K21) appeared to have only epithelial reticular cells separating thymocytes from parathyroid principal cells (Fig. 8.12b); no basal laminae or connective tissue components could be identified between the two organs.

8.3.5. Ultrastructural Comparisons of Parathyroid Glands from Young and Old Kangaroos

Table 8.5 shows the data for the number of mitochondria in $10\mu m^2$ of cytoplasm for young and old kangaroos. From the table it is noted that three of the four means in the old group are higher than any of the values for the three kangaroos in the young group and that one of the two oldest kangaroos (K26) has the greatest mitochondrial numbers whilst a young kangaroo (K9) has the lowest. However, the analysis of variance showed the means of the number of

mitochondria in 10μm^2 cytoplasm were not similar within the two groups; P=0.016 for young kangaroos (n=3); P<0.0004 for old kangaroos (n=4). A similar degree of difference was noted in the analysis of variance on the data of all seven animals (P<0.0004). Thus the differences observed within each group were as great as the differences seen in the comparison of all animals. Hence it was inappropriate to pool data for young, and for old kangaroos, in order to test if the number of mitochondria per 10μm^2 of cytoplasm was greater in old animals compared with young.

Table 8.5. Number of mitochondria in 10μm^2 cytoplasm for young and old kangaroos.

kangaroo	age	nos. of e/graphs	total cyto. area (μm^2)	total nos. of mitochondria	mean (mito in 10μm^2)	S.D.
K9	young	10	735.9	347	4.75	1.30
K22	young	10	559.3	352	6.32	2.00
K27	young	10	506.2	347	7.00	1.58
K13	old	7	420.1	308	7.26	1.37
K26	old	6	302.2	296	9.70	2.15
K30	old	11	641.5	488	7.68	1.32
K35	old	11	678.8	376	5.57	1.86

8.4. Discussion

8.4.1. Age Determination

The mandibles were lightly crushed to ensure the presence of unerupted permanent teeth was not missed and to avoid misidentification of permanent premolars as deciduous teeth. Unerupted molars exposed in the crushing also helped to confirm the identification of the erupted teeth. The weighing scales that were used in the field had a maximum reading of 50Kg. Hence the weight of animals more than 50Kg could not be recorded accurately.

Only two groups of males, namely juvenile to young adult, and old, were used in the study of the effect of age on the morphology of the parathyroid gland because these groups had clearly defined members and, unlike the females, some of which had pouch young, the demands on the parathyroid were assumed to be likely to show fewer variations within a group. Previous studies (Yamahira et al., 1980) have shown that in mice, the number of mitochondria, lipid droplets, storage granules and the volume of Golgi complex are altered in lactation.

8.4.2. Anatomy

The dimensions quoted for parathyroid glands are approximate values only. In many cases the thick capsules could not be easily delineated from the surrounding connective tissue. The close association of the parathyroid glands with the adventitia of the carotid artery and its branches has been described previously in the possum (Adams, 1955) where, unlike the kangaroo, the gland was freely mobile allowing it to be distinguished with a dissecting microscope. In other marsupials it has been noted that the parathyroid III never occurs cephalic to the transversely running glossopharyngeal nerve (Fraser, 1915; Fraser and Hill, 1915; Adams, 1955). The recorded absence of a parathyroid gland in the vicinity of the left carotid bifurcation in eleven kangaroos was possibly due to insufficient tissue being excised from the animal rather than a reflection of the true anatomy. In most animals, the right carotid bifurcation was removed first and blood pouring from severed blood vessels made dissection of the left side of the neck difficult, particularly the structures cephalic to the carotid bifurcation where the carotid branches course deep to the digastric and omohyoid muscles.

The nature of specimen procurement made anatomical examination of the mediastinal region very difficult. Dissection was done at night, on the ground where each kangaroo fell after being shot, and usually there was insufficient time to examine the thoracic cavity or, if the animal had been shot though the heart, then damage to the mediastinum made specimen collection unsuitable. Hence the location of parathyroid IV was found in only one kangaroo. The arrangement of the major arterial branches from the aortic arch in the kangaroo is similar to that in other diprotodonts where the brachiocephalic artery almost immediately gives rise to the right subclavian artery and a short distance on bifurcates into the right and left common carotid arteries; the left subclavian artery is the other major branch from the aortic arch (Pearson, 1940).

The only diprotodont in which parathyroid IV has been investigated is the brush-tail possum, *T. vulpecula*, (Fraser and Hill, 1915; Adams, 1955) and in both studies parathyroid IV was noted to be much smaller than parathyroid III. A similar size difference was also seen in the kangaroo in the current study suggesting that in *M. fuliginosus* and perhaps other macropod species the more caudal gland, parathyroid IV, is smaller than parathyroid III. However caution should be exercised in drawing conclusions from the examination of only one specimen.

Since both parathyroid IV and thymus IV originate from the same fourth pharyngeal pouch and migrate caudally together then the close association of the two tissues observed in kangaroo K10 is not altogether surprising. The absence of parathyroid IV in the thoracic thymus sections from three kangaroos was possibly a result of the variable location of parathyroid IV in marsupials rather than an indication of parathyroid IV being absent in these individuals.

8.4.3. Light Microscopy

Similar histological features were seen in both sub-species of kangaroos. The lobulation of all specimens of parathyroid III appears to be a unique feature of these animals as similar descriptions have not been found for any other animal (Roth and Schiller, 1976). Light microscopic studies confirmed that the presence of the thick septa and indistinct capsule of the parathyroid glands in kangaroos, made the accurate dimensions of the gland difficult to estimate and probably readings were greater than the true values. The connective tissue content of the parathyroids in kangaroos appeared to be constant in glands from animals of all ages. The increase in interstitium and fat cells that has been described for the parathyroids of elderly humans (Morgan, 1936; Gilmour, 1939; Roth, 1979) and dogs (Setoguti, 1977) was not apparent in kangaroos.

In most species, parathyroid III and IV have similar light microscopic features (Roth and Schiller, 1976) but in kangaroos, there are indications that the unique lobulation of the parathyroid gland occurs only in parathyroid III and not parathyroid IV. However it needs to be stressed again that observations on parathyroid IV were based on the examination of just one specimen and the results may not be an accurate representations for the species, *M. fuliginosus*.

8.4.4. Electron Microscopy

From the examination of many random sections at both the light and electron microscopic levels, it appeared that within a lobule the principal cells were tightly packed and adjacent membranes had lengths of straight membranes interrupted by tortuous portions where canaliculus-like areas were present that possibly provided channels to carry secretions to capillaries. Similar intercellular spaces have been described in the rat parathyroid gland (Wemerson et al., 1995) and serial sections demonstrated continuity of the canaliculi.

Variations in the RER morphology have been described in both normal and pathological parathyroid glands (Nilsson, 1977; DeLellis, 1993). There are perhaps four possible explanations for dilated RER. It may represent principal cell hyperactivity, precursors of vacuoles similar to those in water-clear cells, or may be a normal feature of the secretory cycle. In the first suggestion it is proposed that cellular hyperactivity is manifested by immature forms of PTH, e.g. proPTH, being stored within the cisternae of RER prior to transfer to the Golgi complex where PTH is formed (Kemper, 1984). Similar dilated RER profiles are typical of gonadotrophs in the anterior pituitary after ovariectomy and are interpreted as being sites of increased hormone production following the loss of negative feed-back control (Kovacs and Horvath, 1975). However studies on the synthesis of PTH have indicated that once PTH

elaboration has begun it is completed within 30 minutes and the PTH in secretory granules is the only form of storage of the hormone or its precursors in the cell (Kemper, 1984). Furthermore, hyperactivity in parathyroid cells is recognised by increased amounts of RER, not dilatation of RER (DeLellis, 1993).

The second explanation for the dilated RER proposes that it is possibly a precursor of the vacuoles characteristic of water-clear cells. Similar structures have been reported in water-clear cells in the parathyroid glands of the golden hamster (Emura et al., 1990) and have been considered to be the sources of the large, clear vacuoles typical of these cells. However no water-clear cells were observed in any kangaroo specimen and so such a precursor role for the dilated RER in this species does not appear to be likely.

The third suggestion as an explanation for the presence of the distended RER is that it is part of the normal ultrastructure of the secretory principal cells and characterises a transitional state between resting and secreting phases (Wild, 1980). Similar structures have been observed in dogs of all ages (Wild, 1980), particularly in light principal cells at the end of the resting stage and before the presence of the pronounced Golgi complex, secretory granules, and numerous flattened cisternae of RER herald active hormone synthesis (Roth and Capen, 1974). In the present study, dilated RER was not restricted to light cells, which contrasts to the situation in dogs (Wild, 1980). However, the division of principal cells into light (inactive) and dark (active) categories appears to be somewhat artefactual (See chap. 11, General Discussion, section 11.4) Perhaps species differences account for the lack of distended RER in normal human, bovine, and rat parathyroid glands which have been used in studies linking ultrastructure with hormone synthesis and secretion (MacGregor et al., 1975; Kemper, 1984; Kendall et al., 1993).

Initially, the true identity of the close concentric layers of RER that were observed in several specimens was questioned. The morphology of the organelle was similar to that of annulate lamellae and confirmation of the correct identification was influenced largely by the interpretation of whether the electron dense granules on the concentric lamellae were interpreted as ribosomes or pore complexes, unique to annulate lamellae (Kessel, 1992). Both whorls of RER (Nilsson, 1977; DeLellis, 1993) and annulate lamellae (Bergdahl and Boquist, 1973; Boquist, 1980; de Menezes and Sesso, 1988; Kessel, 1992) have been described previously in parathyroid glands. Closely packed cisternae of RER are common in principal cells actively synthesising PTH (Roth and Capen, 1974); concentric arrangement of the RER is less common (Nilsson, 1977; DeLellis, 1993), although in the pituitary gland, concentric whorls of RER (nebenkern) are characteristic of chromophobes entering an active phase of protein synthesis (Imura, 1994). Annulate lamellae are not widespread in normal parathyroid principal cells and

most reports have been associated with parathyroid adenomas (de Menezes and Sesso, 1988). Their transient appearance in normal cells has been linked to mitochondrial proliferation and oxyphil cell formation (Boquist, 1980). Examination of electron micrographs showed the spaces between concentric layers of the organelle were more in keeping with structural details of whorls of RER rather than annulate lamellae. Similar conclusions were made about the nature of the electron dense particles associated with the layers.

The variations that were recorded in the size and appearance of mitochondria in old and young animals of both sexes suggest that in kangaroos mitochondrial morphology does not exhibit age-related changes. In the older members of many species mitochondria enlarge, assume irregular profiles, and have a variety of granular inclusions (Roth and Schiller, 1976). These changes are usually associated with the transformation of principal cells to oxyphil cells where mitochondrial proliferation also occurs (Nilsson, 1977, DeLellis, 1993). Whether mitochondrial proliferation occurs without morphological alteration is discussed in the next section.

The lack of barriers between parathyroid and thymic tissues that was observed in a minority of specimens has been noticed in several other marsupial species in the present study and the somewhat unusual relationships are discussed in chapter 11, General Discussion, section 11.4.

8.4.5. Ultrastructural Comparisons of Parathyroid Glands from Young and Old Kangaroos

There is not an entirely even distribution of mitochondria throughout the cytoplasm of a parathyroid principal cell with few near the cell surface where granules accumulate before being released, and they are not abundant in the juxtanuclear cytoplasm (DeLellis, 1993). However, in the random selection of electron micrographs an assumption was made that a similar range of cytoplasmic areas was sampled for all specimens.

The statistical analyses did not support the hypothesis that there was a significant increase in the number of mitochondria per $10\mu m^2$ of cytoplasm in the parenchymal cells of old kangaroos compared with young kangaroos. Furthermore analyses of data showed there was a wide variation in the number of mitochondria per $10\mu m^2$ of cytoplasm in parenchymal cells of animals of similar ages. However the data also showed that the lowest and highest values for the number of mitochondria per $10\mu m^2$ occurred in a young and an old animal respectively and that three of the four old kangaroos had means higher than all the young kangaroos. Maybe if more male kangaroos had been available to include in the old and juvenile groups then the statistical results may have been different.

If mitochondrial volume instead of number had been assessed for old and young animals a similar lack of difference probably would have been found because similar variations in mitochondrial size and shape were noticed in kangaroos of all ages rather than just old animals.

The lack of statistical support for increased mitochondrial numbers in old animals is consistent with the observed absence of oxyphil cells in all kangaroo specimens. Oxyphil cells develop via transitional cells from principal cells that undergo mitochondrial proliferation (DeLellis, 1993) The lack of transitional cells may indicate that principal cells had not yet begun the transformation into oxyphil cells or that oxyphil cells are not a feature of the parathyroid in old kangaroos. Maybe ten years is not enough time to allow the manifestation of oxyphil cells in kangaroos although oxyphil cells have been detected in younger, apparently healthy, individuals of other species with a comparable lifespan to kangaroos - e.g. 8.5-year-old dogs (Setoguti, 1977) and 4-year-old cows (Capen et al., 1965).

Fig. 8.1. Location of parathyroid IV in kangaroo K10

Fig. 8.1. The simplified drawing of the left latero-ventral view of the mediastinum of kangaroo K10 shows the locations of thymic and parathyroid tissues in relation to the major branches of the aortic arch. Veins are not shown. Note there are only two major branches from the aorta: the brachiocephalic and the left subclavian artery. The brachiocephalic artery gives rise to the right subclavian artery and then bifurcates into the common carotids.

1. thymus
2. thymus
3. lymph node
4. parathyroid gland
5. thymus with tiny patch of parathyroid
6. thymus and separate parathyroid

Kangaroo K10
Bar: 10mm

8.1

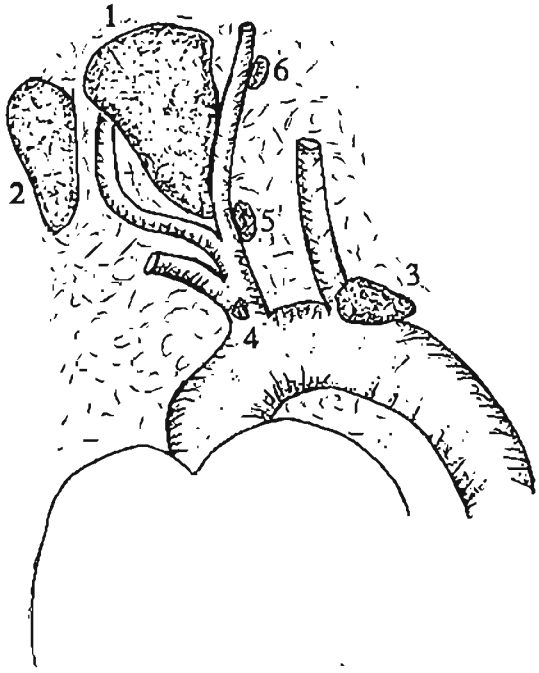

Plate 8.2. Lobulation of parathyroid III

Fig. 8.2a. Low power light micrograph shows the arrangement of the principal cells into compact lobules separated by wide connective tissue septa with fat cells (F) and small blood vessels.
1μm resin section, toluidine blue
Kangaroo K12
Bar: 40μm.

Fig. 8.2b. Shows mast cells (M) and a small nerve (N) with myelinated and unmyelinated fibres in a wide septum between lobules of parathyroid principal cells. Light and dark cells can be distinguished in the lobules.
resin section, toluidine blue
Kangaroo K27
Bar: 20μm.

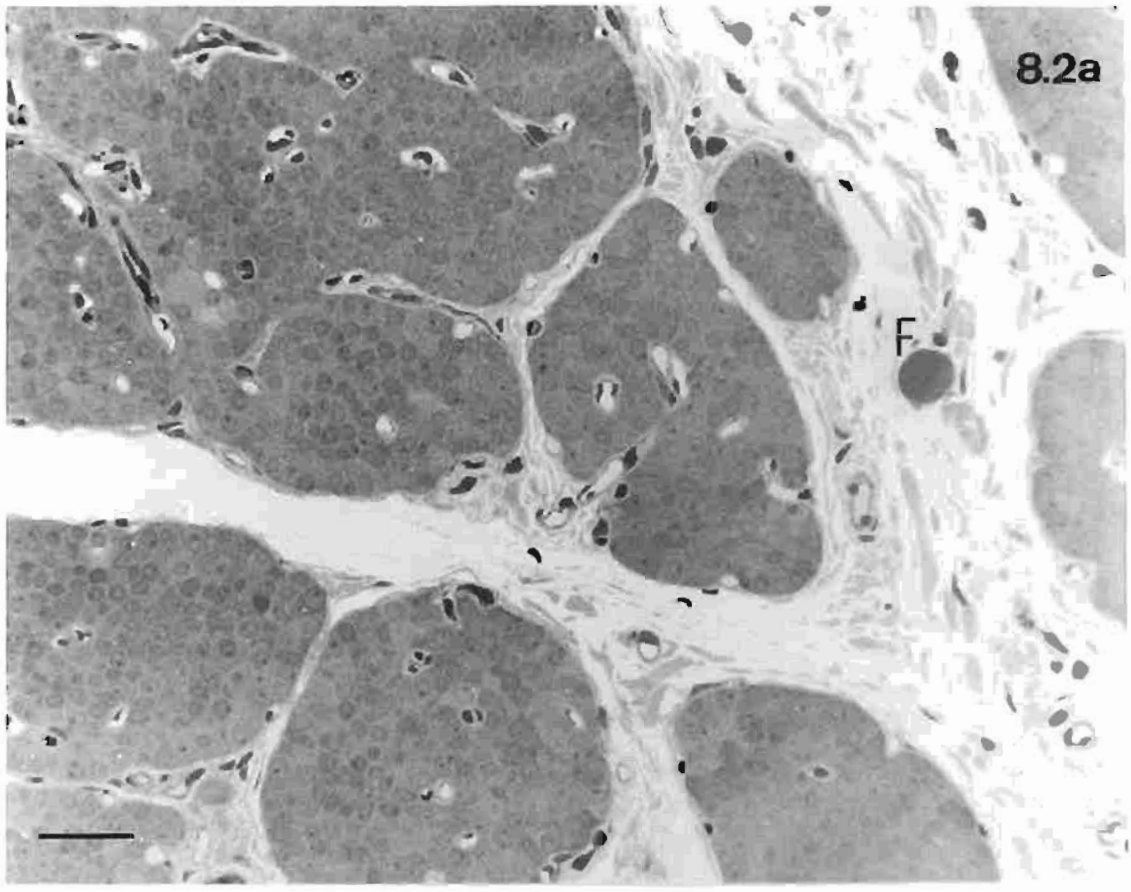
8.2a
F

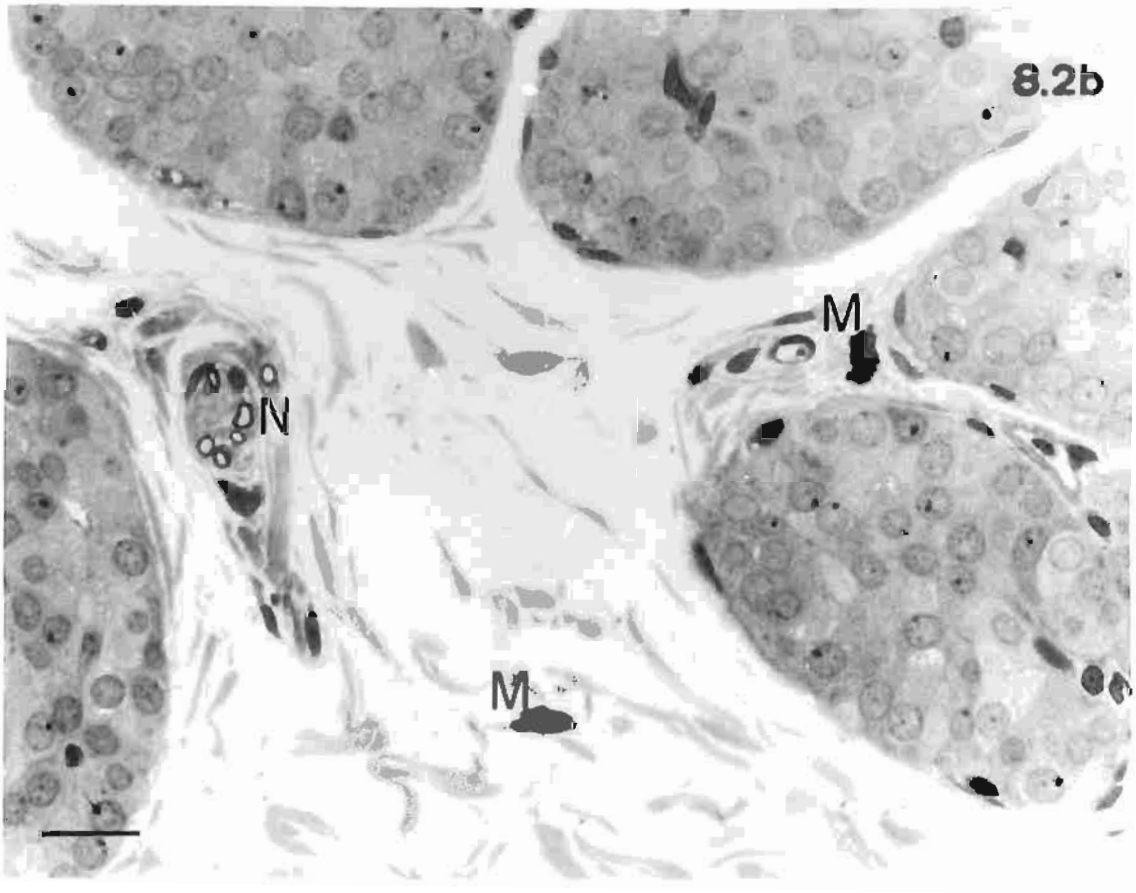
8.2b
M
N
M

Plate 8.3. Septal mast cells, light and dark principal cells in parathyroid III

Fig. 8.3. Shows the compact arrangement of light (arrows) and dark cells within a lobule and the minimal amount of connective tissue accompanying blood vessels and capillaries. Mast cells (M) are reasonably common in the connective tissue.
resin section, toluidine blue
Kangaroo K7
Bar: 30µm.


8.3
M
M
M

Plate 8.4. Light microscopic appearance of principal cells

Fig. 8.4a. Shows a variety of cytoplasmic structures in the principal cells. Some have dark granules; others have many small clear vesicles.
resin section, toluidine blue
Kangaroo K22
Bar: 6μm.

Fig. 8.4b. Shows many large, clear vacuoles in a group of principal cells.
resin section, toluidine blue
Kangaroo K16
Bar: 6μm.

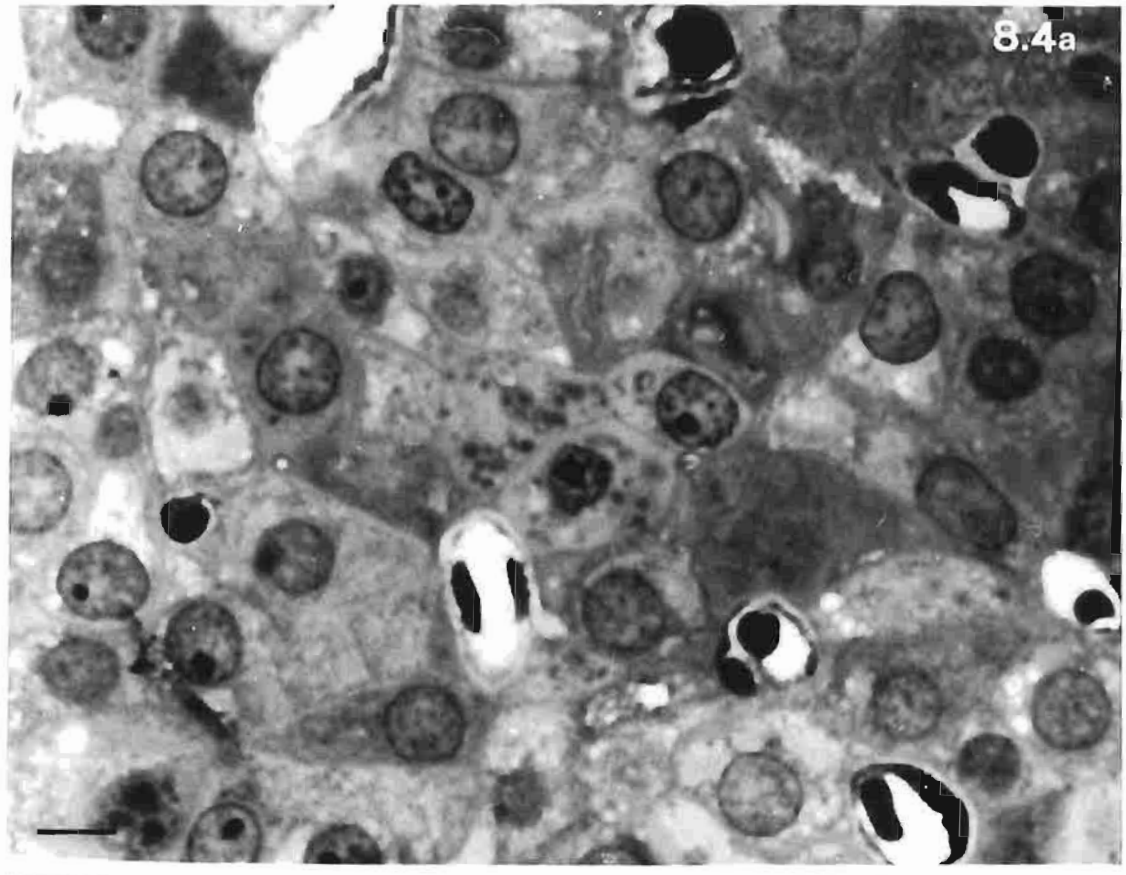
8.4a

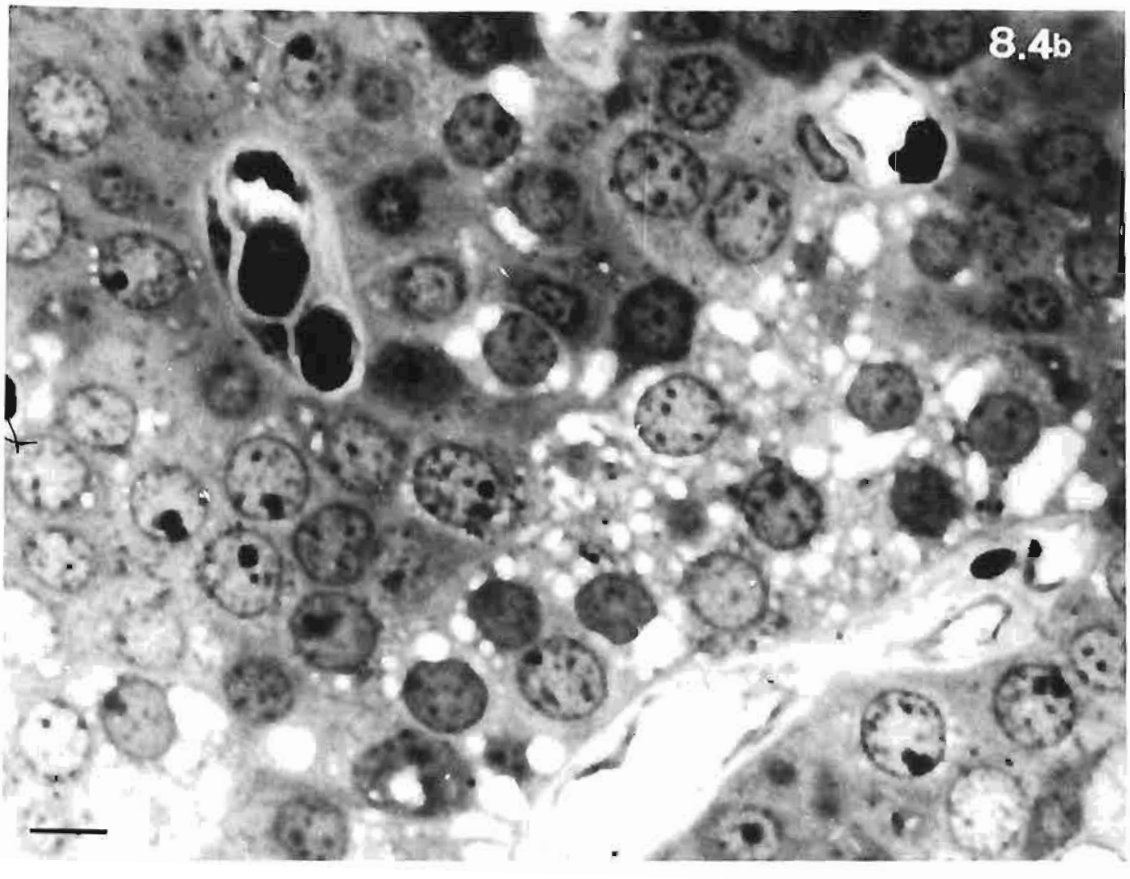
8.4b

Plate 8.5. Mingling of parathyroid III and thymus

Fig. 8.5a. Shows parathyroid tissue encapsulated by a thin band of connective tissue that separates the glandular cells from the surrounding thymus.
resin section, toluidine blue
Kangaroo K1
Bar: 30μm.

Fig. 8.5b. Shows the apparent intermingling of parathyroid and thymic tissues. At this resolution intervening barriers between the two tissues cannot be identified.
resin section, toluidine blue
Kangaroo K13
Bar: 20μm.

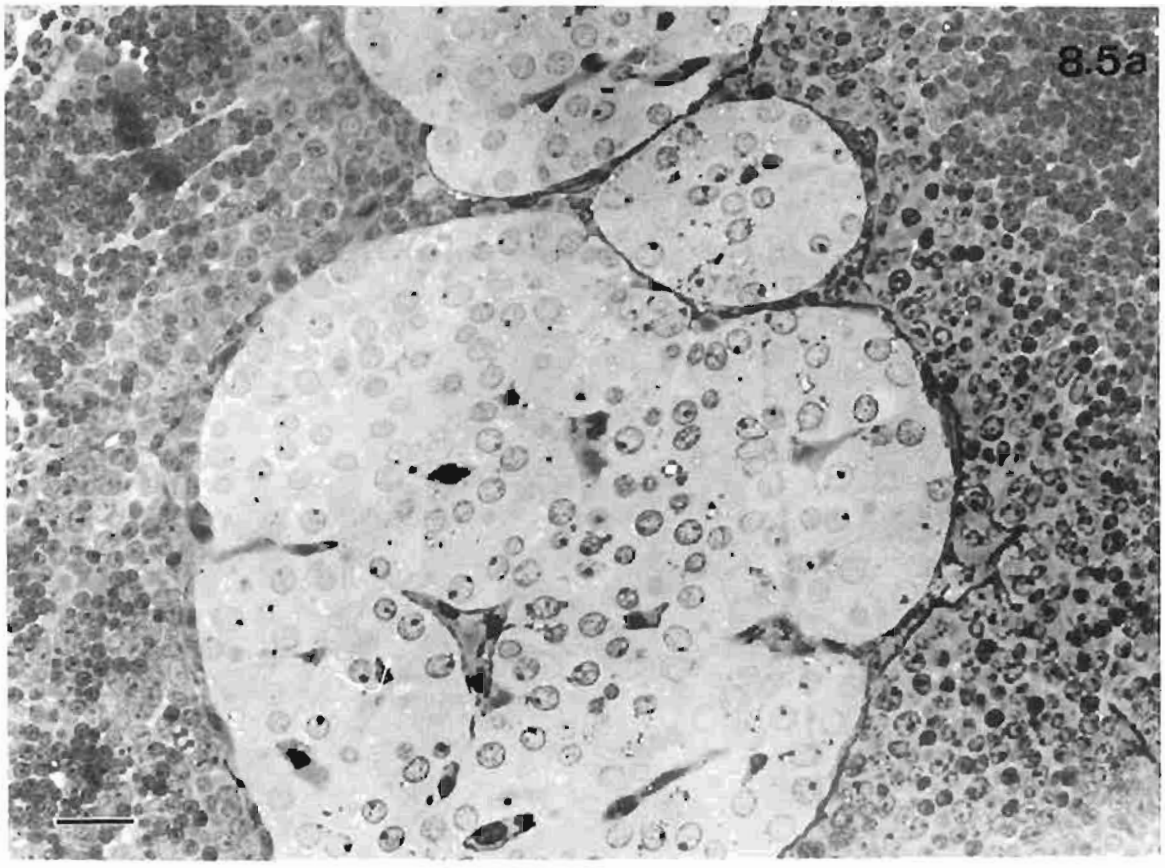
8.5a

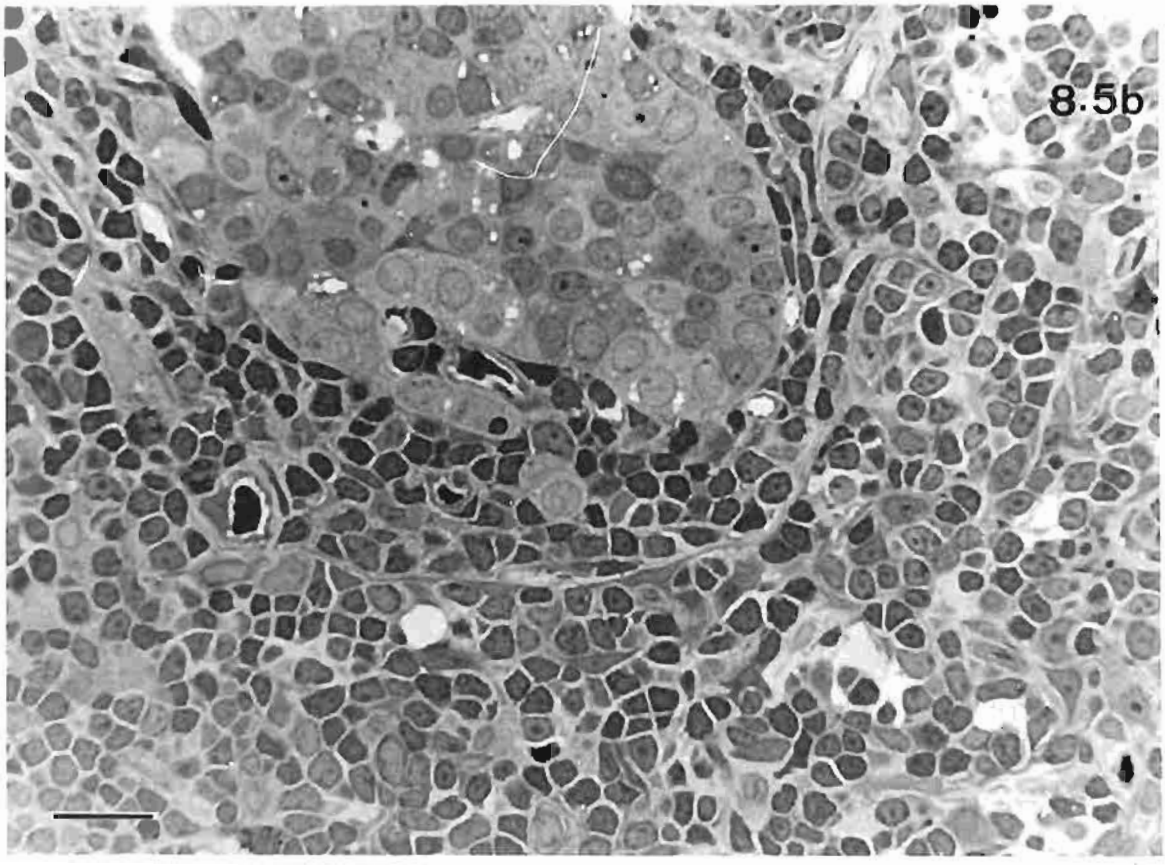
8.5b

Plate 8.6. General ultrastructure of parathyroid III and basal laminae

Fig. 8.6a. The electron micrograph shows a basal lamina (arrows) separating the parathyroid cells (upper right) from the connective tissue components of a septum. A mast cell (M), a lymphocyte?(L), cytoplasmic processes of fibrocytes (F) and collagen fibrils are present in the septum. Note the basal lamina (arrow head) around the mast cell.
Kangaroo K27
Bar: 1μm.

Fig. 8.6b. Shows the rectangular outline of a principal cell with an eccentric nucleus and the compact arrangement of the principal cells. Note the relatively even distribution of granules in the cell suggesting that secretion is released from all sides of the cell not just the surface adjacent to the capillary (right edge). All the cells have a similar cytoplasmic staining intensity.
Kangaroo K9
Bar: 1μm.

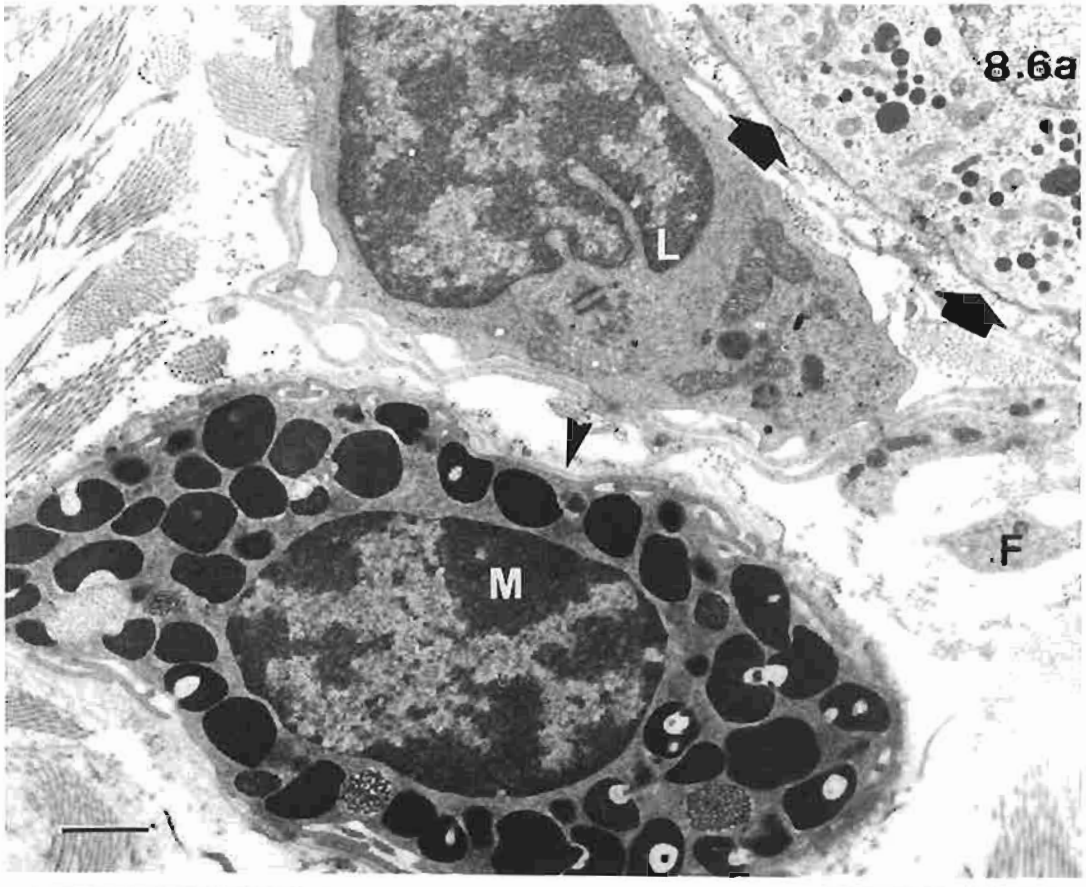
8.6a
L
M
F

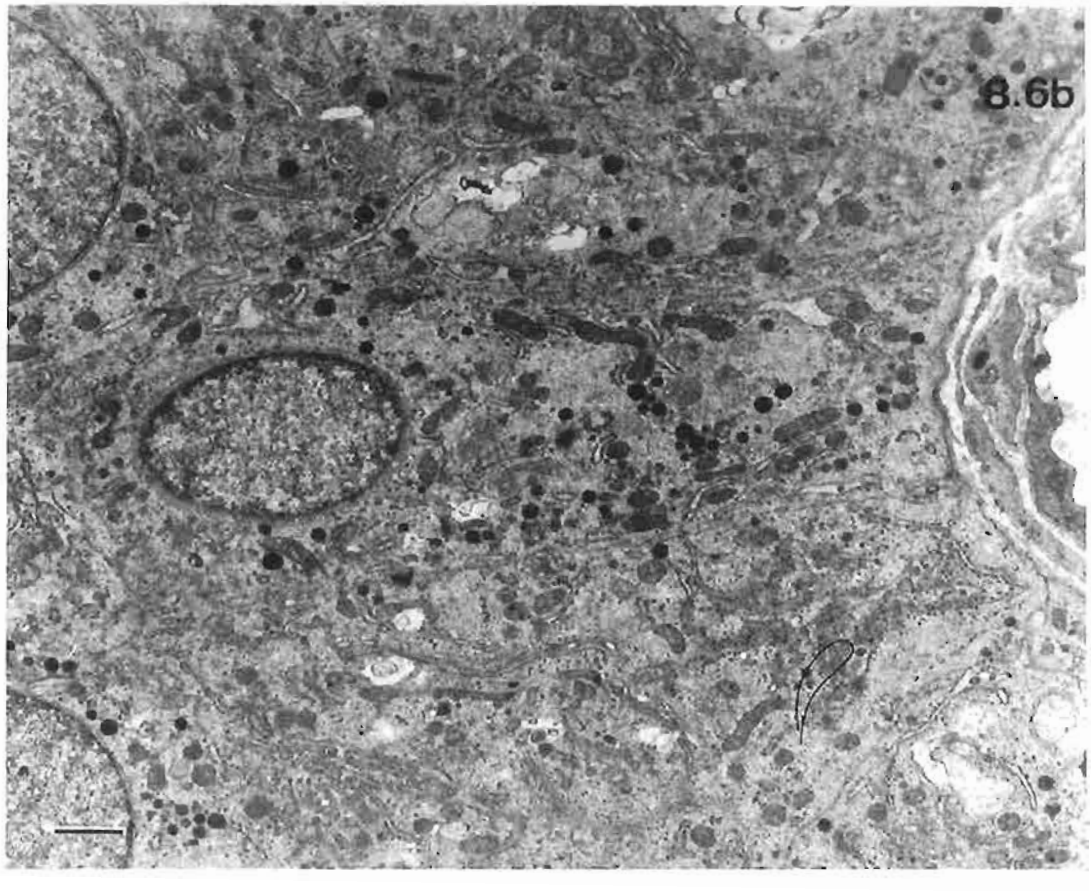
8.6b

Plate 8.7. General ultrastructure of principal cells

Fig. 8.7. Shows light and dark cells with desmosomes (D) between cells and relative straight cell membranes except where short cytoplasmic processes protrude into localised, enlarged intercellular spaces, canaliculi (one shown by an arrow). Note the variation in mitochondrial morphology. In the cell at the centre right of the micrograph areas of cytoplasm appear to be enclosed within the mitochondria whereas mitochondria in the upper left and lower left cells have large pale staining areas of matrix. An array of granules and vesicles is present ranging from electron dense granules (X) to large vesicles with sparse particulate contents (Y) or electron lucent interior (Z).
Kangaroo K22
Bar: 1µm.


8.7
D
X
Y
Z

Plate 8.8. Ultrastructure of light and dark cells

Fig. 8.8a. Shows light and dark cells in a specimen fixed by perfusion suggesting the appearance of the cells, i.e. classification as light and dark cells, is independent of the mode of fixation.
Kangaroo K16
Bar: 1μm.

Fig. 8.8b. Shows similar amounts of RER in light and dark cells. Note the abundant glycogen in the light cell. Nuclei of both the light and dark cells show similar chromatin patterns which suggests similar levels of synthetic activity in the two cells.
Kangaroo K11
Bar: 1μm.

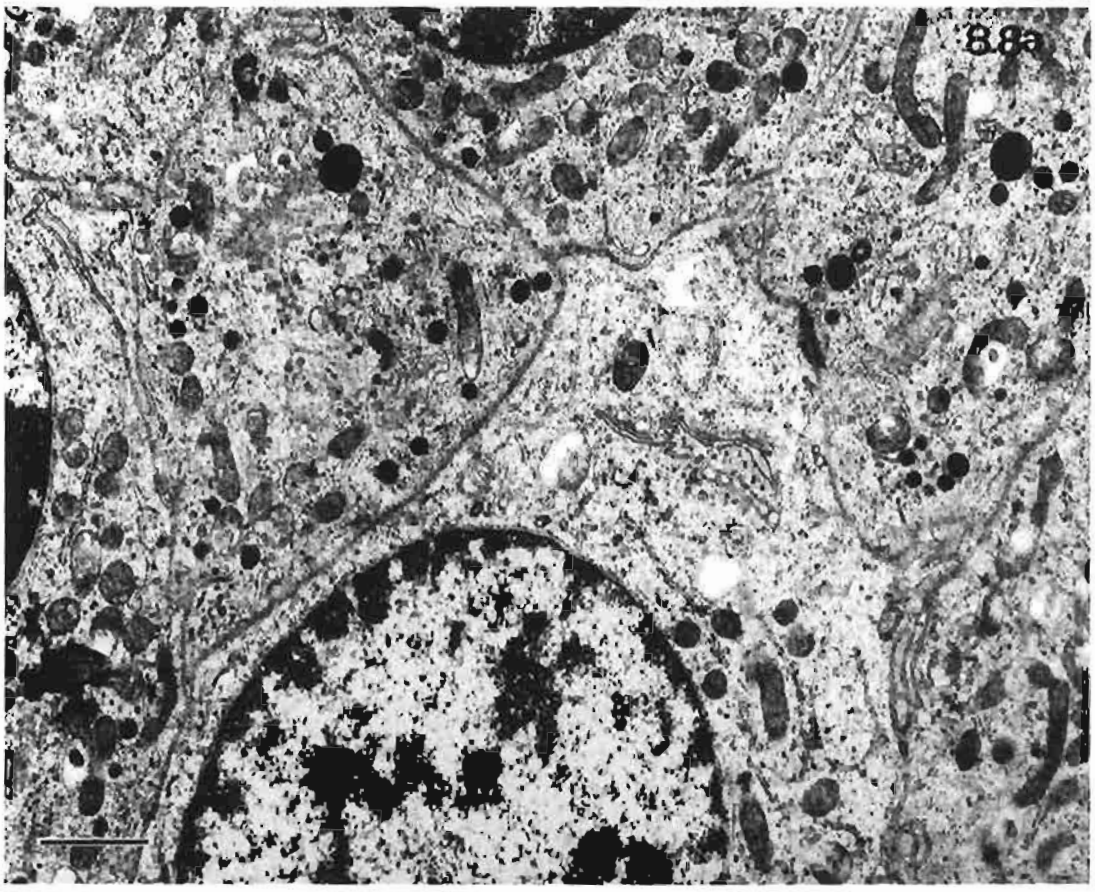
8.8a

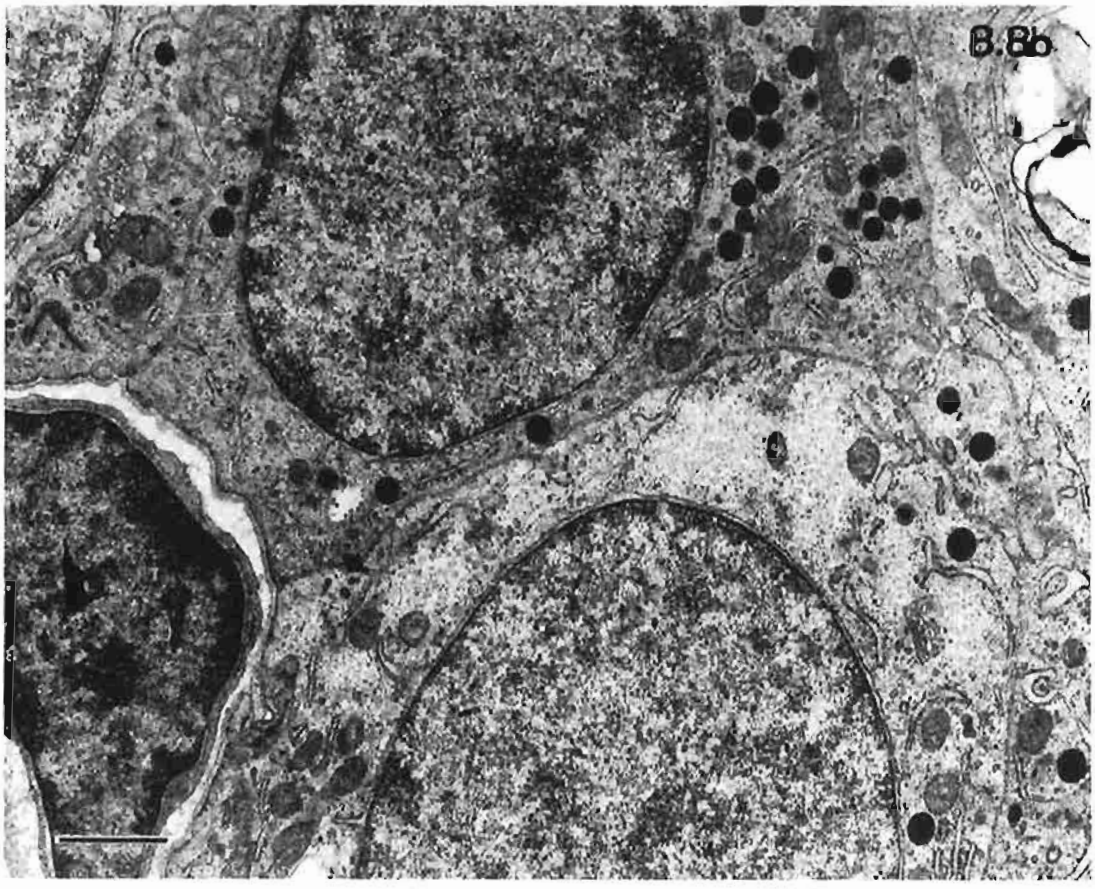
8.8b

Plate 8.9. Rough endoplasmic reticulum in principal cells

Fig. 8.9a. Shows a variety of profiles for RER from narrow tubular structures (N) to distended shapes (D). Note the variation in mitochondrial morphology where some appear to be quite curved.
Kangaroo K8
Bar: 1μm.

Fig. 8.9b. Shows a section through a distended cisterna of RER (arrow) which is continuous with the nuclear envelope.
Kangaroo K9
Bar: 1μm.

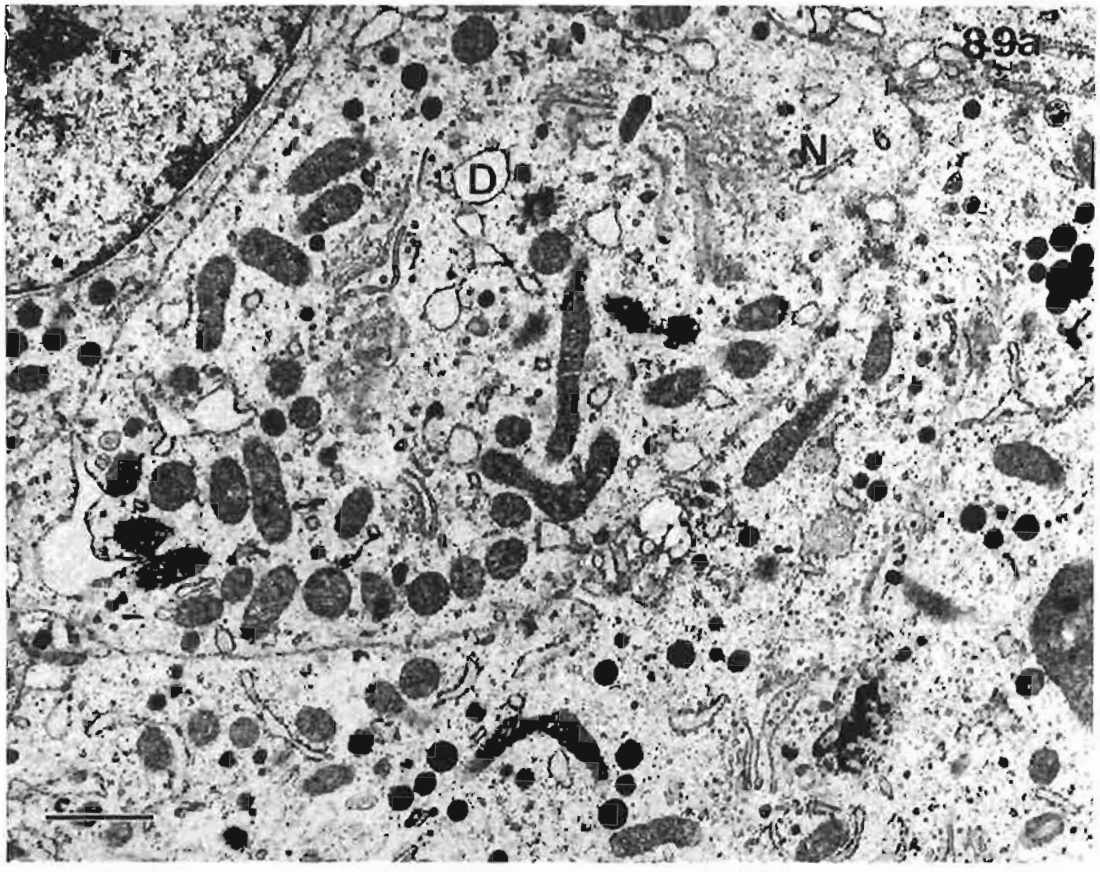
89a
D
N

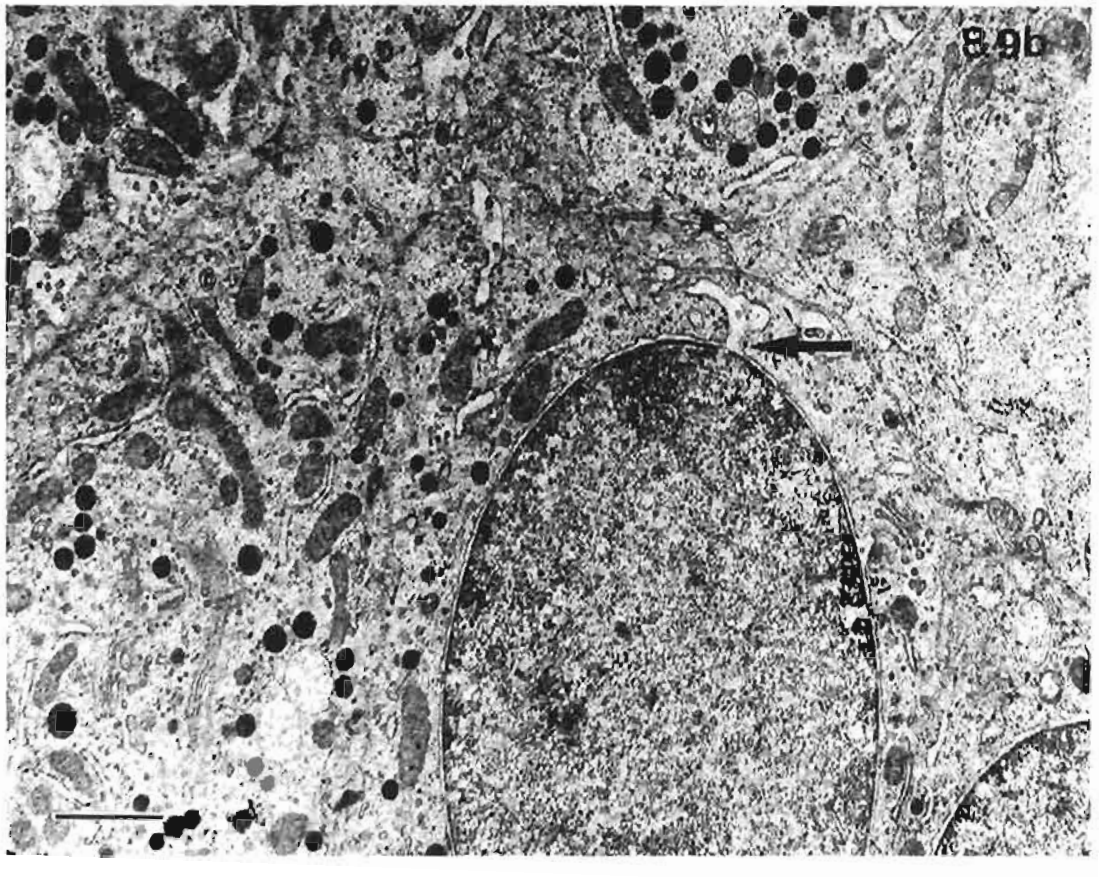
89b

Plate 8.10. Ultrastructure of RER, Golgi body and nuclear pores

Fig. 8.10a. Shows concentric layers of RER with mitochondria associated with central and peripheral regions.
Kangaroo K35
Bar: 0.5µm.

Fig. 8.10b. Shows a relatively small Golgi body with transfer vesicles and secretory vesicles. Several nuclear pores are evident in the glancing section of the nucleus (upper right).
Kangaroo K30
Bar: 0.5µm.


8.10a

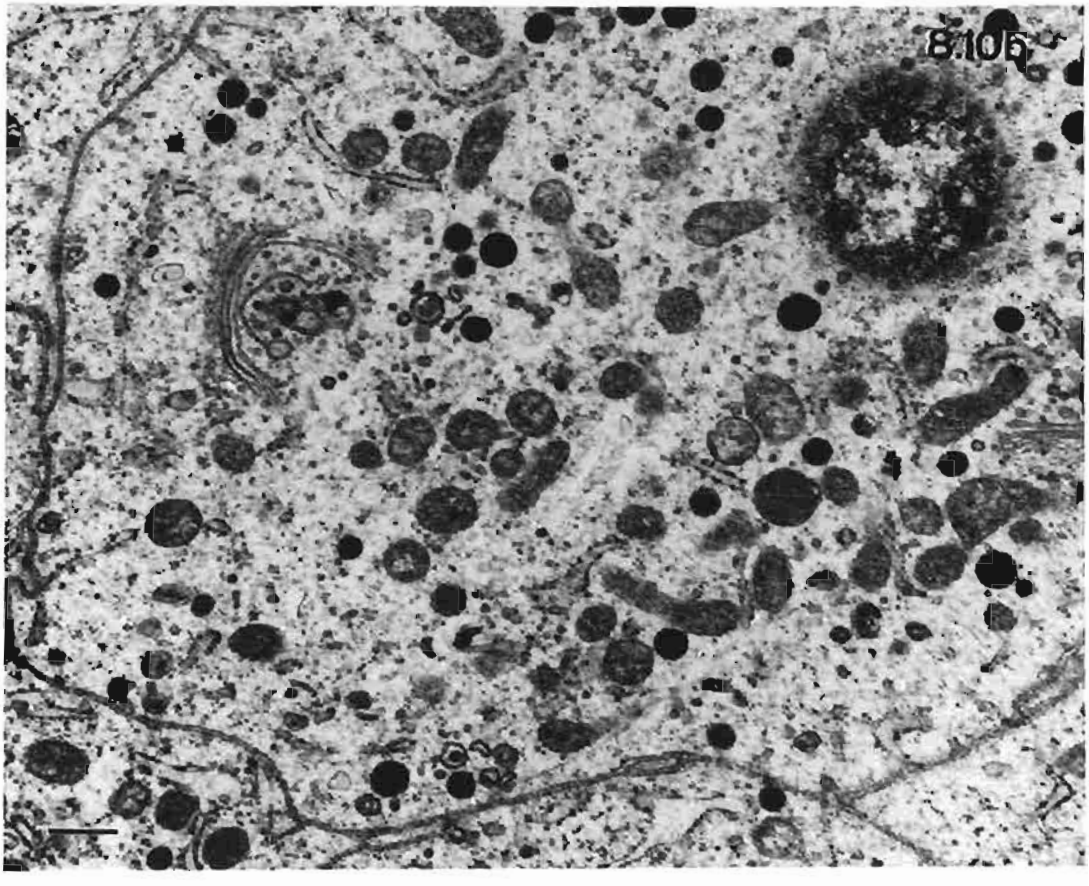
8.10b

Plate 8.11. Ultrastructure of vesicles and vacuolated cells

Fig. 8.11a. Shows small electron dense secretory granules, large membrane bound structures with particulate contents (X) and relatively empty vacuole type inclusions (Y). Label Z indicates a secondary lysosome or a lysosomal derived residual body.
Kangaroo K22
Bar: 0.5µm.

Fig. 8.11b. Shows the unusual appearance of two cells adjacent to more typical parathyroid cells (upper right). Numerous, irregular, electron lucent areas, enclosed by membranes, feature in the cytoplasm. Note many mitochondria lack the morphological detail of those in adjacent cells, perhaps suggesting the two cells are dying and that associated membrane degeneration is responsible for the cytological appearance.
Kangaroo K6
Bar: 1µm.

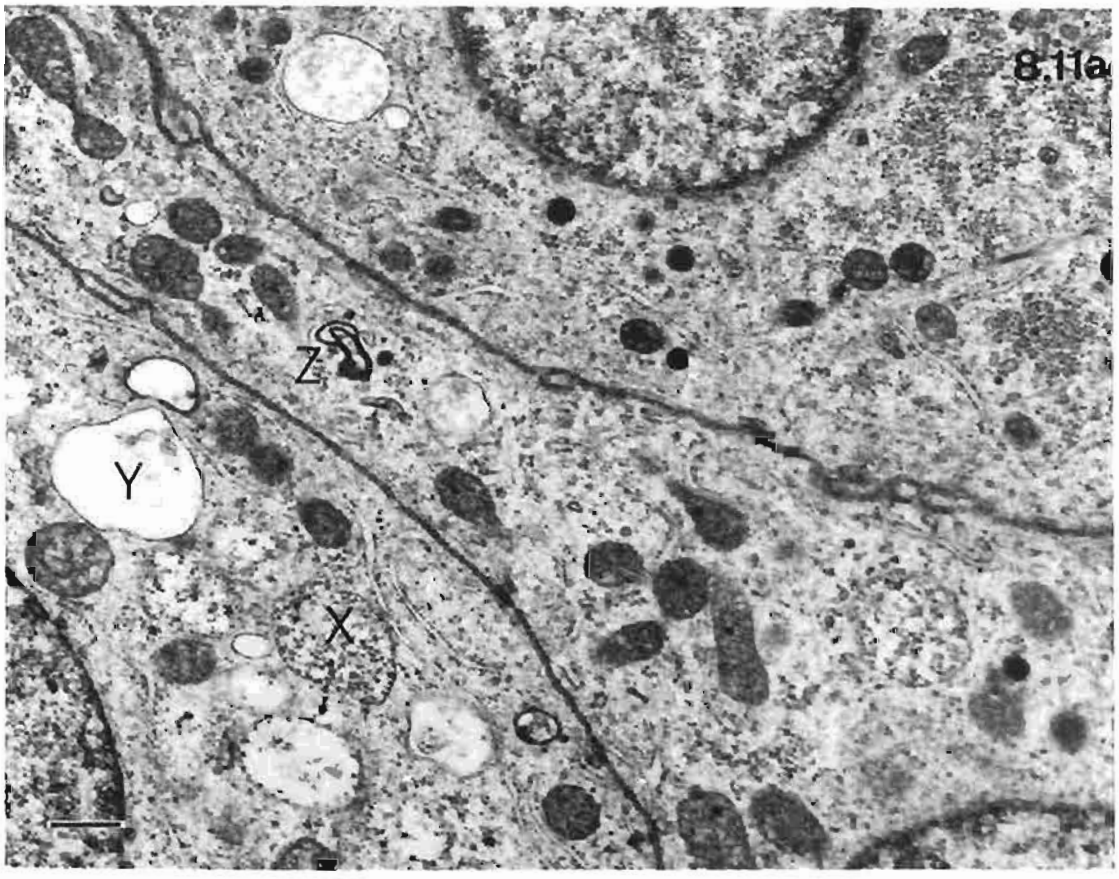
8.11a
Z
Y
X

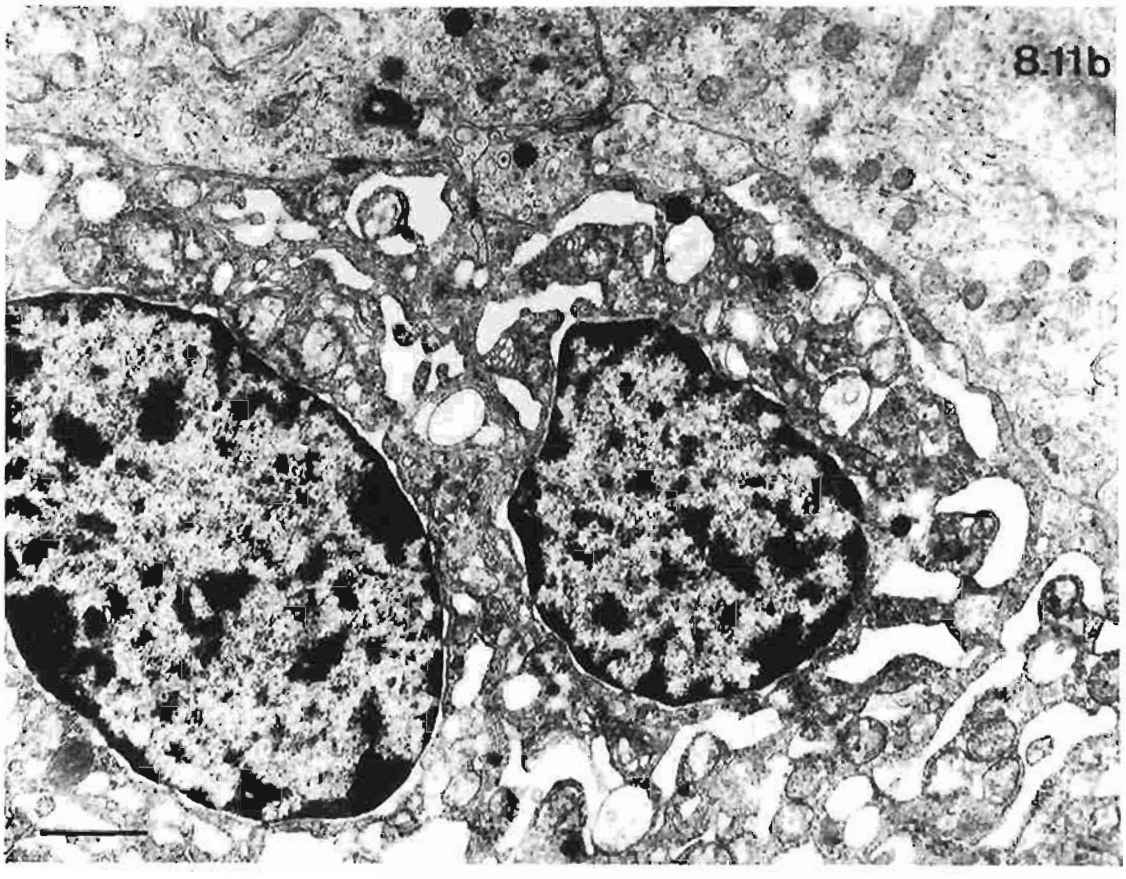
8.11b

Plate 8.12. Ultrastructure of parathyroid, thymus barrier

Fig. 8.12a. Shows layers of connective tissue components and basal laminae (arrows) separating parathyroid (P) (left) and thymic tissue (T) (right).
Kangaroo K1
Bar: 1μm.

Fig. 8.12b. Shows a parathyroid principal cell (P) (left) adjacent to thymic tissue (T) (right) without intervening connective tissue or basal laminae. Processes of an epithelial reticular cell, identified by tonofilaments (arrows), separate principal cells and thymocytes.
Kangaroo K21
Bar: 1μm.

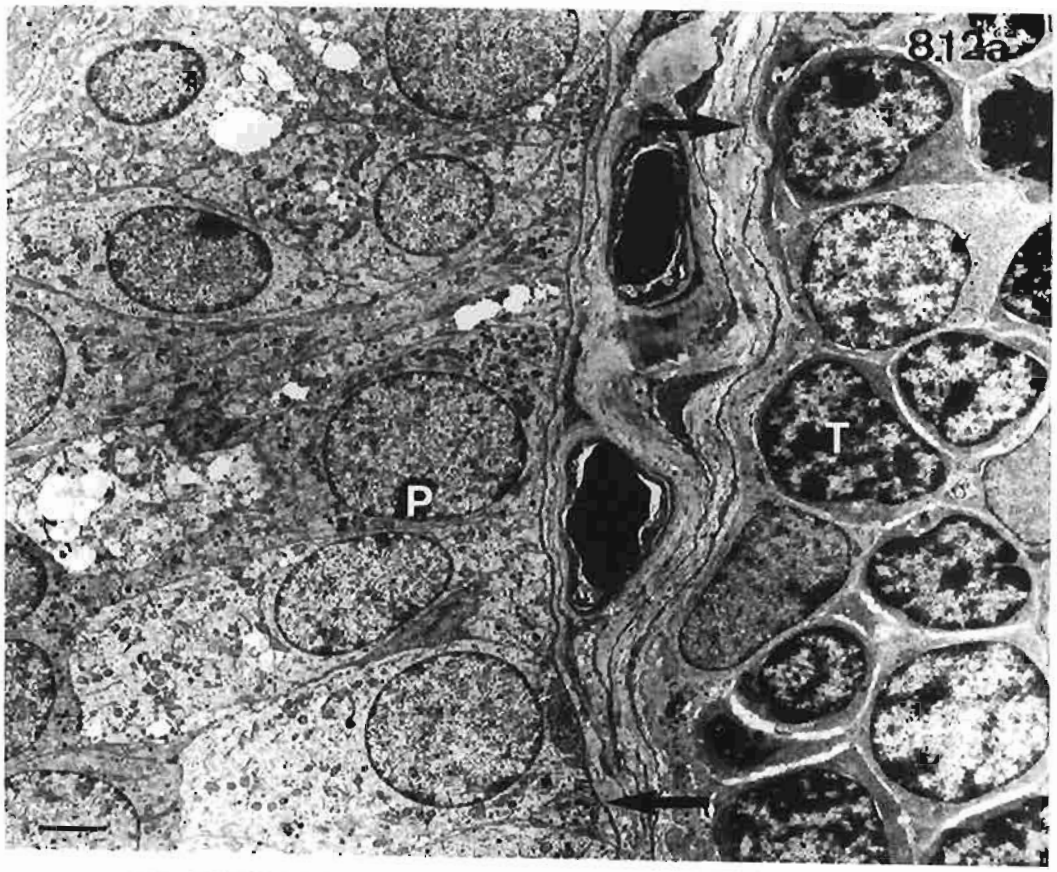
8.12a
P
T

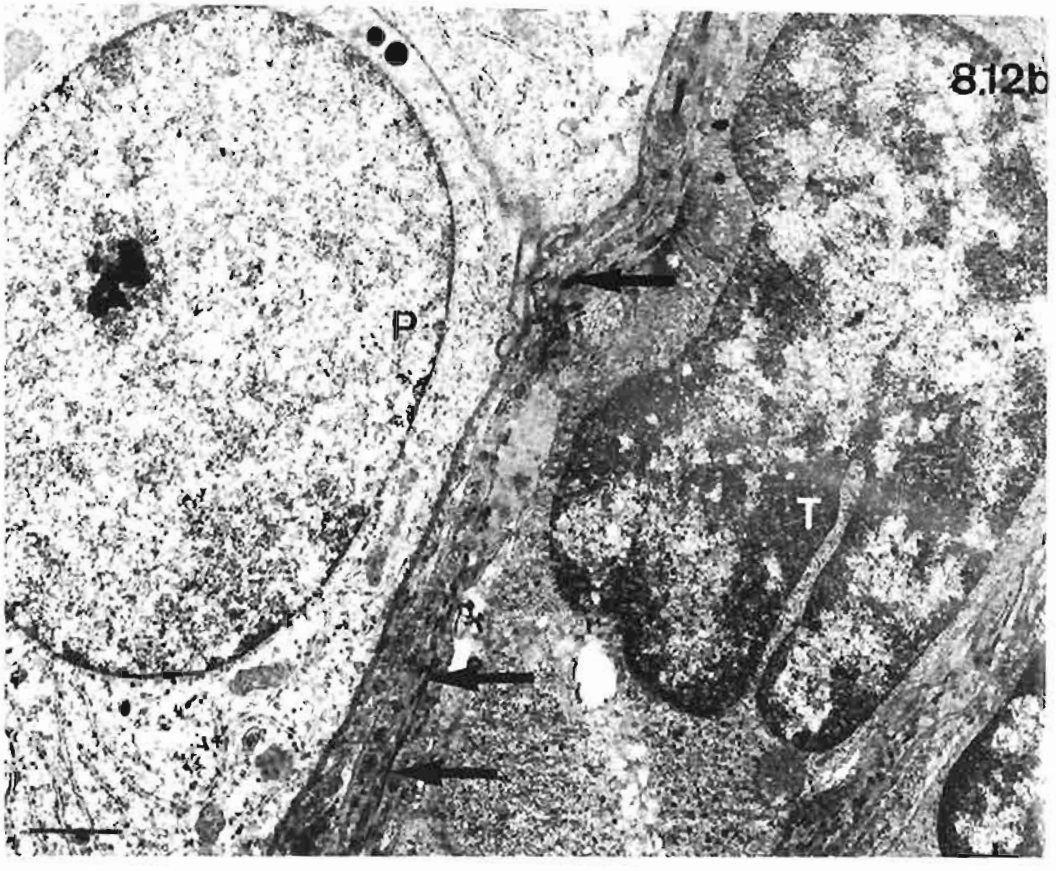
8.12b
P
T

Chapter 9

Parathyroid Glands in Monotremes

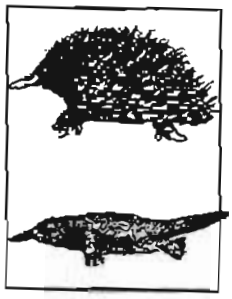

9.1 Introduction

The current description of the monotreme parathyroid gland is based on material obtained from twelve echidnas (two females, ten males), and two platypuses (one female, one male). The echidna, *Tachyglossus aculeatus*, has a wide distribution throughout mainland Australia and Tasmania and six subspecies have been identified (Griffiths, 1978). The echidnas used in this study belong to the subspecies, *T. a. multiaculeatus*, which is found on Kangaroo Island located south of South Australia. The platypus, *Ornithorhynchus anatinus*, inhabits most river systems east of the Great Dividing Range in eastern Australia from northern Queensland to Victoria. It is also found in rivers in Victoria and Tasmania with small populations in the Adelaide Hills and Kangaroo Island (Grant, 1992).

There are only two known studies of the monotreme parathyroid glands in the scientific literature. The embryology of the parathyroids in the echidna, *Tachyglossus aculeatus*, has been thoroughly described by Maurer (1899) and a somewhat incomplete study of the parathyroids has been made in the platypus, *Ornithorhynchus anatinus*, (MacKenzie and Owen, 1919). These studies are described in more detail in chap. 2, Literature Review, sections 2. In addition to the main aims that are given in chap 1, Introduction, Aims and Objectives, the aims of this chapter are to describe the gross anatomy, including the relationship to the parathyroid glands, and the histology of the thymus, thyroid, ultimobranchial bodies, and cervical and mediastinal lymph nodes in mature echidnas and platypuses.

The determination of the locations of parathyroid glands in *Tachyglossus* proved to be a very tedious process that required modifications of the initial method in order to meet the demands of light and electron microscopic examinations. In all animals the superficial salivary glands and muscles were reflected or removed from the ventral neck, and the thorax opened to reveal the heart with its major vessels and mediastinal tissue. In the first two animals examined (E1, E2) serial, paraffin sections were made from the carotid bifurcations and tissues in these

vicinities as well as tissue extending from the level of the larynx to the ascending aorta and surrounding mediastinum and pericardium. The trachea and oesophagus were on the dorsal aspects of these serial sections.

From the laborious preparation and examination of hundreds of serial sections, the general locations of parathyroid glands were noted, and then electron microscopic specimens were taken from these areas in four other animals. In these four echidnas (E4, E7, E8, E9) over sixty resin blocks were produced for each animal by methods described previously (See chap. 3, Materials and Methods, and appendices C and E). Time restraints prevented every block from being cut for survey sections and this technique was later abandoned after no parathyroid tissue was found in any of the sections prepared from forty blocks for each animal.

The most successful method for obtaining good light and electron microscopic specimens of parathyroid tissue from the echidna involved noting the size and exact location of each likely specimen during dissection, and then placing it in fixative. Each fixed specimen, 1mm in diameter or larger, was halved and frozen sections cut and stained from one half. If microscopic examination showed parathyroid tissue then appropriate processing was done on the other half. For specimens less than 1mm in diameter standard processing was not preceded by frozen section sampling. Routine light microscopic and electron microscopic studies were each done on three echidnas; E3, E5, and E6 were used in the former technique and E10, E11, and E12 were used in the latter. Some paraffin sections from E3 and E6 were stained with alcian blue - PAS.

The specimens from the three echidnas used for ultrastructural descriptions formed a very homogeneous group. All were male, killed at the same time in winter (June), perfused with low glutaraldehyde-containing electron microscopic fixative, and *en bloc* stained with uranyl acetate prior to tissue processing (See chap. 3, Materials and Methods, and appendices B and C). Echidnas E3, E5, and E6 that were used for light microscopic studies were a diverse group. Echidna E3 was female, killed in March and dissected approximately eight hours after death; the other two, E5 and E6, were males killed in September and immediately placed in fixation after death. Specimens, both paraffin sections and resin sections, from all echidnas were examined with the light microscope, not just E3, E5 and E6.

For the study of the parathyroid gland in the two platypuses, a large piece of tissue extending from the tongue to the heart and lungs was excised from both animals and placed in buffered formalin. Various stages of dissection were recorded with drawings and photographs; many structures encountered could be identified only after examining histological sections. In platypus #1 discrete structures were excised, whereas in platypus #2 specimens consisted of larger blocks of tissue that were subsequently prepared for

serial sections. Details of techniques used in dissecting and producing routine sections are given in Materials and Methods, chap. 3. Both platypuses had been dead for about eight hours before specimens were collected and so they were unsuitable for electron microscopic studies.

9.2. Results

9.2.1.1. Anatomy - Echidna

Twelve parathyroid glands were found in eight echidnas, four animals (E2, E5, E6, E11) having two each (i.e. left and right gland), the others (E1, E3, E10, E12) only one. Ultimobranchial bodies were also identified in two echidnas (E3 and E5), each animal having two. The carotid bifurcation was just cephalic to the larynx and serial sections of the bifurcations and surrounding tissues did not reveal any parathyroid tissue. However, many lymph nodes which had a histological structure (Figs. 9.3a & b) peculiar to monotremes were present here as well as the ventral neck and mediastinal regions. The diffuse scattering of small lymph nodes is indicated on Figures 9.1a, b, and c which illustrates the typical anatomy based on all the dissections of the echidnas.

All parathyroid glands were located in the mediastinum. In eight echidnas a parathyroid was found near the origin of the right carotid artery and associated with the initial part of the right internal thoracic artery that arises ventrally from the right carotid, very close to its origin (Figs. 9.1a, b, & c). In five animals the right parathyroid gland was identified as a discrete ovoid structure approximately 2 x 1 mm. In the other three echidnas the gland was obscured by surrounding thymic tissue and its identification was possible only from examining serial sections. A left parathyroid gland was found in four echidnas. It was adjacent to the left carotid artery near the origin of the left internal thoracic artery (Figs. 9.1a, b, & c). In three animals the structure was obvious in fibrofatty tissue, but in the fourth it was indistinguishable with the dissecting microscope from overlying thymic tissue.

Parathyroid glands were often closely associated with thymic tissue but never with thyroid tissue. In the echidna the thyroid gland was ventral to the caudal end of the trachea (Fig. 9.1c). It was loosely framed laterally by the common carotid arteries and caudally by the aortic arch but in many cases the thyroid gland extended beyond these anatomical borders to form very irregular boundaries with the thymus. The thymus was diffuse, set in the fibrofatty tissue of the mediastinum. Thymic lobules were found surrounding the aortic arch and its major branches, between the aortic arch and trachea, and even extending over the ventral surface of the pericardium (Figs. 9.1b, & c). Numerous lymph nodes were also present in the mediastinal tissue.

Ultimobranchial bodies, identified by their histological appearance and immunostaining (See section 9.2.2.1 and chap. 10), were found in echidnas E3 and E5. They were located

in fibrofatty tissue adjacent to the trachea, just caudal to the larynx. Each body consisted of tiny nodular structures, the larger ones of which were approximately 1 mm in diameter and indistinguishable with the dissecting microscope from lymph nodes (Fig. 9.1b).

9.2.1.2. Anatomy - Platypus

Dissection of the neck and mediastinum in both platypuses revealed many small nodular structures in fibro-fatty tissue associated with the carotid bifurcations, trachea, aortic arch and major aortic branches (Fig. 9.2). Disappointingly, most of these structures proved to be lymph nodes like those found in echidnas (See above section, 9.2.1.1.). Set within fibro-fatty tissue on the ventral surface of the caudal end of the trachea was a flattened, dark red, oval structure, 18 x 12 x 4 mm (Fig. 9.2), that was framed laterally by the initial segments of the carotid arteries and caudally by the aortic arch. The fibro-fatty tissue appeared to merge with the pericardium. From histological examination the oval structure was identified as thyroid tissue and small involuted lobules of thymus were scattered throughout the fibrofatty tissue attached to the thyroid and the ventral surface of the pericardium. Two parathyroid glands were found associated with this involuted thymic tissue in platypus #2; none was found in the other animal. One gland was on the dorsal side of the origin of the right brachiocephalic artery and the other was on the medial side of the origin of the left common carotid (Fig. 9.2). From measurements done on serial sections the elongated ovoid structures were approximately 3 x 2 x 1 mm and 2.5 x 1.5 x 1 mm respectively. No other endocrine glands or thymic tissue were found in the neck or mediastinum.

9.2.2.1. Light Microscopy - Echidna

Each parathyroid glands was surrounded by a thin, fibrous capsule with generally little connective tissue accompanying the numerous capillaries (Fig. 9.4a). The glands showed a typical reticulate endocrine arrangement of parenchymal cells. No follicles or cysts were present. Most principal cells had a distinctive elongated shape with polarised morphology as indicated by the nuclear position. In cells adjacent to narrow septa or the capsule, nuclei were towards the ends of the cells next to the connective tissue (Figs. 9.4a, b). In routine paraffin sections all cells had a similar pale acidophilic cytoplasm but the number of vacuoles varied (Fig. 9.4b). Principal cells in parathyroids from echidna E6 were PAS positive. Cytoplasmic staining was patchy with unstained vacuoles in a bright pink matrix.

In resin sections of a parathyroid from echidna E12, there was an ovoid clump of very lightly stained cells which were labelled water-clear cells (Figs. 9.5a, b). Water-clear cells appeared about twice the size of the other parenchymal cells and were filled with clear vesicles, some of which had a small dark staining central core (Fig. 9.5b). Other cytoplasmic contents were peripherally located, accentuating the outline of the cells.

The parathyroid gland formed a distinct encapsulated structure in the fibrofatty mediastinum except for one gland from echidna E3 where parathyroid and thymic tissue merged together (Fig. 9.6a) and principal cells and lymphocytes appeared to mingle. The lymphoid tissue was positively identified as thymus by the presence of Hassall's corpuscles (Fig. 9.6a) and incomplete lobules consisting of a darker cortex and paler medulla.

Left and right ultimobranchial bodies were found in echidnas E3 and E6. No other tissue resembling ultimobranchial bodies was found in the other ten echidnas. As described above in section 9.2.1.1, the gland was lateral to the origin of the trachea. Unlike parathyroid glands, the ultimobranchial body was not encapsulated. Clumps of glandular cells and small follicles that consisted of a single layer of cuboidal cells surrounding pale staining, acellular colloid were dispersed within a band of fibrofatty tissue (Fig. 9.6b). The follicular colloid was PAS positive. The small size of the body and the presence of clumps of cells as well as follicles distinguished it from the thyroid gland where follicular formation of endocrine cells dominated the histology. Identification of the structure as the ultimobranchial body was confirmed by the results of immunocytochemical staining (See chap. 10).

The thyroid gland consisted of typical thyroid follicles each of which had an acidophilic colloid surrounded by a single layer of cells. Generally very large follicles had flattened cells and in smaller follicles cuboidal cells surrounded the central colloid. In routine paraffin and resin sections only one type of parenchymal cell, the follicular cell, appeared to be present. Numerous capillaries were present in the connective tissue between the follicles.

Numerous lymph nodes were present in the ventral neck and mediastinum; they had an unusual structure in monotremes (Figs. 9.3a & b). Nodes often occurred where lymph vessels joined together to form larger vessels. Each ovoid node was suspended within the lumen of a thin walled vessel and attached to the wall by a vascular cord of fibrous tissue (Fig. 9.3a). Small blood vessels and capillaries with minimal accompanying connective tissue fanned out from this central region of attachment into the lymph node. The periphery of the node was demarcated by a single row of large, acidophilic reticular cells (Fig. 9.3b). Dense lymphoid tissue, composed of many small lymphocytes formed a cortex whereas in some nodes, the area adjacent to the vascular connection had medullary characteristics consisting of a looser arrangement of lymphocytes often intermingled with macrophages, plasma cells and reticular cells. In some lymph nodes there was a single pale germinal centre (Fig. 9.3b) where mitotic and larger blast-like cells were present. Two nodes in echidna E1 showed brown granular pigmentation in scattered macrophages but not in the peripheral reticular cells.

9.2.2.2. Light Microscopy - Platypus

Both parathyroid glands were set in fibrofatty tissue of the mediastinum with fibrous connective tissue encapsulating the glands and outlining involuting lobules of thymic tissue (Fig. 9.7a). At the periphery of the left gland, intermingling of parenchymal cells and thymic tissue was apparent (Fig. 9.7b). Lymphoid tissue was identified as thymus due to the presence of Hassall's corpuscles (Fig. 9.7c).

Within the glands cells were densely arranged with minimal connective tissue accompanying vascular elements (Figs. 9.7a, b). Only principal cells were present. They were quite small, approximately 20μm in diameter, with the nucleus, approximately 10μm in diameter, occupying much of cell. Light and dark cells were not distinguishable but some cells showed patchy cytoplasmic staining indicative of glycogen. No cysts or follicles were observed.

Lymph nodes, thyroid gland and thymus in the platypus had similar histology to those in the echidna. Descriptions of the light microscopic structure of these organs were given in the preceding section.

9.2.3. Electron Microscopy - Echidna

Only tissue from echidnas, not platypuses, was suitable for electron microscopy; specimens from three animals, E10, E11, and E12, were examined. The typical endocrine structure of the parathyroids was confirmed with the electron microscope. Parenchymal cells were packed tightly together with minimal amounts of connective tissue accompanying capillaries and larger blood vessels (Fig. 9.8a). Most parenchymal cells were principal cells that showed similar cytoplasmic electron density; light and dark cells were not apparent (Fig. 9.8a). In one gland from echidna, E12, there was a clump of large cells filled with electron-lucent vacuoles (Fig. 9.9b). These cells were identified as water-clear cells; similar cells were scattered in a gland from animal E11. Also scattered sparsely among the principal cells were unidentified cells with a non-secretory appearance (Fig. 9.8a, Fig. 9.9b). These irregularly shaped cells had a relatively homogeneous cytoplasmic matrix with very few vesicles and mitochondria. Nuclei were larger, more irregular in shape and had more heterochromatin that nuclei of principal cells.

Principal cells showed partial polarisation in that they were columnar in shape with the nucleus at one end of the cell and a variety of organelles and inclusions clustered at the other end (Fig. 9.9a). Nuclei were mainly round with abundant euchromatin and clumping of peripheral heterochromatin. Cellular outline was accentuated by extensive folding of the membrane into long, thin microlamellar projections, arranged parallel to the plasmalemma and interdigitating with similar processes of adjacent cells (Fig. 9.9b).

These plasmalemmal modifications formed a system of canaliculi. Desmosomes were scattered along straight lengths of principal cells and water-clear cells (Fig. 9.11b).

Principal cells had abundant organelles and inclusions (Fig. 9.9b) and there was no obvious correlation between the amount of nuclear euchromatin and types of cytoplasmic structures. Ribosomes were either single, clustered as polyribosomes, or in parallel stacks of RER where in most cases at least five lamellae were present (Fig. 9.10a). Golgi bodies and mitochondria showed typical features (Fig. 9.10b) except the former were quite small. The latter were elongated with a matrix more electron dense than that of the cytoplasm. Mitochondria were numerous in most cells (Figs. 9.8a, 9.9a, 9.10a, & b) but no oxyphil cells, characterized by vast numbers of mitochondria were present.

Membrane bound, electron dense vesicles, identified as secretory granules, were quite small with diameters similar to the width of mitochondria (Fig. 9.11a). Larger vesicles either had particulate contents surrounded by a halo (Fig. 9.11a) or a heterogeneous interior and were identified as either storage secretory granules or lysosomal bodies. Large electron lucent vacuoles were present in many cells (Fig. 9.9b, Fig. 9.10a). There was evidence that these vacuoles were released from the cells and remained intact within the canaliculi. Often additional concentric membranes could be seen outlining the vacuoles in the intercellular spaces (Fig. 9.10a). Lipid inclusions were not uncommon and again their appearance could not be related to a particular phase of the secretory cycle (Fig. 10).

Water-clear cells were larger than principal cells and packed with electron lucent vacuoles (Fig. 9.8b). Nuclei had more heterochromatin than those of principal cells and often the shape of the nucleus was distorted presumably by the pressure of the many vacuoles crowded into the cell (Fig. 9.8b). Organelles and inclusions other than the vacuoles were confined to small areas between the vacuoles and at the periphery of the cell. Mitochondria, RER, and desmosomes (Fig. 9.11b) were identified, their presence indicating a living rather than dying cell. Vacuoles were large; some formed by the coalescence of adjacent vacuoles and the subsequent degeneration of membranes (Fig. 9.8b). Contents varied from very fine particulate material to collections of electron dense substances and whorls of membranes (Fig. 9.11b).

9.3. Discussion

9.3.1.1. Anatomy - Echidna

Results from the current study on 12 echidnas suggest that one pair of parathyroid glands is characteristic of this species and the glands are located in the mediastinum in the vicinity of the origins of the common carotid and the internal thoracic arteries. If the gland is enveloped by thymic tissue then its identification is very difficult in dissection.

This probably partially explains why varying numbers were found in the dissected echidnas. From the examination of embryos, one 'half grown' (12cm) echidna, and one adult specimen, Maurer (1899) concluded that during development there were two pairs of parathyroids in *Tachyglossus*. His drawings illustrate increasing proximity of parathyroid III and parathyroid IV during development and from examining adult specimens in the present study, a suggestion is made that in maturity either the glands merge together or one pair degenerates. Maurer (1899) failed to find any trace of the parathyroid glands in the adult echidna he examined. His anatomical findings were incorrectly described in the review article by Roth and Schiller (1976) where not only was the description of the 'half-grown' 10cm echidna instead of the adult given but also the location of parathyroid IV was inaccurate: "Therefore in the adult, where both pairs of glands are found in the thorax, parathyroid III is found on the dorsal aspect of the thymus or embedded within it and parathyroid IV remains as a separate gland at the carotid bifurcation".

In determining the location of the parathyroid glands in *Tachyglossus*, several unusual anatomical features were noticed in the ventral neck and mediastinum. For example, the presence of thoracic thymic lobules fused with the superficial surface of the pericardium seems to be a feature of both platypus and echidna and not just the former as was suggested by a previous study (MacKenzie and Owen, 1919). Another unusual finding was the prominence of the internal thoracic artery. This artery and major thoracic branches of the aorta were illustrated in a drawing by Hochstetter (1896, cited by Griffiths, 1968). In all the echidnas examined in this current study, the internal thoracic artery branched from the common carotid, whereas Hochstetter indicated the internal thoracic artery arose at the site of the origins of the subclavian and common carotid arteries from the brachiocephalic.

Perhaps the most curious feature of the ventral neck region was the presence of ultimobranchial bodies in the adult. All four bodies that were identified in two echidnas were smaller than the glands indicated in a drawing by Maurer (1899) and were not discrete nodular structures like those described by that author. Similarly the association of the bodies with the trachea was not as close as Maurer stated. Instead glandular elements were quite dispersed in the fatty tissue between the trachea and deep muscles of the neck. Failure to identify ultimobranchial bodies in all echidnas was probably related to removing the fatty tissue during dissection when the deep ventral muscles were severed and reflected in order to expose the trachea.

Monotremes are the only class of mammals in which the thyroid is located in the mediastinum and the ultimobranchial tissue does not fuse with the thyroid gland during embryonic development but instead, remains as a separate body. The thoracic location of the thyroid and the separate entity of the ultimobranchial body are both reptilian, not mammalian characteristics (Gorbman et al., 1983). In the past decades taxonomic

arguments have focused on the justification of classifying monotremes as mammals because monotremes have many anatomical features usually associated with reptiles (Griffiths, 1968; Griffiths, 1978). Reptiles usually have one or two pairs of parathyroid glands which, as in monotremes, lie near the heart associated with the common carotid arteries and aortic arch (Srivastav et al., 1995). The thyroid is at the caudal end of the trachea (Gorbman et al., 1983) and the thymus is ventral and lateral to the thyroid. The ultimobranchial bodies are loosely attached to the ventrolateral aspects of the caudal end of the trachea (Anderson and Capen, 1976; Gorbman et al., 1983; Singh and Kar, 1983; Padgaonkar et al., 1992). From the current study, the presence of the ultimobranchial body and the thoracic location of the thyroid in *Tachyglossus* are therefore additional reptilian characteristics that have not previously been noted (Griffiths, 1968; Griffiths, 1978). Although the number and precise location of these glands and structures vary in the different reptilian genera, there does appear to be more structural similarities between reptiles and monotremes than between marsupials and monotremes.

9.3.1.2. Anatomy - Platypus

The descriptions that have been given in the current investigation of tissues in the ventral neck and mediastinum of the platypus do not correlate well with descriptions previously provided by MacKenzie and Owen (1919). No endocrine glands were found at the commencement of the trachea and no large "parathymus gland" in the mediastinum. The former glands were probably overlooked in the dissections in spite of great care being exercised. However the identity of these glands as parathyroids by MacKenzie and Owen is disputed when comparisons are made with the embryology and anatomy of the echidna, the only other extant monotreme genus. From the meticulous studies done by Maurer (1899) the ultimobranchial body persists as a separate entity at the origin of the trachea in the echidna and assuming that there are strong embryological similarities between these two closely related monotremes, then it seems reasonable to suggest that MacKenzie and Owen mis-identified ultimobranchial bodies as parathyroid glands in the platypus.

In the current study, the association of parathyroid glands with thymic tissue in the mediastinum is similar to descriptions previously given for the echidna (Maurer, 1899). The thymic tissue examined in both platypuses was involuted but positive identification was supported by the presence of Hassall's corpuscles. The continuation of the thymus caudally to regions of the fibrous pericardium appears to be very unusual for mammals and was also noticed by MacKenzie and Owen (1919).

9.3.2.1. Light Microscopy - Echidna

Descriptions given for the parathyroid gland in the echidna represent the first report based on a study of the glands from 12 echidnas. This is a considerable advance on the earlier report (Maurer, 1899) where only one mature echidna was examined. Principal and water-clear cells, but not oxyphil cells, were present. Water-clear cells are discussed in the following section (9.3.3). Of all the marsupial and monotreme species examined in the current study the principal cells of the parathyroids in *Tachyglossus* showed the most obvious polarity with the cells being quite elongated and the nuclei eccentric in position. However arrangement of principal cells into follicles was not seen. Cysts were also absent. The absence of these features in monotremes distinguishes them from most marsupials where follicles and cysts were part of the parathyroid histology for all marsupial species, except *Antechinus* spp., *Sarcophilus harrisii*, and *Macropus fuliginosus* examined in this current study (See chap. 11, General Discussion). The absence of oxyphil cells appears not unusual considering that their presence has been recorded in only a few reptilian and mammalian species (Roth and Schiller, 1976, Srivastav et al., 1995; Wild and Setoguti, 1995). The noted absence of light and dark categories of principal cells in paraffin and resin sections of parathyroid glands and the merging of parathyroid and thymic tissues have also been described for several marsupials and are discussed in chapter 11, General Discussion. However since the histology of the parathyroid glands, ultimobranchial bodies, thyroid and thymus in *Tachyglossus* shares many similarities with those of reptiles then comparisons with reptiles will be discussed in this chapter.

There appear to be strong affinities between the histology of the parathyroid, ultimobranchial, thyroid glands and thymus in *Tachyglossus* and those in reptilian species that share a similar anatomy for these organs. For example results of the current study are similar to findings in lizards (suborder Lacertilia) and snakes (suborder Serpentes) (Roth and Schiller, 1976; Srivastav et al., 1995). The parathyroid glands in the snakes, *Cerberus rhynchops* and *Eryx johnii* have principal cells with partial polarity arranged in cords, and cells of the ultimobranchial bodies are arranged mainly in follicles (Singh and Kar, 1983; Padgaonkar et al., 1992). The distinction between the histology of the parathyroids and ultimobranchial bodies was as apparent in these reptilian studies as it was in the current study on *Tachyglossus*.. Another common feature for these three species was the close association of the parathyroid gland with the thymus but not the thyroid.

The unique structure of lymph nodes in monotremes has been noticed in a previous study (Diener and Ealey, 1965) where the morphology was interpreted as being intermediate between amphibian jugular bodies and eutherian lymph nodes. Diener and Ealey described each lymph node as consisting of a dark cortex surrounding a pale medulla, formed by a germinal centre. However, my interpretation of lymph node structure differed slightly. A cortex and medulla were not obvious in all nodes. In nodes without a

germinal centre the tissue immediately adjacent to the vascular connection had fewer small lymphocytes present and was only slightly paler in staining compared with the cortex. The distinction of dark cortex and pale medulla that is seen in other mammalian lymph nodes was not apparent. The appearance was more like mucosal associated lymphoid tissue but with a peripheral layer of reticular cells. From the serial sections done in the current study the nodes were present linearly in the lymph vessels and each node had vascular connections to the wall of these vessels. Earlier descriptions of the nodes interpreted them as a complex of nodes joined by interlinking lymph vessels, instead of being in a lineal series. The peripheral covering of the nodes by a layer of reticular cells was also not reported in the earlier study (Diener and Ealey, 1965).

9.3.2.2. Light Microscopy - Platypus

The microscopic structure of parathyroid gland is similar to that of many other air-breathing vertebrates (Roth and Schiller, 1976). If the platypus has similar embryology of the branchial pouches to that of the echidna (Maurer, 1899) then the observed close association of thymic tissue with the parathyroid glands supports the identification of these endocrine glands as parathyroids and not ultimobranchial bodies because the derivation of the parathyroids is similar to that of the thymus but different from that of the ultimobranchial body.

9.3.3. Electron Microscopy - Echidna

Ultrastructural descriptions were based on the examination of specimens from only three echidnas. Although the number of specimens was low, the heterogeneity of the samples was minimal because all animals were male, all were taken from the wild and killed at the same time, and all specimens were treated similarly with excellent fixation and staining. Hence differences that were noted between specimens taken from different animals could be interpreted as individual variations rather than effects caused by different physiological or technical influences. Conversely, no data were recorded on the possible structural variations imposed on the parathyroid by seasonal influences, sexual differences, or physiological conditions (e.g. lactation).

The array of vesicles that were seen in the principal cells of the echidna parathyroid gland is similar to that described in most of the marsupials studied (see chaps. 4 - 8). The classification of granules as secretory or storage/lysosomes was influenced by a previous study where electron dense vesicles without a wide halo and more granular vesicles with a wide halo were found to represent secretory and storage granules respectively (Wernerson et al., 1995).

Unusual features that characterized the echidna parathyroid gland were the presence of water-clear cells with their large vacuoles, the non-secretory cells interspersed with the

other parenchymal cells, the extensive network of canaliculi formed by the interdigitating short microlamellar projections, and the lack of follicles and cysts. The last feature has already been discussed in section 9.3.2.

Water-clear cells are not widespread in mammalian parathyroid glands. They are almost never found in normal human parathyroid glands (DeLellis, 1993) and have been noted occasionally in hamsters (Emura et al., 1990), possums (Haynes, 1995), and rabbits (Wild and Setoguti, 1995). The appearance of vacuoles in water-clear cells is somewhat variable. In humans they range from small to large (i.e. 0.1 - 4μm in diameter) are membrane-bound, often contain fine particulate and thread-like material and sometimes appear to coalesce (Sheldon, 1964; Roth, 1970; Nilsson, 1977; DeLellis, 1993; Wild and Setoguti, 1995). Occasional structures have been reported within the electron lucent vacuoles including lipid droplets, concentric layered "myelin bodies" (Roth, 1970), and electron dense material (DeLellis, 1993). In addition to these variations, in hamsters (Emura et al., 1990; Emura et al., 1991), rabbits (Wild and Setoguti, 1995), and possums (Haynes, 1995) the membrane of some vacuoles has been studded with ribosomes. In humans, vacuoles of water-clear cells are devoid of ribosomes (Sheldon, 1964; Roth, 1970; Nilsson, 1977). The vacuoles that were present in some cells of the echidna parathyroid glands (see section 9.2.3 above) fit within the spectrum of these documented descriptions. The vacuoles often appeared to have coalesced, had fine particulate contents in which dense bodies or lamellar structures were present and no ribosomes were present. The nuclei were misshapen by the surrounding vacuoles and in humans similar nuclear distortions in water-clear cells have also been noted (Nilsson, 1977).

There are three theories that have been proposed on the origin of the vacuoles in water-clear cells. Either the vacuoles arise from the Golgi region and result from the manufacture of cytomembranes by this organelle (Roth, 1970), the vacuoles are distended cisternae of RER (Emura et al., 1991; Wild and Setoguti, 1995), or they are derived from secretory granules (Cinti and Sbarbati, 1995). The supporting pieces of evidence for these hypotheses are respectively, the similarity of the contents of the vacuoles and the cisternae of Golgi region (Roth, 1970), the presence of ribosomes on the vacuolar surface (Emura et al., 1991; Wild and Setoguti, 1995), and finally the appearance of membrane-bound structures with characteristics intermediate between secretory granules and water-clear vacuoles (Cinti and Sbarbati, 1995). In the current study on the echidna parathyroid glands, the concentric lamellar structures that were in some vacuoles may represent cytomembranes and hence add support for the origin of the vacuoles from Golgi region cisternae. Because water-clear cells are never seen in normal human parathyroid glands but sometimes in hyperparathyroidism it is proposed that their rare presence in other vertebrates may be a result of a pathological condition. In possums (see chap. 7) water-clear cells were only found in animals that appeared to be stressed and the appearance of the cells was linked to possible renal insufficiencies in these stressed animals. In echidnas

however no possible explanations for the presence of water-clear cells can be provided because no additional information on the physiological status of the animals is available except that body condition and reproductive status of each animal was normal at the time of death.

The non-secretory cells that were interspersed with principal cells and not separated by basal laminae were unique to echidna; they were not observed in parathyroid glands from marsupials (see preceding chapters), nor have they been described in other mammalian parathyroid glands (Roth and Schiller, 1976). However, similar stellate cells have been identified in the reptilian parathyroid of the iguana (Anderson and Capen, 1976). No function was suggested for the stellate cells. Since they resemble some epithelial reticular cells of the thymus and since the thymus and parathyroid glands have common embryonic origins then a suggestion is made that they are indeed epithelial reticular cells atypical in embryonic development and migration. Epithelial reticular cells in the thymus have been shown to have considerable heterogeneity and subgroups have been identified on grounds of ultrastructural, histochemical and immunological studies (van de Wijngaert et al., 1984; von Gaudecker et al., 1986; Bodey and Kaiser, 1997). In the echidna, the non-secretory cells had characteristics similar to those found in epithelial reticular cells that are either undifferentiated or are not active in the synthesis and secretion of humoral substances (van de Wijngaert et al., 1984; von Gaudecker et al., 1986).

The most unusual ultrastructural feature of the echidna parathyroid was the extensive network of canaliculi that penetrated the glands. Short cytoplasmic processes have been associated with active secretion of parathyroid hormone although delayed and poor fixation can influence the morphology (Wild and Setoguti, 1995). In view of the good preservation of the parathyroid glands by perfusion fixation, it is suggested that the parathyroid glands were very active in secreting parathyroid hormone and the network of minute intercellular spaces formed a pathway for the hormone to pass into the vascular system.

Fig. 9.1. Anatomy of ventral neck and mediastinum in the echidna

The three drawings illustrate the typical anatomy of endocrine glands and lymphoid structures in the ventral neck and thorax of the echidna. Superficial salivary glands have been removed and ventral neck muscles have been cut near their attachment to the larynx.

Fig. 9.1a. Shows the major arterial branches of the aortic arch and the course of the common carotid arteries. The carotid bifurcation occurs at the level of the larynx deep to the ventral neck and digastric muscles. The vagus nerve is shown accompanying the common carotid arteries. Note the prominent internal thoracic arteries that arise from the carotid arteries near their origins and then course caudally ventrolateral to the aortic arch. The most common locations of parathyroid glands, adjacent to the origins of the common carotid and internal thoracic arteries, are shown by solid red squares.

Fig. 9.1b. Shows numerous small lymph nodes (solid black) and the deepest layer of mediastinal tissue (mainly thymus) around the major arteries. Mediastinal tissue consists of thymic lobules and fibrofatty tissue as well as lymph vessels, nodes, neurovascular components and occasionally parathyroid glands.

Fig. 9.1c. Shows the extent of the thyroid gland (dotted) at the caudal end of the trachea, and ventral to it is fibrofatty tissue that is continuous with the pericardium and contains thymic tissue. The locations of the ultimobranchial bodies are indicated by solid blue squares.
Bar: 10mm

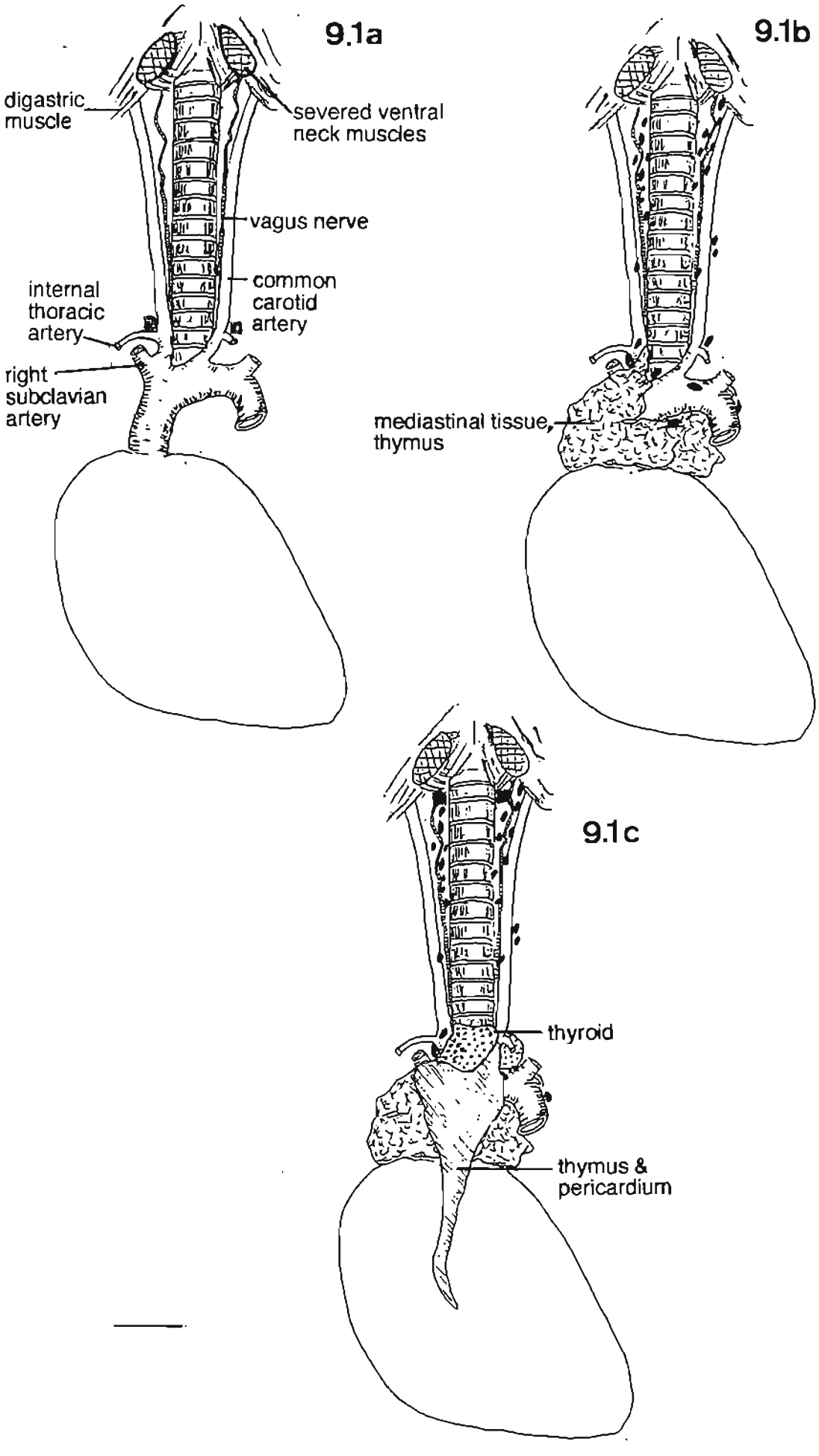
9.1a
digastric muscle
severed ventral neck muscles
vagus nerve
common carotid artery
internal thoracic artery
right subclavian artery
9.1b
mediastinal tissue, thymus
9.1c
thyroid
thymus & pericardium

Plate 9.2. Gross anatomy of the neck and thorax in the platypus

The photograph shows the anatomy of the ventral neck and mediastinum of the platypus. Some of the many nodular structures can be seen in the tissues surrounding the trachea (T) and major arteries. The thyroid (Tr) has been reflected from its usual position at the base of the trachea with the carotid arteries as its lateral borders. A lymph node (L) is dorsal to the thyroid gland. Thymic tissue and parathyroid glands were located in the fibrofatty mediastinal tissue (Th). Arrows indicate where parathyroid glands were found in the serial sections; their locations are hidden in this ventral view.

Platypus #2

Bar: 5mm

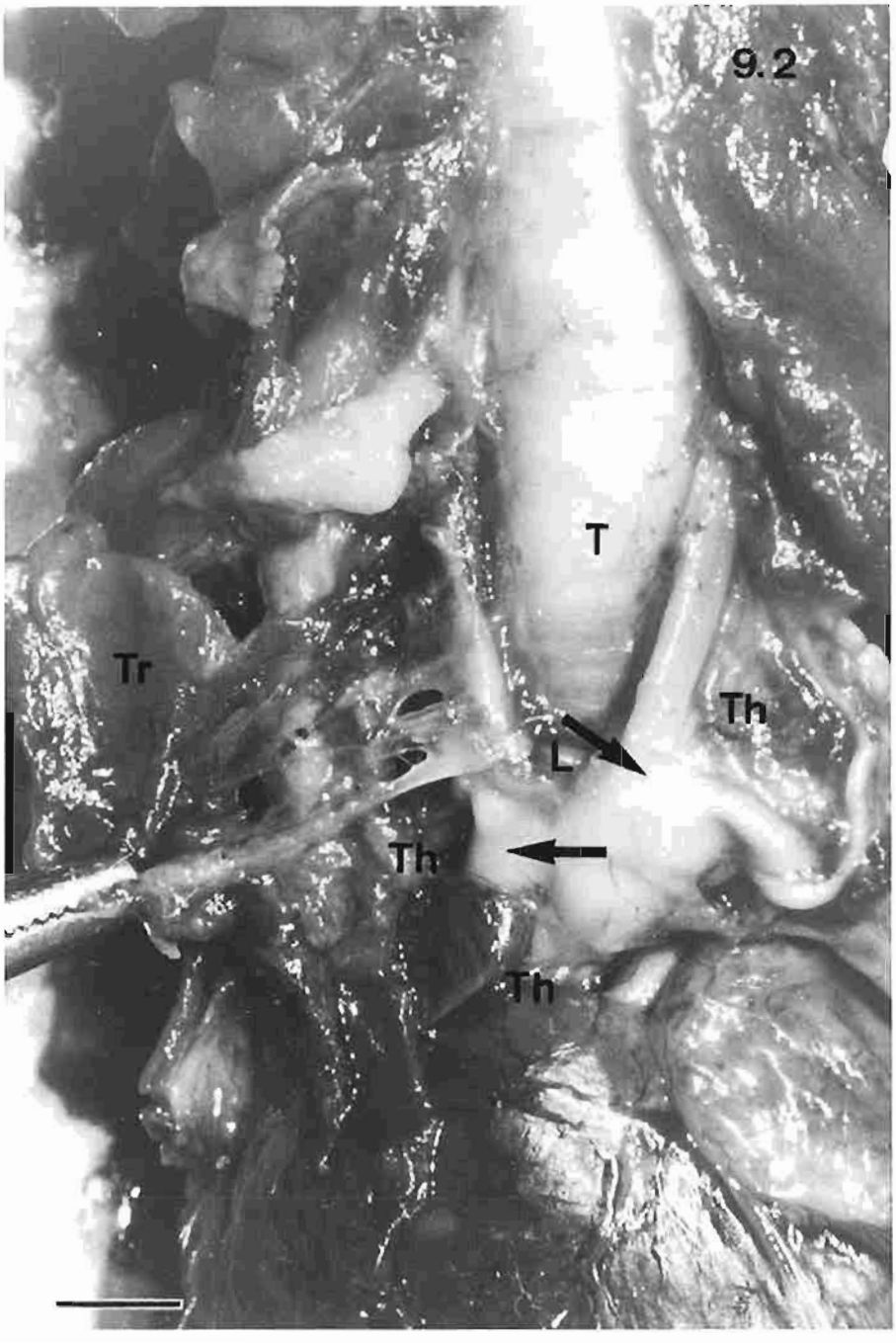
9.2
T
Tr
Th
L
Th
Th

Plate 9.3. Monotreme lymph node

Fig. 9.3a. Shows the typical ovoid shape of a monotreme lymph node suspended in a lymph vessel and the fine vascular connection between the node and the wall. Note the slightly different medullary tissue in the vicinity of the vascular connection. Lymphocytes and other leukocytes, but not red blood cells are present in the surrounding lymph.
Echidna E3, mediastinal tissue
Bar: 50μm

Fig. 9.3b. Shows part of a lymph node with a germinal centre surrounded by small lymphocytes of the cortex. Note the reticular cells (R) at the periphery of the cortex.
Echidna E1, mediastinal tissue
Bar: 30μm

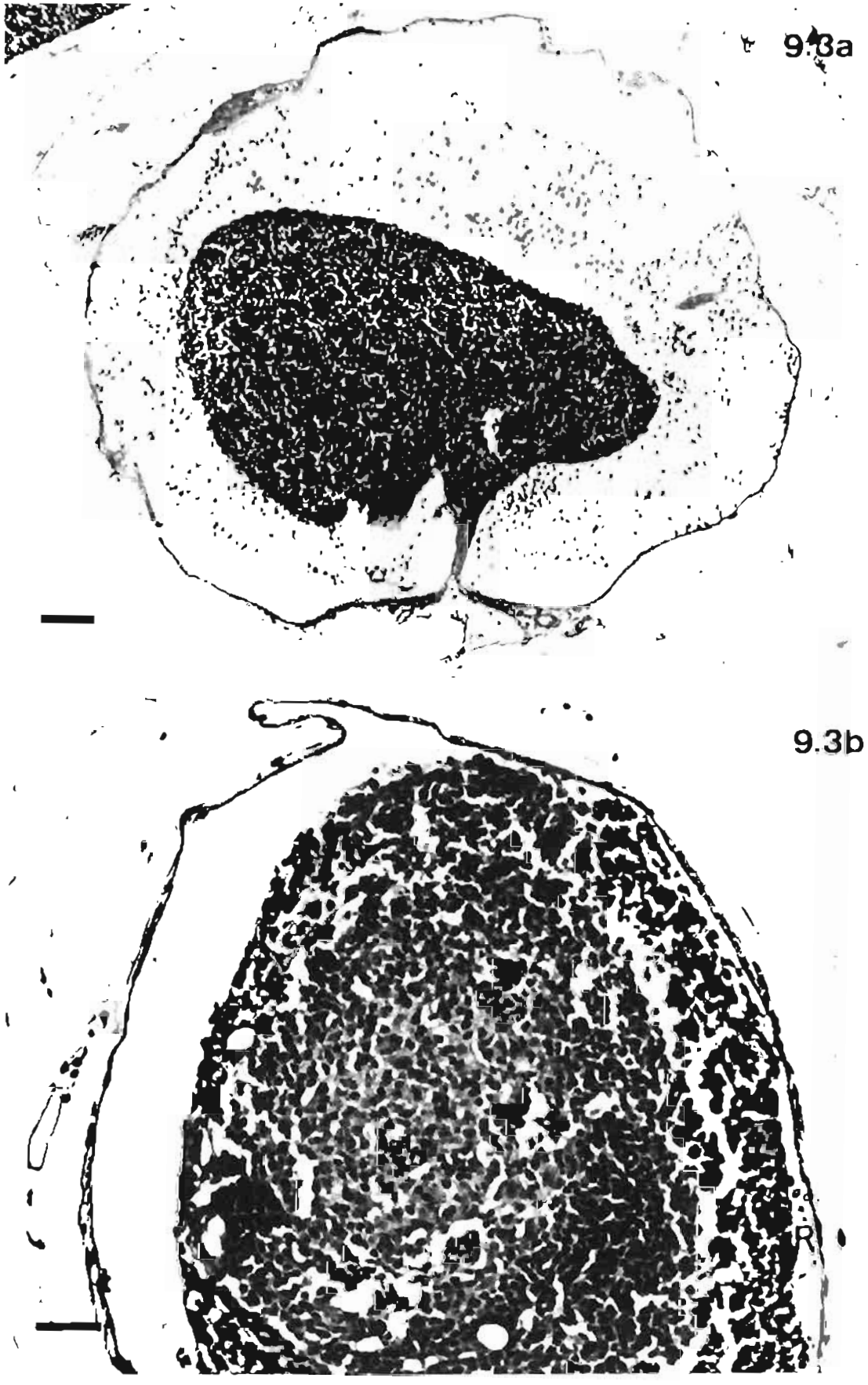
9.3a
9.3b
R

Plate 9.4. Light microscopic structure of parathyroid glands in the echidna

Fig. 9.4a. Shows the typical reticulate endocrine structure of a parathyroid gland. Note the elongated principal cells with eccentric nuclei. Intercellular space has been accentuated. Echidna E1, mediastinal tissue, paraffin section.
Bar: 20μm

Fig. 4b. Shows the cytoplasm of parathyroid principal cells is pale with many vacuoles. Nuclei of the elongated cells are at the ends adjacent to the perivascular connective tissue.
Echidna E6, paraffin section.
Bar: 50μm

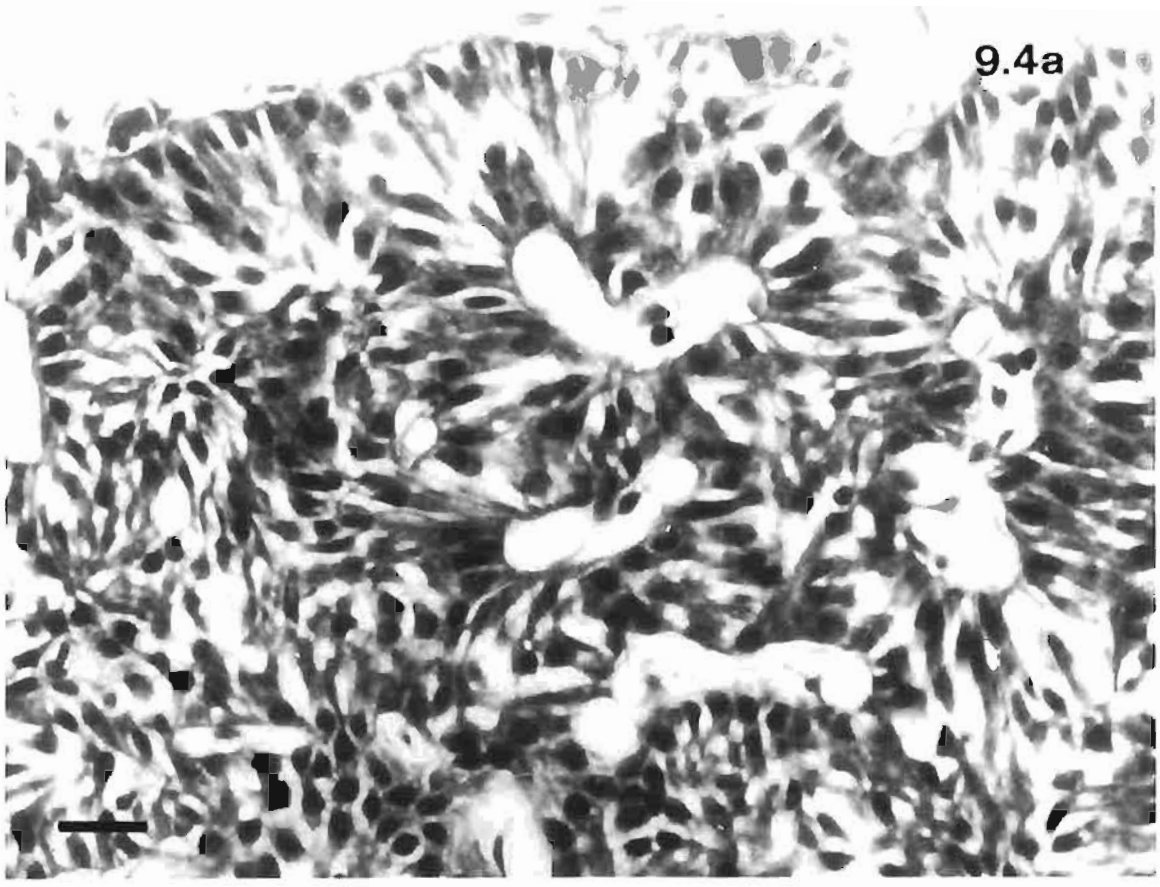
9.4a

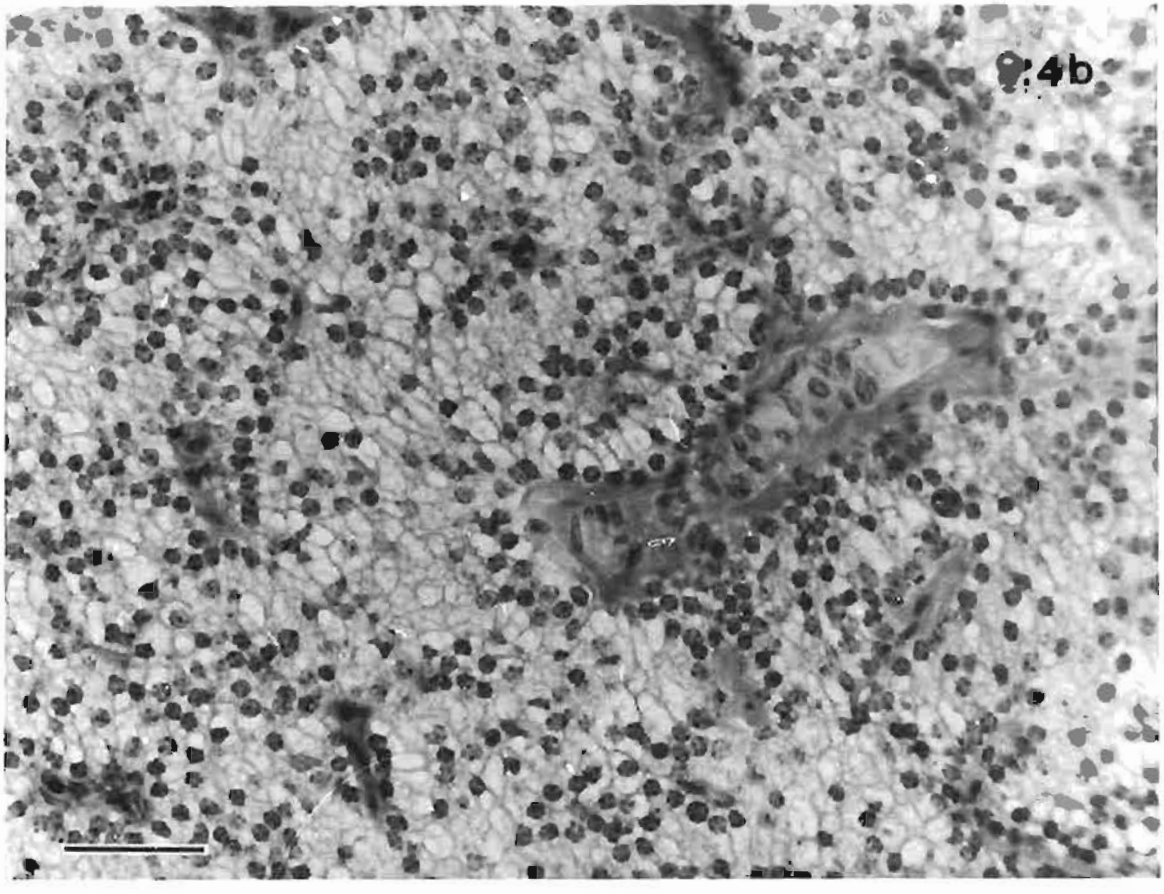
9.4b

Plate 9.5. Light microscopic structure of water-clear cells in echidna

Fig. 9.5a. Shows a patch of water-clear cells in the parathyroid gland of echidna E12. The rich vascularity of the gland is obvious because the capillaries and small blood vessels are distended and clear due to fixation by perfusion.
Echidna E12, resin section, toluidine blue.
Bar: 200μm

Fig 9.5b. Shows the light microscopic appearance of water-clear cells. They are about twice the size of the darker principal cells and are filled with small clear vesicles. Note the central dark core of some vesicles.
Echidna E12, resin sections, toluidine blue.
Bar: 20μm

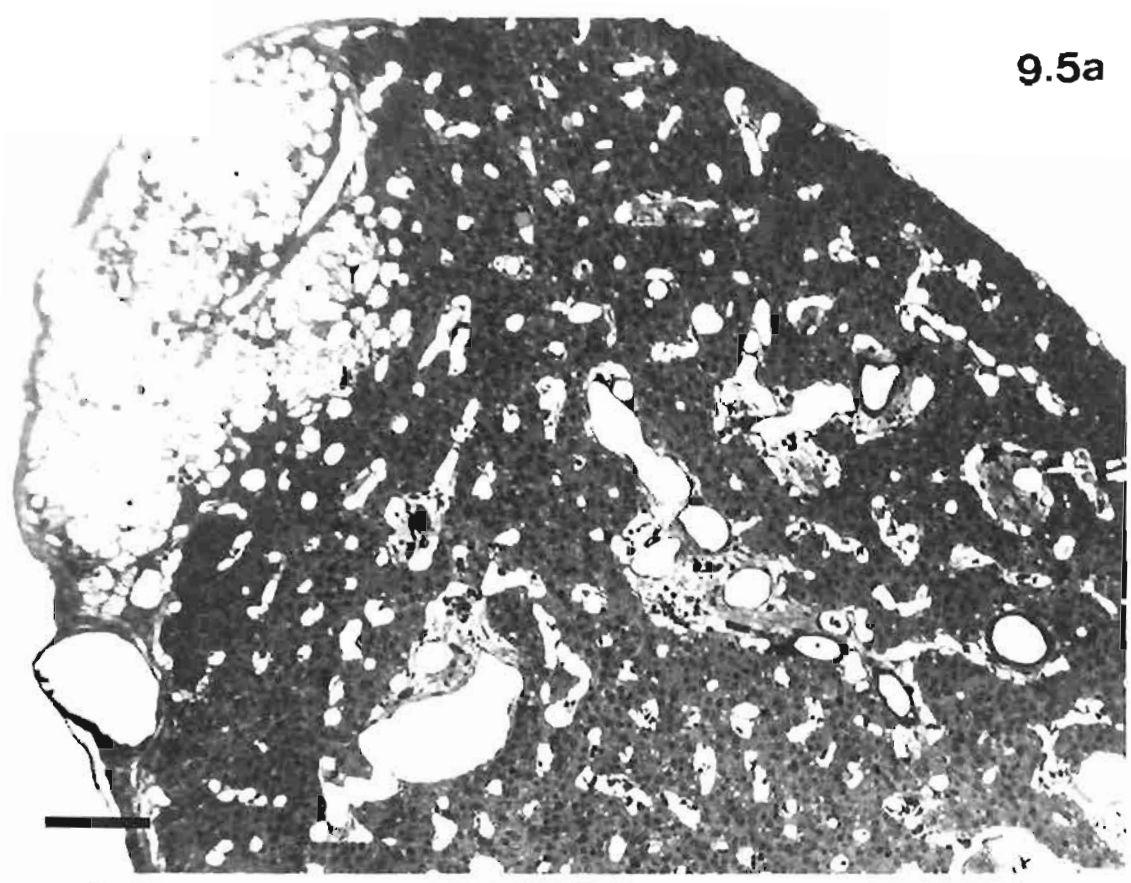

9.5a

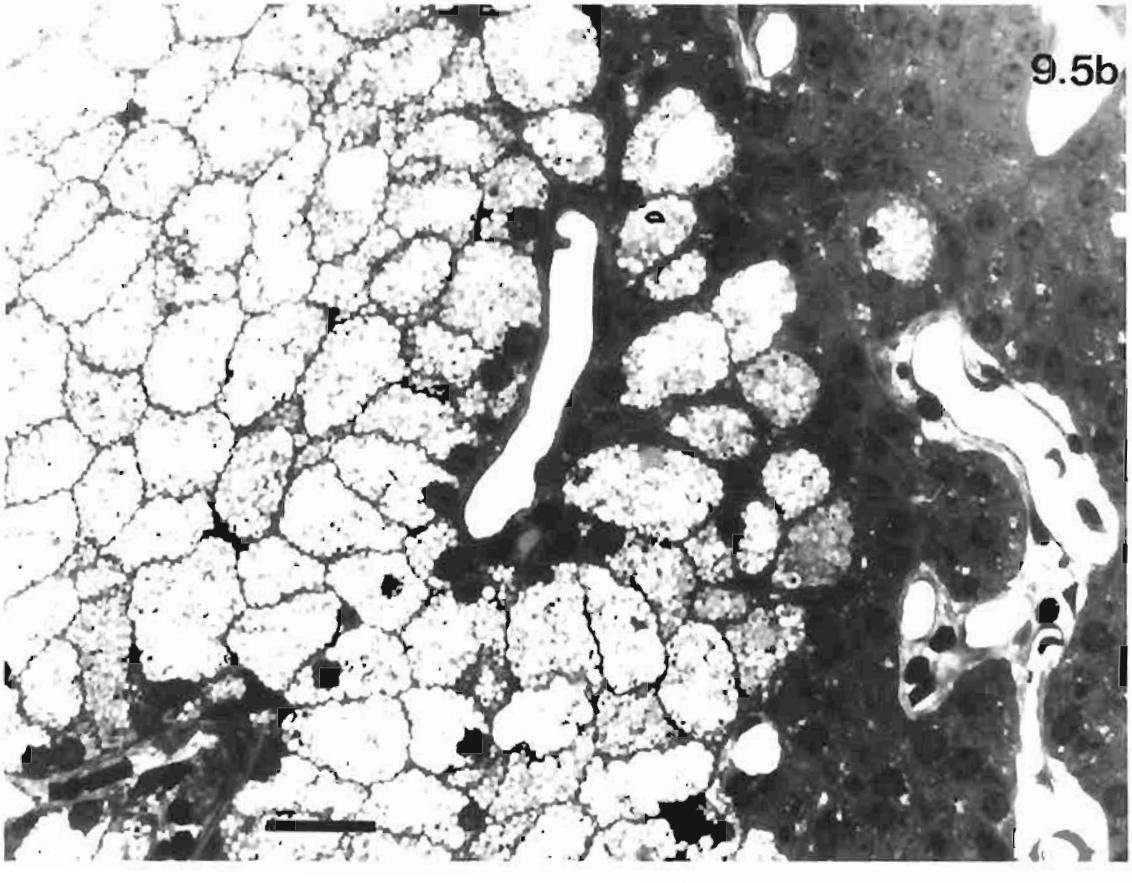

9.5b

Plate 9.6. Thymus-parathyroid barrier and ultimobranchial body in the echidna

Fig. 9.6a. Shows the apparent lack of connective tissue barriers between the pale staining principal cells of the parathyroid gland and the small dark lymphocytes of the thymus. A Hassall's corpuscle (H) is present at the top of the micrograph.
Echidna E3, paraffin section.
Bar: 50μm

Fig. 9.6b. Shows the histology of the ultimobranchial body. Endocrine cells are in clumps or arranged in small follicles. Note glandular cells are not encapsulated but clusters are scattered in the fibrous tissue.
Echidna E3, paraffin section.
Bar: 50μm

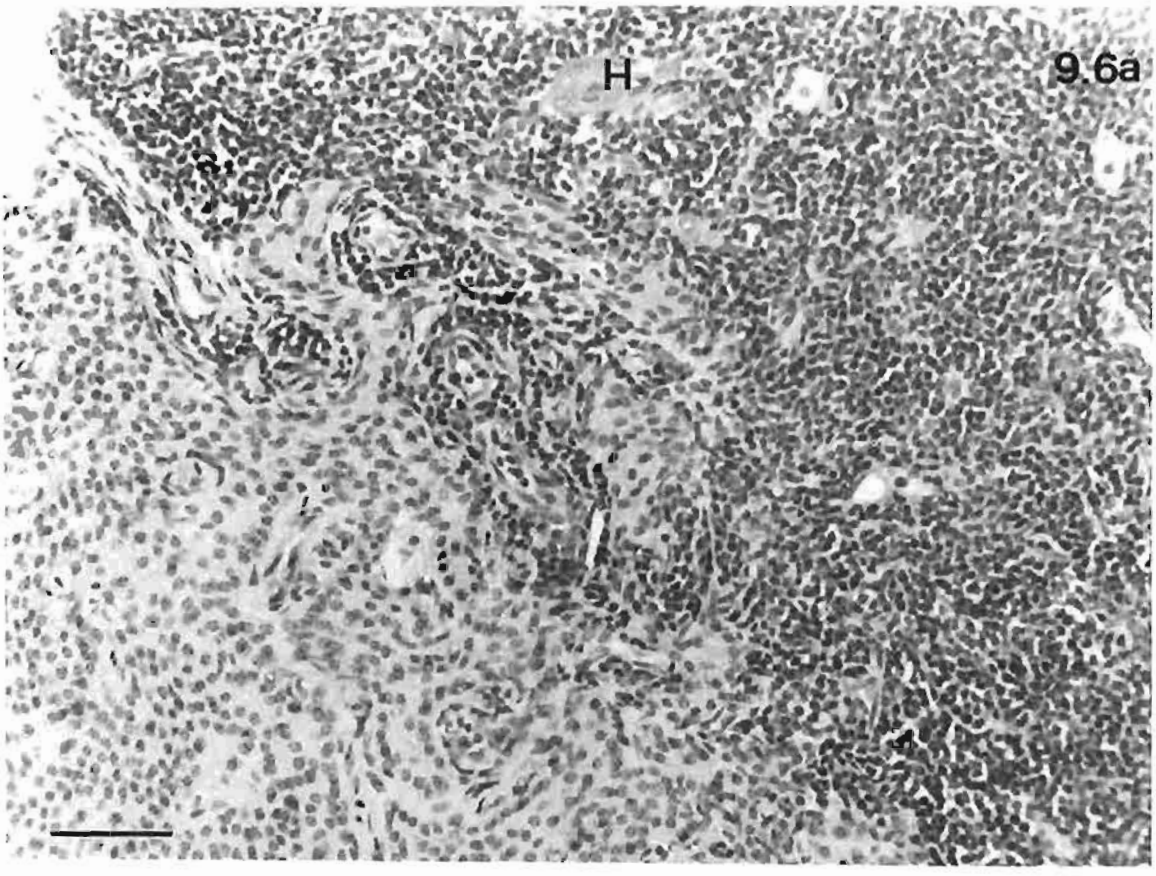
H
9.6a

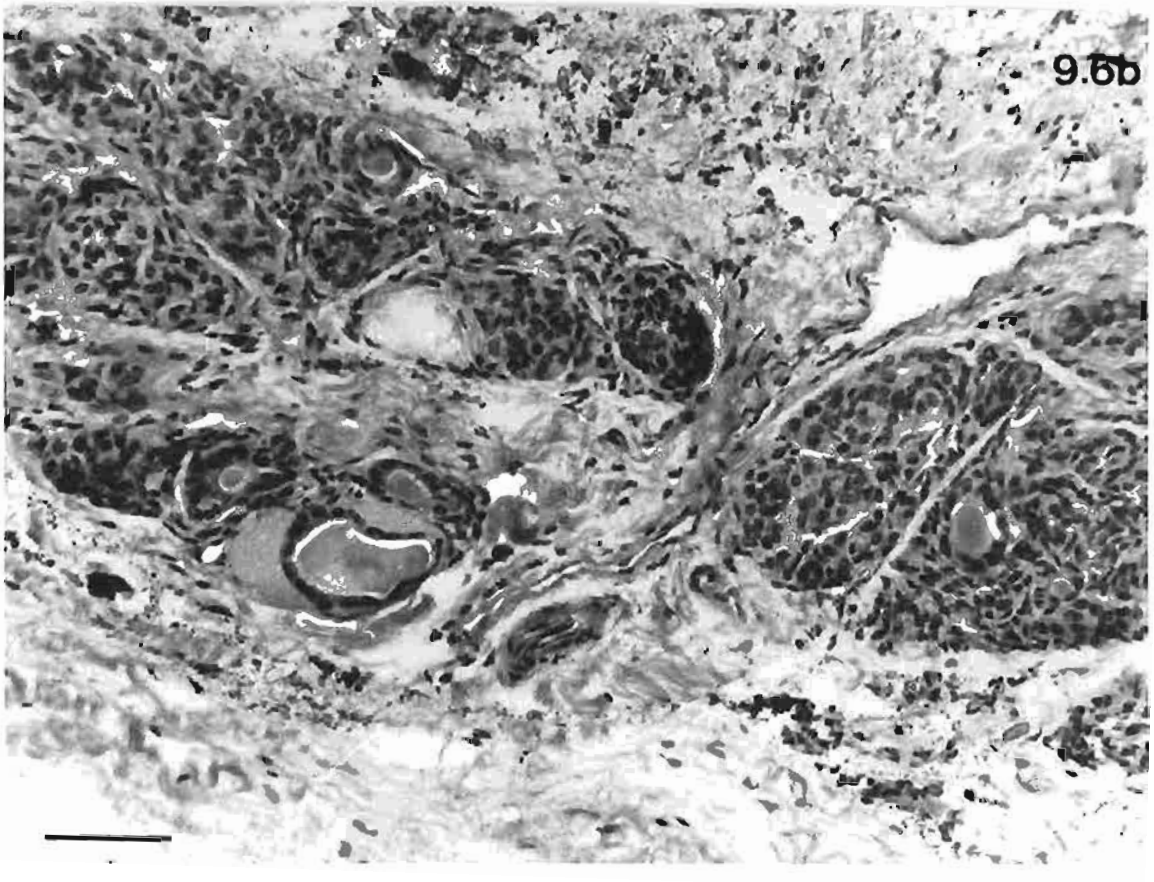
9.6b

Plate 9.7. Light microscopic structure of the parathyroid gland and thymus in the platypus

Fig. 9.7a.. Shows parathyroid gland and thymic lobule set in the fibro-fatty tissue of the mediastinum. Note the compact arrangement of the principal cells in the parathyroid gland and the high nuclear to cell volume ratio.
Platypus 2
Bar: 30μm

Fig. 9.7b. Shows the mingling of thymic tissue (T) (small dark nuclei on the left) with principal cells of the parathyroid. The pale, foamy appearance of the cytoplasm of many principal cells suggests glycogen storage.
Platypus 2
Bar: 30μm

Fig. 9.7c. Shows an involuting thymic lobule without a clearly demarcated cortex and medulla and a Hassall's corpuscle (H) on the upper left.
Platypus 2
Bar: 30μm

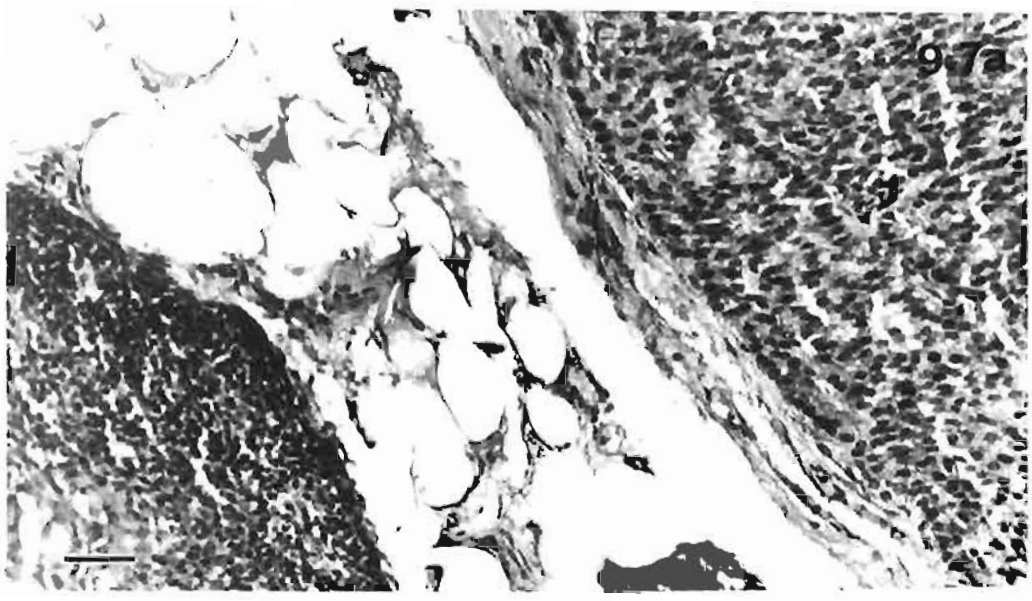
9.7a

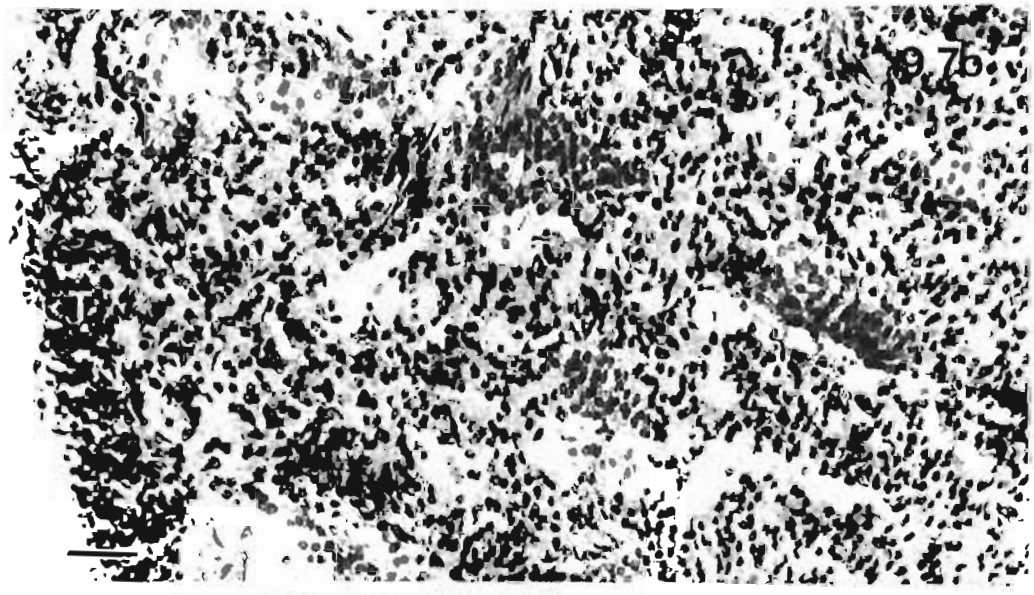
9.7b


9.7c

Plate 9.8. Ultrastructure of principal and water-clear cells in the echidna

Fig. 9.8a. Shows a low power view of the parathyroid gland. Little connective tissue surrounds the capillary and parenchymal cells have similar density of staining to their cytoplasm. Note the non-secretory cell (N) with a triangular nucleus in the upper left quadrant of the micrograph.
Echidna E10
Bar: 5μm

Fig. 9.8b. Shows water-clear cells. The nucleus is hyperchromatic and distorted by large vesicles that fill the cytoplasm almost to the exclusion of other cytoplasmic structures. Some coalescence of vesicles is apparent.
Echidna E12
Bar: 2μm

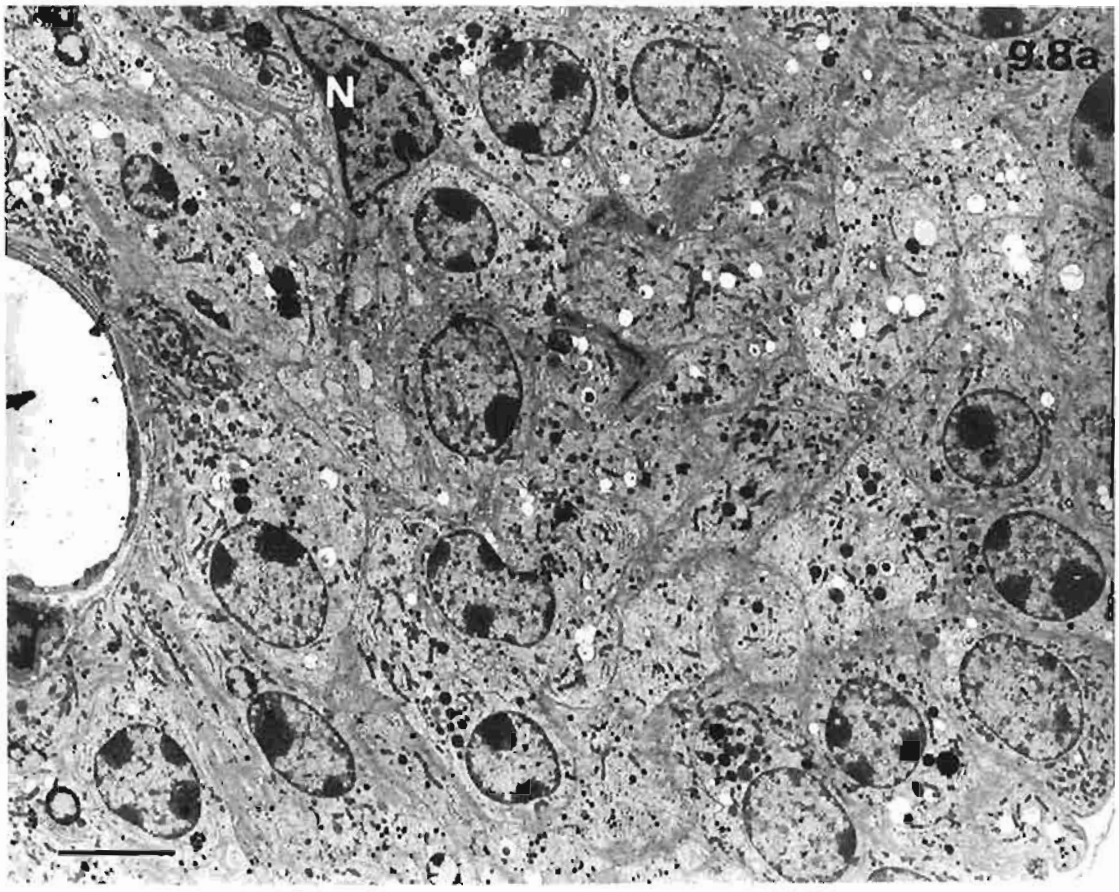
N
9.8a

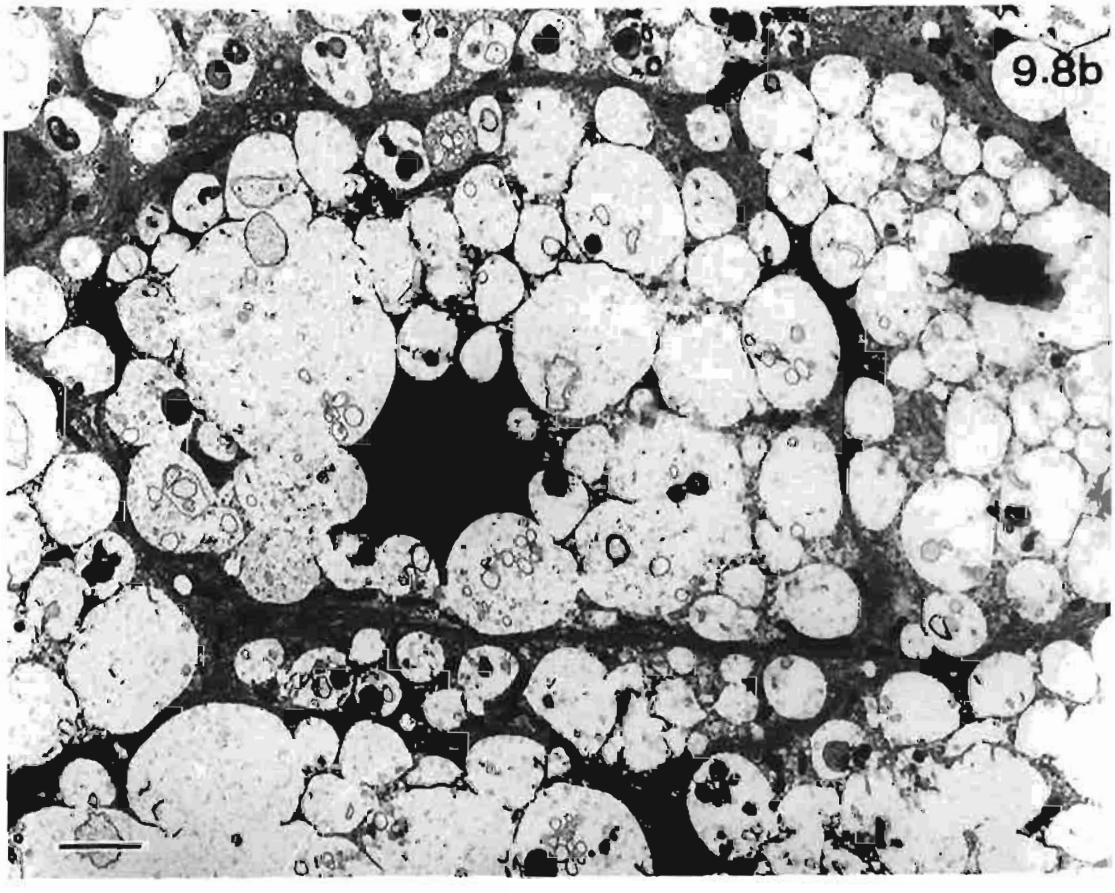
9.8b

Plate 9.9. Polarity of principal cells and intercellular canaliculi in the echidna parathyroid gland

Fig. 9.9a. Shows polarisation of principal cells. In the elongated columnar cells, nuclei and RER are at one end and granules and Golgi bodies at the other. Note the system of canaliculi is between the cells.
Echidna E11
Bar: 2μm

Fig. 9.9b. Cellular outline is accentuated by the microlamellar processes forming canaliculi. Note the abundant organelles and inclusions in the principal cells compared with the non-secretory cell (N) in the top left corner of the micrograph.
Echidna E11
Bar: 2μm

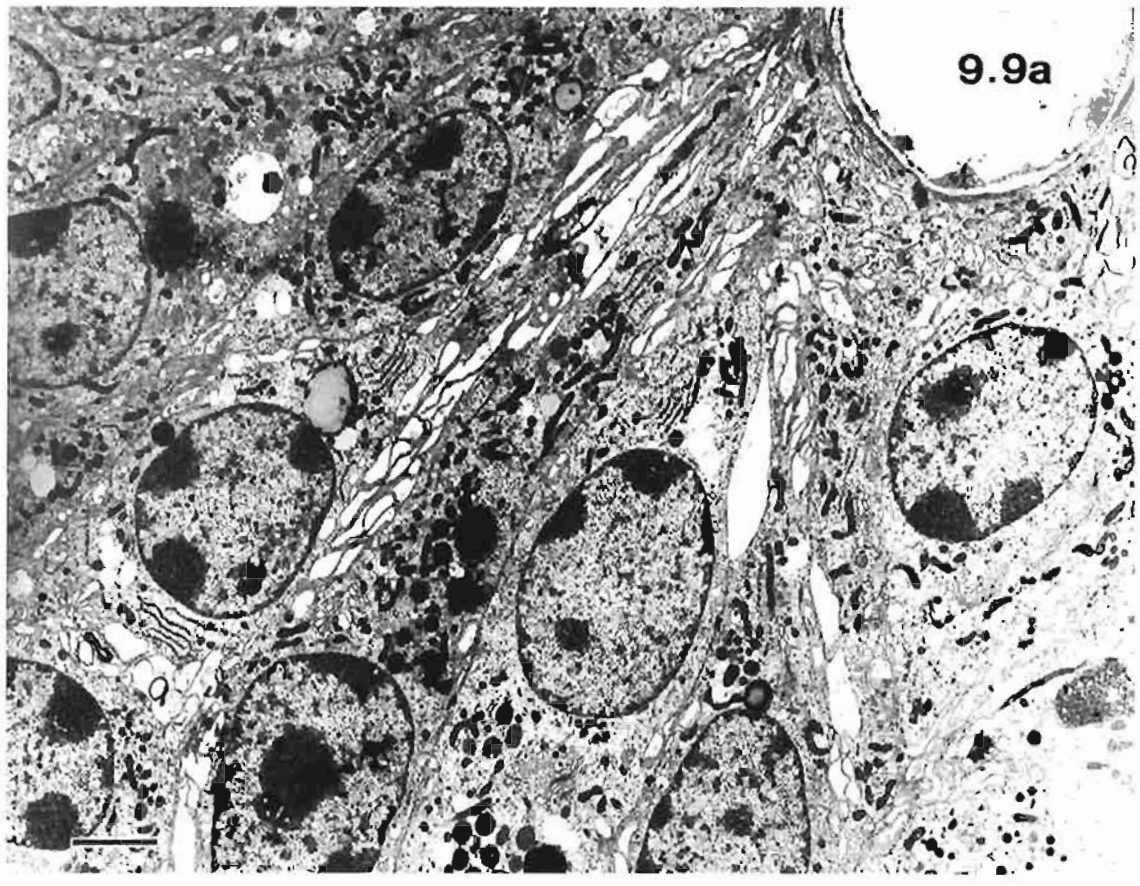
9.9a

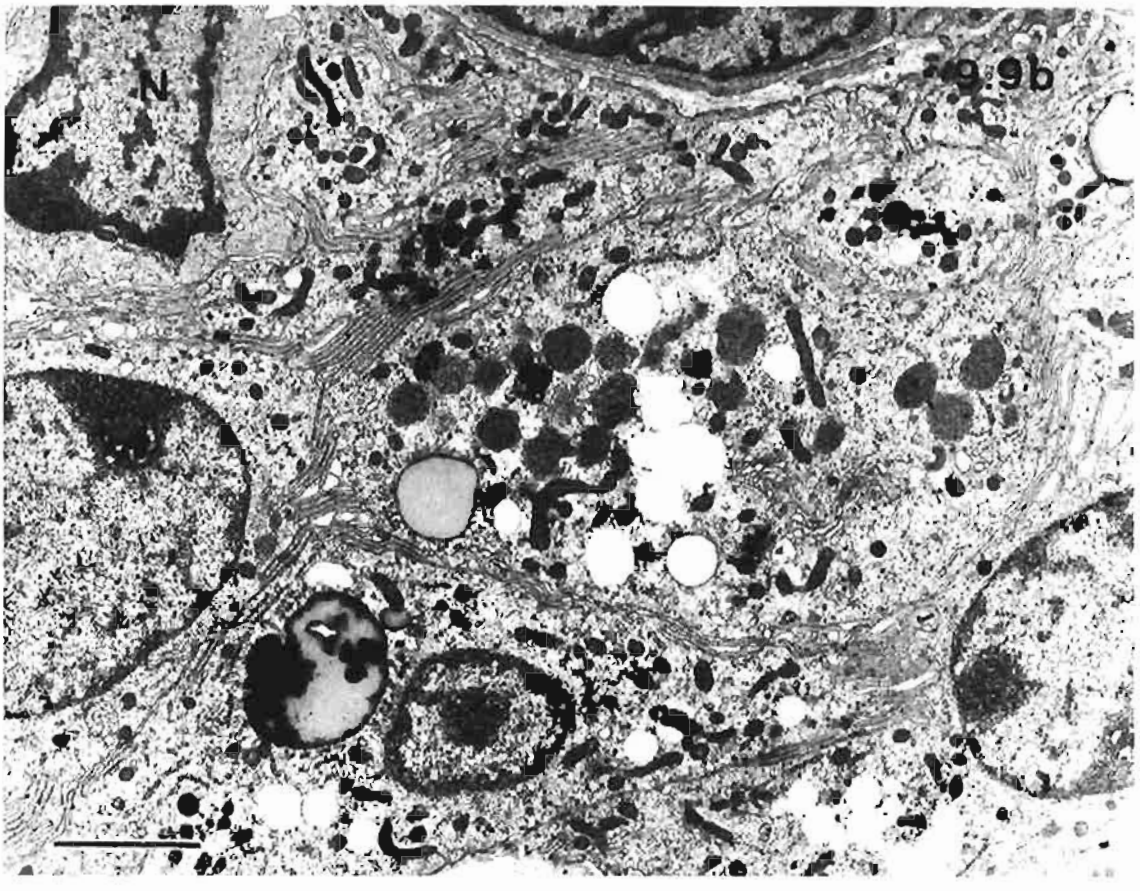
N
9.9b

Plate 9.10. Clear vesicles and Golgi complex in the parathyroid gland of the echidna

Fig. 9.10a. Shows stacks of parallel RER lamellae and details of the intercellular canaliculi formed by microlamellar projections. Clear, membrane-bound vesicles can be seen stored intracellularly (S) and remaining intact (R) in the intercellular canaliculi.
Echidna E11
Bar: 1µm

Fig. 9.10b. Shows the typical appearances of a Golgi complex and mitochondria in an echidna parathyroid gland. Mitochondrial matrix is very electron dense.
Echidna E11
Bar: 500nm


9.10a
S
R

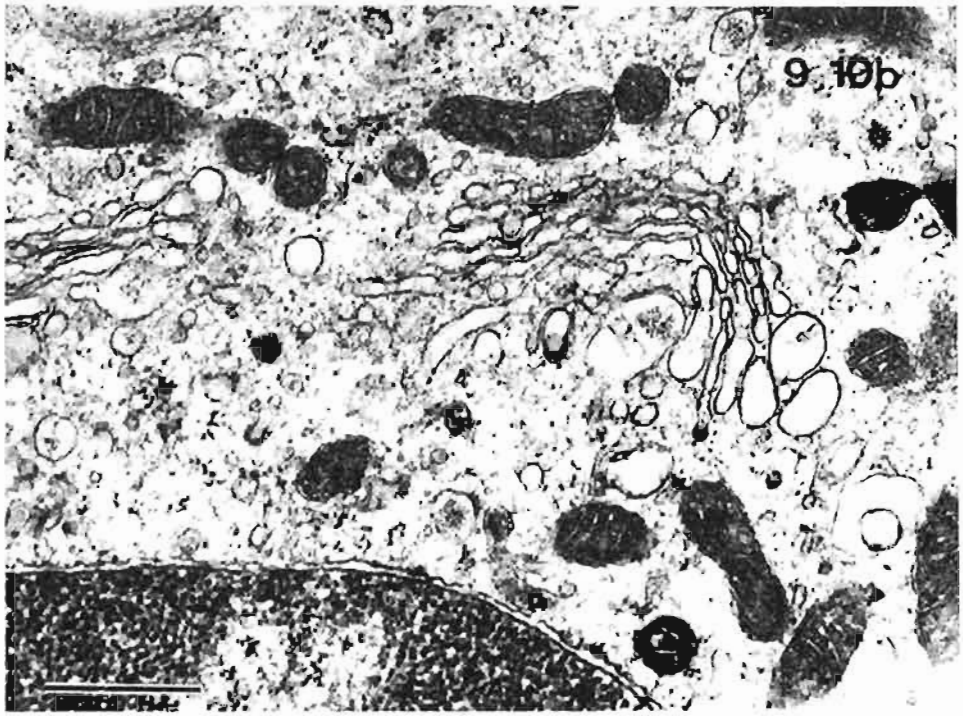
9.10b

Plate 9.11. Vesicles in principal and water-clear cells in the parathyroid gland of the echidna

Fig. 9.11a. Shows electron dense secretory granules (S), larger vesicles (H) where the particulate contents are surrounded by a halo, and two lipid inclusions (L).
Echidna E11
Bar: 500nm

Fig. 9.11b. Shows details of typical vesicles in a water-clear cell. The contents are variable ranging from very sparse particulate matter (P) to heterogeneous structures (G). The presence of a mitochondrion, RER (arrow) and desmosomes indicate a living rather than dying cell.
Echidna 12
Bar: 500nm

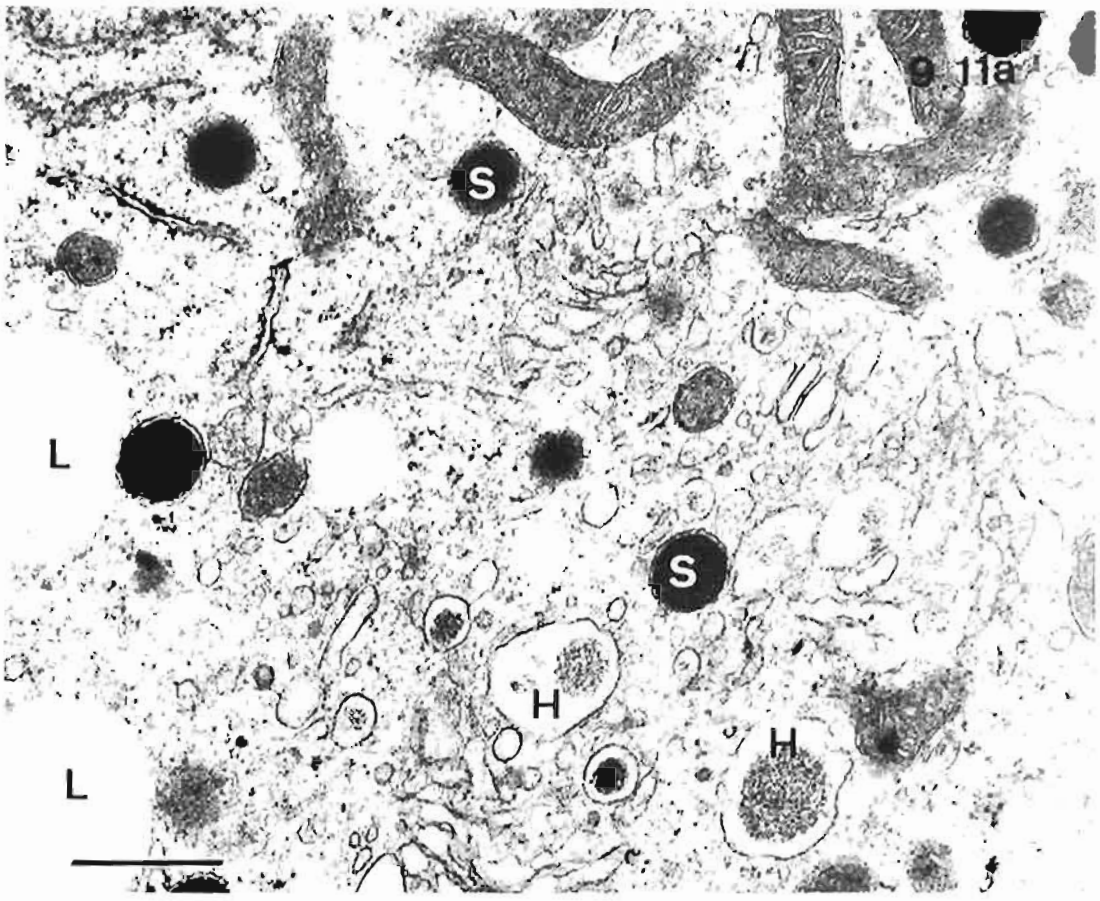

Fig. 11a

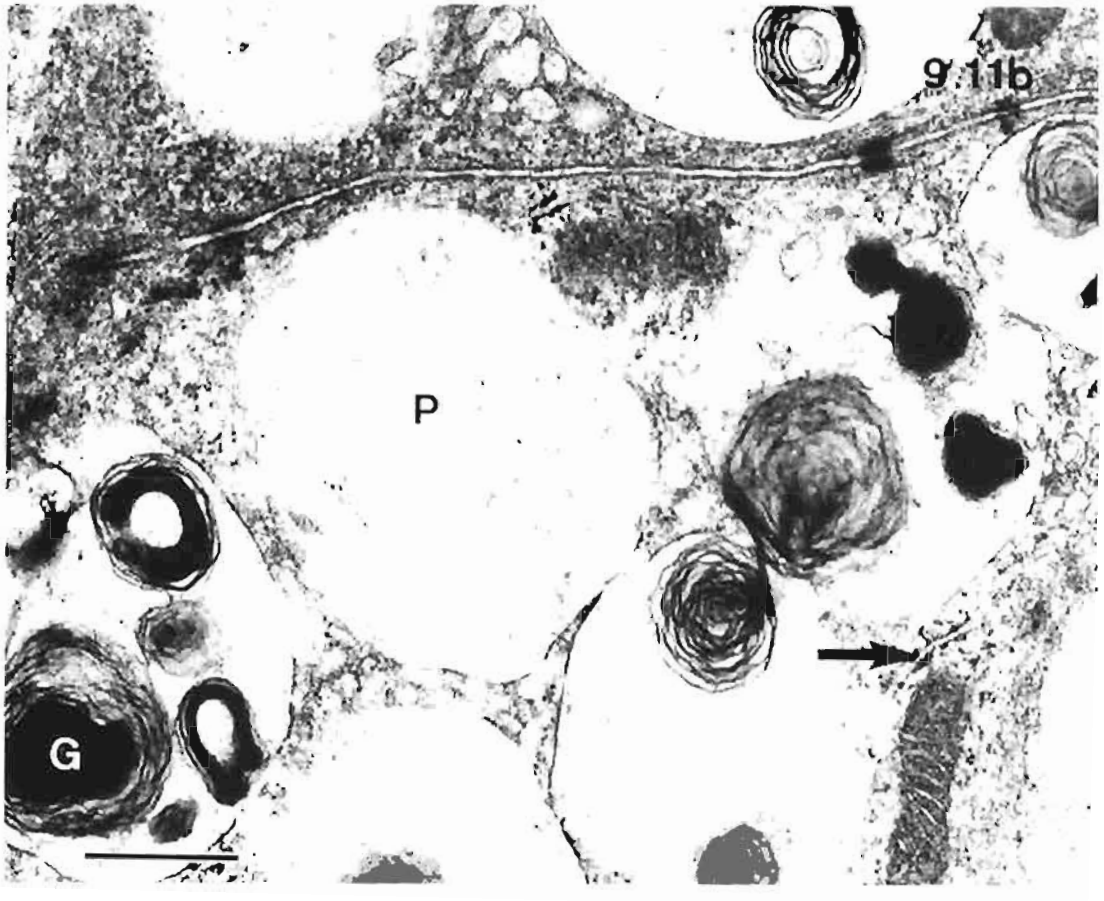

Fig. 11b

Chapter 10

Immunocytochemical Study of Marsupial and Monotreme Parathyroid Glands and the Ultimobranchial body in the Echidna

10.1. Introduction

The aims of this chapter are -

1. To identify parathyroid hormone in tissue sections of parathyroid glands of marsupials and echidnas by using immunocytochemistry at the light and, where possible, the electron microscopic levels.

2. To confirm the identification of ultimobranchial bodies in the echidna using light microscopic immunostaining techniques to detect calcitonin and calcitonin gene-related peptide (CGRP).

The presence of parathyroid hormone has been demonstrated successfully by immunocytochemical techniques in many mammalian parathyroid glands including human (DeLellis, 1993), rat, gerbil, mouse, dog (Inoue and Setoguti, 1986), rabbit (Shoumura et al., 1988), cow (Arps et al., 1987), and hamster (Shoumura, Ishizaki et al., 1988). No information is available on the immunocytochemical staining of marsupial or monotreme parathyroid glands.

Light microscopic techniques have included immunofluorescent staining (Hargis et al., 1964; Ali, 1980) and indirect peroxidase labelled antibody (Futrell et al., 1979; Oka et al., 1988; DeLellis, 1993). Parathyroid hormone has also been demonstrated at the ultrastructural level. Of the several techniques available, two that have been used successfully are the indirect peroxidase labelled antibody method (Futrell et al., 1979) and the protein A-gold technique (Inoue and Setoguti, 1986). In the former method, secretory granules of parathyroid hormone in bovine glands and human adenomas were illustrated, and in the latter, the distribution of parathyroid hormone in parathyroid glands from several mammalian species was shown.

The cells of the ultimobranchial body are identical in origin and function to the parafollicular cells, i.e. C cells, of the thyroid (Wendelaar Bonga

and Pang, 1991). Their known function is to secrete calcitonin in response to hypercalcemia. The gene responsible for the formation of calcitonin also codes for another peptide, calcitonin gene-related peptide (CGRP) and the expression of the specific mRNA for the precursor of calcitonin or CGRP depends on the site of the cell. Calcitonin and CGRP are present within the same cells, even within the same secretory granule, but normally only small amount of CGRP are found in C cells where calcitonin is the major product of the gene, and in the nervous and circulatory system, CGRP is the major peptide (Wendelaar Bonga and Pang, 1991). Across the species, significant homology has been conserved in the amino acid residues of CGRP but fewer similarities are found in calcitonin. For example bovine calcitonin has only 14 out of 32 amino acid residues in common with human calcitonin (Collyear et al., 1991). The degree of homology of these two peptides across the species may influence the immunostaining of C cells or the ultimobranchial body.

10.2. Materials and Methods

The tissue blocks used for immunocytochemical studies came from the same sources that have been described in the preceding chapters. Difficulties were experienced in obtaining paraffin embedded parathyroid glands from *S. crassicaudata* because of the minute dimensions of these glands. All glands were fixed in either buffered formalin or electron microscopic fixative with low glutaraldehyde concentration, i.e. 0.25%, (See chap. 3, Materials and Methods), and embedded in either paraffin for light microscopy or LR White resin for electron microscopy. Details of embedding procedures are given in Appendices A and C.

Immunostaining for light microscopy was done using the indirect peroxidase labelled antibody method. The details of the technique are given in Appendix K1. Briefly the immunocytochemical staining involved initially employing a protein blocking agent, followed by incubation with the primary antibody, then a biotinylated universal secondary antibody and a streptavidin peroxidase reagent. Finally diaminobenzidine was used to produce the staining at the site of the antigen, parathyroid hormone. The protein blocking agent, the secondary antibody and the peroxidase agent were components of a commercial kit, supplied by Immunon, Pittsburgh, USA. The primary antibody, anti-parathyroid hormone came from BioGenex Laboratories, San Ramon, California, USA. Antibodies to calcitonin and CGRP that were used to identify the ultimobranchial body in the echidna were both kindly donated by the Histopathology Department, Institute of Medical and Veterinary Science, Adelaide. The visualisation of the immunoreaction was done using the chromagen 3,3'-diaminobenzidine tetrahydrochloride, also supplied commercially in substrate kit from ZYMED Laboratories, San Francisco, USA.

The immunostaining of parathyroid hormone for light microscopy was done on parathyroid glands from the following marsupials and monotremes:

a. Tasmanian devil, *Sarcophilus harrisii*
b. wombat, *Lasiorhinus latifrons*
c. koala, *Phascolarctos cinereus*
d. possum, *Trichosurus vulpecula*
e. kangaroo, *Macropus fuliginosus*
f. echidna, *Tachyglossus aculeatus* (sections of ultimobranchial body were also used)

Human parathyroid glands removed at autopsies were used as positive and negative controls. For negative controls, incubation with the primary antibody was omitted in the immunostaining protocol.

The immunostaining of calcitonin and CGRP for light microscopy was done on sections of ultimobranchial body (E3, E6), parathyroid gland (E6), and composite tissues (E2) including thyroid, thymus, lymph nodes and parathyroid glands. Positive control was formalin fixed possum thyroid.

Immunostaining for electron microscopy was done using protein A-gold and a modified avidin-gold, extravidin-gold. The gold conjugate in both techniques was 10 nm. In the former technique gold-labelled protein A binds to the primary antibody; in the latter technique the binding site of the primary antibody with parathyroid hormone is amplified by the attachment of biotinylated secondary antibody to which extravidin-gold combines. The protocols for the two techniques and the sources of the reagents are given in Appendix K2.

The immunostaining of parathyroid hormone for electron microscopy was done in the following marsupials:

b. wombat, *Lasiorhinus latifrons*
c. koala, *Phascolarctos cinereus*
d. possum, *Trichosurus vulpecula*
e. kangaroo, *Macropus fuliginosus*

10.3. Results

10.3.1. Light Microscopy - Parathyroid Gland

A positive result for immunostaining of PTH was seen in all the parathyroids stained. The negative control showed that in the oxyphil cells there was some colouration and after viewing routine H & E sections it was decided this staining was due to yellow-brown lipofuscin pigment. In the positive control, human parathyroid gland, PTH was diffusely

distributed in most principal cells (Fig. 10.1a). Some cells were clear and oxyphil cells were intensely stained. Except for the presence of oxyphil cells, a similar diffuse pattern of staining was seen in the parathyroids of the Tasmanian devil, possum (Fig. 10.1b), wombat (Fig. 10.2a), and koala (Fig. 10.2b). Nuclei appeared stained for PTH in some cells (Fig. 10.1b) although positive staining in the cytoplasm above and below the nucleus probably accounted for most of the apparent nuclear staining. Most cells forming follicles in the wombat (Fig. 10.2a) were negative whereas they were positive in the koala (Fig. 10.2b). Smooth muscle in the wall of blood vessels was also noticed to be positive (Fig. 10.2b). Follicular colloid in both species was negative (Figs. 10.2a & 10.2b).

In the kangaroo parathyroid gland staining was quite patchy; with positive staining in scattered cells (Fig. 10.3a). Within the principal cells, granules often appeared to be concentrated on one edge of the cell (Fig. 10.3c). In the wide septa between the lobules mast cells were obvious (Fig. 10.3a). In kangaroo K19, where there was intermingling of parathyroid and thymic tissue, principal cells adjacent to thymic tissue were positively stained (Figs. 10.3b & 10.3c) and contrasted to the negatively stained thymocytes.

The immunostaining of the principal cells in the echidna was paler than that in marsupials. The amount of staining varied from cell to cell (Fig. 10. 4a) with some negative and others with dark granules concentrated in the cytoplasm. Some background staining was apparent in the echidna thymus but yellow-brown stain was very obvious and concentrated in the Hassall's corpuscles. The corpuscles were also positive for the immunostaining of CGRP.

Mast cells in connective tissue adjacent to the parathyroid and thymus were positive for PTH and CGRP. The ultimobranchial body was negative for PTH.

10.3.2. Light Microscopy - Ultimobranchial Body

Immunostaining of calcitonin and CGRP was quite weak and generally inconclusive. In the positive control of possum thyroid, C cells were stained for calcitonin (Fig. 10.5a) and CGRP but some follicular cells were also positive. No parenchymal cells in the echidna thyroid or parathyroid were positive for either peptide. In the ultimobranchial body very weak staining for calcitonin was present in some cells (Fig. 10.5b); CGRP staining was moderate and more widespread (Fig. 10.5c). Mast cells and, as mentioned above, Hassall's corpuscles were intensely stained with CGRP.

10.3.3. Electron Microscopy

Very weak immunolabelling was obtained using protein A-gold technique. Some background staining was present (Fig. 10.6a). Unfortunately most granules had just a handful of gold particles; the best example of labelling was in the koala (Fig. 10.6a).

Labelling was too light to determine if PTH was associated with particular types of granules.

Extravidin-Gold technique resulted in a widespread protein precipitate (Fig. 10.6b) that mainly obscured the gold labelling. However more labelling was obtained with Exravidin-Gold than Protein A-Gold and it appeared more specific. Mitochondria (Fig. 10.6b), RER, and large electron dense vesicles (Fig. 10.6c) were devoid of gold. Particles were associated with very small vesicles (Figs. 10.6b & 10.6c).

10.4. Discussion

10.4.1. Light Microscopy - Parathyroid Gland

The successful immunostaining for PTH using human anti-PTH in marsupial and monotreme parathyroid glands indicates cross-reactivity across the species from monotremes to humans. Similar good cross-reactivity of bovine anti-PTH was found in dogs, rats, gerbils and mice, with dogs showing the strongest intensity of immunostaining and mice the weakest (Inoue and Setoguti, 1986). The intense staining of the periphery of some cells (see Fig. 10.3c) was thought to be a fixation or processing artefact because electron microscopic studies have not shown a similar concentration of vesicles adjacent to the plasmalemma. In the current study the weaker result that was seen in echidnas may reflect a species difference in the amino acid sequence of PTH or fixation of echidna tissue was not optimal for the immunostaining. All the echidnas used in the current study were first used in other scientific investigations that ultimately determined the choice of fixative and the interval between death and fixation.

The apparent staining of oxyphil cells in the human positive control sections was not entirely due to immunostaining. The negative control and the H & E section indicated the presence of a naturally yellow-brown pigment, presumably lipofuscin, in these cells. Previous studies on the immunostaining of PTH in oxyphil cells have been equivocal. Negative staining for PTH has been obtained by Futrell and co-workers (1979) in both bovine and human parathyroid adenomas and Kendall and co-workers (1993) in normal and diseased human parathyroids. Conversely immunostaining of parathyroid adenomas (Ordonez et al., 1982) and nodular hyperplastic glands (Oka et al., 1988) demonstrated PTH in oxyphil cells. Perhaps cross-reactivity between anti-PTH and parathyroid related protein (PRP) (see chap. 2, Literature Review, section 2.3) occurred in the oxyphil cells where PTH expression was noticed. This suggestion is supported by the results of other studies. *In situ* hybridization was used to determine that oxyphil cells had little or no mRNA for the precursor of PTH, namely pre-proparathyroid hormone (Kendall et al., 1991) and a combined immunostaining and *in situ* hybridisation study of PRP in normal parathyroid glands (Kitazawa et al., 1992) showed PRP was present in oxyphil and transitional cells with only scant amounts in principal cells. Thus in conclusion, it is

suggested that the coloured reaction product seen in oxyphil cells in the human positive control was partly lipofuscin and maybe partly PRP.

The intense staining of mast cells was probably due to factors other than immunostaining of PTH. Mast cells can be demonstrated using avidin labelled horseradish peroxidase (Tharp et al., 1985). The conjugated avidin binds to granules in the mast cell and the binding site is visualised by the reaction of the peroxidase on hydrogen peroxide and DAB. In the current study the intense staining seen in mast cells in most marsupial (e.g. Fig. 10.3a) and echidna sections was probably of a histochemical and not immunological nature. Marsupial mast cells have previously been demonstrated using the conjugated avidin technique (Haynes, 1991).

The positive immunostaining of Hassall's corpuscles for PTH and CGRP has not been previously recorded. Epithelial cells in the thymus are heterogeneous and several subclasses have been established with different morphological and physiological properties (von Gaudecker et al., 1986; von Gaudecker et al., 1989; Bodey and Kaiser, 1997). Immunostaining techniques have demonstrated the presence of anterior pituitary hormones in the epithelial cells associated with Hassall's corpuscles (Batanero et al., 1992) and it is proposed that from the result in the current study, either PTH, and CGRP are also found in mammalian and monotreme Hassall's corpuscles or cross reactivity can occur between the antibodies and similar antigens, for example PRP. The epithelial cells in the thymus control the microenvironment for the production and maturation of thymocytes (Bodey and Kaiser, 1997) and it appears to be a reasonable suggestion that PRP and CGRP, two widespread hormones and paracrine secretions, contribute to the physiological microenvironment.

10.4.2. Light Microscopy - Ultimobranchial Body

The anti-calcitonin used in the current study showed poor cross species reactivity. Parafollicular cells in the possum thyroid were stained but specificity was lacking somewhat with some follicular cells also staining. No staining was present in the echidna thyroid or parathyroid and only very faint colouration could be seen in the ultimobranchial cells. Calcitonin shows considerable amino acid variations and hence cross immunoreactivity in different species (Gorbman, 1983). From the current study, assuming antigen fixation was good, the human anti-calcitonin cross reacted with possum calcitonin weakly and negligibly with echidna calcitonin.

Unlike calcitonin, CGRP has strong inter species homology (Wendelaar Bong and Pang, 1991). Anti-CGRP stained cells in the ultimobranchial body and C cells in the possum thyroid but not the thyroid or parathyroid in the echidna. In summary immunostaining was successful in confirming the identification of the ultimobranchial body that was

characterised by staining with anti-CGRP, negligibly with anti-calcitonin, and not at all with ánti-PTH. Additionally, C cells were shown to be absent from the thyroid.

10.4.3. Electron Microscopy

Limited success was achieved in the immunolabelling of PTH in the marsupial parathyroid glands. Only small granules were occasionally labelled (Plate 10.6) which is similar (on a reduced scale) to results obtained by Futrell and her co-workers (1979) but differs from the study by Inoue and Setoguti (1986) on rats, gerbils, mice and dogs where gold labelling of large and small, secretory and storage granules was achieved. Parathyroid hormone is known to have several heterogeneous forms (see chap. 2, Literature Review, section 2.3) and it is proposed that these different forms were not recognised by the anti-PTH. The larger electron dense granules that were unlabelled in the current study (Fig. 10.6c) may have represented lysosomal vesicles with PTH undergoing degradation.

Plate 10.1. Immunostaining of PTH in Human and Possum Parathyroid Gland

Fig. 10.1a. Shows the result of PTH immunostaining of human parathyroid gland that was used as a positive control. Note the variation in the amount of staining in the principal cells and the intense staining in the oxyphil cells (O).
Human paraffin section
Bar: 50µm

Fig. 10.1b. Shows PTH immunostaining of the possum parathyroid gland. Note cells vary slightly in staining intensity and the concentration of stain at the periphery of many cells. Much of the apparent nuclear staining is due to stain in the cytoplasm above and below the nucleus.
Possum P1
Bar: 10µm

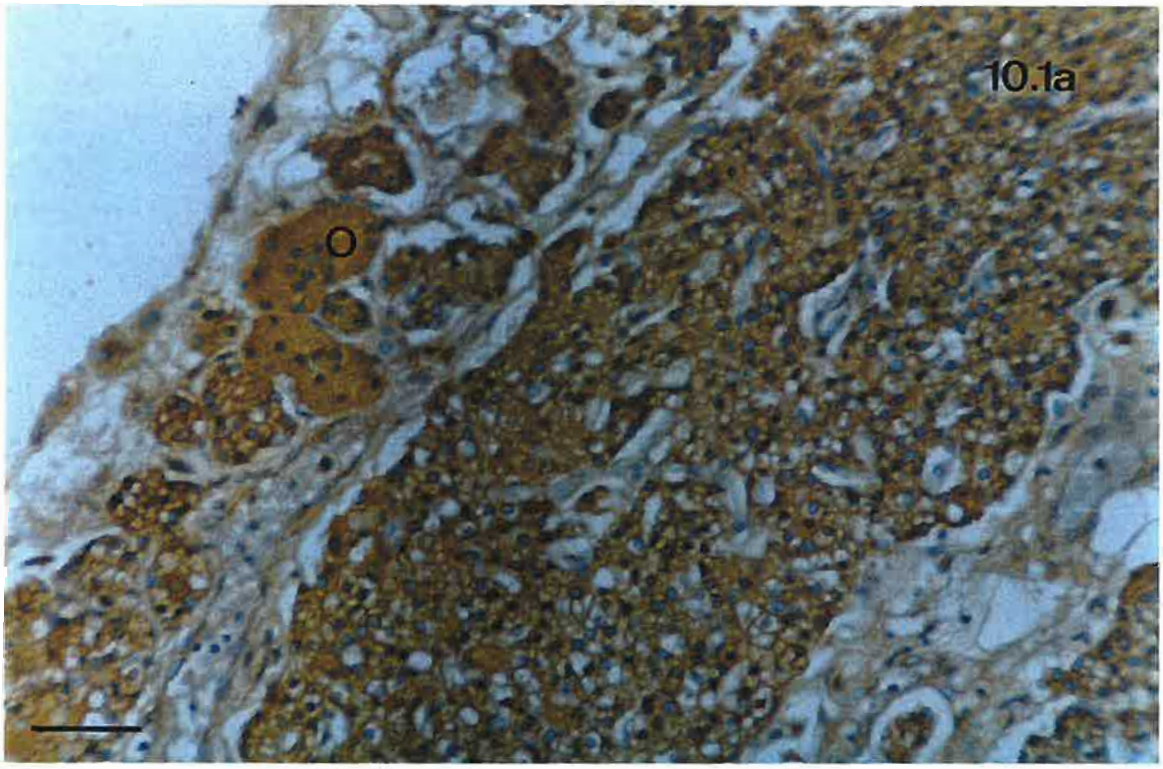
10.1a
O

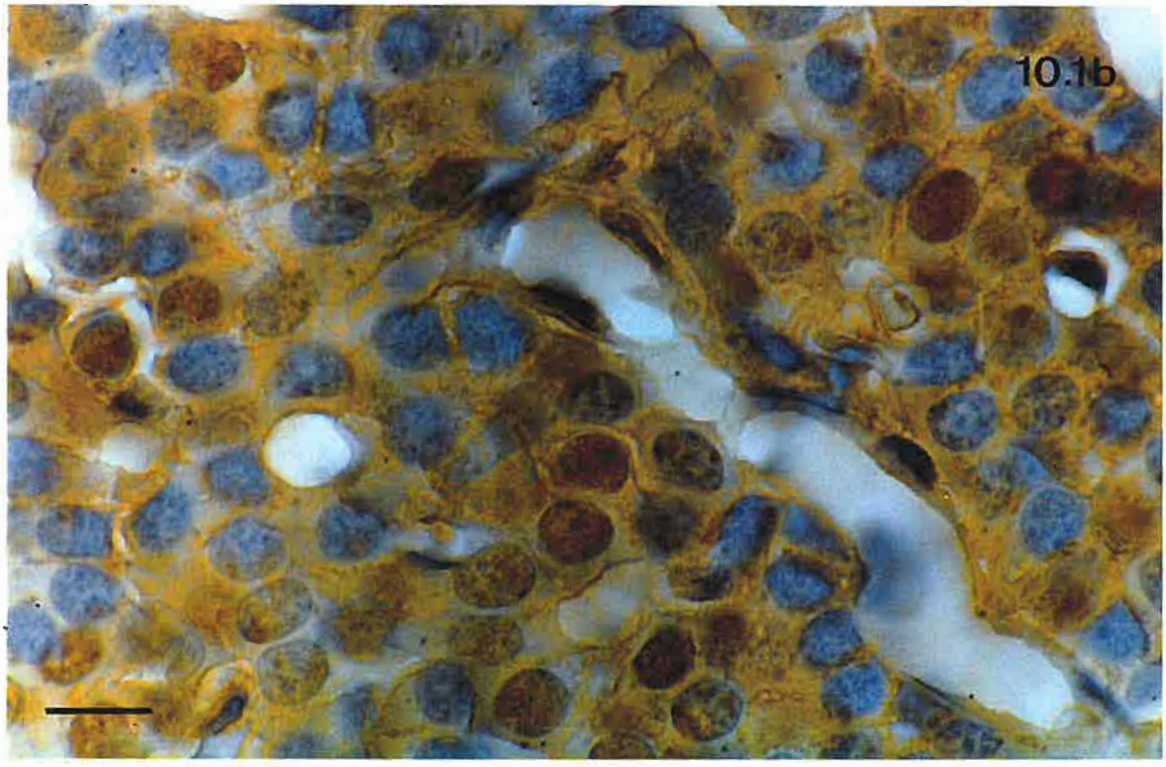
10.1b

Plate 10.2. PTH Immunostaining in Wombat and Koala Parathyroid Glands

Fig. 10.2a. Shows positive staining of PTH in most principal cells of the wombat parathyroid gland. Note that most of the follicular cells (F) and the follicular colloid in the centre of the micrograph are negative.
Wombat W12
Bar: 50µm

Fig. 10.2b. Shows variation in the staining of the principal cells in the koala and positive staining of the follicular cells; colloid (F) is negative. Note the smooth muscle cells of small arterioles (A) have also been stained.
Koala Ko6
Bar: 50µm

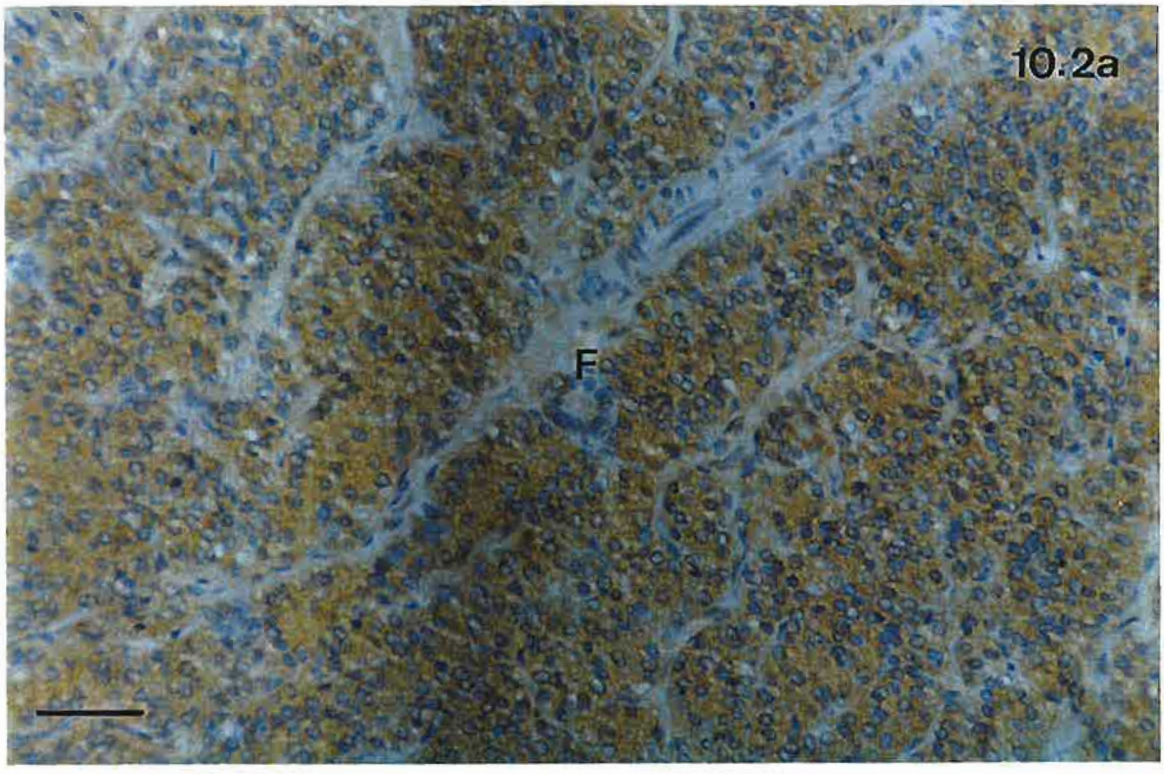
10.2a
F

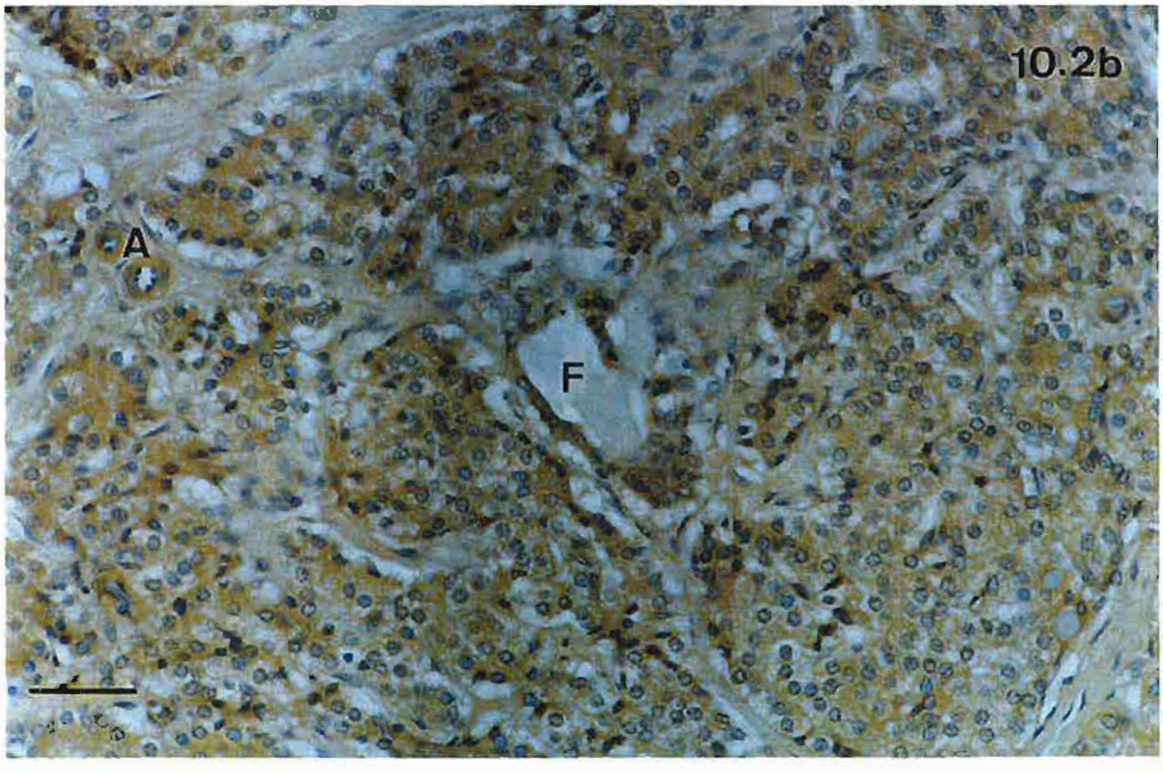
10.2b
A
F

Plate 10.3. Immunostaining of PTH in Kangaroo Parathyroid Gland

Fig. 10.3a. Low power view of kangaroo parathyroid gland. Positively stained principal cells are scattered throughout the lobules; many principal cells are negative. Note the positive staining of the mast cell (M) in the connective tissue.
Kangaroo K17
Bar: 50μm

Fig. 10.3b. Shows positive staining of parathyroid principal cells that are intermingled with thymocytes.
Kangaroo K19
Bar: 50μm

Fig. 10.3c. The high power view of principal cells adjacent to thymic tissue shows the positive staining of some cells is intensified at the periphery. Note that other principal cells are unstained.
Kangaroo K19
Bar: 10μm

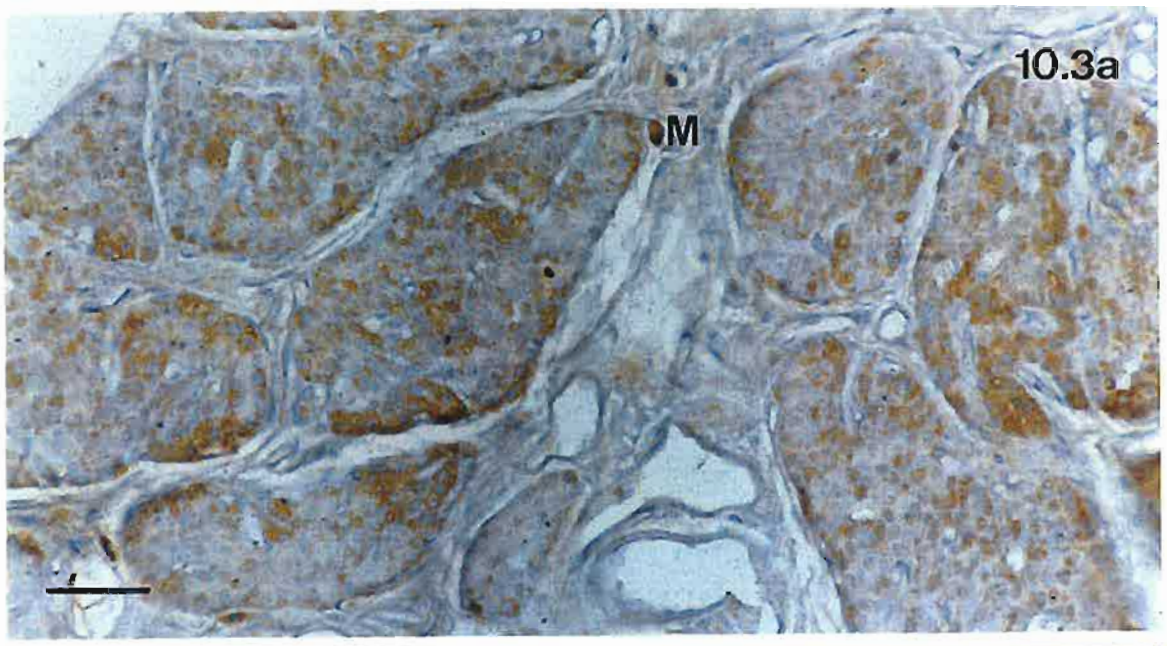
10.3a
M

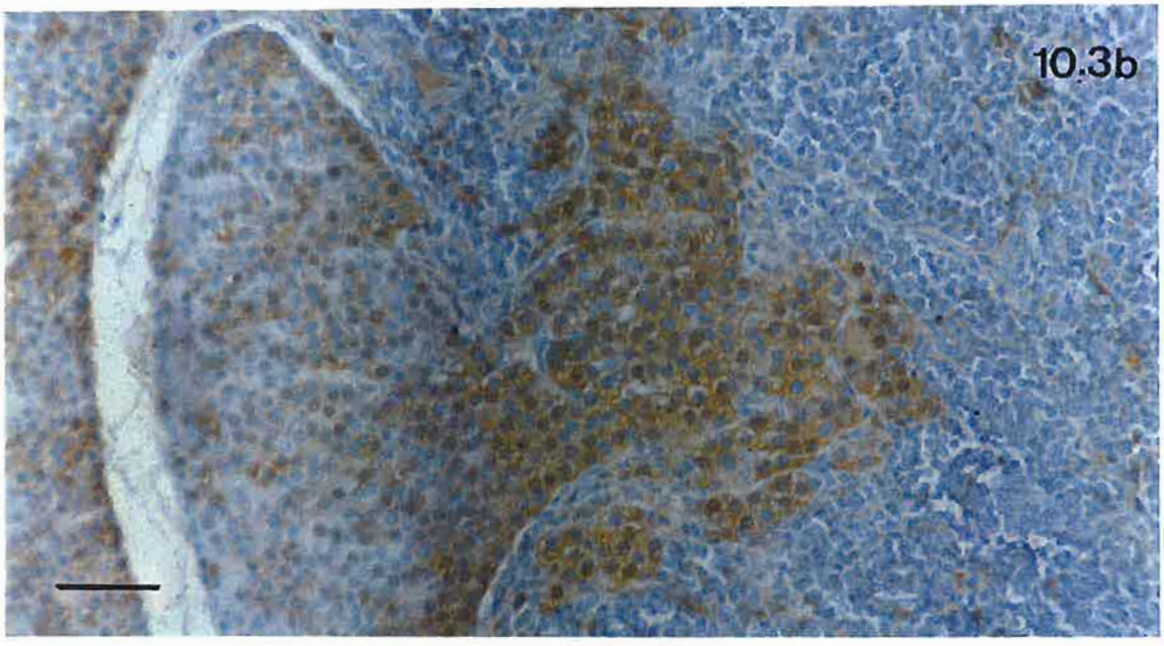
10.3b

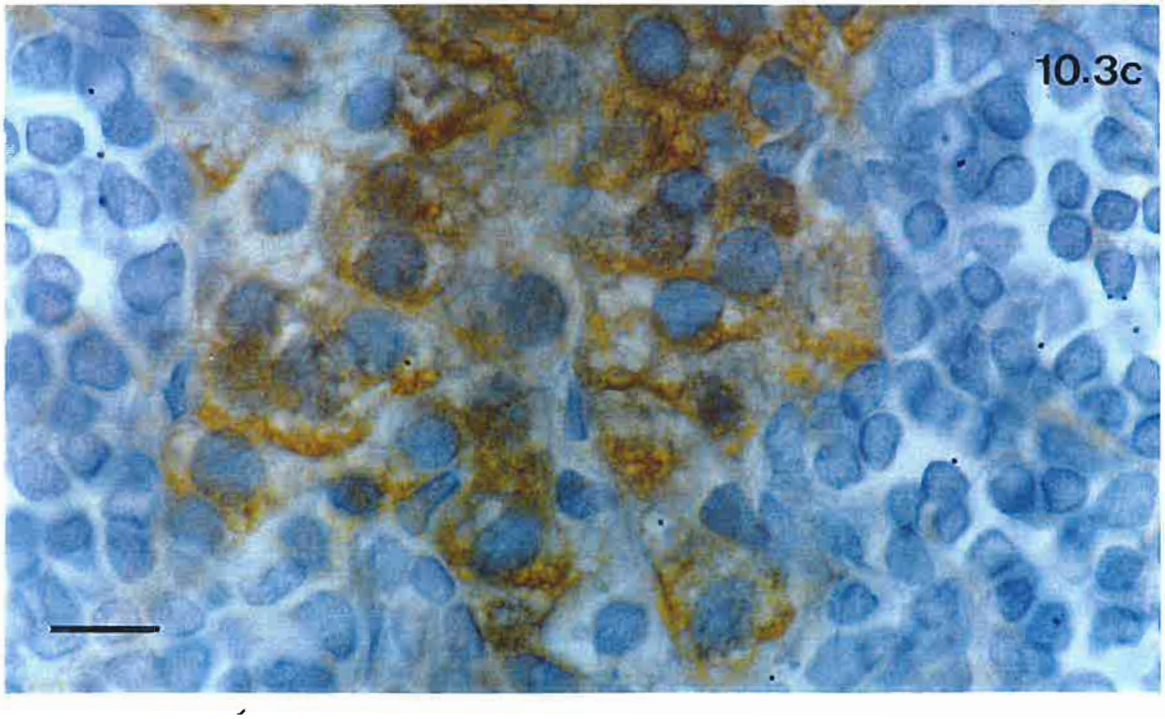
10.3c

Plate 10.4. Immunostaining of PTH in the Echidna Parathyroid Gland and Thymus

Fig. 10.4a. Shows diffuse positive reaction in the principal cells of the echidna parathyroid gland. Many cells are negative and staining is quite pale in the other cells.
Echidna E2
Bar: 20μm

Fig. 10.4b. Shows a thymic lobe stained for PTH. Some background staining is present but note the intense positive reaction in the Hassall's corpuscles.
Echidna E2
Bar: 50μm

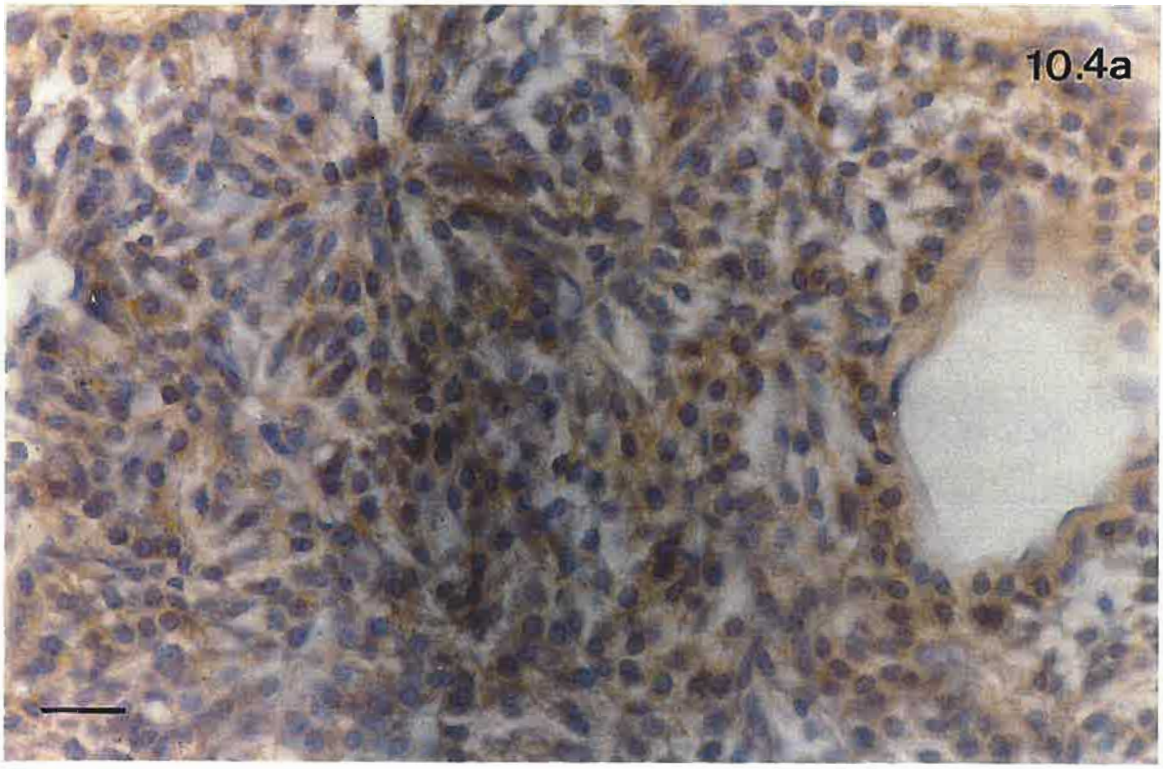
10.4a

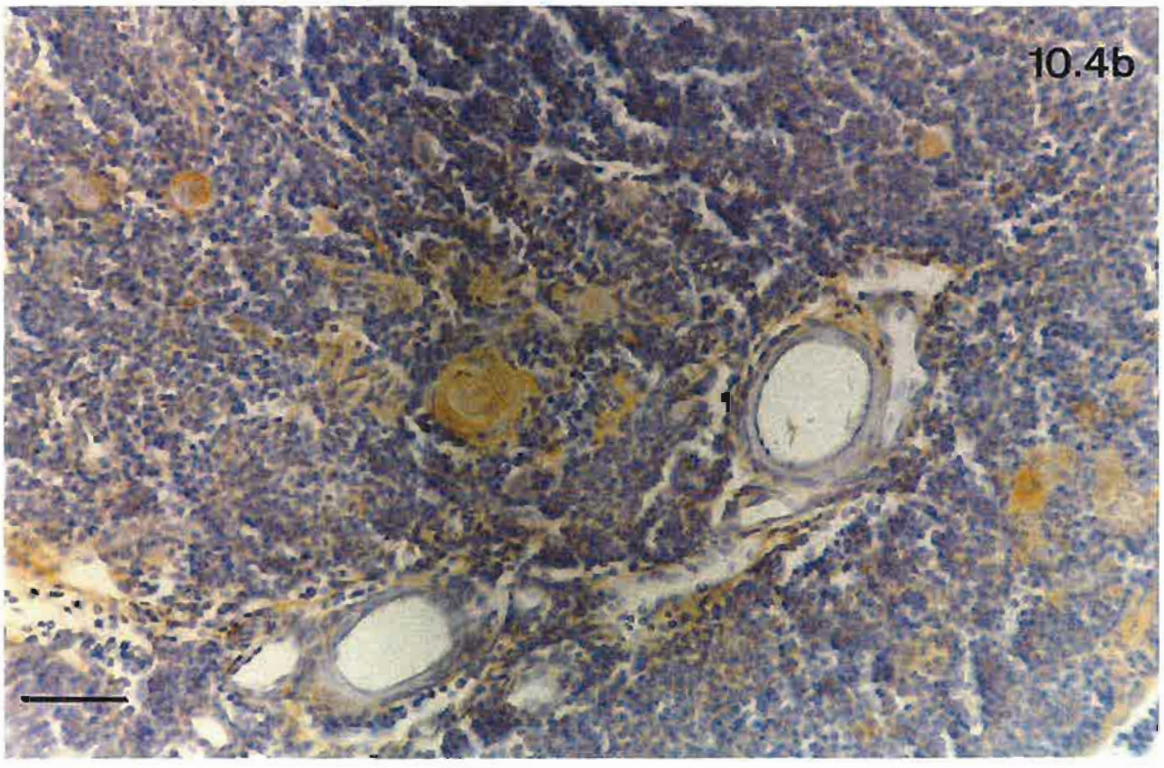
10.4b
1

Plate 10.5. Immunostaining of Calcitonin and CGRP in the Ultimobranchial Body of the Echidna

Fig. 10.5a. Shows C cells stained for calcitonin in the positive control, possum thyroid. Note some follicular cells are also positive.
Possum P1
Bar: 50µm

Fig. 10.5b. Shows very faint immunostaining (arrows) for calcitonin in some cells of the ultimobranchial body.
Echidna E6
Bar: 50µm

Fig. 10.5c. Shows positive staining for CGRP in the cells of the ultimobranchial body. Note that the amount of stain varies in the cells.
Echidna E6
Bar: 20µm

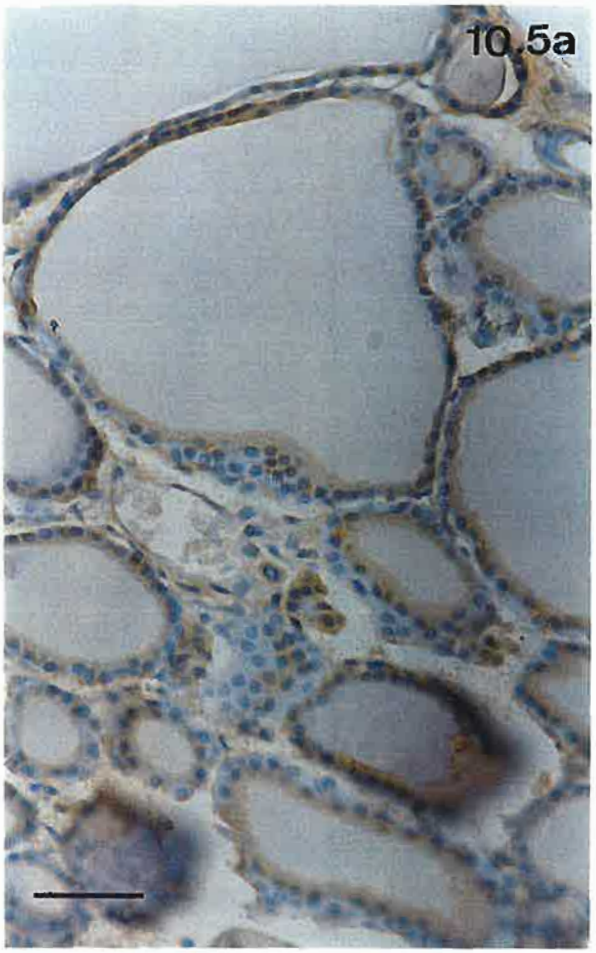
10.5a

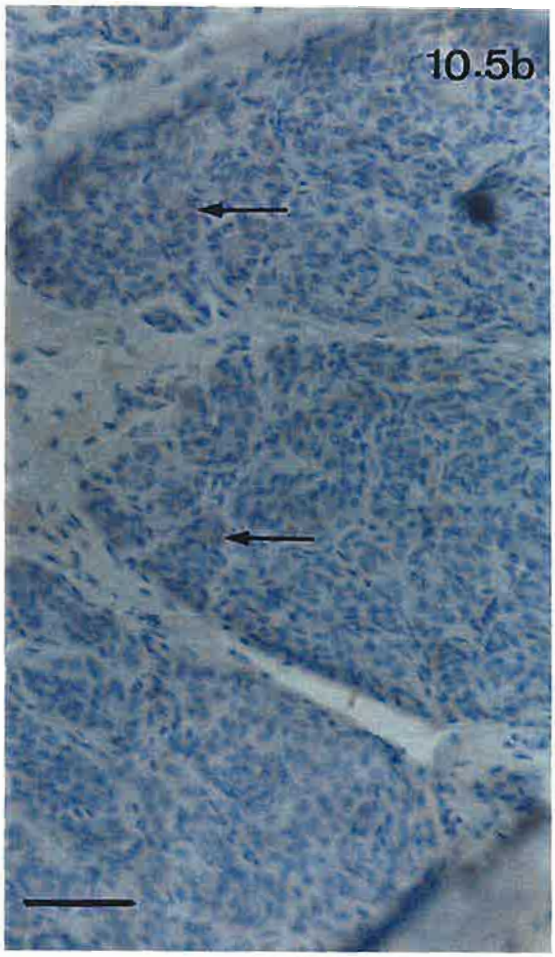
10.5b

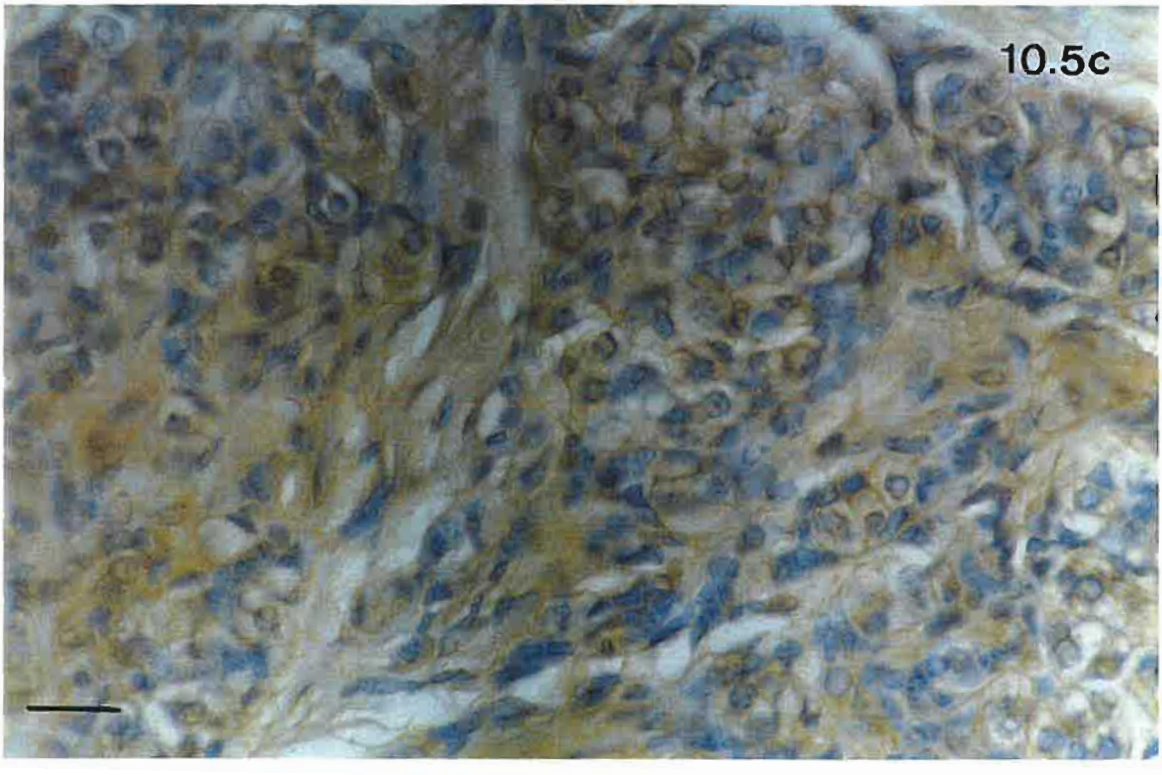
10.5c

Plate 10.6. Electron Microscopic Immunolabelling of PTH in Marsupials

Fig. 10.6a. Shows koala parathyroid gland and the immunolabelling of PTH in a small granule by Protein A-Gold technique. The mitochondrion on the lower right and the vesicular organelle (V) are not labelled.
Koala #1
Bar: 200nm

Fig. 10.6b. Shows immunolabelling by Extravidin-Gold technique in the kangaroo parathyroid. Although a protein precipitate was widespread throughout the sections (lower left) labelling was quite specific as indicated by the lack of gold particles on the mitochondrion and RER (arrow). Gold particles are clustered on a small granule.
Kangaroo K12
Bar: 200nm

Fig. 10.6c. Shows immunolabelling by Extravidin-Gold technique in the wombat parathyroid. Note small granules have been labelled and the larger electron dense granules (G) appear not to contain PTH.
Wombat W8
Bar: 250nm

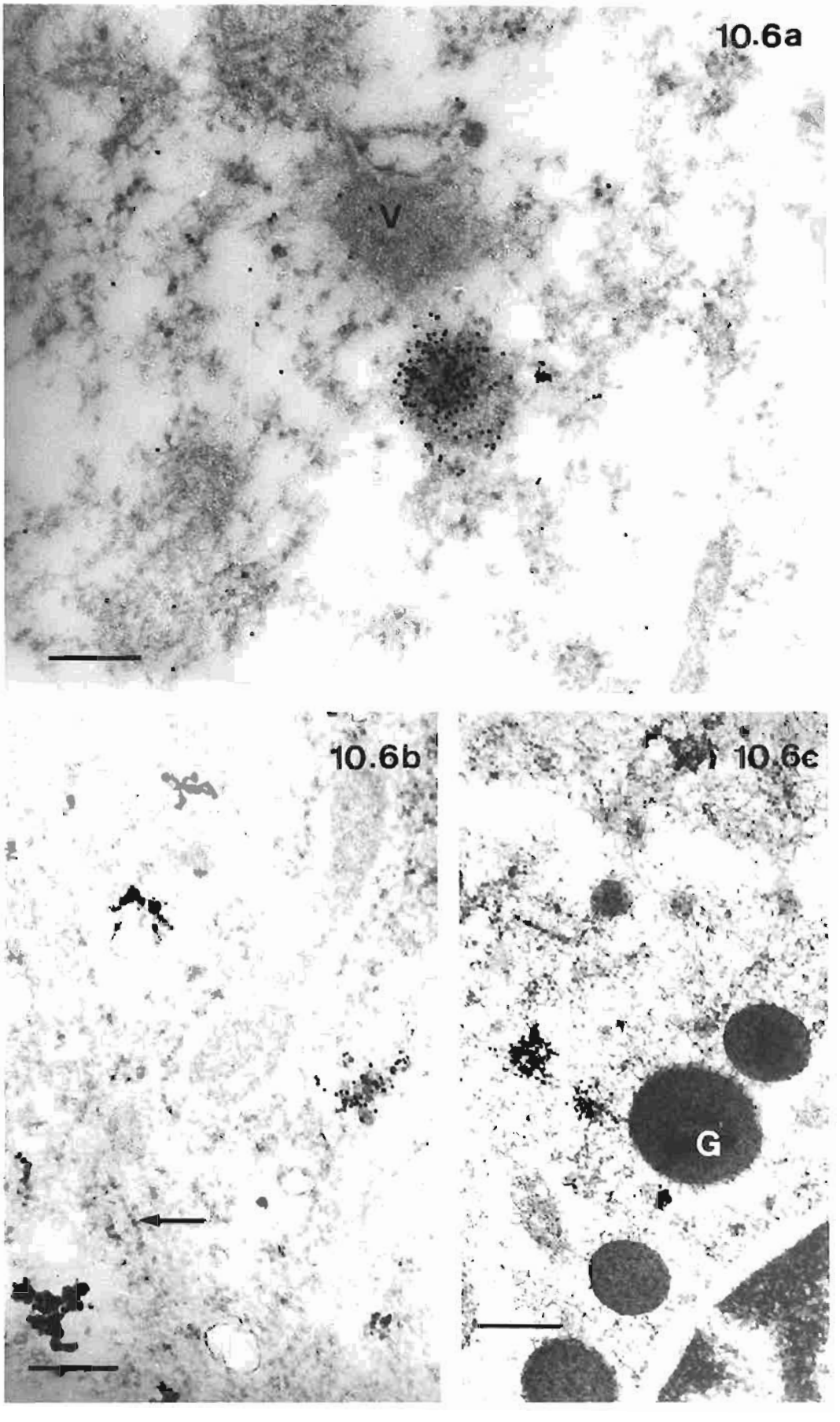
10.6a
V
10.6b
10.6c
G

Chapter 11

General Discussion

11.1. Gross Anatomy

From this study it has been concluded that Australian marsupials usually possess one pair of parathyroid glands, parathyroid III, and each gland is located bilaterally in the neck, in the vicinity of the carotid bifurcation that is dorsolateral to the larynx. The presence, number and location of the more caudally located glands, parathyroid IV, varied for the different species. In all animals examined the positive identification of parathyroid glands was only possible after histological examination because accompanying lymph nodes, small ganglia and thymic tissue often had similar features with the dissecting microscope. Serial sectioning of the ventral neck and mediastinum was necessary in order to detect parathyroid IV that was very variable in location. In kangaroos (*Macropus fuliginosus*), possums (*Trichosurus vulpecula*), wombats (*Lasiorhinus latifrons*), bandicoots (*Isoodon* spp) two glands were present; one gland was characteristic of dunnarts (*Sminthopsis crassicaudata*) and no gland was detected in the koala (*Phascolarctos cinereus*). Compared with eutherians, the variability in locations for parathyroids III and IV was the reverse for the marsupials examined. In the eutherian species which have parathyroids III and IV, the latter has a constant position usually associated with the cephalic dorsal aspects of the thyroid (Roth and Schiller, 1976; Wang, 1976) whereas the position of parathyroid III is variable. In rats and mice where only one pair of glands (parathyroid III) is found (Roth and Schiller, 1976; Wernerson et al., 1995) the glands are found in or on the thyroid. The complete lack of association of parathyroid glands with the thyroid appears to be a constant feature of the marsupial glands.

In the monotreme species, echidna (*Tachyglossus aculeatus*) and platypus (*Ornithorhynchus anatinus*), only one pair of parathyroid glands was found, in the mediastinum associated with the origins of the carotid arteries. The location of the monotreme parathyroids, the persistence of the ultimobranchial body as a separate gland in the adult, and the presence of the thyroid gland in the thorax are unique anatomical features for a mammal but typical of many reptiles (Srivastav et al., 1995). These anatomical features have not previously been listed as reptilian features

characteristic of these 'primitive' mammals (Griffiths, 1976). The morphology of the lymph nodes in monotremes was also unusual for mammals.

Each parathyroid gland in marsupials and monotremes was small, round to oval, flattened structure. In the smallest marsupials examined, *Sminthopsis crassicaudata* with an average adult weight of 15g, the approximate dimensions of the ovoid gland were 1 x 0.5 x 0.5 mm whereas in the largest marsupial, *Macropus fuliginosus* with an average adult male weight of 30 Kg, the ovoid gland was 7 x 3x 1.5 mm. There was no direct correlation between the weight of the animal and the size of the gland but the longest dimension of any gland was rarely more than 10 mm. Similar sizes of less than 10 mm have been recorded for eutherian mammals and even in elephants the diameter of the gland was estimated to be only 10 mm (Roth and Schiller, 1976). Based on the knowledge gained from the dissections of 140 marsupials and monotremes, a very general statement can be made that the average size of the parathyroid gland is similar to the diameter of the common carotid artery.

A report on the comparative anatomy of parathyroid glands in marsupials and monotremes seems incomplete without including comments on the thymus because these two organs share similar embryological origins from the third and sometimes fourth branchial pouches (Maurer, 1899; Fraser, 1915; Fraser and Hill, 1915) and often similar anatomical locations. Furthermore, in all the species examined in the current study, intermingling of thymic and parathyroid tissues was seen. The nature of the junction between the thymus and the parathyroid is discussed below in section 11.5. Diprotodont marsupials have a cervical thymus as well as a thoracic thymus except for the koala and wombat where the thoracic thymus is not always present (Yadav, 1973). Polyprotodont marsupials (Fraser, 1915; Fraser and Hill, 1915) and monotremes (Maurer, 1899) have only a thoracic thymus. In the current study the absence of a cervical thymus in the polyprotodonts *Sminthopsis* and *Antechinus* was verified and the presence of large cervical lymph nodes in all individuals noted. The large cervical lymph nodes proved to be a normal feature of the lymphoid system and contained an usually high density of mast cells (Haynes, 1991).

In the bandicoot, *I. macrourus*, the finding of two separate thymic structures in the neck of both animals examined is interesting in view of the fact that these marsupials do not have a true cervical thymus and the occurrence of the thymus in both animals makes the possibility of a developmental anomaly unlikely. The cervical thymus arises mainly from the cervical sinus with minor contributions from the second, third and maybe fourth branchial pouches (Fraser, 1915) and is located superficial to the hyoid and sternomastoid muscles in the neck. The deeper location of the thymic structures in the bandicoot suggests they have developed from the branchial pouches rather than the cervical sinus and the presence of the thymuses in both animals indicates that the thymuses are found normally in the neck as well as the thorax. Although bandicoots are classified as polyprotodonts, they also show several

diprotodont features (Dawson, 1984; Seebeck et al., 1990). The skull, teeth and serology are typical of polyprotodonts but the hind feet exhibit diprotodont characteristics. It seems that the deep cervical thymus is another feature that adds to the uniqueness of the bandicoots.

From the dissections of wombats and koalas in the current study, a cervical thymus was found in both species and a thoracic thymus was found in the wombat but not the koala. These results disagree with descriptions made by Yadav (1973) who reported a thoracic thymus in the koala but not the wombat. Some of these differences may have arisen from the different techniques used. The examination by Yadav of histological sections of specimens selected during dissection is not as thorough as the preparation of serial sections of mediastinal tissues. Small, involuted thymic lobules can easily be overlooked in the former method. In conclusion, the presence of the thoracic thymus in the koala and wombat is yet to be confirmed or denied but when the results of this current study are added to previous investigations (Symington, 1898; Johnstone, 1898; Symington, 1900; Fraser, 1915; Yadav, 1973), a thoracic thymus has been identified in only three out of twenty koalas (15%) and in five out of eighteen wombats (28%).

The role of the cervical thymus in diprotodonts is unclear. It has a similar function to the thoracic thymus in the development of immunity but the increased volume of thymic tissue formed by the cervical thymus offers no supplementary, additional functions (Yadav, 1973). In diprotodonts in spite of the larger volume of thymic tissue, lymphocyte and antibody production in the pouch young does not occur at an earlier developmental stage than in polyprotodonts, i.e. day 8 for *Didelphis*, a polyprotodont, and day 10 for *Setonix branchyurus*, a diprotodont (Yadav, 1973). Perhaps the additional epithelial reticular cells that are provided by the presence of the cervical thymus have an important role in the immunity of diprotodonts. Numerous hormones and cytokines have been identified in thymic epithelial reticular cells (Batanero et al., 1992; Bodey and Kaiser, 1997) and the suggestion is made that the cervical thymus in diprotodonts may provide a greater quantity of cellular secretions to fine-tune the immune process. In the current study the deep cervical thymus that was found in *Isoodon macrourus* may somehow also supplement the function of the thoracic thymus, providing the species with an immunological advantage that is yet to be identified.

11.2. Light Microscopy

The parathyroid glands in both marsupials and monotremes generally showed a compact arrangement of parenchymal cells and numerous capillaries that were supported by a delicate connective tissue framework. This histological appearance is shared almost universally with other vertebrates (Roth and Schiller, 1976; Srivastav, Das, et al., 1995; Srivastav et al., 1995; Wild and Setoguti, 1995). However, unlike human parathyroids (Akerström et al.,

1981; Abu-Jawdeh and Roth, 1992), in marsupials and monotremes fat cells were not a feature and intraglandular fat did not increase with age . The kangaroo parathyroid was distinctive from the others by the lobulation in the gland. Fibrous connective tissue septa appeared the same composition and thickness in young and old specimens. From previous studies of serial sections of rat parathyroid glands principal cells have been interpreted as forming a very folded, single layer of epithelial cells on a basal lamina and as a consequence of this arrangement, structural polarity was present in the cells (Krstic, 1980; Wernerson et al., 1995). Findings from the current study suggest that the degree of polarity in principal cells varies between species. The eccentric nucleus in many marsupial principal cells indicated some structural polarity, similar to the structural organisation in the rat but polarity was very accentuated in monotremes where principal cells were narrow and columnar.

An incidental finding from the study of parathyroid glands in marsupials and monotremes is the lack of brown adipose tissue in all animals examined. Brown adipose tissue in eutherians is where non-shivering thermogenesis occurs and has an important role in maintaining body temperature in the newborn and in hibernation and torpor. In eutherians brown adipose tissue is found around the major vessels in the neck and mediastinum, in the shoulder girdle and other locations (Geiser et al., 1996). However the absence of brown adipose tissue in the marsupial and monotreme species examined in the current study confirms the hypothesis put forward by Hayward and Lisson (1992) that brown adipose tissue only occurs in eutherian animals and evolved early in the radiation of the eutherian subclass (Hayward and Lisson, 1992).

11.3. Follicles and Cysts

In marsupial parathyroid glands, follicles and cysts were quite common in the different species examined in this study. Follicles and cysts were defined in chap. 2, Literature Review, section 2.5.1. The definitions were based mainly on Gilmour's descriptions (1939) and similar criteria were used in the current study to categorise a structure as a follicle or a cyst, except for the size. The luminal diameters of many follicles encountered in marsupial parathyroid glands were often 150μm, considerably greater than 40μm stated by Gilmour (1939) as the maximum diameter. Follicles and cysts, not distinguished from each other in all studies (e.g. Nilsson, 1977), are widespread in parathyroids from many species and their numbers may or may not be indicative of certain physiological or pathological states. In humans, parathyroid follicles are considered a normal histological feature (Cinti and Sbarbati, 1995) and numbers are not related to age (Cinti et al., 1983). However an increase in follicles and/or cysts has been noticed in hyperparathyroidism (DeLellis, 1993). In rats, the number of small cysts with cellular debris increased in hypercalcemic and phosphate-depleted animals (Wernerson et al., 1995) and an increase in follicles and cysts sometimes increased in reptiles during periods of hypoactivity in winter (Akbarsha, 1985). In the current study follicles and/or cysts were present in parathyroids of *S. crassicaudata*,

Isoodon spp., *L latifrons*, *P. cinereus*, and *T. vulpecula*. In wombats 12 of the 25 glands had cysts and/or follicles and in koalas follicles but not cysts were found in 10 of the 13 glands examined. Further investigations are needed to test if the high frequency of follicles and/or cysts in koalas and wombats is a structural characteristic of the species or if it is related to fluctuating calcium and phosphate levels.

In several ultrastructural investigations of the human parathyroid, the follicular lumina have been considered to be continuous with intercellular spaces and similarly staining material, characteristic of amyloid, found at both sites (Nilsson, 1977). In the current study, serial sections showed no continuity of the follicles with intercellular spaces and follicular colloid was distinctly different from intercellular material. In wombats (chap. 6) and possums (chap. 7), PAS staining demonstrated glycans in the follicular colloid but not the intercellular spaces. Immunostaining for PTH indicated the hormone was not present in the colloid (see chap. 10). Ultrastructural studies showed colloid had a fine granular texture and similar material was not present intercellularly but similarities were noted between luminal colloid content and that of some vesicles in the lining cells suggesting the colloid was a product of the cells. This suggestion is supported by similar observations that have previously been reported in humans (Cinti and Sbarbati, 1995).

Several structures identified in the current study as cysts appeared to be embryological anomalies instead of structures formed in response to altered parathyroid function. These cysts (e.g. Plate 7.7) had lining cells reminiscent of respiratory epithelium and were at the periphery of the glands. These features are similar to human parathyroid cysts formed from small tubular diverticula that arise during the embryological formations of the parathyroid and thymus from the branchial pouches (Morgan, 1936; Gilmour, 1939).

11.4. Ultrastructure and the Effects of Fixation on Ultrastructure

The ultrastructure of the parathyroid glands in marsupials and monotremes showed general similarities to that described for other vertebrates (Roth and Schiller, 1976) including humans (DeLellis, 1993), reptiles (Srivastav et al., 1995), and amphibians (Srivastav, Das, et al., 1995). These similarities included a small cellular volume compared with cells of other endocrine glands (e.g. anterior pituitary), light and dark variants of principal cells, small Golgi complex, moderate amounts of RER, and an array of granules that consisted of secretory, storage and lysosomal vesicles. Features of the marsupial and monotreme parathyroid that were not widespread in other species included the intercellular canaliculi formed by the surface irregularities of the principal cells and the presence of non-principal cells or cells not derived from principal cells.

11.4.1. Ultrastructure of Vesicles

The vesicles found in all marsupials and monotremes included small electron dense granules and granules with heterogeneous contents or halo around dense core material. Similar granules in the rat have been classified as secretory and storage granules respectively (Setoguti et al., 1995). Secretory granules contain newly formed PTH that is constantly being hydrolysed and if exocytosis does not occur then the electron dense core of each granule diminishes with a halo increasing in size. Thus secretory granules are transformed into storage granules and eventually vacuolar bodies (Setoguti et al., 1995). These structural interpretations were influenced by earlier immunocytological studies of PTH (Inoue and Setoguti, 1986). In the current study morphological evidence indicated that similar cytological activities were occurring in the secretion, storage and degradation of PTH in marsupials and monotremes. However the immunocytological staining of PTH (chap. 10) provided inconclusive evidence because at the light microscopic level immunostaining demonstrated a diffuse distribution of PTH in the cells, indicating that many granules contained PTH, but at the electron microscopic level immunolabelling was extremely light and confined to sparse, small granules; electron dense secretory granules were unlabelled. It is believed that the lack of support at the ultrastructural level was due to technical problems and that in future studies the technique could be refined and adapted to marsupials to give an intensity of labelling for PTH similar to that achieved at the light microscopic level.

The koala, kangaroo and echidna all showed numerous large membrane-bound vacuoles that suggests much degradation of PTH occurs in these cells. In the koala the presence of many lipid droplets also suggests low secretory activity; lipid inclusions are relatively abundant in the resting phase of principal cells (Roth and Capen, 1974; Nilsson, 1977; DeLellis, 1993; Cinti and Sbarbati, 1995).

11.4.2. Intercellular Canaliculi

In the species examined in the current study there was considerable variation in cellular outline and the presence of intercellular canaliculi. In the kangaroo and particularly the echidna canaliculi were present in between the tightly packed parenchymal cells. A suggestion is made that the role of the canaliculi is to convey secretions released from the surface of the cells to the capillaries. From the examination of many random sections in the kangaroo it was evident that not every site of secretion from principal cells was adjacent to a capillary and canaliculi may provide an intercellular pathway. Similar intercellular spaces have been described in the rat parathyroid gland (Wemerson et al., 1995) and serial sections have demonstrated continuity of the canaliculi. In the echidna the canaliculi were formed by unusual parallel microlamellar projections. In the koala canaliculus-like channels were seen between the lining cells of follicles and from the similarity of the colloid and vesicles in the follicular cells, a suggestion is made that the canaliculi provided the pathway for

transportation of the vesicular content into the colloid. Similar connections between intracellular vesicles and colloid have been proposed for the human (Cinti and Sbarbati, 1995) and rat (Wernerson et al., 1995) parathyroid glands.

11.4.3. 'Non-Secretory' Cells

In antechinus, wombat and echidna 'non-secretory' cells were present in amongst the principal cells and not separated from them by a basal lamina. However in each species the nature of these cells was different. In antechinus, the cells were identified as neutrophils and lymphocytes and their presence in the parathyroids was perhaps related to the chronic stress experienced by the animals. In the wombat, the cells were identified as macrophages but no reason for their presence could be offered and macrophages in parathyroids from other species have not been recorded (Nilsson, 1977; DeLellis, 1993; Cinti and Sbarbati, 1995). The 'non-secretory' cells observed in the echidna were distinctive from those in the other two species because they lacked numerous granules and short cytoplasmic processes suggesting that they did not share a haematopoietic origin. They were similar to stellate cells that have been described in the parathyroid of the iguana (Anderson and Capen, 1976). Since mingling of thymic tissue and parathyroid tissue has been noticed in all marsupial and monotreme species studied in the current investigation it was suggested that in the echidna the 'non-secretory' cells were epithelial reticular cells atypical in embryonic development and migration. Features of these cells were similar to the subgroup of undifferentiated epithelial reticular cells that are not active in the production of humoral substances in the thymus (van de Wijingaert et al., 1984: von Gaudecker et al., 1986).

11.4.4. The Effects of Fixation on Ultrastructure

In the current study, many principal cells, in addition to microvilli and microlamellar projections, had irregular cytoplasmic outlines and varied from dark to light staining. Irregular outlines of parathyroid cells have been shown to be characteristic of active secretory cells (Roth, 1979) and cells with dark staining cytoplasm have been considered to represent cells in the active phase of the secretory cycle (Roth and Raisz, 1966; Roth, 1979). However the appearance of these morphological features has been shown to be influenced by fixation and tissue processing (Wild and Setoguti, 1995). Consequently this discussion centres around distinguishing artefactual influences from actual ultrastructure in the marsupials and monotremes examined. In the first part the effect of fixation on the tortuosity of the plasmalemma is discussed and in the second part the significance of light and dark cells.

11.4.5. Fixation and Plasmalemmal Tortuosity

The plasmalemma of principal cells was very irregular in some animals examined. For example, in possums P10 and P11 (see p104) and antechinus Af1 (see p37), which were all perfused with fixative, principal cells had very irregular outlines, appearing almost

crenated with enlarged intercellular spaces. Similar morphology was also seen in possum P12 (see p104) and wombat W9 (Fig. 6.9b) that were fixed by immersion. In all these examples, this morphology was thought to be partly artefactual and maybe related to the duration of primary fixation in glutaraldehyde /paraformaldehyde electron microscopic fixative.

The irregularity of the plasmalemma is known to be influenced by the type of fixative, mode of fixation and the time between death and fixation (Wild and Setoguti, 1995). For example, in animals where the parathyroid gland on one side has been removed and immersed in fixative while the gland on the other side has been fixed by perfusion, uniformity in cell shape, integrity of the plasmalemma, and folds and interdigitations have been retained in the perfused group but varying morphologies have resulted from fixation by immersion (Wild and Setoguti, 1995). In fixation by immersion, tortuous outlines have resulted after glutaraldehyde fixation and straight outlines after osmium tetroxide (Faccini, 1970).

In the current study electron microscopy was only done on specimens fixed by perfusion or when only a few minutes had elapsed between death and fixation by immersion, thus minimising autolysis. However several specimens, (e.g. possum P12 and wombat W9), showed that fixatives did not penetrate completely into the centre resulting in crenated cells with enlarged intercellular spaces. This situation could have arisen if at the time of specimen collection the gland was excised with adhering layers of fatty tissue that impeded the infiltration of the fixative into the tissue. However lack of penetration by the primary fixative does not explain the morphology seen in some perfused specimens, (e.g. possums P10, P11, and antechinus Af1), where cellular shrinkage and enlarged intercellular spaces were apparent. A possible suggestion for this result comes from the study done by Wild and Setoguti (1995) where it was noticed that morphology was altered during osmium tetroxide post-fixation and even during dehydration. In the current investigations the only variable factor in the fixation and tissue processing protocols was the duration of primary fixation and hence the interval between death and post-fixation with osmium tetroxide. It is consequently proposed that in a minority of specimens in the current study the membranes were not stabilised by the primary fixatives that resulted in fluid moving between the intracellular and intercellular compartments and cellular shrinkage. Alternatively, the fixative solutions inadvertently contained incorrect concentrations and the resultant hypertonic solutions caused cellular shrinkage.

11.4.6. Light and Dark Cells

Descriptions of the ultrastructure of the parathyroid glands, whether they are from humans (DeLellis, 1993), vertebrates generally (Roth and Schiller, 1976), mammals (Wild and Setoguti, 1995), reptiles (Srivastav et al., 1995) or amphibians (Srivastav, Das et al.,

1995) invariably include mention of light , dark, and intermediate variants of the principal cells. In the current study variation in the staining density of the principal cells was also noticed in most marsupial and monotreme species except bandicoots (*Isoodon* spp), koalas and echidnas. Previous studies have linked light and dark cells with the inactive and active phases respectively of the secretory cycle (Roth and Raisz, 1966; Roth, 1979). However the presence of light cells has been shown in several experiments to be partly artefactual and related to the mode of fixation. In perfused specimens, parenchymal cells tend to show similar cytoplasmic densities with the distinction between light and dark cells obscure (Clark and Khairallah, 1972; Setoguti, 1977; Larsson et al., 1985; Wild and Setoguti, 1995).

From the current study the following three topics are discussed:-

1. The influence of the mode of fixation on the ultrastructure of glands from dunnarts, possums and kangaroos and the comparison of these results with other mammals.
2. The validity of the results in other marsupial and monotreme species - i.e. Was the ultrastructure a true representation of the morphology or was it altered by the mode of fixation?
3. Ultrastructural evidence that associates light and dark cells with inactive and active phases of the secretory cycle.

For dunnarts, possums, and kangaroos two groups of animals could be identified in each species where environmental conditions at the time of death and the subsequent processing of specimens were similar for the two groups with the only known difference being the mode of fixation. For dunnarts and kangaroos the mode of fixation appeared not to influence the proportions of light and dark cells but for possums all cells had similar cytoplasmic density after fixation by perfusion with variants only noticeable in specimens fixed by immersion. The results that were obtained for the possum support similar findings in studies on mice, rats, rabbits, cats, dogs, pigs, cattle, sheep , goats, and horses (Wild and Setoguti, 1995) where light cell formation was initiated during immersion fixation and eliminated by perfusion fixation. However the results for dunnarts and kangaroos indicate that light cells are inherent features of the parathyroid gland and not manifested by immersion fixation. Time lapse between death and immersion in fixative and the concentration of calcium ions in the fixative have shown to affect parathyroid cells (Wild and Setoguti, 1995) but since the interval between death and fixation, and the composition of the fixative were similar for all animal groups, a conclusion is reached that light cells are part of the normal ultrastructure of the parathyroids from dunnarts and kangaroos but not possum.

In the current study light cells were not present in bandicoots (*Isoodon* spp), koalas and echidnas. Glands from the first two species were immersed in fixative while the echidnas were perfused. Since fixation protocol and processing were standardised for all specimens in the study an assumption can be made that if light cells were absent after immersion

fixation they are absent from the actual ultrastructure. In the echidna no light cells were seen in the perfused specimens which condition reflects the normal ultrastructure.

In summary, in studies on eutherians, light cells have only been present in parathyroid glands fixed by immersion and their presence is instigated by a prolonged interval between death and fixation and by varying calcium ion concentrations in the buffered fixing solutions (Wild and Setoguti, 1995). In dunnarts and kangaroos, the persistence of light cells in the parathyroids after fixation by perfusion indicates their presence is an inherent feature and not artefactual; similarly the absence of differing cell densities in glands of koalas and bandicoots demonstrates light cells are not part of the normal parathyroid ultrastructure.

Although morphometric analyses on the ultrastructure of light and dark cells were not done in the current investigation, observations of many principal cells were made that enabled generalised compositions of the two cell variants to be compiled and compared with previous studies. In dunnarts (chap. 4) and kangaroos (chap. 8), the two marsupials which showed light and dark variants of principal cells in specimens fixed by either immersion or perfusion, the matrix of dark cells had a denser arrangement to its fine particles compared with light cells. The only other cytoplasmic differences were in dunnarts where dark cells had less glycogen and more RER compared with light cells. Plasmalemmal irregularities, the array of secretory and other vesicles, and the amount of nuclear heterochromatin appeared the same in light and dark cells. These morphological differences, or rather, similarities between light and dark cells do not correlate well with the classical descriptions of principal cells in the various phases of the secretory cycle (Shannon and Roth, 1974). In this secretory cycle inactive light cells have few plasmalemmal irregularities, abundant glycogen, lipid, lysosomes and lipofuscin, small Golgi complex and free ribosomes. As the cell starts PTH production the dark variant of the principal cell is formed. Glycogen, lipid, lysosomes decrease, stacks of RER form, and vesicles accumulate near the enlarging Golgi apparatus. Cellular outline becomes irregular and cellular volume decreases.

In the current study the lack of changes in vesicular numbers in light and dark cells supports a study by MacGregor and his co-workers (1975) who noted that the number of vesicles was not indicative of secretory activity. It is concluded that the appearance of light and dark cells in dunnarts and kangaroos may be related to changes in the volume of the cell where at certain times expansion of the cell results in dispersal of the cytoplasmic contents and reduced density of the cytoplasmic matrix. Little correlation appears to exist between the classification of light and dark cells and the secretory activity of the cell. The changes in cellular volume could not be detected by casual observation.

11.5. Parathyroid and Thymus Junction.

Epithelial reticular cells of the thymus and principal cells of parathyroid III are derived from the lining of the same third branchial pouch. Therefore it seems logical that a basal lamina may be absent between two similar epithelial structures of the same embryological origin but it would arise between epithelial and underlying mesenchyme tissues. Previous descriptions of parathyroid-thymus junctions have always shown that connective tissue separates the aberrant gland and thymus (Kendall, 1988). In humans, the gland is clearly encapsulated (Kurtay and Crile, 1969; Thompson et al., 1982) and in the rat, parathyroid tissue occurs in the interlobar connective tissue of the thymus (Kendall, 1988). These descriptions contrast to the present study where sometimes only epithelial reticular cells separated parathyroid and thymic tissues.

11.6. Future Studies

Future studies on the marsupial and monotreme parathyroid glands will, like the current study, be limited by the availability of animals. In several species, for example, platypus, bandicoot, antechinus, and Tasmanian devil, more animals need to be examined so that descriptions representative of the species overall and not an individual animal can be compiled. Immunocytochemical studies at the electron microscopic level should be expanded whereby the distribution of PTH, parathyroid secretory protein (chromogranin A), and acid phosphatase can be determined to identify the nature of follicular colloid, and the types of granules (e.g. secretory, storage, lysosomal). If available, more wombat parathyroid specimens should be examined to investigate the frequency of oxyphil cells in these animals.

Assuming animals are available, future studies should investigate the relationship between parathyroid morphology and levels of calcium and PTH in the blood. The structure of the parathyroid gland in several species in the current study indicate that variations between individuals are present and future studies might attempt to correlate structural changes with physiological changes as well as attempting to identify the causes driving the changes. For example, the current study suggested that in possums there is a link between chronic stress and parathyroid morphology. In future studies physiological data could be linked to morphological data to test if renal insufficiencies occur in possums suffering chronic stress and if this alters parathyroid ultrastructure. Similarly the effects of chronic stress on the parathyroid in the antechinus could be studied.

Summary

Parathyroid Glands in Marsupials and Monotremes

The gross anatomy and microscopic morphology of the parathyroid glands were studied in 140 animals from ten species of marsupials from Dasyuridae, Peramelidae, Phalangeridae, Macropodidae, Vombatidae and Phascolarctidae and in the monotreme species, *Tachyglossus aculeatus* (echidna) and *Ornithorhynchus anatinus* (platypus).

Investigations were done on animals which had been killed either as part of other scientific research unrelated to parathyroid studies, or as part of culling programs. The gross anatomy of the parathyroids was described either from dissections of whole animals or from large pieces of tissue removed from the ventral neck and mediastinum or from the examination of serial sections of the same regions. Histological studies used routine paraffin and resin sections for light microscopy and routine transmission electron microscopic techniques for descriptions of the ultrastructure. Some paraffin sections were stained with PAS, alcian blue or Altmann's stain to demonstrate glycans and mitochondria respectively. Specimens were used for electron microscopy only if less than twenty minutes had lapsed between death and fixation. Fixation was done by either perfusion or immersion and the influence of the mode of fixation on ultrastructure was investigated in several species. Where possible, specimens for immunocytochemistry were collected for the identification of parathyroid hormone in tissue sections of the parathyroid glands at the light and electron microscopic levels.

In marsupials one parathyroid gland was found in the vicinity of each carotid bifurcation dorso-lateral to the larynx. Another pair of parathyroid glands were found in the mediastinum of most species; no gland was found associated with the thyroid. Monotremes had one pair of glands located adjacent to the origins of the carotid arteries in the mediastinum. Glands were encapsulated and parenchymal cells were arranged in strands and clumps separated by capillaries and supported by minimal connective tissue except in the kangaroo, *Macropus fuliginosus*, where principal cells were clustered into lobules separated by quite wide septa. The histology of parathyroid III, the more cephalic of the glands, was similar to that of parathyroid IV with the kangaroo again forming an exception. Follicles and cysts were observed in parathyroids of fat-tailed dunnart (*Sminthopsis crassicaudata*), bandicoots (*Isoodon* spp.), hairy-nosed wombat (*Lasiorhinus latifrons*), koala (*Phascolarctos cinereus*), and brush-tail possum (*Trichosurus vulpecula*). Light and dark variants of principal cells were seen in most marsupial but not monotreme species; variations were sometimes related to the mode of fixation by perfusion or immersion. Generally the principal cells showed similar features. The nucleus was euchromatic and in the cytoplasm RER was sparse, Golgi complex small, and various granules were present,

ranging from small electron dense granules to larger vesicles with heterogeneous contents. Principal cells in the echidna, *Tachyglossus aculeatus*, showed partial polarity with the nucleus in an eccentric location and grouping of organelles and inclusions. Between the cells were canaliculi bordered by microlamellar projections. Lipid inclusions were common in the principal cells of the koala. Oxyphil cells were identified in glands of the wombat, and water-clear cells in parathyroids of *T. vulpecula* and *T aculeatus*. The presence of water-clear cells in some possums was thought to be a result of stress that resulted from their captivity. The relationship between chronic stress and the ultrastructure of the parathyroid glands was investigated in *Antechinus* spp. in which chronic stress of males in the post-mating period is well documented. Apart from an increase in intraglandular leukocytes no apparent histological differences, including the presence of water-clear cells and oxyphil cells, were noticed. The effect of age on parathyroid morphology was studied in *M. fuliginosus*. The age of the kangaroos was estimated by the pattern of molar eruption and the number of mitochondria per $10\mu m^2$ of parenchymal cell cytoplasm analysed for young adult male and very old (more than ten years) male kangaroos. No increase in the number of mitochondria was detected in the old group.

In some parathyroid glands from all species examined except antechinus, Tasmanian devil, bandicoot, and koala, thymic tissue was present. There appeared to be mingling of the two tissue types and electron microscopy showed that epithelial reticular cells formed the only barrier between thymic and parathyroid tissues. It was concluded that the thymic tissue and the parathyroid were derived from the endodermal lining of the same branchial pouch and abnormal cleavage and migration of the anlagen resulted in the mingling of the tissues.

In determining the anatomy of the parathyroid glands it was natural to note the locations of thymuses. The presence of only a thoracic thymus was confirmed in dasyurid marsupials whereas thoracic as well as cervical thymuses were found in possums and kangaroos. In bandicoots a thoracic and a deep cervical thymus were present. The latter has not previously been documented and is another unique anatomical characteristic of bandicoots which have a mixture of polyprotodont and diprotodont structural features with the skull and teeth being typical of polyprotodonts but hind feet typical of diprotodonts. In the current project a cervical thymus was found in both the koala and wombat; a thoracic thymus was found in the koala and not the wombat. This finding was contrary to previous studies that have described the reverse situation for the presence of a thoracic thymus in these two marsupials.

The anatomy of the parathyroid, thyroid and ultimobranchial bodies in the echidna was more akin to reptiles than mammals. Monotremes appear to be the only mammals that have a thyroid and one pair of parathyroid glands in the mediastinum of the thoracic cavity, no parathyroids in the neck, and separate ultimobranchial bodies near the commencement of the trachea. The similarities of these anatomical features to those of reptiles have not previously

been included in lists of reptilian characteristics in monotremes. The unusual morphology of the lymph nodes in monotremes was confirmed with slight modifications made to earlier descriptions.

An immunocytochemical study of the marsupial and monotreme parathyroid glands showed the diffuse distribution of parathyroid hormone in the principal cells at the light microscopic level. At the electron microscopic level parathyroid hormone was found confined to small granules. It was not detected in the colloid of follicles or cysts or extracellularly.

The identification of the ultimobranchial body in the echidna was confirmed with immunostaining. A weak positive result for calcitonin, a stronger result for calcitonin gene-related peptide and negative result for PTH were found in the cells of the ultimobranchial body; thyroid and parathyroid cells were negative but mast cells were positive for calcitonin gene-related peptide.

Appendix A

Routine processing, Sectioning, and Staining of Paraffin Embedded Tissue

After fixation, small pieces of tissue are placed in the carriers of the automatic tissue processor and processed for either - (a) eight or - (b) sixteen hours depending on the size of the tissue.

Solution	Time (a)	Time (b)
70% alcohol	30 mins	45 mins
80% alcohol	45 mins	30 mins
95% alcohol (x2)	45 mins ea.	45 mins ea.
absolute alcohol (x3)	30, 45, 45 mins	45 mins ea.
safsolvent (x3)	30 mins ea.	60 mins ea.
molten paraffin wax I	30 mins	90 mins
molten paraffin wax II	75 mins	390 mins

Tissue is blocked and 7μm sections cut on a rotary microtome.
Sections are floated out onto water and placed onto aluminised glass slides and dried at 40°C.

Routine Staining of Paraffin Sections

1. Safsolvent - 5 mins.
2. Safesolvent - 5 mins.
3. Absolute alcohol - 2 mins.
4. Absolute alcohol - 2 mins.
5. 70% alcohol - 2 mins.
6. 30% alcohol - 2mins
7. Water - 2mins.
8. Harris's haematoxylin - 4 mins.
9. Wash in water, differentiate in weak acid and blue in weak ammonia (0.5%).
10. Wash in water, stain with eosin - 2mins.
11. Absolute alcohol - 3 x 3 mins.
12. Safsolvent - 2 x 4 mins.
13. Mount in PIX.

Appendix B

1. Rinse Solution for Perfusion

9.0g NaCl
25g polyvinylpyrrolidone (PVP 40)
0.25g heparin
5g procaine-HCl

Preparation

Dissolve in distilled water to obtain a final volume of 1 litre; adjust to pH 7.4 with IN NaOH.

2. Electron Microscopic Fixative (Modified from Forssmann et al., 1977).

(3% formaldehyde/ 3% glutaraldehyde in 0.1M phosphate buffer pH 7.4)

45ml	0.2M NaH_2PO_4
405ml	0.2M Na_2HPO_4
120ml	25% paraformaldehyde
120ml	25% glutaraldehyde
25g	polyvinylpyrrolidone (PVP 40)

Preparation

Adjust pH to 7.4 with 1N NaOH and add distilled water to obtain a final volume of 1 litre.
25% paraformaldehyde is freshly prepared from paraformaldehyde powder in the following manner :-

a. Heat 100mls of distilled water to 60°C.
b. Add 25g of paraformaldehyde and 12 drops of 1N NaOH.
c. Stir until solution clears and then filter.

Electron microscopic fixatives used for immunocytochemical studies contained 10mls instead of 120mls of 25% glutaraldehyde which gave a final concentration of 0.25%.

Appendix C1

Processing for Routine Transmission Electron Microscopy

1. After fixation, the pots containing the specimens are placed on a rotator for the duration of processing.
2. Wash in 0.2M phosphate buffer (pH 7.4); 3 x 15 mins.
3. Post-fix in 1% osmium tetroxide in 0.1M phosphate buffer for 60 mins.
4. Wash in 0.2M phosphate buffer for 15 mins.
5. Dehydrate for 20 mins in each of the following alcoholic solutions :-
   30%, 50%, 70%, 75%, 80%, 85%, 90%, 95%, absolute alcohol.
6. Complete dehydration with 3 x 30 min. changes in anhydrous absolute alcohol.
7. Transfer to propylene oxide for 2 x 30 mins changes.
8. Infiltrate with:- propylene oxide: TAAB resin 2:1 - overnight.
   propylene oxide: TAAB resin 1:2 - 8 hours.
   pure TAAB resin - overnight
9. Embed in fresh TAAB resin and polymerise at 60°C for 24 hours.

Appendix C2

Processing for Electron Microscopic Immunostaining

1. After fixation, the pots containing the specimens are placed on a rotator for the duration of processing.
2. Wash in distilled water; 2 x 15 mins.
3. Dehydrate for 20 mins in each of the following alcoholic solutions :-
   30%, 50%, 70%, 75%, 80%, 85%, 90%, 95%, absolute alcohol.
4. Complete dehydration with 3 x 30 min. changes in anhydrous absolute alcohol.
5. Infiltrate with:- abs. alcohol: LR White resin 1:1 - overnight.
   fresh pure LR White resin - 8 hours.
   fresh pure LR White resin - overnight
6. Embed in fresh LR White resin and polymerise at 60°C for 24 hours.

Appendix D

En bloc Staining with Uranyl Acetate

1. After post-fixation with osmium tetroxide, wash in 0.2M phosphate buffer for 15 mins.
2. Wash in maleate buffer pH 5.2 - 2 x 15 mins.
3. Stain with 1% uranyl acetate in maleate buffer pH 6.0 at 4°C in the dark for 1 to 2 hours.
4. Wash in maleate buffer pH 5.2 - 15 mins.
5. Proceed with dehydration - Step 5, Appendix C.

Maleate Buffer

Stock Solutions

A 0.2M maleic acid
Dissolve 5.8g maleic acid in distilled water, add 50mls 1N NaOH and distilled water to 250mls.

B 1N NaOH

Working Solutions

Adjust 25mls of stock solution A with stock solution B to pH 5.2 or pH 6.0 and add distilled water to 50mls.

Appendix E

Toluidine Blue Staining of 1μm Resin Sections

Resin sections are transferred with a fine glass rod from the water bath of the glass knife onto a drop of 0.025% toluidine blue (C.I. 52040) in 0.05% sodium tetraborate on a glass microscope slide. Slides are placed on a hot-plate at 65°C and the stain is evaporated.

Appendix F

Staining Sections for Electron Microscopy

Sections are stained first with uranyl acetate and then with lead citrate.

Uranyl Acetate Staining

1. Make small 'boats' out of 1.5cm^2 pieces of dental wax and place in a petri dish containing a small amount of 70% alcohol.
2. Millipore a few drops of uranyl acetate into each boat and float inverted grids on the uranyl acetate.
3. Place lid on petri dish and leave in a dark covered container for 25 minutes.
4. Dip grids into 70% alcohol about 20 times, then repeat with distilled water.
5. Finally wash grids gently in distilled water.
6. Dry grids with pieces of filter paper.

Stain Preparation

1. Place uranyl acetate powder up to the 0.5ml mark in a disposable centrifuge tube and fill to 10ml with 70% alcohol.
2. Leave on a rotator for 45 minutes.
3. Centrifuge for 15 minutes and use immediately.

Lead Citrate Staining

Method

1. Centrifuge lead stain for 15 minutes.
2. To one of the chambers of a divided petri dish add 10 - 20 pellets of NaOH.
3. Pipette a few drops of stain into the other chamber and float inverted grids on the drops.
4. Add a pipette full of water onto the pellets and place a lid on the petri dish.
5. Stain for 12 minutes.
6. Dip grids 20 times into two changes of distilled water and then wash grids gently in a third change of distilled water.
7. Dry grids with pieces of filter paper.

Stain Preparation

1. Mix 1.33g lead nitrate with 1.76g sodium citrate in 30ml distilled water in a 50cc volumetric flask. Shake thoroughly for one minute and intermittently for 30 minutes to ensure complete conversion of lead nitrate to lead citrate.
2. Add 8ml N NaOH and dilute the suspension to 50mls with distilled water. Mix by inversion. Centrifuge solution before use.

Appendix G

Altmann's Technique for Mitochondria (Bancroft and Stevens, 1982).

1. Remove wax and bring sections to water.
2. Flood sections with aniline-acid fuchsin solution.
3. Gently heat the slide until steam rises and leave for 5 mins.
4. Rinse in tap water.
5. Differentiate in first picric acid differentiator until excess red stain is removed.
6. Continue differentiation in the second picric acid differentiator and control microscopically until stain is removed from tissue components other than mitochondria.
7. Dehydrate rapidly in two changes of absolute alcohol.
8. Clear in xylene (or substitute) and mount in PIX.

Solutions

Aniline acid fuchsin.

Prepare a saturated solution of acid fuchsin (approximately 15%) in 5% aniline in distilled water. Filter before use.

First Differentiator	
saturated alcoholic picric acid	10 ml
30% alcohol	40 ml
Second Differentiator	
saturated alcoholic picric acid	5 ml
30% alcohol	40 ml

Appendix H

Periodic Acid, Schiff's (PAS) Method (modified from Cook, 1982).

1. Remove wax and bring sections to water.
2. Oxidize in 1% periodic acid for 10 mins.
3. Wash in running water for 10 mins.
4. Immerse in Schiff's reagent for 10 mins.
5. Wash in running water for 10 mins.
6. Counterstain with Harris's haematoxylin for 10 secs.
7. Wash in tap water, blue in dilute ammonia (0.25%) solution for 5 secs.
8. Wash in water, dehydrate, clear and mount in PIX.

Solutions

Schiff's Reagent

1. Dissolve 1g pararosanilin in 200ml of boiling distilled water which is removed from the heating source just before the addition of the dye.
2. Allow the solution to cool to 52°C and add 200ml of 0.15N HCl.
3. Allow the solution to cool further to 25°C and add 1g potassium metabisulphite.
4. Stir, then cover and leave the solution in a dark place for 24 hours.
5. Add 2g of activated charcoal; shake and filter the colourless solution which is then ready for use.

Appendix I

Toluidine Blue Method

1. Remove wax and bring sections to water.
2. Cover each slide with toluidine blue solution for 10 seconds.
3. Drain off excess stain; blot dry on filter paper.
4. When completely dry, clear sections and mount in PIX.

Staining Solution

Toluidine blue	0.25g
Sodium Acetate	1.943g
Sodium barbiturate (veronal)	2.943g
Distilled water	100ml

Appendix J

Alcian Blue pH2.5 and Alcian Blue pH1.0 Techniques
(modified from Bancroft and Stevens, 1982).

Alcian Blue pH2.5

1. Bring sections to water.
2. Stain in alcian blue pH2.5 solution for 30 mins.
3. Rinse in distilled water, wash in running water for 5 mins.
4. Counterstain in 0.1% nuclear fast red in 5% aluminium sulphate for 10 mins.
5. Rinse in distilled water.
6. Dehydrate, clear and mount in PIX.

Alcian Blue pH1.0

1. Bring sections to water.
2. Stain in alcian blue pH1.0 solution for 30 mins.
3. Rinse briefly in 0.1N hydrochloric acid; blot dry.
4. Stain in 0.1% nuclear fast red in 5% aluminium sulphate for 10 mins.
5. Rinse in distilled water.
6. Dehydrate, clear and mount in PIX.

Staining Solutions

Alcian Blue pH2.5

Alcian blue	0.5g
Glacial acetic acid	3ml

Distilled water to make solution 100ml.

Alcian Blue pH1.0

Alcian blue	1.0g
Hydrochloric acid	100ml of 0.1N HCl

Appendix K1

Immunostaining of Paraffin Sections

The immunostaining uses commercially prepared kits (Immunon, Biogenex, ZYMED Laboratories) that contain reagents and antibodies prediluted, buffered and ready to use.

1. Bring sections to water.
2. Wash in 0.1M phosphate buffered saline (PBS), pH 7.6, for 5 mins.
3. Incubate with freshly prepared 3% hydrogen peroxide for 30 mins.
4. Wash in PBS for 5 mins.
5. Incubate with protein blocking agent (Immunon) for 30 mins.

6*. Incubate with prediluted human anti-parathyroid hormone (Biogenex) further diluted 1:40 with 1% ovalbumin in PBS and 10% wallaby serum overnight at 4°C.

7. Rinse in PBS.
8. Incubate with biotinylated universal secondary antibody (Immunon) for 120 mins.
9. Rinse in PBS.
10. Incubate with streptavidin peroxidase reagent (Immunon) for 90 mins.
11. Wash in buffer.
12. Incubate in buffered 3,3'diaminobenzidine and hydrogen peroxide solution (ZYMED Laboratories) for approximately 5 mins. Check chromagen development with a microscope.
13. Rinse in water.
14. Counterstain with haematoxylin.
16. Dehydrate and mount sections in PIX.

6* For immunostaining of calcitonin and CGRP, the appropriate antibody was prediluted in PBS and sections were incubated overnight at 4°C.

Reagents

Protein blocking agent, biotinylated universal secondary antibody and streptavidin peroxidase reagent were all part of an immunostaining kit supplied by Immunon, Pittsburgh, USA.

Human anti-parathyroid hormone supplied by Biogenex, lot #PUO 410596.

Human anti-calcitonin and anti-CGRP were in prediluted aliquots kindly donated by the Histopathology Department, Institute of Medical and Veterinary Science, Adelaide.

The buffer, 3,3'diaminobenzidine, and hydrogen peroxide solutions were all part of a substrate kit supplied by ZYMED Laboratories, San Francisco, USA.

Appendix K2

Protein A-Gold Immunostaining for Electron Microscopy

1. Silver-gold resin sections are mounted onto nickel grids coated with formvar (6% formvar in chloroform).
2. Place each grid on 1% ovalbumin in 0.1M PBS, pH 7.6, for 15 -20 minutes.
3 Blot off excess fluid on filter paper.
4. Place each grid on a drop (15 - 20 µl) of diluted primary antibody and leave overnight at 4°C. Human anti-parathyroid hormone, prediluted and supplied by Biogenex was further diluted 1:40 with PBS pH 7.6, 1% ovalbumin and 10% wallaby serum.
5. Rinse, 6 x 5 minutes, in PBS.
6. Blot off excess fluid on filter paper.
7. Place each grid on a 20 µl drop of prediluted Protein A - Gold complex, further diluted 1:20 for 90 minutes.
8. Rinse, 6 x 5 minutes, in PBS.
9. Rinse four times in double distilled water.
10. Stain with uranyl acetate for 4 minutes.
11. Rinse well in 70% alcohol and then 4 lots of double distilled water.

Avidin-Gold Immunostaining for Electron Microscopy

Steps 1 - 6 are the same as steps 1 - 6 in Protein A-Gold immunostaining.

7. Place each grid on a drop of biotinylated universal secondary antibody (Immunon) for 120 minutes.
8. Rinse, 4 x 5 minutes in PBS.
9. Blot off excess fluid on filter paper
10. Place each grid on a 20µl drop of prediluted Avidin-Gold complex (Extavidin-Gold), further diluted 1:20 for 90 minutes.
11. Rinse, 6 x 5 minutes, in PBS.
12. Rinse four times in double distilled water.
13. Stain with uranyl acetate for 4 minutes.
14. Rinse well in 70% alcohol and then 4 lots of double distilled water.

Reagents

Human anti-parathyroid hormone supplied by Biogenex, lot # PUO 410596.

Protein A-Gold supplied by Amersham. Product name is AuroProbe™EM protein A G10.

Biotinylated universal secondary antibody supplied by Immunon.

Avidin-Gold complex supplied by Sigma. Reagent is actually a modified avidin - ExtrAvidin™-Gold 10nm gold conjugate.

Appendix L

Age Determination of Western Grey Kangaroos

Group 1 - Juvenile to Young Adult Males (1yr, 8mth to 3yrs)

kangaroo	weight (Kg)	dentition
K9	23	one incisor, two deciduous premolars, 1st fully erupted, 2nd molar partially erupted
K14	14.25	one incisor, two deciduous premolars, 1st fully erupted, 2nd molar partially erupted
K22	12	one incisor, two deciduous premolars, 1st molar
K27	15.5	one incisor, two deciduous premolars, 1st molar
K32	23	one incisor, two deciduous premolars, 1st fully erupted, 2nd molar partially erupted

Group 2 - Mature Adult Males (4 to 9 yrs)

kangaroo	weight (Kg)	dentition
K1	35	one incisor, one permanent premolar, three molars
K8	28	one incisor, one deciduous premolar, 1st molar fully erupted, 2nd molar partially erupted
K31	28	one incisor, one deciduous premolar, two molars
K33	25	one incisor, one permanent premolar, two molars

Group 3 - Old Adult Males (more than 10 yrs)

kangaroo	weight (Kg)	dentition
K2*	> 50	not available
K7	> 50	one incisor, no deciduous or permanent premolars, 1st molar shed, 2nd, 3rd and 4th molars present
K13	> 50	one incisor, no deciduous or permanent premolars; 3 molars, 4th molar half erupted
K26	> 50	one incisor, no deciduous or permanent premolars; 1st molar shed, 2nd, 3rd and 4th molars present
K30	> 50	one incisor, no deciduous or permanent premolars; 1st molar shed, 2nd, 3rd and 4th molars present
K35	> 50	one incisor, no deciduous or permanent premolars; four molars present

K2* From the size and weight of the kangaroo, it was estimated to be more than ten years old.

Group 4 - Juvenile to Young Adult Females (1yr, 8mth to 3yrs)

kangaroo	weight (Kg)	dentition
K15 + PY*	20	one incisor, no premolars (unerupted perm. premolar within jaw), two molars
K17	17	one incisor, two deciduous premolars, two molars
K23	14.5	one incisor, two deciduous premolars, 1st molar fully erupted, 2nd molar partially erupted

* PY - pouch young

Group 5 - Mature Adult Females (4 to 6 yrs)

kangaroo	weight (Kg)	dentition
K19	22	one incisor, one permanent premolar, 1st and 2nd molars fully erupted, 3rd molar partially erupted
K20 +PY(7cm)		one incisor, one permanent premolar, 1st and 2nd molars fully erupted, 3rd molar partially erupted
K21+PY (0.58Kg)	22	one incisor, one deciduous premolar, two molars
K24+PY (0.75Kg)	25.5	one incisor, one deciduous premolar, 1st molar fully erupted, 2nd molar partially erupted.
K29 (lactating)	23	one incisor, one permanent premolar, 1st and 2nd molars fully erupted, 3rd molar partially erupted

Group 6 - Old Adult Females (more than 7 yrs)

kangaroo	weight (Kg)	dentition
K6	32	not available
K16 +PY		one incisor, no deciduous or permanent premolars, 1st molar shed, 2nd, 3rd and 4th molars present
K18 +PY	29	one incisor, no deciduous or permanent premolars, four molars present
K25+PY (0.4Kg)	27	one incisor, no deciduous or permanent premolars; 1st molar shed, 2nd, 3rd and 4th molars present
K28+PY (2.3Kg)	33	one incisor, no deciduous or permanent premolars, four molars present
K34+PY (1.2Kg)	30	one incisor, no deciduous or permanent premolars; 1st molar shed, 2nd, 3rd and 4th molars present

Bibliography

Abu-Jawdeh, G.M. and S.I. Roth, (1992) Parathyroid glands. In: 'Histology for Pathologists'. SS Sternberg, ed. Raven Press, New York, pp 311 - 320.

Adams, W.E. (1955) The carotid sinus complex, "Parathyroid" III and thymo-parathyroid bodies, with special reference to the Australian opossum *Trichosurus vulpecula*. Am J Anat 97: 1 - 58.

Akbarsha, M.A. (1985) Seasonal morpho- and histometric changes in parathyroids of the lizard, *Calotes versicolor* (Daudin). Z Mikrosk Anat Forsch 99: 929 - 936.

Akerstrom, G., L. Grimelius, H Johansson, H Lundqvist, H. Pertoft, and R. Bergstrom. (1981) The parenchymal cell mass in normal human parathyroid glands. Acta Pathol Microbiol Scand A 89: 367 - 375.

Alberts, B., D. Bray, J. Lewis, M. Raff, K. Roberts and J.D. Watson. (1994) In 'Molecular biology of the cell, 3rd ed.' Garlang Publishing, New York.

Ali, S.S. (1980) Immunofluorescent staining experiments in parathyroid glands. Acta Histochem 67: 28 - 31.

Anderson, M.P. and C.C. Capen. (1976) Ultrastructural evaluation of parathyroid and ultimobranchial glands in iguanas with experimental nutritional osteodystrophy. Gen Comp Endocrinol 30: 209 - 222.

Arps, H., M. Dietel, B. Lauritzen, J.J. Elting, A. Niendorf, D.V. Cohn. (1987) Co-localization of parathyroid hormone and secretory protein-I in bovine parathyroid glands: a double immunocytochemical study at the electron microscopical level. Bone Mineral 2: 175 - 183.

Aurbach, G.D. and L.R. Chase. (1976) Cyclic nucleotides and biochemical actions of parathyroid hormone and calcitonin. In: 'Handbook of Physiology; section 7: Endocrinology', vol. 7 Parathyroid gland. chap. 15. American Physiological Society, Washington, D.C., pp 353 - 381.

Baber, E. (1881) Researches on the minute structure of the thyroid gland. Philos Trans 172: 577 - 608.

Balogh, K. and R.B. Cohen. (1961) Oxidative enzymes in the epithelial cells of normal and pathological human parathyroid glands. Lab Invest 10: 354 - 360.

Bancroft, J.D. and A. Stevens. (1982) Cytoplasmic granules, organelles and special tissue. In: 'Theory and Practice of Histological Techniques'. J.D. Bancroft and A. Stevens, ed. Churchill Livingstone, Edinburgh, chap. 18, pp 364 - 378.

Barbour, R.A. (1963) Musculature and limb plexuses of *Trichosurus vulpecula*. Aust J Zool 11: 488 - 610.

Barker, I.K., I. Beveridge, A.J. Bradley and A.K. Lee. (1978) Observations on spontaneous stress-related mortality among males of the dasyurid marsupial *Antechinus stuartii* (Macleay). Aust J Zool 26: 435 - 444.

Batanero, E., F.E. de Leeuw, G.H. Jansen, D.F. van Wichen, J. Huber and H.J. Schuurman. (1992) The neural and neuro-endocrine component of the human thymus. II. Hormone immunoreactivity. Brain Behav Immun 6: 249 - 264.

Bennett, J.H., W.G. Breed, D.L. Hayman, and R.H. Hope. (1990) Reproductive and genetical studies with a laboratory colony of the dasyurid marsupial *Sminthopsis crassicaudata*. Aust J Zool 37: 207 - 222.

Bergdahl, L. and L. Boquist. (1973) Parathyroid morphology in normal dogs. Path Europ 8: 95 - 103.

Bertoni, G., T. Torresani, E.M. Schraner, and P. Wild. (1988) Unimpaired membrane dynamics in parathyroid cells in insulin delicient rats. Virchows Arch B Cell Pathol 55: 31 - 37.

Blind, E., H. Schmidt-Gayk, S. Scharla, D. Flentje, S. Fischer, U. Gohring and W. Hitzler (1988) Two-site assay of intact parathyroid hormone in the investigation of primary hyperparathyroidism and other disorders of calcium metabolism compared with a mid-region assay. J Clin Endocrinol Metab 67: 353 - 360.

Blum, J.W., G.P. Meyer, and J.T. Potts Jr. (1974) Parathyroid hormone response during spontaneous hypocalcemia and induced hypercalcemia in cows. Endocrinology 95: 84 - 92.

Bodey, B. and H.E. Kaiser. (1997) Development of Hassall's bodies of the thymus in humans and other vertebrates (especially mammals) under physiological and pathological conditions: immunocytochemical, electronmicroscopic and *in vitro* observations. In Vivo 11: 61 - 85.

Boquist, L. (1980) On the relationship between annulate lamellae and mitochondria in human parathyroid adenomas. Z Mikrosk Anat Forsch 94: 241 - 249.

Bradley, A.J., I.R. McDonald, and A.K. Lee. (1980) Stress and mortality in a small marsupial (*Antechinus stuartii* Macleay). Gen Comp Endocrinol 40: 188 - 200.

Breed, W.G. and C.M. Leigh. (1988) Morphological observations on sperm-egg interactions during in vivo fertilization in the dasyurid marsupial *Sminthopsis crassicaudata*. Gamete Res 19: 131 - 149.

Broadus, A.E., M. Mangin, K. Ikeda, K. Insogna, E.C. Weir, W.J. Burtis, and A.F. Stewart. (1988) Humoral hypercalcemia of cancer. Identification of a novel parathyroid hormone-like peptide. N Engl J Med 319: 556 -563.

Calaby, J.H. (1968) Observations on the teeth of marsupials, especially kangaroos. Dental Mag and Oral Topics 85: 26 - 27.

Capen, C.C., A. Koestner, and C.R. Cole. (1965) The ultrastructure and histochemistry of normal parathyroid glands of pregnant and non pregnant cows. Lab Invest 14: 1673 - 1690.

Cheal, P.D., A.K. Lee, and J.L. Barnett. (1976) Changes in the haematology of *Antechinus stuartii* (Marsupialia), and their association with male mortality. Aust J Zool 24: 299 - 311.

Christie, A.C. (1967) The parathyroid oxyphil cells. J Clin Pathol 20: 561 - 602.

Cinti, S., G. Balercia, M.C. Zingaretti, S. Amati and F. Osculati. (1983) The normal parathyroid gland. J Submicrosc Cytol 15: 661 -679.

Cinti, S. and A. Sbarbati. (1995) Ultrastructure of human parathyroid cells in health and disease. Microsc Res Tech 32: 164 - 179.

Clark, N.B. and L.H. Khairallah. (1972) Ultrastructure of the parathyroid gland of fresh-water turtles. J Morphol 138: 131 - 140.

Cohn, D.V. and J. Elting. (1983) Biosynthesis, processing and secretion of parathormone and secretory protein-I. Recent Prog Horm Res 39: 181 - 209.

Cohn, D.V. and R.R. MacGregor. (1981) The biosynthesis, intracellular processing, and secretion of parathormone. Endocr Rev 2: 1 - 26.

Cohn, D.V., R. Zangerle, R. Fischer-Cobrie, L.L.H. Chu, J.J. Elting, J.W. Hamilton, and H. Winkler. (1982) Similarity of secretory protein I from parathyroid gland to chromogranin A from adrenal medulla. Proc Natl Acad Sci USA 79: 6056 - 6059.

Collip, J.B. (1925) Extraction of a parathyroid hormone which will prevent or control parathyroid tetany and which regulates the level of blood calcium. J Biol Chem 63: 395 - 438.

Collyear, K., S.I. Girgis, G. Saunders, I. MacIntyre and G. Holt. (1991) Predicted structure of the bovine calcitonin gene-related peptide and the carboxy-terminal flanking peptide of calcitonin precursor. J Mol Endocrinol 6: 147 - 152.

Cook, H.C. (1982) Carbohydrates. In: 'Theory and practice of histological techniques'. Bancroft and A. Stevens, ed. Churchill Livingstone, Edinburgh, chap. 11, pp 180 - 216.

Cooper, D., A. Schermer, and T.T. Sun. (1985) Classification of human epithelia and their neoplasm using monoclonal antibodies to keratins: Strategies, applications, and limitations. Lab Invest 52: 243 - 256.

Cormack, D.H. (1987) In: 'Ham's Histology', 9th ed. Lippincott Co., Philadelphia

Dawson, T.J. (1983) In: 'Monotremes and Marsupials: the Other Mammals.' Studies in Biology no 150. Camelot Press, Southhampton.

de Campos Soares, J., A.L. Ferreira and I. Vugman. (1987) Some characteristics of the mast cells of atrioventricular valves and pericardium of South American opossum (*Didelphis azurae*). Zool Jb Anat 116: 361 - 365.

de Menezes, Y. and A. Sesso. (1988) Annulate lamellae as a precursor or a product of paired cisternae in human adenomatous parathyroid cells. Acta Anat 131: 3 - 8.

DeGroot, L.J. (1979) Endocrinology, vol 2. DeGroot, ed. Grune and Stratton, New York.

DeLellis, R.A. (1993) Tumours of the parathyroid Gland, Third Series, Fascicl 6. Atlas of Tumour Pathology. Armed Forces Institute of Pathology, Washington, DC., pp 1 - 102.

Diener, E. and E.H.M. Ealey. (1965) Immune system in a monotreme. Nature 208: 950 - 953.

Dufour, D.R. and S.Y. Wilkerson. (1982) The normal parathyroid revisited: percentage of stromal fat. Hum Pathol 13: 717 - 721.

Emly, J.F., J. Gregory, S.J. Bowden, A. Ahmed, M.J. Whittle, D.I. Rushton and Ratcliffe, W.A. (1994) Immunohistochemical localization of parathyroid hormone-related protein (PTHrP) in human term placenta and membranes. Placenta 15: 653 -660.

Emura, S., S. Shoumura, M. Utsumi, T. Yamahira, H. Chen, M. Arakawa, H. and Isono. (1990) Ultrastructure of a water-clear cell in the golden hamster parathyroid gland. J Electron Microsc 39: 172 - 177.

Emura, S., S. Shoumura, M. Utsumi, T. Yamahira, H. Chen, M. Arakawa, H. and Isono. (1991) Origin of the water-clear cell in the parathryoid gland of the golden hamster. Acta Anat 140: 357 - 361.

Faccini, J.M. (1970) The ultrastructure of parathyroid glands removed from patients with primary hyperparathyroidism: a report of 40 cases, including four carcinomata. J Path 102: 189 - 199.

Faccini, J.M., and A.D. Care. (1965) The effect of fluoride on the ultrastructure of the parathyroid glands of sheep. Nature 207: 1399 - 1401.

Fairney, A. (1983) Parathyroid hormone. In 'Hormones in blood'. 3rd ed., vol. 5. C.H. Gray and V.H.T. James, ed. Academic Press, London, pp 1 - 9.

Fasciotto, B.H., S.U. Gorr, A.M. Bourdeau, and D.V. Cohn. (1990) Autocrine regulation of parathyroid secretion: inhibition of secretion by chromogranin A (secretory protein I) and potentiation of secretion by chromogranin A and pancreastatin antibodies. Endocrinology 127: 1329 - 1335.

Feldman, P.S., E. Horvath and K. Kovacs. (1972). Ultrastructure of three Hürthle cell tumours of the thyroid. Cancer 30: 1279 - 1289.

Forssman, W.G., S. Ho, E. Weihe, A. Aoki, M. Dym and D.W. Fawcett. (1977) An improved perfusion fixation method for the testis. Anat Rec 188: 307 - 314.

Forsyth, D. (1908) The comparative anatomy, gross and minute, of the thyroid and parathyroid glands in mammals and birds. J Anat 42: 141-169; 302 - 319.

Fraser, E. (1915) The development of the thymus, epithelial bodies, and thyroid in the Marsupialia II *Phascolarctos*, *Phascolyms* and *Perameles*. Philos Trans R Soc Lond, Series B, 207: 87 - 112.

Fraser, E., and J. Hill (1915) The development of the thymus, epithelial bodies, and thyroid in the Marsupialia I. *Trichosurus vulpecula*. Philos Trans R Soc Lond, Series B, 207: 1 - 85.

Frigerio, B., C. Capella, E. Wilander, L. Grimelius. (1982) Argyrophil reaction in parathyroid glands: a light and electron microscopic study. Acta Pathol Microbiol Immunol Scand A 90: 323 - 326.

Futrell, J.M., S.I. Roth, S.P.C. Su, J.F. Habener, G.V. Segre, J.T. Potts Jr. (1979) Immunocytochemical localization of parathyroid hormone in bovine parathyroid glands and human parathyroid adenomas. Am J Pathol 94: 615 - 619.

Geiser, F., A.J. Hulbert and S.C. Nicol. (1996) Adaptations to the cold. Tenth International Hibernation Symposium. Geiser, A.J. Hulbert and S.C. Nicol, ed. University of New England Press, Armidale, Australia.

Gilmour, J.R. (1937) The embryology of the parathyroid glands, thymus and associated rudiments. J Pathol Bacteriol 45: 507 - 522.

Gilmour, J.R. (1939) The normal histology of the parathyroid glands. J Pathol Bacteriol 48: 187 - 222.

Godwin, M.C. (1937) Development of parathyroids in the dog with emphasis upon origin of accessory glands. Anat Record 68: 305 - 325.

Gorbman, A., W.H. Dickhoff, S.R. Vigna, N.B. Clark, and C.L. Ralph. (1983) The thyroid gland. In 'Comparative Endocrinology', chap 6. A. Gorbman, W.H. Dickhoff, S.R. Vigna, N.B. Clark, and C.L. Ralph, ed. John Wiley and Sons, New York, pp 185 - 276.

Grant, T.R. (1992) The historical and current distribution of the platypus, *Ornithorhynchus anatinus*, in Australia. In 'Platypus and echidnas'. M.L. Augee, ed. The Royal Zoological Society of NSW, Sydney, pp 232 - 254.

Green, W.Q. (1984) A review of the ecological studies relavant to management of the common brushtail possum. In 'Possums and Gliders', chap 49. A.P. Smith and I.D. Hume, ed. Australian Mammal Society, Sydney, pp 483 - 499.

Griffiths, M. (1968) 'Echidnas', Pergamon Press, London.

Griffiths, M. (1978) 'The biology of monotremes', Academic Press, London.

Habener, J.F. (1979) Parathyroid hormone synthesis. In 'Endocrinology, vol 2'. chap 43. L.J. De Groot, ed. Grune and Stratton, New York, pp. 599 - 605.

Hackenbrock, C.R. (1968) Ultrastructural bases for metabolically linked mechanical activity in mitochondria. II. Electron transport-linked ultrastructural transformations in mitochondria. J Cell Biol 37: 345 - 369.

Hammer, J.A. (1908) Glandula parathyreoideae (Sandstromi) En historisk ofverblick Hygiea (Festband) 42: 1 - 24. (Translated by C.M. Seipel. Bull Hist Med 6: 179 - 222, 1938.)

Hansson, C.G., S. Mathewson, and K. Norrby. (1971) Parathyroid cell growth and proliferation in nephrectomised rats. Pathol Eur 6: 313 - 321.

Hargis, G.K., V.J. Gakulis, G.A. Williams and A.A. White. (1964) Cytological detection of parathyroid hormone by immunofluorescence. Proc Soc Exptl Biol Med 117: 836 - 839.

Harper, H.A., V.W. Rodwell and P.A. Mayes. (1979) Review of Physiological Chemistry, 17th ed. Lange Medical Publications, Los Altos, California.

Hasleton, P.S. and H.H. Ali. (1980) The parathyroid in chronic renal failure - a light and electron microscopical study. J Pathol 132: 307 - 323.

Haynes, J.I. (1991) Cervical lymph nodes and mast cells in the marsupial *Sminthopsis crassicaudata*. Anat Rec 231: 7 - 13.

Haynes, J.I. (1995) Parathyroid morphology of the brush-tail possum, *Trichosurus vulpecula*. Anat Rec 241: 401 - 410.

Hayward, J.S. and P.A. Lisson. (1992) Evolution of brown fat: its absence in marsupials and monotremes. Can J Zool 70: 171 - 179.

Imura, H. (1994) Morphology of adenohypophyseal cells and pituitary adenomas. In: 'The Pituitary Gland' 2nd ed. Raven Press, New York, pp 29 - 62.

Inoue, Y. and T. Setoguti. (1986) Immunocytochemical localization of parathormone in mammalian parathyroid gland using the protein A-gold technique. Cell Tissue Res 243: 3 - 7.

Irving, J.T. (1973) Calcium and Phosphorus Metabolism, Academic Press, London.

Johnson, C.N. (1983) Variations in group size and composition in red and western grey kangaroos, *Macropus rufus* and *Macropus fuliginosus*. Aust Wildl Res 10: 25 - 32.

Johnstone, J. (1898) The thymus in the marsupials. J Linn Soc (Zool) 26: 537 - 557.

Juhlin, C., J. Rastad, L. Klareskog, L. Gremelius, and G. Akerstrom. (1989) Parathyroid histology and cytology with monoclonal antibodies recognizing a calcium sensor of parathyroid cells. Am J Pathol 135: 321 - 328.

Kemper, B. (1984) Biosynthesis and secretion of parathyroid hormone. In: 'Cell Biology of the Secretory Process'. M. Cantin, ed. Karger, Basel, Switzerland, pp 443 - 480.

Kendall, C.H., L. Potter, R. Brown, B. Jasani, J.H. Pringle, and I. Lauder. (1993) *In situ* correlation of synthesis and storage of parathormone in parathyroid gland disease. J Pathol 169: 61 - 66.

Kendall, C.H., P.A. Roberts, J.H. Pringle, and I. Lauder. (1991) The expression of parathyroid hormone messenger RNA in normal and abnormal parathyroid tissue. J Pathol 165: 111 - 118.

Kendall, M.D. (1988) Anatomical and physiological factors influencing the thymic environent. In: 'Thymus Update. 1- The microenvironment of the human thymus'. M.D. Kendall and M.A. Ritter, ed. Harwood Academic Publishers, Chur, Switzerland, chap. 3, pp 27 - 66.

Kessel, R.G. (1992) Annulate lamellae: a last frontier in cellular organelles. Int Rev Cytol 133: 43 - 120.

Kingsbury, B.F. (1940) The development of the phayngeal derivatives of the opossum (*Didelphys virginiana*) with special reference to the thymus. Am J Anat 67: 393 - 435.

Kirkpatrick, T.H. (1964) Molar progression and macropod age. Queensl J Agric Anim Sci 21: 163 - 165.

Kirkpatrick, T.H. (1965) Studies of the Macropodidae in Queensland. 3. Reproduction in the grey kangaroo in southern Queensland. Queensl J Agric Anim Sci 22: 319 - 328.

Kirkpatrick, T.H. (1978) The development of the dentition of *Macropus giganteus* (Shaw). An attempt to interpret the marsupial dentition. Aust Mammol 2: 29 - 35.

Kirkpatrick, T.H. (1985) Biology for management. In: 'The Kangaroo Keepers.' H.J. Lavery, ed. University of Queensland Press, St Lucia, Australia, chap 6, pp 135 - 160.

Kirsch, J.A.W. and W.E. Poole. (1972) Taxonomy and distribution of the grey kangaroos, *Macropus giganteus* Shaw and *Macropus fuliginosus* (Desmarest), and the subspecies (Marsupialis: Macropodidae). Aust J Zool 20: 315 -339.

Kitazawa, R., S. Kitazawa, M. Fukase, T. Fujita, A. Kobayashi, K. Chihara, and S. Maeda. (1992) The expression of parathyroid hormone-related protein (PTHrP) in normal parathyroid: histochemistry and in situ hybridization. Histochemistry 98: 211 - 215.

Klahr, S., E. Slatopolsky and K. Martin. (1985) An overview of recent advances in mineral metabolism. In: 'Chronic renal disease. Causes, complications and treatment'. N.B. Cummings and S. Klahr, ed. Plenum Publishing Corporation, New York, chap. 13, pp 117 - 125.

Kovacs, K., and E. Horvath. (1975) Gonadotrophs following removal of the ovaries: a fine structural study of human pituitary glands. Endokrinologie 66: 1 - 8.

Kramer, S., F.H. Reynolds, M. Castillo, D.M. Valenzuela, M. Thorikay and J.M. Sorvillo. (1991) Immunological identification and distribution of parathyroid-likeprotein polypeptides in normal and malignant tissues. Endocrinology 128: 1927 - 1937.

Krstic, R. (1980) Three-dimensional organisation of the rat parathyroid glands. Z Mikrosk Anat Forsch 94: 445 - 450.

Kurtay, M. and G. Crile. (1969) Aberrant parathyroid glands in relationship to the thymus. Am J Surg 117: 705 - 705.

Langman, J. (1969) Digestive tube and its derivatives. In: 'Medical Embryology, 2nd ed,' chap 13. Williams and Wilkins, Baltimore, pp 237 - 275.

Larsen, W.J. (1997) Development of the head, the neck, and the eyes and ears. In: 'Human Embryology, 2nd ed,' chap 12, part 1. Churchill Livingstone, New York, pp 347 - 374.

Larsson, H., R. Lorentzon and L. Boquist. (1985) Quantitative morphological assessment of parathyroid activity in response to variations in calcium concentrations *in vitro*. Virchows Arch [Cell Pathol] 48: 97 - 105.

Leigh, C.M. and N. Edwin. (1991) An immunocytochemical study of the endocrine pancreas in the fat-tailed dunnart (*Sminthopsis crassicaudata*). Cell and Tissue Res 263: 195 - 198.

MacCallum, W.G. and C. Voegtlin. (1908) On the relation of the parathyroid to calcium metabolism and the nature of tetany. Bull Johns Hopkins Hosp 19: 91 - 92.

MacCallum, W.G. and C. Voegtlin. (1909) On the relation of tetany to the parathyroid glands and to calcium metabolism. J Exptl Med 11: 118 - 151.

MacGregor, R.R., J. W. Hamilton and D.V. Cohn. (1975) The by-pass of tissue hormone stores during secretion of newly synthesized parathyroid hormone. Endocrinology 97: 178 - 188.

MacKenzie, W.C. and W.J. Owen. (1919) The glandular system in monotremes and marsupials. Jenkin, Buxton and Co., Melbourne, Australia.

Malluche, H.H. and M.-C. Faugere. (1986). 'Atlas of Mineralized Bone Histology.' Karger, Basel, pp.-14 - 15.

Malmaeus, J., L. Grimelius, H. Johansson, G. Åkerström and S.Ljunghall. (1984) Parathyroid pathology in hyperparathyroidism secondary to chronic renal failure. Scand J Urol Nephrol 18: 157 - 166.

Martin, T.J. and J.M. Moseley. (1995) Parathyroid Hormone-Related Protein. In: 'Endocrinology, 3rd ed, vol 2', chap 57. L.J. DeGroot, ed. Saunders, Philadelphia, pp 967 - 977.

Matsushita, H., M. Hara, H. Nakazawa, Y. Shishiba, and T. Matuhasi. (1992) The presence of immunoreactive parathyroid hormone-related protein in parathyroid adenoma cells. Acta Pathol Jpn. 42: 35 - 41.

Maurer, F. (1899) Schilddruse, Thymus, und sonstige Schlundspalten derivate bei Echidna und ihre Beziehungen zu den gleichen Organen bei anderen Wirbelthieren. Denkschr Med Naturwiss Ges Jena 6: 403 - 444.

Mayer, G.P. (1979) Parathyroid hormone secretion. In: 'Endocrinology, vol. 2'. L.J.De Groot, ed. Grune and Stratton Inc, New York, chap 44, pp. 607 - 611.

McCrady, E. (1938) The embryology of the opossum. Am Anat Mem 16: 1 - 233.

McCrady, E. (1941) Parathyroids in the adult opossum. Anat Rec suppl 79: 45.

Miettinen, M., R. Clark, V-P Lehto, I. Virtanen and I. Damjanov. (1985) Intermediate-filament proteins in parathyroid glands and parathyroid adenomas. Arch Pathol Lab Med 109: 986 - 989.

Millzner, R.J. (1931) The normal variations in the position of the human parathyroid glands. Anat Rec 48: 399 - 405.

Morgan, J.R.E. (1936) Parathyroid glands: study of normal gland. Arch Pathol 21: 10 - 26.

Morrissey, J.J. and D.V. Cohn. (1978) The effects of calcium and magnesium on the secretion of parathormone and parathyroid secretory protein by isolated porcine parathyroid cells. Endocrinology 103: 2082 - 2090.

Müller-Höcker, J. (1992) Random cytochrome-c-oxidase deficiency of oxyphil cell nodules in the parathyroid gland. A mitochondrial cytopathy related to cell ageing? Path Res Pract 188: 701 - 706.

Munger, B.L. and S.I. Roth. (1963) The cytology of the normal parathyroid glands of man and Virginia deer. A light and electron microscopic study with morphologic evidence of secretory activity. J Cell Biol 16: 379 - 400.

Nicholas, J.S. and W.W. Swingle. (1925) An experimental and morphological study of the parathyroid glands of the cat. Am J Anat 34: 469 - 509.

Nilsson, O. (1977) Studies on the ultrastructure of the human parathyroid glands in various pathological conditions. Acta Pathol Microbiol Immunol Scand (A) 263 (Suppl): 1 - 88.

Norris, E.H. (1937) The parathyroid glands and the lateral thyroid in man: their morphogenesis, histogenesis, topographic anatomy and prenatal growth. Carnegie Inst Wash Contrib Embryology 59: 249 - 294.

Nunez, E.A., J.P. Whalen, and L.Krook. (1972) An ultrastructural study of the natural sescretory cycle of the parathyroid gland of the bat. Am J Anat 134: 459 - 480.

O'Connor, D.T., M.S. Burton, and L.J. Deftos. (1983) Chromogranin A: immunohistology reveals its universal occurrence in normal polypeptide hormone producing endocrine glands. Life Sci 33: 1657 - 1663.

Oka, T., T. Yoshioka, G.R. Shrestha, T. Koide, T. Sonoda, S. Hosokawa, K. Onoe, and M. Sakurai. (1988) Immunohistochemical study of nodular hyperplastic parathyroid glands in patients with secondary hyperparathyroidism. Virchows Archiv A Pathol Anat 413: 53 - 60.

Orloff, J.J., T.L. Wu, A.F. Stewart. (1989) Parathyroid hormone-like proteins: biochemical responses and receptor interactions. Endocr Rev 10: 476 - 484.

Ordenez, N.G. M.L. Ibanez, B. Mackay, N.A. Samaan and R.C. Hickey. (1982) Functioning oxyphil cell adenomas of parathyroid gland: immunoperoxidase evidence of hormonal activity in oxyphil cells. Am J Clin Pathol 78: 681 - 689.

Owen, R. (1862) On the anatomy of the Indian Rhinoceros (*Rh unicornis*, L). Trans Zool Soc Lond 4: 31 - 58.

Padgaonkar, A.S., M.V. Kagwade and A.P. Warbhuwan. (1992) Parathyroid and ultimobranchial glands of the estuarine snake, *Cerberus rhynchops* (Schneider). Gen Comp Endocrinol 86: 395 - 397.

Parsons, J.A. (1979) Physiology of parathyroid hormone. In: 'Endocrinology, vol 2', L.J. De Groot, ed. Grune and Stratton,, New York, chap. 46, pp 621 - 629.

Pearse, A.G.E. (1980) The chemistry and practice of fixation. In: 'Histochemistry Theoretical and Applied, vol 1. Preparative and optical technology', Churchill Livingstone, London, chap. 5, pp 97 - 158.

Pearson, J. (1940) Notes on the blood system of the Marsupialia. Pap & Proc Roy Soc Tasmania 1939: 77 - 94.

Perry, S.F., D. Seguin, F.P.J.G. Lafeber, S.E. Wendelaar Bonga, and J.C. Fenwick. (1989). Depression of whole-body calcium uptake during acute hypercalcemia in American eel, *Anguilla rostrata*, is mediated exclusively by corpuscles of Stannius. J Exp Biol 147: 249 - 262.

Poole, W.E. (1973) A study of breeding in grey kangaroos, *Macropus giganteus* (Shaw) and *M. fuliginosus* (Desmarest), in central New South Wales. Aust J Zool 21: 183 - 212.

Poole, W.E. (1976) Breeding biology and current status of the grey kangaroo, *Macropus fuliginosus fuliginosus*, of Kangaroo Island, South Australia. Aust J Zool 24: 169 - 187.

Poole, W.E., J.C. Merchant, S.M. Carpenter, and J.H. Calaby. (1985) Reproduction, growth and age determination in the yellow-footed rock-wallaby *Petrogale xanthopus* (Gray), in captivity. Aust Wildl Res 12: 127 - 136.

Potts, J.T. Jr, F.R. Bringhurst, T. Gardella, S. Nussbaum, G. Segre, and H. Kroneberg. (1995) Parathyroid hormone: physiology, chemistry, biosynthesis, secretion, metabolism, and mode of action. In: 'Endocrinology, 3rd ed, vol 2'. L.J. DeGroot, ed. Saunders, Philadelphia, chap 56, pp 920 - 966.

Presidente, P.J.A. (1982) Common brushtail possum,*Trichosurus vulpecula*: Maintenance in captivity, blood values, disease and parasites. In: 'The Management of Australian Mammals in Captivity". D.D. Evans, ed. Zoological Board of Victoria, Melbourne, pp 55 - 66.

Ravazzola, M., L. Orci, J.F. Habener and J.T. Potts Jr. (1978) Parathyroid secretory protein immunocytochemical localisation within cells that contain parathyroid hormone. Lancet 8085: 371 - 372.

Rogers, W.M. (1929) The development of the pharynx and the pharyngeal derivatives in the white rat (*Mus norvegius albinus*). Am J Anat 44: 283 - 330.

Roth, S.I. (1970) The ultrastructure of primary water-clear cell hyperplasia of the parathyroid glands. Am J Path 61: 233 - 248.

Roth, S.I. (1979) Anatomy of the parathyroid glands. In 'Endocrinology, vol 2'. L.J. DeGroot, ed. Grune and Stratton, New York, chap. 41, pp 587 - 592.

Roth, S.I. and C.C. Capen. (1974) Ultrastructural and functional correlations of the parathyroid gland. Int Rev exp Path 13: 161 - 221.

Roth, S.I. and R.B. Marshall. (1969) Pathology and ultrastructure of the human parathyroid glands in chronic renal failure. Arch Intern Med 124: 397 - 407.

Roth, S.I. and B.L. Munger. (1962) The cytology of the adenomatous, atrophic and hyperplastic parathyroid glands of man, a light and electron microscopic study. Virchows Arch Abt A Pathol Anat Physiol 335: 389 - 410.

Roth, S.I. and L.G. Raisz. (1966) The course and reversibility of calcium effect on the ultrastructure of the rat parathyroid gland in organ culture. Lab Invest 15: 1187 - 1211.

Roth, S.I. and A.L. Schiller. (1976) Comparative anatomy of the parathyroid glands. In: 'Handbook of Physiology, Section 7, vol 7', R.O. Greep and E.B. Astwood, section ed. Endocrinology. G.D. Aurbach, vol. ed. American Physiological Society, Washington, D.C., chap 12, pp 281 - 311.

Sandström, I. (1880) Om en ny kortel hos menniska och atskilliga daggdjur. Upsala Lakareforenings Forh 15: 441 - 554. (Translated by C.M. Seipel., 1938, Bull Hist Med 6: 179 - 222).

Seebeck, J.H., P.R. Brown, R.L. Wallis and C.M. Kemper. (1990) 'Bandicoots and Bilbies'. J.H. Seebeck, P.R. Brown, R.L. Wallis and C.M. Kemper, ed. Surrey Beatty and Sons, Sydney.

Segre, G.V. (1979) Heterogeneity and metabolism of parathyroid hormone. In: 'Endocrinology, vol 2'. L.J. De Groot, ed. Grune and Stratton, New York, chap. 45, pp 613 - 619.

Segre, G.V., J.F. Habener, D Powell, G.W. Tregear and J.T. Potts Jr. (1972) Parathyroid hormone in human plasma: immunochemical characterization and biological implications. J Clin Invest 51: 3163 - 3172.

Seipel, C.M. (1938) An English translation of Sandström's "Glandulae Parathyreoideae". Bull Hist Med 6: 179 - 222.

Setoguti, T. (1977) Electron microscopic studies of the parathyroid gland of senile dogs. Am J Anat 148: 65 - 84.

Setoguti, T., Y. Inoue, and P. Wild. (1995) The biological significance of storage granules in rat parathyroid cells. Microsc Res Tech 32: 148 - 163.

Shannon, W.L., and S.I. Roth. (1974) An ultrastructural study of acid phosphatase activity in normal, adenomatous and hyperplastic (chief cell type) human parathyroid glands. Am J Pathol 77: 493 - 506.

Sharman, G.B., H.J. Frith, and J.H. Calaby. (1964) Growth of the pouch young, tooth eruption and age determination in the red kangaroo *Megaleia rufa*. CSIRO Wildlife Res 9: 20 - 49.

Sheldon, H. (1964) On the water-clear cell in the human parathyroid gland. J Ultrastruct Res 10: 377 - 383.

Shoumura, S., S. Emura, N. Ishizaki, T. Yamahira, H.Y. Chen and H. Isono. (1988) Immunocytochemical localization of parathyroid hormone in hamster parathyroid gland. Acta Anat Basel 133: 107 - 110.

Shoumura, S., N. Ishizaki, S. Emura, Y. Iwasaki, T. Yamahira, and H. Isono. (1988) Immunocytochemical localization of parathyroid hormone in rabbit parathyroid glands. Histol Histopathol 3: 93 - 95.

Singh, R. and I. Kar. (1983) Parathyroid and ultimobranchial glands of the sand boa, *Eryx johnii* Daudin. Gen Comp Endocrinol 51: 66 - 70.

Sonntag, C.F. (1921) The comparative anatomy of the koala (*Phascolarctos cinereus*) and the vulpine phalanger (*Trichosurus vulpecula*). Proc Zool Soc Lond 1921: 547 - 577.

Speare, R., A.T. Haffenden, P.W. Daniels, A.D. Thomas and C.D. Seawright. (1984) Diseases of the Herbert River ringtail, *Pseudocheirus herbertensis* and other north Queensland rainforest possums. In: 'Possums and Gliders'. A.P. Smith and I.D. Hume, ed. Australian Mammal Society, Sydney, pp 283 - 302.

Strahan, R. (1983) In: 'The Complete Book of Australian Mammals'. R Strahan, ed. Angus and Robertson Publishers, Sydney.

Srivastav, A.K., V.K. Das, S. Das, Y. Sasayama and N. Suzuki. (1995) Amphibian parathyroids: morphological and functional aspects. Microsc Res Tech 32: 79 - 90.

Srivastav, A.K., Y. Sasayama, and N. Suzuki. (1995) Morphology and Physiological significance of parathyroid glands in reptilia. Microsc Res Tech 32: 91 - 103.

Symington, J. (1898) The thymus gland in the marsupialia. J Anat Physiol Lond 32: 278 - 291.

Symington, J. (1900) A note on the thymus gland in the koala (*Phascolarctus cinereus*). J Anat Physiol Lond 34: 226 - 227.

Taggart, D.A., C.M. Leigh and W.G.Breed. (1995)....Ultrastructure and motility of spermatozoa in the male reproductive tract of peramelid marsupials. Reprod Fertil Dev 7: 1141 - 1156.

Taggart, D.A., V.R. Steele, D. Schultz and P.D. Temple-Smith. (1996) Semen collection and cryopreservation in the southern hairy-nosed wombat (*Lasiorhinus latifrons*): Implications for the conservation of the northern hairy-nosed wombat (*Lasiorhinus krefftii*). In: 'Wombats in Australia: Biology, History, Art and Literature'. R. Wells, ed. Surrey Beatty: Sydney.

Taggart, D.A., V.R. Steele, D. Schultz and P.D. Temple-Smith. (1994) Semen collection and cryopreservation in the southern hairy-nosed wombat (*Lasiorhinus latifrons*): Implications for the conservation of the northern hairy-nosed wombat (*Lasiorhinus krefftii*). In: 'Proceedings of Wombats in Australia: Biology, history, art and literature'. Roy Zoo Soc SA, Adelaide.

Taggart, D.A. and P.D. Temple-Smith. (1990a). The effects of breeding season and mating on the total number and relative distribution of spermatozoa in the epididymis of the brown marsupial mouse, *Antechinus stuartii*. J Reprod Fert 88: 81-91.

Taggart, D.A. and P.D. Temple-Smith. (1990b). An unusual mode of progressive motility in spermatozoa from the dasyurid marsupial, *Antechinus stuartii*. Reprod Fert Dev 2: 107-14.

Taggart, D.A. and P.D. Temple-Smith. (1991). Postnatal development of the epididymis in dasyurid marsupial (*Antechinus stuartii*., Marsupialia). Anat Embryol 186: 259-270.

Taggart, D.A. and P.D. Temple-Smith. (1991) Transport and storage of spermatozoa in the female reproductive tract after mating and structural morphology of the oviducal sperm storage crypts in the brown marsupial mouse, *Antechinus stuartii*., (Dasyuridae). J Reprod Fert 93: 97-110.

Talmage, R.V., S.A. Grubb, C.J. Vander Wiel, S.H. Doppelt, and H. Norimatsu. (1978) The demand for bone calcium in maintenance of plasma calcium concentrations. Proceedings, Mechanisms of Localized Bone Loss. JE Horton, TM Tarpley and WF Davis, ed. Special Supplement to Calcified Tissue Abstracts: 73 - 91.

Tandler, B., R.V.P. Hutter and R.A. Erlandson. (1970) Ultrastructure of oncocytoma of the parotid gland. Lab Invest: 567 - 580.

Taylor, J.M. (1984) The Oxford guide to mammals of Australia. Oxford University Press, Melbourne.

Tedman, R.A. (1990) Some observations on the visceral anatomy of the bandicoot *Isoodon macrourus* (Marsupialia: Peramelidae) In: 'Bandicoots and Bilbies'. J.H. Seebeck, P.R. Brown, R.L. Wallis and C.M. Kemper, ed. Surrey Beatty and Sons, Sydney, pp 107 - 116.

Tharp, M.D., L.S. Leonard, R.E. Tigelaar, and P.R. Bergstresser. (1985) Conjugated avidin binds to mast cell granules. J Histochem Cytochem 33: 27 - 32.

Thiele, J. (1984) Fine structure of normal human parathyroid gland as revealed by thin section and freeze-fracture with regard to some pathological conditions. In: 'Ultrastructural of endocrine cells and tissues'. P.M. Motta, ed. Martinus Nijhoff Publishers, Boston, chap. 26. 302 - 312.

Thompson, N.W., F.E. Eckhauser and J.K. Harness. (1982) The anatomy of primary parathyroidism. Surgery 92: 814 - 821.

Tremblay, G. (1969) Oncocytes, a review. Methods and Achievements in Exp Path 4: 121 - 140.

Tremblay, G. and G.E. Cartier. (1961) Histochemical study of oxidative enzymes in human parathyroid. Endocrinology 69: 658 - 661.

Tremblay, G. and A.G.E. Pearse. (1959) Cytochemical study of oxydative enzymes in parathyroid oxyphil cells and their functional significance. Br J Exp Pathol 140: 66 - 70.

Trier, J.S. (1958) The fine structure of the parathyroid gland. J Biophys Biochem Cytol 4: 13 - 22.

Triggs, B. (1988) The Wombat. New South Wales University Press, Sydney.

van de Wijngaert, F.P., M.D. Kendall, H.J. Schuurman, L.H. Rademakers, and L. Kater. (1984) Heterogeneity of epithelial cells in the human thymus. An ultrastructural study. Cell Tissue Res 237: 227 - 237.

von Gaudecker, B., G.G. Steinmann, M.L. Hansmann, J. Harpprecht, N.M. Milicevic, and H.K. Muller-Hermelink. (1986) Immunohistochemical characterization of the thymic microenvironment. A light-microscopic and ultrastructural immunocytochemical study. Cell Tissue Res 244: 403 - 412.

von Gaudecker, B., M. Larche, H.J. Schuurman, and M.A. Ritter. (1989) Analysis of the fine distribution of thymic epithelial microenvironmental molecules by immuno-electron microscopy. Thymus 13: 187 - 194.

Walton, D.W. and B.J. Richardson. (1989) 'Fauna of Australia. Mammalia.' vol 1B D.W. Walton and B.J. Richardson, ed. Australian Government Publishing Service, Canberra.

Wang, C.A. (1976) The anatomic basis of parathyroid surgery. Ann Surg 183: 271 - 275.

Wang, L.C.H. (1982) Hibernation and the endocrines. In: 'Hibernation and Torpor in Mammals and Birds.' C.P. Lyman, J.S. Willis, A. Malan and L.C.H. Wang, ed. Academic Press, London, chap. 12, pp 206 - 236.

Wells, R.T. (1989) Vombatidae. In: 'Fauna of Australia. Mammalia.' Vol. 1B D.W. Walton and B.J. Richardson, ed. Australian Government Publishing Service, Canberra, chap. 32, pp 755 - 768.

Welsh, D.A. (1898) Concerning the parathyroid glands: A critical, anatomical and experimental study. J Anat (Lond) 32: 292 - 307; 380 - 403.

Wendelaar Bonga, S.E. and P.K.T. Pang. (1991) Control of calcium regulating hormones in vertebrates: parathyroid hormone, calcitonin, prolactin, and stanniocalcin. Int Rev Cytol 128: 139 - 213.

Wernerson, A., O. Svensson, and F.P. Reinholt. (1995) Quantitative and three-dimensional aspects of the rat parathyroid gland in normo-, hypo, and hypercalcemia. Microsc Res Tech 32: 129 - 147.

Wild, P. (1980) Correlative light- and electron-microscopic study of parathyroid glands in dogs of different age groups. Acta Anat 108: 340 - 349.

Wild, P. and T. Setoguti. (1995) Mammalian parathyroids: Morphological and functional implications. Microsc Res Tech 32: 120 - 128.

Wilson, G.R. (1975) Age structures of populations of kangaroos (Macropodidae) taken by professional shooters in New South Wales. Aust Wildl Res 2: 1 - 9.

Yadav, M. (1973) The presence of the cervical and thoracic thymus lobes in marsupials. Aust J Zool 21: 285 - 301.

Yamahira, T., S Shoumura, N Ishizaki, S. Emura, K. Hayashi and H. Isono. (1980). Electron microscopic observations on the parathyroid glands of the pregnant and puerperal mice: A morphometric study. J Clin Electron Microsc 13: 517.

Zuckerkandl, E. (1902) Die Epithelkorperchen von *Didelphys azara* nebst Bemerkungen uber die Epithelkorperchen des Menschen. Anat Hefte 19: 59 - 84.

Addendum

Wild, P., E.M. Schraner, H. Augsburger, R. Beglinger, and R. Pfister. (1986) Ultrastructural alterations in mammalian parathyroid glands induced by fixation. Acta Anat 126: 87 - 96.

Sources of Figures used on the First Page of Each Chapter

Animal	book	page
Sminthopsis crassicaudata	Brazenor, 1950	21
Antechinus flavipes	Ride and Fry, 1970	117
Sarcophilus harrisii	Lyne, 1967	21
Isoodon obesulus	Brazenor, 1950	30
Lasiorhinus latifrons	Lyne, 1967	34
Phascolartos cinereus	Lyne, 1967	71
Trichosurus vulpecula	Lyne, 1967	43
Macropus fuliginosus	Brazenor, 1950	51
Tachyglossus aculeata	Lyne, 1967	7
Ornithorhynchus anatinus	Lyne, 1967	6

Brazenor, C.W. (1950) 'The Mammals of Victoria. Handbook no. 1. National Museum of Victoria'. Brown, Prior and Anderson, Melbourne.

Lyne, A.G. (1967) 'Marsupials and Monotremes of Australia'. Angus and Robertson, Sydney.

Ride, W.D.L. and E. Fry. (1970) 'A Guide to the Native Mammals of Australia'. Oxford University Press, Melbourne.

Addendum

The anatomy, light and electron microscopic structure of the parathyroid glands that are presented in this comparative study of marsupials and monotremes have been described from observations made on specimens subjected to standardised fixation and histological techniques. Artefacts relating to imperfect fixation and processing are also described. ***The study was done with the assumption that the parathyroid tissue of different species reacted similarly when subjected to the standardised techniques. However if this assumption is not valid then some of the observed differences in structural details between species may need to be re-interpreted as additional artefacts.***

For example, in antechinus (chap. 4), wombat (chap. 6), and echidna (chap. 9) the presence of 'non-secretory cells' amongst parathyroid principal cells was noted. These cells were devoid of desmosomes and were identified as neutrophils and lymphocytes in the antechinus, macrophages in the wombat, and epithelial reticular cells in the echidna. Reasons supporting these identifications are given in the relevant chapters. ***Alternatively*** these cells may be artefactual products resulting from imperfect fixation and actually represent shrunken, atrophic, principal cells. Previous studies (Wild et al., 1986) on the effect of different fixatives on the ultrastructure of parathyroid glands from several species have shown various species reacted inconsistently to the different fixatives and the morphological variations were considered to be artefactual manifestations. For example, cells similar to the non-secretory cells described above, were found to be present in cat parathyroid tissue only after certain fixative protocols had been applied (Wild et al., 1986).

Chapter 4.

p37, second paragraph. Add after the second sentence -

No desmosomes were observed between these cells identified as leukocytes and adjacent principal cells.

Chapter 8

p134, last paragraph. Change third sentence -

Alternatively, the distention of RER may be a fixation artefact.

p135, insert between the third and fourth paragraph -

The distention of RER has been shown to be a fixation artefact (Wild et al., 1986) However the fact that both distended and narrow profiles of RER were present within the same cells suggests the observed morphology reflected the actual structure and was not entirely moulded by the effects of fixation.